PERTURBATION THEORY OF ELECTROMAGNETIC SCATTERING FROM LAYERED MEDIA WITH ROUGH INTERFACES

DISSERTATION

Presented in Partial Fulfillment of the Requirements for

the Degree Doctor of Philosophy in the

Graduate School of The Ohio State University

By

Metin A. Demir, M.S., B.E., B.S.

* * * * *

The Ohio State University

2007

Dissertation Committee:

Prof. Joel T. Johnson, Adviser

Prof. Fernando L. Teixeira

Prof. Lee C. Potter

Approved by

Adviser

Graduate Program in
Electrical and Computer
Engineering

ABSTRACT

The Small Perturbation Method (SPM) is a low frequency approximation to the electromagnetic scattering from rough surfaces. The theory involves a small height expansion in conjunction with a perturbation series expansion of the unknown scattering coefficients. Recently, an arbitrary order, iterative solution procedure has been derived for SPM: kernels at any order are expressed as a summation over lower order kernels in an iterative fashion. Such a form is very useful, because it allows evaluation of the field statistical moments in a direct manner, when considering stochastic surfaces. In this dissertation, this procedure is extended to the two layer (two rough surfaces on top of each other) problem and the complete solution is given.

Utilizing this formulation, the second and fourth order bi-static scattering coefficients for two rough surfaces characterized by two uncorrelated Gaussian Random Processes (GRP) are obtained. The effects of upper and lower roughnesses and the interaction effect in the total fourth order cross section can be identified in the theory. Studies on the ratio of the interaction effect to the total cross section are presented for example cases, investigating the relative importance of interactions among surfaces. Results show the interaction term contributes most to the cross-pol cross sections when surfaces are close to each other at near grazing incidence.

In addition, the previously developed arbitrary order SPM solution for the single layer problem is utilized to derive the fourth order term in the small slope approximation (SSA) of thermal emission from the sea surface. It is shown that this term has the form of a four-fold integration over a product of two sea spectra for a Gaussian random process sea, thereby describing emission "interaction" effects among pairs of sea waves. Interaction effects between "long" and "short" waves are considered, both through numerical and approximate evaluations of the fourth order theory. The approximation developed is a theoretical alternative to the "two-scale" model, and enables comparisons of short wave "tilting" effects between the two models in terms of spectrum independent "weighting" functions. The weighting functions obtained are found to be similar, but not identical.

To my wife and my parents

ACKNOWLEDGMENTS

First, I would like to express my sincere appreciation to my adviser, Prof. Joel T. Johnson, for his support, patience and encouragement during my graduate study. This work will not be possible without him, and I feel very lucky working with him.

I would also like to thank to my PhD. committee members: Prof. Potter and Prof. Teixera, both for their valuable discussions during my candidacy exam and for their suggestions on my dissertation.

I gratefully acknowledge help and support from my professors in ESL, especially, Prof. Pathak, Prof. Rojas, Prof. J.F. Lee and Dr. Sertel. I really learned a lot from them.

I also thank my colleagues in our group, Barış Güner, Guangdong Pan, Noppasin Niamsuwan and Praphun Naenna for their valuable discussions and their friendship. It was an honor, working with them.

In addition, I thank to my colleagues in ESL, Koray Tap and Yakup Bayram, for being such nice friends. My office mates Hyoung-Sun Youn and Jae-Young Chung are also acknowledged for their friendship and practical EM related discussions.

And, the final thanks goes to my family, especially my wife, for her constant understanding, love and support.

VITA

November 20, 1978	Born - Kayseri, Turkey
June 2001	B.E., Electronics and Communication Engineering, College of Engineering, Istanbul, Technical University of Istanbul, Turkey
June 2001	B.S., Mathematical Engineering, College of Science and Literature, Istanbul, Technical University of Istanbul, Turkey
June 2003	M.S., Electrical and Computer Engineering, College of Engineering, Columbus, The Ohio State University, Ohio
2001-present	Graduate Research Associate, The Ohio State University.

PUBLICATIONS

Research Publications

M. A. Demir, J. T. Johnson, "Fourth order small slope theory of sea brightness temperatures". *IEEE Trans. Geosc. Rem. Sens*, vol. 45, pp. 175-186, 2007

M. A. Demir, J. T. Johnson, "Calculation of the fourth order small slope theory of thermal emission from the sea surface". *IGARSS '04. Proceedings*, vol.4, pp. 2768 - 2771, Sept. 2004

M. A. Demir, J. T. Johnson, "Fourth and higher-order small perturbation solution for scattering from dielectric rough surfaces". *J. Opt. Soc. Am. A*, vol. 20, no. 12, pp. 2330-2337, 2003

M. A. Demir, "Fourth and higher-order small perturbation solution for scattering from dielectric rough surfaces". *The Ohio State University*, Master Thesis, 2003.

M. A. Demir, J. T. Johnson, "Fourth and higher-order small perturbation solution for scattering from dielectric rough surfaces". *IEEE AP-S International Confernence Proceedings*, vol. 3, pp.412-415, Jun. 2003.

M. A. Demir, J. T. Johnson, "Fourth order small slope theory of thermal emission from the sea surface". *PIERS 2002 International Confernence Proceedings*, pp. 150, Jun. 2002.

FIELDS OF STUDY

Major Field: Electrical and Computer Engineering

Studies in:

Electromagnetic Scattering	Prof. Joel T. Johnson
Microwave Remote Sensing	Prof. Joel T. Johnson

TABLE OF CONTENTS

Page

LIST OF FIGURES

CHAPTER 1

INTRODUCTION

This dissertation is about high order SPM solutions of electromagnetic scattering from rough interfaces. Recently developed arbitrary order SPM solution procedure is applied to layered roughness problem. The purpose of this chapter is to:

- Describe the motivation of the work and introduce the problems addressed in this dissertation.
- Summarize the current state of scattering models for layered roughness and emission based models.
- Provide a description of the approach taken in this study by pointing out the main contributions and an outline of the dissertation.

1.1 The two-layer problem

Scattering of electromagnetic waves from rough layered media is of interest in many areas of engineering such as remote sensing and optics[1]-[71]. In remote sensing, many natural surface-subsurface structures such as soil and multi-year ice can easily be modeled as rough layered surfaces; a reliable electromagnetic scattering model can be useful in several practical applications such as soil moisture estimation[2],

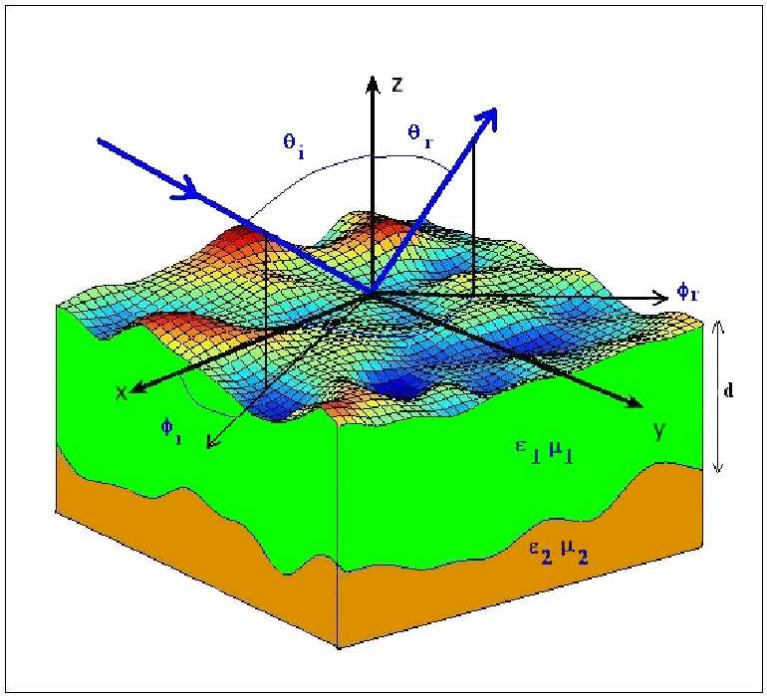

Figure 1.1: Two layer problem geometry

ice thickness calculations[4], subsurface sensing, Ground Penetrating Radar (GPR), and so forth. The application areas can easily be extended into optics, such as design of multi-layer coated optical components, thin films, and optical scattering from nanoscale structures

In this study, scattering from 2-D, homogeneous, dielectric media with two rough interfaces is considered. A descriptive sketch is given in Figure 1.1. For an incident plane wave of either horizontal or vertical polarization, a complete perturbation based solution, meaning , all the reflected, intermediate and transmitted fields at any order in surface height, is sought. Both numerical and analytical solutions of the perturbation series are investigated for either deterministic or random scenarios. The coherent

and incoherent scattered powers and corresponding radar cross sections(RCS) are calculated. The effects of upper and lower roughness and the interactions of roughness effects are identified. For the case when the upper and lower surfaces are uncorrelated random processes, the importance of the interaction of roughness effects is examined.

1.2 Emission theory of a single layer

Emission from naturally occuring rough surfaces is one of the fundemental interests in passive microwave remote sensing. Applications such as satellite based wind speed-direction retrival over the ocean surface are of interest, and SPM theory is commonly used in this field. Kirchhoff's Law requires computation of the total surface reflectivity in order to determine surface emissivity. The total surface reflectivity is determined by integrating the total power scattered into the upper hemisphere under plane wave illumination. The formulation of these models is based on SPM solution for scattering from a single layer rough surface [22], which has been shown to yield a Small Slope Approximation (SSA) theory when applied to the computation of surface emission [73].

In this dissertaion, derivation of the fourth order SSA theory is considered, utilizing the previously developed arbitrary order SPM solution for a single layer. This term has the form of a four-fold integration over a product of two sea spectra for a Gaussian random process sea, thereby describing emission interaction effects among different scales of roughnesses. An approximation for "long - long" wave interactions (i.e. the optical limit) is considered, in comparison the physical optics theory. Interaction effects between "long" and "short" waves are also considered, both through

numerical and approximate evaluations of the fourth order theory. The approximation developed has a form similar to an expanded "two-scale" model, and enables comparisons of short wave "tilting" effects between the two models in terms of spectrum independent "weighting" functions. In addition, azimuthal harmonics from the fourth order SSA expansion of long-short wave interactions for a particular sea surface model are compared against the full fourth order theory and the two-scale model.

1.3 Background

1.3.1 Rough surface scattering models for layered media

Rough surface scattering is a challenging branch of electromagnetics. A closed form solution for this problem, even in the simplest, deterministic case is not available today[1]. Although recent advances in numerical solution techniques can be applied[7],[11], they lack physical insight and usually are very expensive in terms of computation. Due to this fact, researchers tend to choose approximation based approaches such as the Kirchhoff approximation or perturbation type theories for the solution of rough surface scattering problems[10],[19],[21].

Originally derived by Rice [22] in the 1950's, the small perturbation method(SPM) is one of the most common techniques for rough surface scattering problems. It is also known as the Fourier-Rayleigh approach [25]. As in any other perturbation based model, the SPM is an approximate method that exploits the smallness of an inherent parameter, which is the height variations of the surface in this case. The SPM assumes the Rayleigh hypothesis, which basically states that the scattered (or transmitted) field can be expressed as a sum of up (or down) going plane waves (Floquet modes)([68],[69],[70]); the method has been proven to work for gentle roughness[26].

The derivations of the theory involve a small height expansion in conjunction with a perturbation series expansion of the unknown scattering coefficients. Terms of the same order are collected together to solve the scattering coefficients as the elements of the perturbation series [9],[12].

The main deficiency of the theory is that the solution for the scattering coefficients becomes highly complicated as the order of the solution increases[69]. When a multi-layer rough surface structure is considered, the complexity increases significantly with increasing number of layers. Due to this fact, most of the previous analytical studies of the multi-layer SPM method are usually limited to the two-layer, first order formulation. Usually, for single rough interface problems higher order solutions are not vital, except for some special applications [71]. But for structures involving two or more rough interfaces, this is not the case. In order to investigate interaction effects between the surfaces, the order of solution required increases with the number of interfaces.

Recently, an arbitrary order recursive solution procedure has been developed for the single interface SPM[69],[70]. The main idea of this procedure was to express the N^{th} order SPM weighting function in terms of lower order SPM weighting functions, enabling a recursive formulation of the solution. Such an approach is advantageous in terms of programming and compact formulation. An important portion of this study is to extend similar ideas to the two layer and N-layer problem.

As mentioned before, the interaction between rough surfaces is also of interest in this study. Previous analytical results, limited to the first order solution, can only investigate the interaction between correlated rough surfaces, which provide a

limited amount of information[2]. A higher order solution of the scattering coefficients is needed when interaction of uncorrelated surfaces is considered[6]. In fact, in the minimum, a solution up to third order is necessary for the two layer problem. Interesting wave scattering phenomena such as back-scattering enhancement of rough layers then can be analyzed for more realistic cases. Although such an investigation is already available using another perturbation type approach, called the reduced Rayleigh integrals[5], this previous study is semi-numerical, since the field expressions involve integrals which were handled numerically.

1.3.2 Emission Theory of Rough Surfaces

In recent years, models based on the small slope approximation (SSA) for emission from a single layer rough surface have been applied to study sea surface brightness temperatures [73]-[77]. The formulation of these models is based on a small perturbation method (SPM) solution for scattering from a rough surface [22], which has been shown to yield a small slope theory when applied to the computation of surface emission [73]. One consequence of the small slope nature of the theory is the fact that the SSA model produces agreement with a physical optics (PO) theory for the contributions of large-scale waves when the PO theory is expanded in long-wave slope [78], while retaining agreement with SPM emission predictions for small scale surfaces.

The majority of previous studies have employed the second order SSA theory [73]-[75], either alone or in combination with a full geometrical optics approach to obtain a "two scale" model [79]-[80]. These second order SSA based theories predict that the influence of surface roughness on brightness temperatures can be expressed

as an integration over the surface directional spectrum multiplied with an emission "weighting function" [75]. A third order SSA theory has also been derived recently [76]-[77], and obtains a correction to the second order results in terms of a quadruple integration over the surface bi-spectrum. Because the bi-spectrum vanishes identically for a surface described as a Gaussian random process, third order SSA results provide only limited information on the accuracy of second order predictions for a near-Gaussian process sea.

Extension of the theory to fourth order requires knowledge of the SPM scattering solution to fourth order. Explicit expressions up to second order in surface height were provided in [22]; explicit expressions up to third order have also been presented [68]. Reference [68] also presented a systematic procedure for determining fourth and higher order solutions, but the simplified results of this procedure were not provided. Recently, the systematic procedure described in [68] was applied to construct a recursive and arbitrary order solution [69] for scattered fields in the SPM method. This solution now enables formulation and evaluation of SSA emission contributions at fourth order.

In the second order SSA theory, emission contributions from individual sea waves are summed without regard to the presence of other waves. One advantage of a fourth order model is its ability to capture emission "interactions" among multiple length scale waves in the sea surface. An example of previous heuristic attempts to model such interactions is found in the two-scale theory of sea surface emission. Under this model, the sea surface spectrum is separated into "long" (i.e. sea wave wavelengths much longer than the electromagnetic wavelength) and "short" (sea waves remaining after long waves are removed) wave portions. Emission from the sea is then modeled

as an average of short-wave surface emissions (each computed using the second order SSA theory) with the short wave "facets" tilted by the slope distribution of the long-wave portion of the sea surface. The tilting process results in a change in the local observation angle of a given short wave facet, as well as a polarization transformation from the short-wave local to the global observation coordinates. The tilting process of the two-scale model represents an interaction between long and short wave portions of the sea surface.

Because no such interactions are included in the SSA2 model, long wave tilting of short waves is neglected in this theory. The fourth order SSA theory then should produce the first SSA modeling of these effects for a near-Gaussian random process sea, and thereby enable comparisons with and evaluations of tilting effects included in the two-scale theory. The results to be presented here have been selected to provide an initial examination of these effects.

1.4 Overview of the dissertation

In Chapter 2, detailed formulation of the perturbation solution for rough surface scattering is provided, for one dimensional (1-D), Perfect Electric Conductor (PEC) interfaces. Other approximate models are also considered, including the second order small slope approximation (SSA2), the physical optics (PO), and the lowest order modified non-local SSA (MNLSSA). As an exact numerical solution, the extended boundary condition (EBC) method is presented. The 1-D Dirichlet treatment of the SPM is highlighted in great detail for the deterministic case, since the rest of the dissertation is about the advanced applications of SPM theory and many ideas introduced here will directly apply to the following chapters. The rest of the chapter is

mostly specialized for a deterministic problem: scattering from sinusoidal gratings, since the sinusoidal scattering problem has a great theoretical importance and provides a lot of insight to the rough surface scattering theory. Formulations of each model mentioned above are presented for the sinusoidal grating problem and one final section is also included, comparing these models for several sinusoidal surfaces, in order to give insight on the limitations of each model.

Then, in Chapter 3, the basic formulation for the two-layer problem is introduced. First, the notational conventions for the rest of the dissertation are provided. Next, the boundary conditions are studied in a similar fashion with the previous chapter. Each boundary condition brings a so called forcing function, which can be utilized to express the solution of the problem as a set of two linear system of equations, for horizontal and vertical polarizations, respectively. The solution for these systems of equations is provided analytically. Later, a Fast Fourier Transform(FFT) based numerical solution is described, in the Fourier-Rayleigh sense. For validation purposes, the numerical perturbation solution is compared against an existing two and a half dimensional extended boundary condition(EBC) solution for two sine surfaces on top of each other, in the propagating modes, for several example cases. Although only the two-layer case is considered analytically in the following chapters, the arbitrary number of layers case is also considered as a final section in this chapter in a numerical sense. This section can also be considered as a generalization of the two-layer numerical solution, which will be very useful in possible future work involving analytical arbitrary layer SPM solutions.

In Chapter 4, an analytical solution procedure for the two-layer problem is presented. First, the zeroth order solution is provided, in terms of functions defined in

Chapter 3. Zeroth and arbitrary order contributions to the general N^{th} order solution are then obtained from the forcing functions. The zeroth order contribution terms are studied separately for horizontal and vertical incidence cases, while arbitrary order contributions are identical for both incidence cases. Next, partial SPM solutions for zeroth and lower order contribution terms are obtained. Later, these partial solutions are utilized to obtain the complete first and second order solutions. Then, a general form of higher order solutions is studied, and based on those generalizations, a new tensor based notation is introduced. The tensor notation is applied to the partial SPM solutions, and the arbitrary order SPM solution procedure is constructed with them. Finally, a convergence analysis of SPM solutions is presented using the ratio test of convergence.

In Chapter 5, an analysis of two-layer problem scattered powers is provided. Given the field solution to the third order in surface height, reflected, intermediate and transmitted powers can also be derived to third order. In this chapter, first, a general discussion on the power calculations is provided. Assumptions on the statistical surface properties are highlighted. Then, under the assumption of Gaussian Random Process (GRP), the zeroth and the second order coherent reflectivity and the second and the fourth order incoherent bi-static Radar Cross Sections (RCS) are derived. For the case when the two random processes are uncorrelated, the bi-static RCS term is studied thoroughly and the effects of upper and lower roughness and the interaction of roughness effects are identified. A special term is defined as the ratio of the interaction effect to the overall RCS, and it is studied for several problems of practical interest.

In Chapter 6, the arbitrary order SPM scattering solution for the one layer problem is applied in Kirchhoff's Law of thermal emission to derive the fourth order correction in the small slope emission theory. First, the SPM scattering solution is reviewed and the notation to be utilized is introduced. These scattered field solutions are then applied with Kirchhoff's Law to derive the fourth order SSA emission term; it is shown that this term has the form of an integration over a product of two spectra for a Gaussian random process sea. Next, the long-long wave expansion analysis is extended to fourth order to demonstrate again that the SSA theory continues to match a slope expanded PO theory for large-scale surface emission contributions. Numerical evaluation of the four-fold SSA4 integral for computing "long-short" wave interactions is discussed, and an approximation for computing such interactions is presented. The form of the approximation obtained allows a sea spectrum independent comparison with the two-scale theory of long-short wave tilting effects to be performed in terms of a set of weighting functions; these functions are found to be similar but not identical between the two theories. To provide more concrete illustrations, azimuthal harmonic coefficients of emitted brightnesses obtained from a numerical four-fold SSA4 integration are presented, and results compared with predictions of the approximation as well as the two-scale theory are compared.

Finally in Chapter 7, final discussions and conclusions are provided along with main contributions of this dissertation.

CHAPTER 2

ROUGH SURFACE SCATTERING FORMULATION FOR SINUSOIDAL GRATINGS

2.1 Introduction

This chapter provides detailed formulations of fundamental rough surface scattering models for one dimensional (1-D) rough Perfectly Electric Conductor (PEC) interfaces. Both approximate and exact models are described. The approximate models include the small perturbation method (SPM), the second order small slope approximation (SSA2), physical optics (PO), and the lowest order modified non-local SSA (MNLSSA). As an exact numerical solution, the extended boundary condition (EBC) method is presented.

In the following sections, a 1-D Dirichlet treatment of the SPM is described in detail for the deterministic case, since the rest of the dissertation is about the advanced applications of SPM theory and many ideas introduced here directly apply to the following chapters. The rest of the chapter is specialized to a deterministic problem: scattering from sinusoidal gratings, since the sinusoidal scattering problem has theoretical importance and provides insight into rough surface scattering theory. Formulations of each model mentioned above are presented for the sinusoidal grating

problem, and a final section compares these models for several surfaces in order to illustrate the limitations of each model.

2.2 SPM Formulation for Dirichlet Problem

Consider a deterministic periodic surface $z = f(x)$ with period P as shown in Figure 2.1. Also assume that the upper region ($z > f(x)$) is free space, while the lower region ($z < f(x)$) is a perfectly conducting medium. Defining the Fourier operator as $\mathcal{F}()_n$, the Fourier series expansion of the surface is given as follows:

$$\begin{aligned} f(x) &= \sum_{n=-\infty}^{+\infty} h_n e^{j\left(\frac{2\pi n}{P}\right)x} \\ h_n &= \mathcal{F}(f(x))_n = \frac{1}{P}\int_0^P dx e^{-j\left(\frac{2\pi n}{P}\right)x} f(x) \end{aligned} \tag{2.1}$$

Assume the following plane wave impinges on the surface:

$$\vec{E}_i = -\hat{y}e^{j\vec{k}_i.\vec{r}}, \qquad \vec{H}_i = \frac{1}{\eta_o}\left(\hat{k}_i \times (-\hat{y})\right) e^{j\vec{k}_i.\vec{r}} \tag{2.2}$$

where $\vec{k}_i = k_{xi}\hat{x} - k_{zi}\hat{z}$ and $k_{xi} = k_o \sin(\theta_i)$, $k_{zi} = k_o \cos(\theta_i)$. The free space wavenumber is defined as $k_o = \frac{2\pi}{\lambda}$. The incidence angle θ_i is defined as the angle between the vector $-\vec{k}_i$ and $\hat{z}$.

Under the Rayleigh hypothesis, the scattered wave can be expressed as a sum over up-going plane waves (Floquet modes), as:

$$\vec{E}_s = -\hat{y}\sum_{n=-\infty}^{+\infty} \alpha_n e^{j\vec{k}_s^n.\vec{r}}, \qquad \vec{H}_s = \frac{1}{\eta_o}\sum_{n=-\infty}^{+\infty}\left(\hat{k}_s^n \times (-\hat{y})\right)\alpha_n e^{j\vec{k}_s^n.\vec{r}} \tag{2.3}$$

Here, α_n are the unknown amplitudes of the scattered Floquet modes. By the Floquet theorem, the scattered wave propagation vectors are defined as $\vec{k}_s^n = k_{xn}\hat{x} + k_{zn}\hat{z}$, with components: $k_{xn} = k_{xi} + \frac{2\pi n}{P}$ and $k_{zn} = \sqrt{k_o^2 - k_{xn}^2}$.

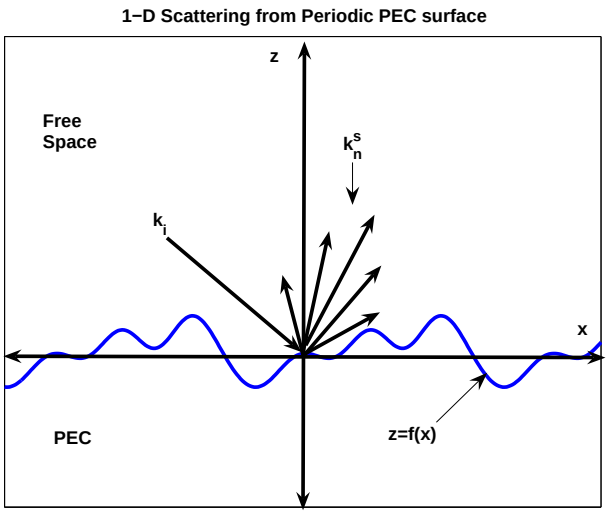

Figure 2.1: 1-D Dirichlet Problem Geometry

The Dirichlet boundary condition enforces that the tangential component of the electric field vanishes on the PEC boundary, and can simply be stated as:

$$\left[\hat{z} - \hat{x}\frac{\partial f}{\partial x}\right] \times \left[\vec{E}_i + \vec{E}_s\right]\Big|_{z=f(x)} = 0 \tag{2.4}$$

Evaluating this boundary condition on the surface, only for the $\hat{x}$ component, results in the following expression:

$$\sum_{n=-\infty}^{+\infty} e^{j\left(\frac{2\pi n}{P}\right)x} \alpha_n e^{jk_{zn}z^*} = -e^{-jk_{zi}z^*}, \tag{2.5}$$

where $z^* = f(x)$. Certainly, if $z^* = f(x)$ is a simple function, eg. a sinusoid, then by applying the operator $\mathcal{F}$ on both sides, this equation can be put in a matrix form. Truncating the number of unknowns to some reasonable number, one can obtain the exact solution by means of a standard matrix inversion procedure. But for arbitrary surfaces, (or when we consider random processes) this approach will not

be convenient. Instead, a perturbation theory can be utilized in which the following series expansions are applied:

$$\begin{aligned} \alpha_n &= \sum_{m=0}^{+\infty} \alpha_n^{(m)} \\ e^{jkz} &= \sum_{q=0}^{+\infty} \frac{(jkz)^q}{q!} \end{aligned} \tag{2.6}$$

The first equation represents the perturbation series expansion of the unknown, and the second equation is simply the Taylor expansion for the exponential term. Using these series expansions in equation 2.5, and considering only the terms of order M, one obtains:

$$\sum_{n=-\infty}^{+\infty} e^{j\left(\frac{2\pi n}{P}\right)x} \left(\sum_{m=0}^{M} \alpha_n^{(m)} \frac{(jk_{zn}z^*)^{(M-m)}}{(M-m)!} \right) = -\frac{(-jk_{zi}z^*)^{(M)}}{(M)!} \tag{2.7}$$

Keeping only the M^{th} order term of the unknown on the left, we obtain:

$$\begin{aligned} \sum_{n=-\infty}^{+\infty} e^{j\left(\frac{2\pi n}{P}\right)x} \alpha_n^{(M)} &= -\frac{(-jk_{zi}z^*)^{(M)}}{(M)!} - \sum_{n=-\infty}^{+\infty} e^{j\left(\frac{2\pi n}{P}\right)x} \left(\sum_{m=0}^{M-1} \alpha_n^{(m)} \frac{(jk_{zn}z^*)^{(M-m)}}{(M-m)!} \right) \\ &= S(x) \end{aligned} \tag{2.8}$$

The right side of the equation is named $S(x)$, the forcing function of the boundary. Applying the Fourier operator on both sides, the M^{th} order solution of the scattered wave amplitude can be expressed as:

$$\alpha_{n'}^{(M)} = \mathcal{F}(S(x))_{n'} \tag{2.9}$$

It can be shown that zeroth order solution will be in the following form:

$$\alpha_{n'}^{(0)} = -\delta(n'), \tag{2.10}$$

which corresponds to flat surface reflection. The first order solution can be given as:

$$\alpha_{n'}^{(1)} = h_{n'}(2jk_{zi}), \tag{2.11}$$

and the second order solution is:

$$\alpha_{n'}^{(2)} = \sum_{n_1} h_{n_1} h_{n'-n_1} (2k_{zi} k_{zn_1}). \tag{2.12}$$

In general, the M^{th} order correction has the form:

$$\alpha_{n'}^{(M)} = \sum_{n_1} ..... \sum_{n_{M-1}} h_{n_1} ... h_{n_{M-1}} h_{n'-\sum_{k=1}^{M-1} n_k} g_\alpha^M(n', n_1, ..., n_{M-1}) \tag{2.13}$$

Here, functions $g_\alpha^M()$ (also called SPM kernels) are defined for convenience, and decouple the surface properties(Fourier coefficients) from the scattering process. In the random scattering point of view, such an expression of the scattered fields is very convenient, since any statistical operator applied on the scattered fields will operate only on the surface Fourier coefficients.

2.2.1 Arbitrary order solution procedure

The presentation of the SPM up-to this point is standard and well known. The following derivations will highlight a new procedure for obtaining the arbitrary order solutions(or $g_\alpha^M()$ functions) in terms of the lower order solutions in a recursive fashion. In order to do that, the forcing function($S(x)$) defined in equation 2.8 has to be studied more throughly. Define functions $S^r(x)$ as:

$$S^{\,r}(x) = \begin{cases} -\frac{(-jk_{zi}z^*)^M}{M!} - \sum_{n=-\infty}^{+\infty} e^{j\left(\frac{2\pi n}{P}\right)x} \alpha_n^{(0)} \frac{(jk_{zn}z^*)^M}{M!} & \text{if } r = 0 \\ -\sum_{n=-\infty}^{+\infty} e^{j\left(\frac{2\pi n}{P}\right)x} \alpha_n^{(M-r)} \frac{(jk_{zn}z^*)^r}{r!} & \text{otherwise} \end{cases} \tag{2.14}$$

so that, $S(x) = \sum_{r=0}^{M-1} S^r(x)$. The corresponding unknown components can be defined as $\alpha_{n'}^{(M,r)} = \mathcal{F}(S^r(x))_{n'}$ with $\alpha_{n'}^{(M)} = \sum_{r=0}^{M-1} \alpha_{n'}^{(M,r)}$. Each component of $\alpha_{n'}^{(M)}$ should be studied separately. First, consider $S^{\,0}(x)$, which involves the zeroth order solution. Plugging in $\alpha_{n'}^{(0)} = -\delta(n')$, one obtains:

$$S^{\,0}(x) = -\frac{(-jk_{zi}z^*)^M}{M!} + \frac{(jk_{zi}z^*)^M}{M!} \tag{2.15}$$

At this point, one can utilize the Fourier series representation formula for the p^{th} power of z^* given below:

$$\mathcal{F}((z^*)^p) = \sum_{n_1} ..... \sum_{n_{p-1}} h_{n_1} ... h_{n_{p-1}} h_{n' - \sum_{k=1}^{p-1} n_k} \tag{2.16}$$

so that $\alpha_{n'}^{(M,0)}$ can be expressed as:

$$\begin{aligned} \alpha_{n'}^{(M,0)} &= \left(\frac{(j)^M - (-j)^M}{M!} \right) k_{zi}^M \mathcal{F}((z^*)^M)_{n'} \\ &= \sum_{n_1} ..... \sum_{n_{M-1}} h_{n_1} ... h_{n_{M-1}} h_{n' - \sum_{k=1}^{M-1} n_k} \frac{(j)^M k_{zi}^M \epsilon}{M!} \end{aligned} \tag{2.17}$$

Here, ϵ equal to 2 if M is an odd integer and zero otherwise. Also, note that for $M = 1$, $S^0(x)$ is the only component that contributes to the solution. Simply by plugging in $M = 1$ to equation 2.17, one obtains:

$$\alpha_{n'}^{(1)} = h_{n'}(2jk_{zi}) \tag{2.18}$$

so that the corresponding first order kernel can be given as:

$$g_{\alpha}^{(1)}(n') = 2jk_{zi} \tag{2.19}$$

For a general $r = 1, 2, ..., M-1$ case, $\alpha_{n'}^{(M,r)}$ can be expressed in terms of $S^r(x)$ as follows:

$$\begin{aligned} \alpha_{n'}^{(M,r)} &= \mathcal{F}\left(- \sum_{n=-\infty}^{+\infty} e^{j\left(\frac{2\pi n}{P}\right)x} \alpha_n^{(M-r)} \frac{(jk_{zn}z^*)^r}{r!} \right)_{n'} \\ &= \frac{-j^r}{r!} \mathcal{F}\left((z^*)^r \sum_{n=-\infty}^{+\infty} e^{j\left(\frac{2\pi n}{P}\right)x} \alpha_n^{(M-r)} k_{zn}^r \right)_{n'} \end{aligned} \tag{2.20}$$

Utilizing the convolution theorem, one obtains:

$$\alpha_{n'}^{(M,r)} = \frac{-j^r}{r!} \sum_n \mathcal{F}((z^*)^r)_{(n'-n)} \alpha_n^{(M-r)} k_{zn}^r \tag{2.21}$$

Here, equations 2.13 and 2.16 can be utilized to express $\alpha_{n'}^{(M,r)}$ in the following form:

$$\begin{aligned}\alpha_{n'}^{(M,r)} &= \frac{-j^r}{r!}\sum_{n}\left(\sum_{n_1}\sum_{n_2}.....\sum_{n_{r-1}} h_{n_1}h_{n_2}....h_{n_{r-1}}h_{n'-n-\sum_{k=1}^{r-1}n_k}\right) \\ &\quad \left(\sum_{m_1}\sum_{m_2}.....\sum_{m_{M-r-1}} h_{m_1}h_{m_2}....h_{m_{M-r-1}}h_{n-\sum_{k=1}^{M-r-1}m_k}\right) \\ &\quad k_{zn}^r g_\alpha^{(M-r)}(n, m_1, m_2, ..., m_{M-r-1}) \end{aligned} \tag{2.22}$$

At this point, a new variable can be defined: $m_{M-r} = n - \sum_{k=1}^{M-r-1} m_k$, resulting in the following:

$$\begin{aligned}\alpha_{n'}^{(M,r)} &= \frac{-j^r}{r!}\sum_{m_{M-r}}\left(\sum_{n_1}\sum_{n_2}.....\sum_{n_{r-1}} h_{n_1}h_{n_2}....h_{n_{r-1}}h_{n'-\sum_{k=1}^{r-1}n_k-\sum_{k=1}^{M-r}m_k}\right) \\ &\quad \left(\sum_{m_1}\sum_{m_2}.....\sum_{m_{M-r-1}} h_{m_1}h_{m_2}....h_{m_{M-r}}\right) \\ &\quad k_{zn}^r g_\alpha^{(M-r)}(n, m_1, m_2, ..., m_{M-r-1}) \end{aligned} \tag{2.23}$$

Finally with some index modifications (i.e. $m_i = n_{r-1+i}, \quad (i = 1, 2, ..., M-r)$) we obtain the following:

$$\begin{aligned}\alpha_{n'}^{(M,r)} &= \frac{-j^r}{r!}\sum_{n_1}\sum_{n_2}.....\sum_{n_{M-1}} h_{n_1}h_{n_2}....h_{n_{M-1}}h_{n'-\sum_{k=1}^{M-1}n_k} \\ &\quad k_{zn^*}^r g_\alpha^{(M-r)}(n^*, n_r, n_{r+1}, ..., n_{M-2}) \end{aligned} \tag{2.24}$$

The variable n^* is defined as:

$$n^* = n^*(r, M) = \sum_{k=r}^{M-1} n_k \tag{2.25}$$

Combining equations 2.17 and 2.24, the M^{th} order SPM kernel can be expressed as:

$$\begin{aligned} g_\alpha^M(n', n_1, ..., n_{M-1}) &= \frac{(j)^M k_{zi}^M \epsilon}{M!} - \sum_{r=1}^{M-1}\frac{(j)^r}{r!}k_{z(n^*)}^r g_\alpha^{(M-r)}(n^*, n_r, n_{r+1}, ...n_{M-2}) \\ &= g_\alpha^{(M,0)} + \sum_{r=1}^{M-1} v_r(n^*) g_\alpha^{(M-r)}(n^*, n_r, n_{r+1}, ...n_{M-2}) \end{aligned} \tag{2.26}$$

Equation 2.26 completes the arbitrary order recursive solution of the 1-D scattering from a PEC surface problem. The procedure described here will be applied to other boundary conditions in Chapters 3 and 4.

In order to highlight the advantages of a solution in the form of 2.26, first consider the $M = 2$ case. Zeroth order contribution drops since $\epsilon = 0$ for even orders. The summation also drops, only $r = 1$ contribution matters, so that we obtain the following:

$$g_\alpha^{(2)}(n', n_1) = -jk_{z(n^*)} g_\alpha^{(1)}(n^*) \tag{2.27}$$

Since, we already know the $g_\alpha^{(1)}$ by equation 2.19 and $n^*(1,2) = n_1$, we obtain:

$$g_\alpha^{(2)}(n', n_1) = 2k_{zi}k_{zn_1} \tag{2.28}$$

Now consider the $M = 3$ case. For this case, equation 2.26 becomes:

$$g_\alpha^{(3)}(n', n_1, n_2) = \frac{-(j)2k_{zi}^3}{3!} - \sum_{r=1}^{2} \frac{(j)^r}{r!} k_{z(n^*)}^r g_\alpha^{(3-r)}(n^*, n_r, n_{r+1}, ...n_1) \tag{2.29}$$

Utilizing equations 2.19 and 2.28, and also noting that $n^*(1,3) = n_1 + n_2$ and $n^*(2,3) = n_2$, equation 2.29 becomes:

$$\begin{aligned} g_\alpha^{(3)}(n', n_1, n_2) &= \frac{-(j)2k_{zi}^3}{3!} - \left[jk_{z(n_1+n_2)} g_\alpha^{(2)}(n_1 + n_2, n_1) - \frac{1}{2!} k_{zn_2}^2 g_\alpha^{(1)}(n_2) \right] \\ &= (-2jk_{zi}) \left[\frac{k_{zi}^2}{3!} + k_{z(n_1+n_2)} k_{z(n_1)} - \frac{k_{z(n_2)}^2}{2!} \right] \end{aligned} \tag{2.30}$$

The ability to express the M^{th} order SPM kernel in terms of lower order (orders of $r = 1, ..M-1$ and implicitly the zeroth order) SPM kernels allows the formulation to be computed to arbitrary order using a simple recursive algorithm.

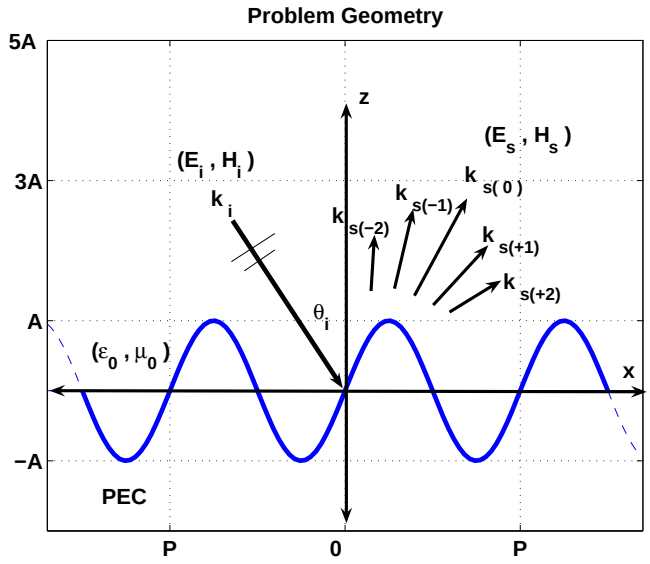

Figure 2.2: Sinusoidal Grating Problem

2.3 Scattering from a sinusoidal surface

In this section, the 1-D Dirichlet problem for a sinusoidal surface is considered. The problem geometry is sketched in Figure 2.2. Here, basic notational conventions are presented and they apply to the following subsections.

The surface being considered here is:

$$z = f(x) = A\sin(\frac{2\pi}{P}x), \tag{2.31}$$

which is periodic with period P. (i.e. $f(x) = f(x+P)$) Defining the Fourier operator as $\mathcal{F}()_n$, the Fourier series expansion of the surface is given as follows:

$$h_n = \frac{A}{2j}\left(\delta(n-1) - \delta(n+1)\right) \tag{2.32}$$

Due to periodicity of the surface, the scattered field above the maximum of the surface can be expressed as sum over Floquet modes as:

$$\vec{E}^s(\vec{r}) = \hat{y} \sum_{n=-\infty}^{+\infty} R(n) e^{i\vec{k}_s^n . \vec{r}} \tag{2.33}$$

The $R(n)$ is in general a complex coefficient, determining the amplitude and phase of the scattered field in each direction. In the following subsections, these coefficients are derived with SPM, EBC, PO, SSA2, and MNLSSA models, based on the underlying approximation, each method suggests a different $R(n)$.

2.3.1 SPM solution

As a reminder, for an arbitrary periodic surface, the following equations were obtained. The scattered field was given by:

$$\vec{E_s} = \hat{y} \sum_{n=-\infty}^{+\infty} \alpha_n e^{j\vec{k}_s^n . \vec{r}} \tag{2.34}$$

The α_n was expanded into a perturbation series of type:

$$\alpha_n = \sum_{m=0}^{+\infty} \alpha_n^{(m)} \tag{2.35}$$

Then the M^{th} order term was expressed in terms of lower order contributions as:

$$\alpha_{n'}^{(M)} = \sum_{r=0}^{M-1} \alpha_{n'}^{(M,r)} \tag{2.36}$$

with

$$\begin{aligned} \alpha_{n'}^{(M,0)} &= \left(\frac{(j)^M - (-j)^M}{M!} \right) k_{zi}^M \mathcal{F}\big((z^*)^M\big)_{n'} \\ \alpha_{n'}^{(M,r)} &= \frac{-j^r}{r!} \sum_n \mathcal{F}\big((z^*)^r\big)_{(n'-n)} \alpha_n^{(M-r)} k_{zn}^r \end{aligned} \tag{2.37}$$

Also, the Fourier operator applied to the p^{th} power of z^* was given by:

$$\mathcal{F}\big((z^*)^p\big)_{n'} = \sum_{n_1} ..... \sum_{n_{p-1}} h_{n_1} ... h_{n_{p-1}} h_{n' - \sum_{k=1}^{p-1} n_k} \tag{2.38}$$

For $z^* = A\sin(\frac{2\pi}{P}x)$ we have:

$$h_n = \frac{A}{2j}\left(\delta(n-1) - \delta(n+1)\right) \tag{2.39}$$

Utilizing these Fourier coefficients, the formula 2.38 becomes:

$$\mathcal{F}((A\sin(\frac{2\pi}{P}x))^p)_{n'} = \sum_{k=0}^{p} \delta(n' - (p-2k)) \left(\frac{A}{2j}\right)^p \begin{pmatrix} p \\ k \end{pmatrix} (-1)^k \tag{2.40}$$

Thus, for $\alpha_{n'}^{(M,0)}$, we obtain:

$$\begin{aligned} \alpha_{n'}^{(M,0)} &= \frac{\epsilon j^M k_{zi}^M}{M!}\left(\frac{A}{2j}\right)^M \sum_{k=0}^{M} \delta(n' - (M-2k)) \begin{pmatrix} M \\ k \end{pmatrix} (-1)^k \\ &= \epsilon\left(\frac{Ak_{zi}}{2}\right)^M \sum_{k=0}^{M} \delta(n' - (M-2k)) \frac{(-1)^k}{(M-k)!k!} \end{aligned} \tag{2.41}$$

where ϵ equal to 2 if M is an odd integer and zero otherwise. For $\alpha_{n'}^{(M,r)}$, we obtain:

$$\begin{aligned} \alpha_{n'}^{(M,r)} &= \frac{-j^r}{r!} \sum_n \left(\sum_{l=0}^{r} \delta(n' - n - (r-2l)) \left(\frac{A}{2j}\right)^r \begin{pmatrix} r \\ l \end{pmatrix} (-1)^l \right) \alpha_n^{(M-r)} k_{zn}^r \\ &= -\sum_n \sum_{l=0}^{r} \delta(n' - n - (r-2l)) \frac{(-1)^l}{(r-l)!l!} \left(\frac{Ak_{zn}}{2}\right)^r \alpha_n^{(M-r)} \\ &= -\sum_{l=0}^{r} \frac{(-1)^l}{(r-l)!l!} \left(\frac{Ak_{z(n'-(r-2l))}}{2}\right)^r \alpha_{(n'-(r-2l))}^{(M-r)} \end{aligned} \tag{2.42}$$

Combining these terms, we obtain the following iterative relation for α_n^M:

$$\begin{aligned} \alpha_{n'}^{(M)} &= \epsilon\left(\frac{Ak_{zi}}{2}\right)^M \sum_{k=0}^{M} \delta(n' - (M-2k)) \frac{(-1)^k}{(M-k)!k!} \\ &\quad - \sum_{r=1}^{M-1} \sum_{l=0}^{r} \frac{(-1)^l}{(r-l)!l!} \left(\frac{Ak_{z(n'-(r-2l))}}{2}\right)^r \alpha_{(n'-(r-2l))}^{(M-r)} \end{aligned} \tag{2.43}$$

Moreover, if we define a new representation for α_n^M as:

$$\tilde{\alpha}_{(k)}^{(M)} = \alpha_{(M-2k)}^{(M)}, \qquad k = 0, 1, .., M \tag{2.44}$$

then equation 2.43 can be transformed into the following form:

$$\sum_{r=0}^{M} \sum_{l=0}^{r} \frac{(-1)^l}{(r-l)!l!} \left(\frac{Ak_{z(M-r-2(k-l))}}{2}\right)^r \tilde{\alpha}_{(k-l)}^{(M-r)} = -\left(\frac{-Ak_{zi}}{2}\right)^M \frac{(-1)^k}{(M-k)!k!} \tag{2.45}$$

By it's iterative nature, equation 2.45 is useful for generating the arbitrary order solutions. Using symbolic math packages like Maple or Matlab, one can even get their functional forms at any order. For the sake of simplicity, only solutions up to 4^{th} order are presented here.

The zeroth order solution for α is independent of the surface and given by:

$$\alpha_{n'}^{(0)} = -\delta(n'), \tag{2.46}$$

The first order solution is given by:

$$\begin{aligned} \alpha_{-1}^{(1)} &= -Ak_{zi} \\ \alpha_{+1}^{(1)} &= Ak_{zi} \end{aligned} \tag{2.47}$$

The second order solution is given by:

$$\begin{aligned} \alpha_{-2}^{(2)} &= \frac{-1}{2}A^2 k_{zi}k_{z(-1)} \\ \alpha_{0}^{(2)} &= \frac{+1}{2}A^2 k_{zi}(k_{z(-1)} + k_{z(-1)}) \\ \alpha_{+2}^{(2)} &= \frac{-1}{2}A^2 k_{zi}k_{z(+1)} \end{aligned} \tag{2.48}$$

The third order solution is given by:

$$\begin{aligned} \alpha_{-3}^{(3)} &= \frac{-1}{24}A^3 k_{zi}^3 - \frac{1}{4}A^3 k_{zi}k_{z(-1)}k_{z(-2)} + \frac{1}{8}A^3 k_{zi}k_{z(-1)}^2 \\ \alpha_{-1}^{(3)} &= \frac{1}{8}A^3 k_{zi}^3 + \frac{1}{4}A^3 k_{zi}k_{z(-1)}k_{z(-2)} + \frac{1}{4}A^3 k_{zi}^2 k_{z(-1)} \\ &\quad + \frac{1}{4}A^3 k_{zi}^2 k_{z(+1)} - \frac{1}{4}A^3 k_{zi}k_{z(-1)}^2 - \frac{1}{8}A^3 k_{zi}k_{z(+1)}^2 \\ \alpha_{+1}^{(3)} &= \frac{-1}{8}A^3 k_{zi}^3 - \frac{1}{4}A^3 k_{zi}^2 k_{z(-1)} - \frac{1}{4}A^3 k_{zi}^2 k_{z(+1)} \\ &\quad - \frac{1}{4}A^3 k_{zi}k_{z(+1)}k_{z(+2)} + \frac{1}{8}A^3 k_{zi}k_{z(-1)}^2 + \frac{1}{4}A^3 k_{zi}k_{z(+1)}^2 \\ \alpha_{+3}^{(3)} &= \frac{1}{24}A^3 k_{zi}^3 + \frac{1}{4}A^3 k_{zi}k_{z(+1)}k_{z(+2)} - \frac{1}{8}A^3 k_{zi}k_{z(+1)}^2 \end{aligned} \tag{2.49}$$

And finally the fourth order solution is given by:

$$\begin{aligned}\alpha_{-4}^{(4)} &= -\frac{1}{8}A^4 k_{zi}k_{z(-1)}k_{z(-2)}k_{z(-3)} + \frac{1}{16}A^4 k_{zi}k_{z(-1)}\left(k_{z(-1)}k_{z(-3)} + k_{z(-2)}^2\right) \\ &\quad -\frac{1}{48}A^4 k_{zi}\left(k_{z(-1)}^3 + k_{zi}^2 k_{z(-3)}\right) \end{aligned} \tag{2.50}$$

$$\begin{aligned}\alpha_{-2}^{(4)} &= +\frac{1}{48}A^4 k_{zi}\left(k_{zi}^2 k_{z(-3)} + k_{z(+1)}^3\right) \\ &\quad +\frac{1}{8}A^4 k_{zi}k_{z(-1)}\left(k_{z(-2)}k_{z(-3)} + k_{zi}(k_{z(+1)} + k_{z(-1)}) + k_{z(-1)}k_{z(-2)} - k_{z(-2)}^2\right) \\ &\quad -\frac{1}{16}A^4 k_{zi}\left(k_{z(-1)}^2(k_{z(-1)} + k_{z(-3)}) + k_{z(+1)}(k_{zi}^2 + k_{z(+1)}k_{z(-1)})\right) \end{aligned} \tag{2.51}$$

$$\begin{aligned}\alpha_{0}^{(4)} &= -\frac{1}{8}A^4 k_{zi}^2(k_{z(-1)} + k_{z(+1)})^2 + \frac{1}{16}A^4 k_{zi}^3(k_{z(-1)} + k_{z(+1)}) \\ &\quad +\frac{1}{16}A^4 k_{zi}(k_{z(-1)}^3 + k_{z(+1)}^3) \\ &\quad +\frac{1}{16}A^4 k_{zi}k_{z(+1)}k_{z(-1)}(k_{z(-1)} + k_{z(+1)}) \\ &\quad +\frac{1}{16}A^4 k_{zi}k_{z(-1)}k_{z(-2)}(k_{z(-2)} - 2k_{z(-1)}) \\ &\quad +\frac{1}{16}A^4 k_{zi}k_{z(+1)}k_{z(+2)}(k_{z(+2)} - 2k_{z(+1)}) \end{aligned} \tag{2.52}$$

$$\begin{aligned}\alpha_{2}^{(4)} &= +\frac{1}{48}A^4 k_{zi}\left(k_{z(-1)}^3 + k_{zi}^2 k_{z(+3)}\right) \\ &\quad +\frac{1}{8}A^4 k_{zi}k_{z(+1)}\left(k_{z(+3)}k_{z(+2)} + k_{zi}(k_{z(+1)} + k_{z(-1)}) + k_{z(+1)}k_{z(+2)} - k_{z(+2)}^2\right) \\ &\quad -\frac{1}{16}A^4 k_{zi}\left(k_{z(+1)}^2(k_{z(+1)} + k_{z(+3)}) + k_{z(-1)}(k_{zi}^2 + k_{z(+1)}k_{z(-1)})\right) \end{aligned} \tag{2.53}$$

$$\begin{aligned}\alpha_{4}^{(4)} &= -\frac{1}{8}A^4 k_{zi}k_{z(+3)}k_{z(+1)}k_{z(+2)} + \frac{1}{16}A^4 k_{zi}k_{z(+1)}\left(k_{z(+3)}k_{z(+1)} + k_{z(+2)}^2\right) \\ &\quad -\frac{1}{48}A^4 k_{zi}\left(k_{z(+1)}^3 + h^4 k_{zi}^2 k_{z(+3)}\right) \end{aligned} \tag{2.54}$$

In fact, there is another approach for calculating α_n, without expanding it into perturbation series. This method is being used in the literature and called "Fourier-Rayleigh" approach.

$$\sum_{n=-\infty}^{+\infty} e^{j\left(\frac{2\pi n}{P}\right)x}\alpha_n e^{jk_{zn}z^*} = -e^{-jk_{zi}z^*}, \tag{2.55}$$

obtained just after applying the boundary condition, can be utilized to calculate α_n, by applying the Fourier operator on both sides.

For $z^* = f(x) = A\sin(\frac{2\pi x}{P})$, the calculations follow as:

$$\begin{aligned}
\frac{1}{P}\int_0^P dx e^{-j\left(\frac{2\pi n'}{P}\right)x}\left(\sum_{n=-\infty}^{+\infty} e^{j\left(\frac{2\pi n}{P}\right)x}\alpha_n e^{jk_{zn}z^*}\right) &= -\frac{1}{P}\int_0^P dx e^{-j\left(\frac{2\pi n'}{P}\right)x}\left(e^{-jk_{zi}z^*}\right) \\
\sum_{n=-\infty}^{+\infty}\alpha_n\frac{1}{P}\int_0^P dx e^{-j\left(\frac{2\pi(n'-n)}{P}\right)x}e^{jAk_{zn}\sin(\frac{2\pi x}{P})} &= -\frac{1}{P}\int_0^P dx e^{-j\left(\frac{2\pi n'}{P}\right)x}e^{-jAk_{zi}\sin(\frac{2\pi x}{P})} \\
\sum_{n=-\infty}^{+\infty}\alpha_n\frac{1}{2\pi}\int_0^{2\pi} dx e^{-j(n'-n)\theta}e^{jAk_{zn}\sin(\theta)} &= -\frac{1}{2\pi}\int_0^{2\pi} dx e^{-jn'\theta}e^{-jAk_{zi}\sin(\theta)} \quad (2.56)
\end{aligned}$$

Finally, by utilizing Lommel's formula 2.67, we obtain:

$$\sum_{n=-\infty}^{+\infty}\alpha_n J_{n'-n}(Ak_{zn}) = -J_{n'}(-Ak_{zi}) \quad (2.57)$$

Certainly, this equation can be truncated with a reasonable number of unknowns, and then can be put in a matrix equation form. An analytical solution to this infinite system of equations is unknown.

2.3.2 EBC Formulation

In this section, the Extended Boundary Condition method will be utilized for the same problem. The EBC method or (T-Matrix method) is based on the extinction theorem or the null field theorem. This theorem can be used as a boundary condition to obtain an extended integral equation. Formulation of [9] will be followed in this section.

For a periodic, one dimensional PEC surface, the EBC formulation reduces to:

$$E_y^i(\vec{r}) - \int_0^P dS' g_p(\vec{r},\vec{r}\,')\,(\vec{n}'.\nabla_{S'}E_y(\vec{r}\,')) = \begin{cases} E_y(\vec{r}) & z > f(x) \\ 0 & z < f(x) \end{cases} \quad (2.58)$$

Here, the periodic 2-D Green's function is given as:

$$g_p(\vec{r},\vec{r}\,') = \frac{i}{2P}\sum_{n=-\infty}^{+\infty}\frac{1}{k_{zn}}e^{ik_{xn}(x-x')+ik_{zn}|z-z'|}, \quad (2.59)$$

with:

$$k_{xn} = k_{xi} + \frac{2\pi n}{P}, \qquad k_{zn} = \begin{cases} \sqrt{k_0^2 - k_{xn}^2} & k_0 > k_{xn} \\ i\sqrt{k_{xn}^2 - k_0^2} & k_0 < k_{xn} \end{cases} \tag{2.60}$$

Hence, for $z > A$ we have:

$$E_y(\vec{r}) = E_y^i(\vec{r}) - \frac{i}{2P} \sum_{n=-\infty}^{+\infty} \frac{1}{k_{zn}} e^{ik_{xn}x + ik_{zn}z} \left[\int_0^P dS' e^{-ik_{xn}x' - ik_{zn}z'} \vec{n}'.\nabla_{S'} E_y(\vec{r}\,') \right] \tag{2.61}$$

and for $z < A$:

$$0 = E_y^i(\vec{r}) - \frac{i}{2P} \sum_{n=-\infty}^{+\infty} \frac{1}{k_{zn}} e^{ik_{xn}x - ik_{zn}z} \left[\int_0^P dS' e^{-ik_{xn}x' + ik_{zn}z'} \vec{n}'.\nabla_{S'} E_y(\vec{r}\,') \right] \tag{2.62}$$

Now, we need to define coefficients β_m such that:

$$dS'\vec{n}'.\nabla_{S'} E_y(\vec{r}\,') = (-2i)dx' \sum_{m=-\infty}^{+\infty} \beta_m e^{ik_{xm}x'} \tag{2.63}$$

Then we have:

$$-\frac{i}{2P} \int_0^P dS' e^{-ik_{xn}x' \mp ik_{zn}z'} \vec{n}'.\nabla_{S'} E_y(\vec{r}\,') = -\sum_{m=-\infty}^{+\infty} \beta_m I^{\mp}(n,m), \tag{2.64}$$

where

$$I^{\mp}(n,m) = \frac{1}{P} \int_0^P dx' e^{i(k_{xm} - k_{xn})x' \mp ik_{zn} A \sin(\frac{2\pi x'}{P})} \tag{2.65}$$

Noting that $(k_{xm} - k_{xn}) = \frac{2\pi}{P}(m-n)$, and utilizing the variable transformation $\theta = \frac{2\pi x'}{P}$ we obtain:

$$I^{\mp}(n,m) = \frac{1}{2\pi} \int_0^{2\pi} d\theta e^{i(m-n)\theta \mp ik_{zn} A \sin(\theta)} \tag{2.66}$$

Utilizing the following identity (also known as Lommel's formula, see Appendix D for a proof) of Bessel function :

$$J_n(z) = \frac{1}{2\pi} \int_0^{2\pi} e^{-in\theta} e^{iz\sin(\theta)} d\theta, \tag{2.67}$$

we obtain:

$$\begin{aligned} I^{-}(n,m) &= J_{(m-n)}(Ak_{zn}) \\ I^{+}(n,m) &= J_{(n-m)}(Ak_{zn}) \end{aligned} \tag{2.68}$$

With these results equations 2.61 and 2.62 reduces to: for $z > A$:

$$E_y(\vec{r}) = E_y^i(\vec{r}) - \sum_{n=-\infty}^{+\infty} \frac{1}{k_{zn}} e^{ik_{xn}x + ik_{zn}z} \sum_{m=-\infty}^{+\infty} \beta_m J_{(m-n)}(Ak_{zn}) \tag{2.69}$$

and for $z < A$:

$$0 = E_y^i(\vec{r}) - \sum_{n=-\infty}^{+\infty} \frac{1}{k_{zn}} e^{ik_{xn}x - ik_{zn}z} \sum_{m=-\infty}^{+\infty} \beta_m J_{(n-m)}(Ak_{zn}) \tag{2.70}$$

To be consistent with reference [9], we can define coefficients b_n and a_n as:

$$\begin{aligned} E_y(\vec{r}) &= E_y^i(\vec{r}) + \sum_{n=-\infty}^{+\infty} e^{ik_{xn}x + ik_{zn}z} b_n \qquad z > A \\ 0 &= E_y^i(\vec{r}) + \sum_{n=-\infty}^{+\infty} e^{ik_{xn}x - ik_{zn}z} a_n \qquad z < A \end{aligned} \tag{2.71}$$

where:

$$\begin{aligned} b_n &= \frac{-1}{k_{zn}} \sum_{m=-\infty}^{+\infty} \beta_m J_{(m-n)}(Ak_{zn}) \\ a_n &= \frac{-1}{k_{zn}} \sum_{m=-\infty}^{+\infty} \beta_m J_{(n-m)}(Ak_{zn}) \end{aligned} \tag{2.72}$$

Here, it is important to note that by the null field theorem we know that $a_n = -\delta(n)$.

The EBC solution of the problem reduces to two infinite matrix equations. Truncating the number of unknowns by a reasonable number, one can obtain the β_m's by inverting a matrix of the second expression, and then b_n can be obtained from the first expressions. It is also true that the EBC method should give the exact solution of the problem since no approximation is involved. But it is also a known fact that the matrices involved in this theory becomes ill conditioned as the height to length ratio of the surface increases .

2.3.3 PO Formulation

In this section the Physical Optics(PO) solution is presented for the 1-D sinusoidal surface. The PO method utilizes the Kirchhoff Approximation(KA), which approximates the surface fields using the tangent plane approximation. For this approximation to be valid, the surface should have large radius of curvature. In general, by Huygens principle, the scattered field in the upper region can be expressed as:

$$E_y^s(\vec{r}) = E_y(\vec{r}) - E_y^i(\vec{r}) = -\int_{S'} dS' g(\vec{r},\vec{r}\,')\,(\hat{n}'\cdot\nabla_{S'}E_y(\vec{r}\,')) \tag{2.73}$$

where the Green's function and the surface normal defined as:

$$g(\vec{r},\vec{r}\,') = \frac{i}{4}H_0^{(1)}(k|\vec{r}-\vec{r}\,'|), \qquad \hat{n}' = \frac{\vec{n}}{L} = \frac{\hat{z}-\frac{df}{dx}\hat{x}}{\sqrt{1+\left(\frac{df}{dx}\right)^2}} \tag{2.74}$$

For a periodic surface, the scattered field should also be periodic. At this point, we can take advantage of the periodic Green's function [9]:

$$g_p(\vec{r},\vec{r}\,') = \frac{i}{2P}\sum_{n=-\infty}^{+\infty}\frac{1}{k_{zn}}e^{ik_{xn}(x-x')+ik_{zn}|z-z'|}, \tag{2.75}$$

with $k_{xn} = k_{xi} + \frac{2\pi n}{P}$ and $k_{zn} = \sqrt{k_0^2 - k_{xn}^2}$, in order to express the infinite integral involved in equation 2.73 as an infinite sum of finite integrals. With this modification and using the fact that $dS' = Ldx'$, equation 2.73 becomes:

$$E_y^s(\vec{r}) = -\int_0^P dx' g_p(\vec{r},\vec{r}\,')\,(\vec{n}.\nabla_{S'}E_y(\vec{r}\,')) \tag{2.76}$$

Here we apply the tangent plane approximation: on the hypothetical tangential plane, we have $\hat{n}\times H = 2\hat{n}\times H^i$. For a 1-D surface, the tangential component of the magnetic field ($\hat{n}\times H$) is proportional to $\vec{n}\times\nabla\times E = \vec{n}\times\nabla E\times\hat{y}$. Using BAC-CAB rule and $\vec{n}.\hat{y} = 0$, we observe that:

$$\hat{n}\times H \sim -\hat{y}(\vec{n}.\nabla E) \tag{2.77}$$

and hence

$$\vec{n}.\nabla E(\vec{r}\,') \simeq 2\vec{n}.\nabla E^i(\vec{r}\,') \tag{2.78}$$

Plugging this approximation into equation 2.76, we obtain:

$$\begin{aligned} E_y^s(\vec{r}) &= -\int_0^P dx' \left(\frac{i}{2P}\sum_{n=-\infty}^{+\infty}\frac{1}{k_{zn}}e^{ik_{xn}(x-x')+ik_{zn}|z-z'|}\right) 2\vec{n}.\nabla E^i(\vec{r}\,') \\ &= -\frac{1}{P}\sum_{n=-\infty}^{+\infty}\frac{1}{k_{zn}}e^{ik_{xn}x+ik_{zn}z}\int_0^P dx' e^{-ik_{xn}x'-ik_{zn}z'}(\frac{df}{dx}k_{xi}+k_{zi})e^{ik_{xi}x'-ik_{zi}z'} \\ &= -\frac{1}{P}\sum_{n=-\infty}^{+\infty}\frac{1}{k_{zn}}e^{ik_{xn}x+ik_{zn}z}I(n) \end{aligned} \tag{2.79}$$

The inner integral can be rewritten with the exact surface expression as:

$$I(n) = \int_0^P dx' e^{-i\frac{2\pi n}{P}x'}e^{-i(k_{zi}+k_{zn})A\sin(\frac{2\pi x'}{P})}\left[\frac{2\pi}{P}A\cos(\frac{2\pi x'}{P})k_{xi}+k_{zi}\right] \tag{2.80}$$

Lets divide $I(n)$ into two parts and study them separately:

$$\begin{aligned} I_1(n) &= \int_0^P dx' e^{-i\frac{2\pi n}{P}x'}e^{-i(k_{zi}+k_{zn})A\sin(\frac{2\pi x'}{P})}k_{zi} \\ I_2(n) &= \int_0^P dx' e^{-i\frac{2\pi n}{P}x'}e^{-i(k_{zi}+k_{zn})A\sin(\frac{2\pi x'}{P})}\left[\frac{2\pi}{P}A\cos(\frac{2\pi x'}{P})k_{xi}\right] \end{aligned} \tag{2.81}$$

Defining the change of variable rule; $\theta = \frac{2\pi}{P}x$, the first integral becomes:

$$I_1(n) = \frac{P}{2\pi}\int_0^{2\pi} d\theta e^{-in\theta}e^{-i(k_{zi}+k_{zn})A\sin(\theta)}k_{zi} \tag{2.82}$$

Utilizing the Bessel function identity given in 2.67, $I_1(n)$ can be evaluated as:

$$I_1(n) = (P)k_{zi}J_n(-A(k_{zi}+k_{zn})) \tag{2.83}$$

For the second integral, the identity given in equation 2.67 has to be manipulated as follows: Applying the change of variable rule defined above backwards, we obtain:

$$J_n(z) = \frac{1}{P}\int_0^P e^{-i\frac{2\pi n}{P}x}e^{iz\sin(\frac{2\pi x}{P})}dx, \tag{2.84}$$

which can be interpreted as the Fourier series representation of the function $h(x) = e^{iz\sin(\frac{2\pi x}{P})}$.

From Fourier theory, we know that for a periodic arbitrary function $h(x)$, we have the following Fourier series representation:

$$\begin{aligned} \alpha_n &= \frac{1}{P}\int_0^P e^{-i\frac{2\pi n}{P}x}h(x)dx \\ h(x) &= \sum_{n=-\infty}^{+\infty}\alpha_n e^{+i\frac{2\pi n}{P}x} \end{aligned} \tag{2.85}$$

If we differentiate $h(x)$, we obtain:

$$h'(x) = \sum_{n=-\infty}^{+\infty}\alpha_n\left(i\frac{2\pi n}{P}\right)e^{+i\frac{2\pi n}{P}x} \tag{2.86}$$

so that the Fourier series representation of $h'(x)$ will be:

$$\beta_n = \frac{1}{P}\int_0^P e^{-i\frac{2\pi n}{P}x}h'(x)dx = \frac{2\pi j}{P}n\alpha_n \tag{2.87}$$

Similarly, Fourier representation for the derivative of $h(x) = e^{iz\sin(\frac{2\pi x}{P})}$ will be in the following form:

$$\frac{1}{P}\int_0^P e^{-i\frac{2\pi n}{P}x}e^{iz\sin(\frac{2\pi x}{P})}\left(iz\frac{2\pi}{P}\cos(\frac{2\pi x}{P})\right)dx = \frac{2\pi i}{P}nJ_n(z) \tag{2.88}$$

The term $\frac{2\pi i}{P}$ cancels from both sides and we are left with:

$$\frac{1}{P}\int_0^P e^{-i\frac{2\pi n}{P}x}e^{iz\sin(\frac{2\pi x}{P})}\cos(\frac{2\pi x}{P})dx = n\frac{J_n(z)}{z} \tag{2.89}$$

Finally, to make it look nice, we can apply the same change of variable again: reaching the following new identity.

$$\frac{1}{2\pi}\int_0^{2\pi} e^{-in\theta}e^{iz\sin(\theta)}\cos(\theta)d\theta = \frac{nJ_n(z)}{z} \tag{2.90}$$

Utilizing this new identity, the second integral can be evaluated as:

$$\begin{aligned} I_2(n) &= Ak_{xi}\int_0^{2\pi} d\theta e^{-in\theta}e^{-i(k_{zi}+k_{zn})A\sin(\theta)}\cos(\theta) \\ &= -k_{xi}(2\pi n)\frac{J_n(-A(k_{zi}+k_{zn}))}{(k_{zi}+k_{zn})} \end{aligned} \tag{2.91}$$

Combining $I_1(n)$ and $I_2(n)$, and plugging in equation 2.79, we have:

$$\begin{aligned} E_y^s(\vec{r}) &= -\frac{1}{P}\sum_{n=-\infty}^{+\infty}\frac{1}{k_{zn}}e^{ik_{xn}x+ik_{zn}z}\left[Pk_{zi}-\frac{k_{xi}(2\pi n)}{(k_{zi}+k_{zn})}\right]J_n(-A(k_{zi}+k_{zn})) \\ &= \sum_{n=-\infty}^{+\infty}e^{ik_{xn}x+ik_{zn}z}\left[\frac{k_{xi}}{k_{zn}}\frac{(k_{xn}-k_{xi})}{(k_{zi}+k_{zn})}-\frac{k_{zi}}{k_{zn}}\right]J_n(-A(k_{zi}+k_{zn})) \end{aligned} \tag{2.92}$$

2.3.4 SSA2 Formulation

In Small Slope Approximation (SSA) method, the scattered field is expressed as:

$$\vec{E}^s(\vec{r},k_{xi}) = \int dk_x \frac{e^{ik_x x+ik_z z}}{\sqrt{k_z}}S(k_x,k_{xi}) \tag{2.93}$$

where k_x and k_{xi} are the $\hat{x}$ components of the scattered field wave number. The scattered field wave vector is defined as $\vec{k}_s = k_x\hat{x}+k_z\hat{z}$ with

$$k_z = \begin{cases} \sqrt{k_0^2-k_x^2} & k_0 > |k_x| \\ i\sqrt{k_x^2-k_0^2} & k_0 < |k_x| \end{cases} \tag{2.94}$$

Here $k_0 = \frac{2\pi}{\lambda}$, is electromagnetic wavenumber. The function (in general a matrix function) $S(k_x,k_{xi})$ is called the scattering amplitude, which is given as:

$$\begin{aligned} S(k_x,k_{xi}) &= \frac{\sqrt{k_z k_{zi}}}{(k_z+k_{zi})}\int\int\frac{dxd\xi}{2\pi}e^{-i(k_z+k_{zi})f(x)-i(k_x-k_{xi})}. \\ &\quad .\left[2B(k_x,k_{xi})\delta(\xi)+\frac{i}{2}\left[B_2(k_x,k_{xi};k_x-\xi)+B_2(k_x,k_{xi};k_{xi}+\xi)\right.\right. \\ &\quad \left.\left.+2(k_z+k_{zi})B(k_x,k_{xi})\right]F(\xi)\right] \end{aligned} \tag{2.95}$$

where

$$\begin{aligned} B(k_x, k_{xi}) &= -1 \\ B_2(k_x, k_{xi}; k'_x) &= 2k'_z \end{aligned} \tag{2.96}$$

In the case of a periodic surface $f(x) = f(x + P)$, expressing the infinite integral as an infinite sum of integrals on a single period, and utilizing the identity:

$$\frac{1}{2\pi} \sum_{n=-\infty}^{+\infty} e^{inx} = \sum_{n=-\infty}^{+\infty} \delta(x - 2\pi n) \tag{2.97}$$

we obtain the following periodic version of the scattering amplitude:

$$\begin{aligned} S(k_x, k_{xi}) &= \sum_{n=-\infty}^{+\infty} S_n \delta(k_x - k_{xi} - \frac{2\pi n}{P}) \\ S_n &= \frac{\sqrt{k_{zn} k_{zi}}}{(k_{zn} + k_{zi})} \sum_{m=-\infty}^{+\infty} Q_{n,m}. \\ &\quad . \left[2B(k_{xn}, k_{xi})\delta(m) + \frac{i}{2} \left[B_2(k_{xn}, k_{xi}; k_{x(n-m)}) + B_2(k_{xn}, k_{xi}; k_{xm}) \right.\right. \\ &\quad \left.\left. + 2(k_{zn} + k_{zi}) B(k_{xn}, k_{xi}) \right] h_m \right] \end{aligned} \tag{2.98}$$

where

$$Q_{n,m} = \frac{1}{P} \int_0^P dx e^{-i(n-m)\frac{2\pi}{P}x - i(k_{zn} + k_{zi})f(x)} \tag{2.99}$$

Plugging in functions B and B_2, S_n simplifies to:

$$S_n = \frac{\sqrt{k_{zn} k_{zi}}}{(k_{zn} + k_{zi})} \sum_{m=-\infty}^{+\infty} Q_{n,m} \left[-2\delta(m) + i \left[k_{z(n-m)} + k_{zm} - k_{zn} - k_{zi} \right] h_m \right] \tag{2.100}$$

Moreover, if we consider $f(x) = A \sin(\frac{2\pi}{P} x)$, then we have:

$$h_n = \frac{A}{2j} \left(\delta(n-1) - \delta(n+1) \right), \tag{2.101}$$

and

$$\begin{aligned} Q_{n,m} &= \frac{1}{P}\int_0^P dx e^{-i(n-m)\frac{2\pi}{P}x - i(k_{zn}+k_{zi})A\sin(\frac{2\pi}{P}x)} \\ &= \frac{1}{2\pi}\int_0^{2\pi} d\theta e^{-i(n-m)\theta - i(k_{zn}+k_{zi})A\sin(\theta)} \\ &= J_{n-m}(-A(k_{zn}+k_{zi})) \end{aligned} \tag{2.102}$$

These modifications simplify equation 2.100 to:

$$\begin{aligned} S_n &= \frac{\sqrt{k_{zn}k_{zi}}}{(k_{zn}+k_{zi})}\sum_{m=-\infty}^{+\infty} J_{n-m}(-A(k_{zn}+k_{zi}))\left[\delta(m-1)-\delta(m+1)\right] \\ &\quad \left[-2\delta(m)+\frac{A}{2}\left[k_{z(n-m)}+k_{zm}-k_{zn}-k_{zi}\right]h_m\right] \\ &= \frac{\sqrt{k_{zn}k_{zi}}}{(k_{zn}+k_{zi})}\left\{\frac{A}{2}\left[k_{z(n-1)}+k_{z(1)}-k_{zn}-k_{zi}\right]J_{n-1}(-A(k_{zn}+k_{zi}))\right. \\ &\qquad -2\ J_n(-A(k_{zn}+k_{zi})) \\ &\qquad \left.-\frac{A}{2}\left[k_{z(n+1)}+k_{z(-1)}-k_{zn}-k_{zi}\right]J_{n+1}(-A(k_{zn}+k_{zi}))\right\} \end{aligned} \tag{2.103}$$

2.3.5 One term MNLSSA Formulation

The Nonlocal Small Slope Approximation (NLSSA) method assumes the following form for the scattering amplitude:

$$S(k_x,k_{xi}) = \frac{1}{4\pi^2}\int \Phi(k_x,k_{xi};\xi)e^{-i(k_x-\xi)x_1 - ik_z f(x_1)}e^{i(k_{xi}-\xi)x_2 - ik_{zi}f(x_2)}dx_1dx_2d\xi \tag{2.104}$$

Originally proposed by Voronovich [15], this form of scattering amplitude has the capability to include multiple (two point) scattering effects. The functional Φ is expanded into a integral-power series and new coefficients are determined in comparison with SPM (SPM-1 and SPM-2)kernels.

Recently, Elfouhaily et. al. [13] suggested a modification to this theory, which they call modified NLSSA (MNLSSA), by enforcing extra conditions on NLSSA, and

they were able to match with Kirchoff Approximation (GO1) solution in the high frequency limit.

The MNLSSA kernel is given [13] by:

$$\begin{aligned}\Phi(k_x, k_{xi;\xi}) &= \frac{k_z + k_{zi}}{2k_z k_{zi}} \left[B_2(k_x, k_{xi}; \xi) + B_2(k_x, k_{xi}; k_x + k_{xi} - \xi) - B(k_x, k_{xi})\right] \\ &\quad + \frac{B(k_x, k_{xi})}{Q_z} \end{aligned} \tag{2.105}$$

Here, for Dirichlet problem, B, Q_z and B_2 are defined as:

$$\begin{aligned} B(k_x, k_{xi}) &= -2k_z k_{zi} \\ Q_z &= k_z + k_{zi} \\ B_2(k_x, k_{xi}; \xi) &= \frac{-2k_z k_{z(\xi)} k_{zi}}{k_z + k_{zi}} \end{aligned} \tag{2.106}$$

Plugging in these functions, the kernel becomes:

$$\Phi(k_x, k_{xi}; \xi) = -\frac{2k_z k_{zi}}{k_z + k_{zi}} - k_{z(\xi)} - k_{z(k_x + k_{xi} - \xi)} + k_z + k_{zi} \tag{2.107}$$

Moreover, for a periodic surface (i.e. $f(x) = f(x + P)$) we can do the following modifications: First, consider equation 2.104 in the following form:

$$\begin{aligned} S(k_x, k_{xi}) &= \int \Phi(k_x, k_{xi}; \xi) I_1(k_x, \xi) I_2(k_{xi}, \xi) d\xi \\ I_1(k_x, \xi) &= \frac{1}{2\pi} \int e^{-i(k_x - \xi)x_1} e^{-ik_z f(x_1)} dx_1 \\ I_2(k_{xi}, \xi) &= \frac{1}{2\pi} \int e^{i(k_{xi} - \xi)x_2} e^{-ik_{zi} f(x_2)} dx_2 \end{aligned} \tag{2.108}$$

Now, we can study I_1 and I_2 separately as:

$$\begin{aligned} I_1(k_x, \xi) &= \sum_n \delta(k_x - \xi - \frac{2\pi n}{P}) \frac{1}{P} \int_0^P e^{-i\frac{2\pi n}{P} x_1} e^{-ik_z f(x_1)} dx_1 \\ &= \sum_n \delta(k_x - \xi - \frac{2\pi n}{P}) J_n(-Ak_z) \end{aligned} \tag{2.109}$$

and

$$\begin{aligned} I_2(k_{xi},\xi) &= \sum_m \delta(\xi - k_{xi} - \frac{2\pi m}{P})\frac{1}{P}\int_0^P e^{-i\frac{2\pi m}{P}x_2} e^{-ik_{zi}f(x_2)}dx_2 \\ &= \sum_m \delta(\xi - k_{xi} - \frac{2\pi m}{P}) J_m(-Ak_{zi}) \end{aligned} \tag{2.110}$$

Hence, we can express the scattering amplitude as:

$$\begin{aligned} S(k_x,k_{xi}) &= \sum_n \sum_m \delta(k_x - k_{xi} - \frac{2\pi(n+m)}{P}) S_{n,m} \\ S_{n,m} &= \left[-\frac{2k_{z(n+m)}k_{zi}}{k_{z(n+m)}+k_{zi}} - k_{zm} - k_{zn} + k_{z(n+m)} + k_{zi} \right]. \\ &\qquad .J_n(-Ak_{z(n+m)}) J_m(-Ak_{zi}) \end{aligned} \tag{2.111}$$

Noting that, one can modify this result as:

$$S(k_x,k_{xi}) = \sum_r \delta(k_x - k_{xi} - \frac{2\pi r}{P}) \sum_m S_{r-m,m}, \tag{2.112}$$

which is more convenient in comparing the method with others.

2.4 Comparison of the Methods

The scattered field amplitudes for all of these these models can be writen in the following general form:

$$\vec{E}^s(\vec{r}) = \hat{y} \sum_{n=-\infty}^{+\infty} R(n) e^{i\vec{k}_s^n . \vec{r}} \tag{2.113}$$

due to periodicity. In the previous subsections, it was shown that $R(n)$ can be given as: in SPM,

$$R(n) = \alpha_n \tag{2.114}$$

in EBC,

$$R(n) = b_n \tag{2.115}$$

in PO,

$$R(n) = \left[\frac{k_{xi}}{k_{zn}}\frac{(k_{xn}-k_{xi})}{(k_{zi}+k_{zn})} - \frac{k_{zi}}{k_{zn}}\right] J_n(-A(k_{zi}+k_{zn})) \tag{2.116}$$

in SSA2,

$$\begin{aligned} R(n) &= \frac{k_{zi}}{(k_{zn}+k_{zi})}\left\{\frac{A}{2}\left[k_{z(n-1)}+k_{z(1)}-k_{zn}-k_{zi}\right]J_{n-1}(-A(k_{zn}+k_{zi}))\right. \\ &\qquad -2\ J_n(-A(k_{zn}+k_{zi})) \\ &\qquad \left.-\frac{A}{2}\left[k_{z(n+1)}+k_{z(-1)}-k_{zn}-k_{zi}\right]J_{n+1}(-A(k_{zn}+k_{zi}))\right\} \end{aligned} \tag{2.117}$$

and finally in MNLSSA,

$$\begin{aligned} R(n) &= \frac{1}{k_{zn}}\sum_m\left[-\frac{2k_{zn}k_{zi}}{k_{zn}+k_{zi}} - k_{zm} - k_{z(n-m)} + k_{zn} + k_{zi}\right]. \\ &\qquad .J_{(n-m)}(-Ak_{zn})J_m(-Ak_{zi}) \end{aligned} \tag{2.118}$$

$R(n)$ of each method is implemented and comparison is done for the following test cases. Note that only the propagating modes are considered in all of these results.

The first test was about the convergence of the SPM solution. For an incidence angle of $\theta_i = 45^\circ$ and a surface height parameter $A = 1\lambda$, surface period is varied for three different cases (i.e. $P = 20\lambda$, $P = 10\lambda$, $P = 5\lambda$). The fourth, the eighth and the 32^{th} order SPM solutions are tested against the 40 mode EBC solution. The results are given in Figure 2.3. The height of the surface is set to a high value, to decrease the convergence rate. But still for the $P = 20\lambda$ case, which is inside the region where the Rayleigh hypothesis is valid($\frac{A2\pi}{P} < 0.448$, due to Millar) , excellent agreement with the EBC method is observed for the 32^{th} order SPM solution. There is no question about the validity of the EBC method for this case, since the matrices involved in this theory are well conditioned. In part (b), results for the $P = 10\lambda$ case are plotted. The EBC matrices are well conditioned, so EBC can be assumed

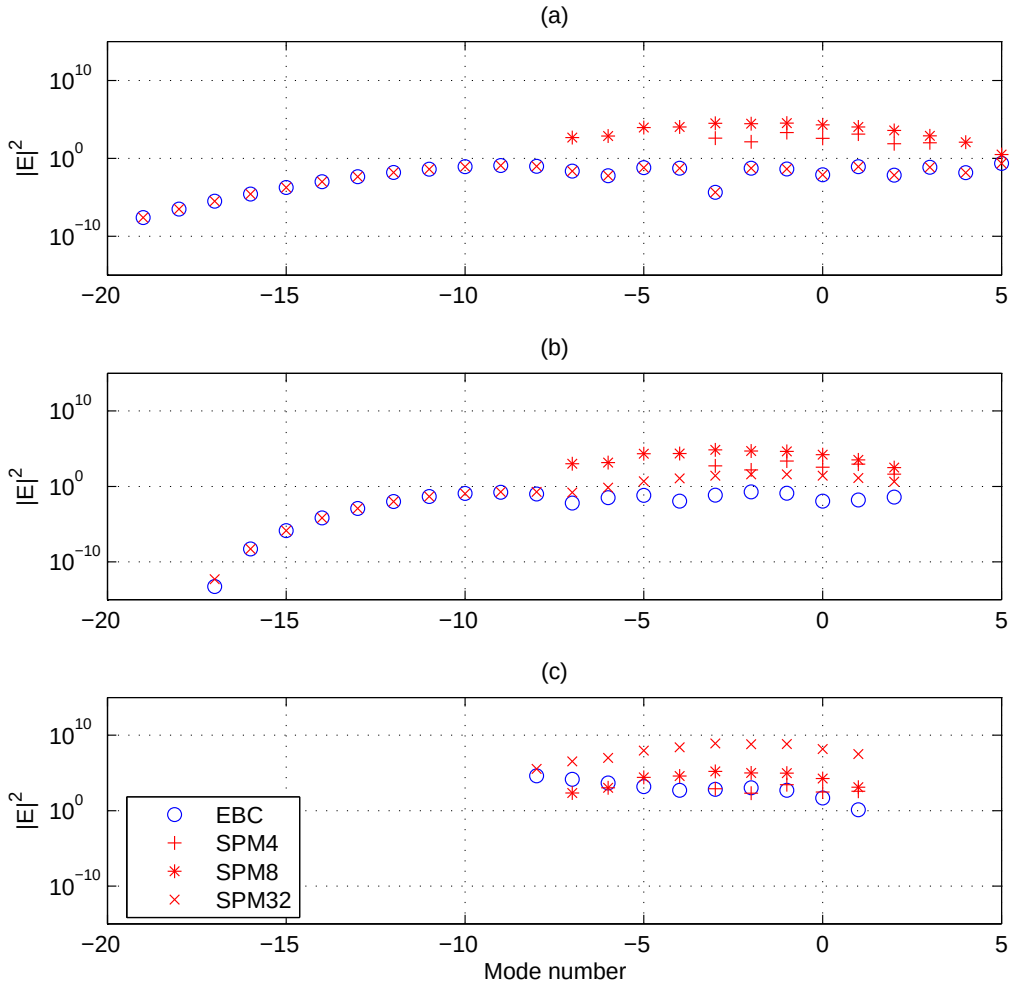

Figure 2.3: SPM convergence study: For incidence angle of $\theta_i = 45°$ and the surface height parameter $A = 1\lambda$, surface period is varied as: (a)$P = 20\lambda$, (b)$P = 10\lambda$, (c)$P = 5\lambda$

as truth. Although this case is slightly out of the Rayleigh region, SPM convergence to the EBC solution can clearly be observed. Also, for the modes far away from the specular mode, excellent agreement with the EBC solution is observed. In Part (c), results for the $P = 5\lambda$ are presented. The EBC matrices are ill conditioned, so the results are not dependable. The divergent nature of the SPM solution can also be observed.

A second test was to compare all of the models in the small height limit. The surface height is set to $A = 0.5\lambda$ and the period is assumed to be $P = 10\lambda$. Then results from each model are given for $\theta_i = 20°, 45°, 70°$ cases in Figures 2.4, 2.5 and 2.6 respectively. The EBC method solution is used for comparison for all other models. The large radius of curvature condition is also satisfied, so the models are in great agreement in all cases, except for the $\theta_i = 70°$ case PO result in the specular direction. The SSA and MNLSSA models implicitly contains SPM information. So it is natural to expect them to match with SPM in the small height limit.

The final test was for the large height limit, where a relatively higher height to length ratio is considered. The height of the surface is set to $A = 0.5\lambda$ and the period of the surface is set to $P = 5\lambda$. Similar to the second test, $\theta_i = 20°, 45°, 70°$ cases are shown in Figures 2.7, 2.8 and 2.9 respectively. Relative differences between the methods can be observed. Again for the $\theta_i = 70°$ case, PO result in the specular direction has a different behavior from the other results. Also, the MNLSSA results are closer to PO results than the SSA, due to the modification of the non-local kernels to match the PO, in the high frequency limit.

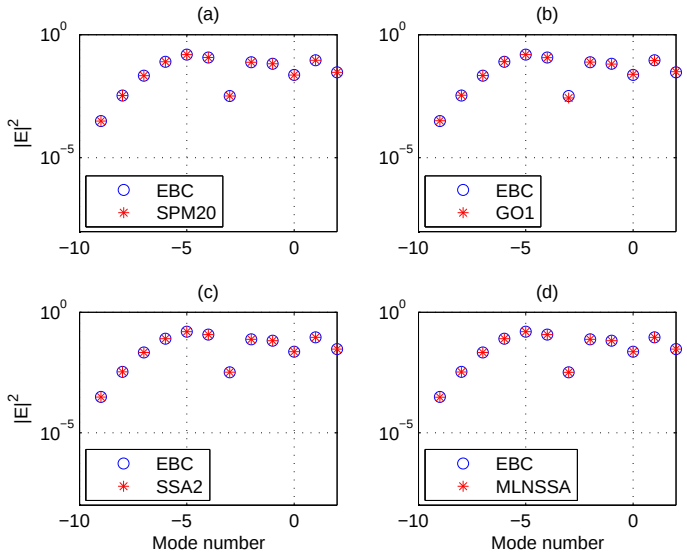

Figure 2.4: Small height example: For $\theta_i = 20°$ incidence angle, the surface height is set to $A = 0.5\lambda$ and the period is assumed to be $P = 10\lambda$.(a)EBC-SPM20, (b)EBC-PO, (c)EBC-SSA2, (d)EBC-MNLSSA

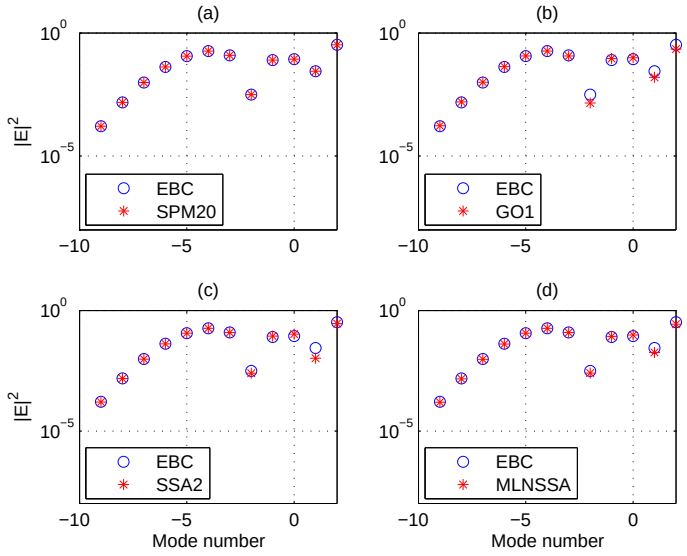

Figure 2.5: Small height example: For $\theta_i = 45°$ incidence angle, the surface height is set to $A = 0.5\lambda$ and the period is assumed to be $P = 10\lambda$.(a)EBC-SPM20, (b)EBC-PO, (c)EBC-SSA2, (d)EBC-MNLSSA

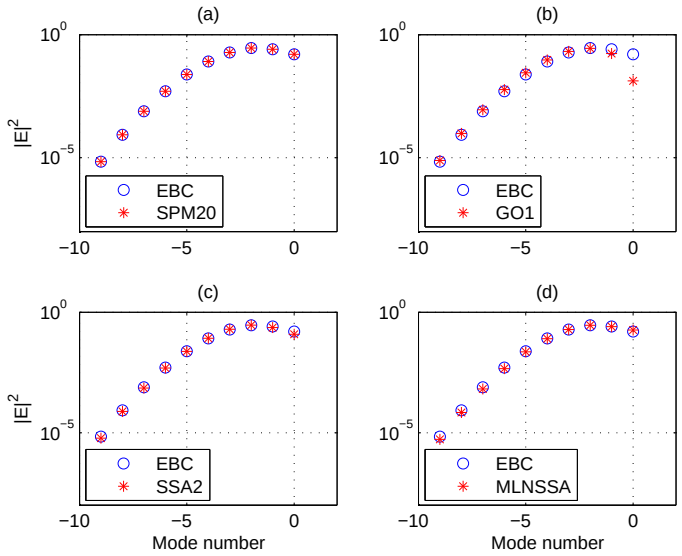

Figure 2.6: Small height example: For $\theta_i = 70°$ incidence angle, the surface height is set to $A = 0.5\lambda$ and the period is assumed to be $P = 10\lambda$.(a)EBC-SPM20, (b)EBC-PO, (c)EBC-SSA2, (d)EBC-MNLSSA

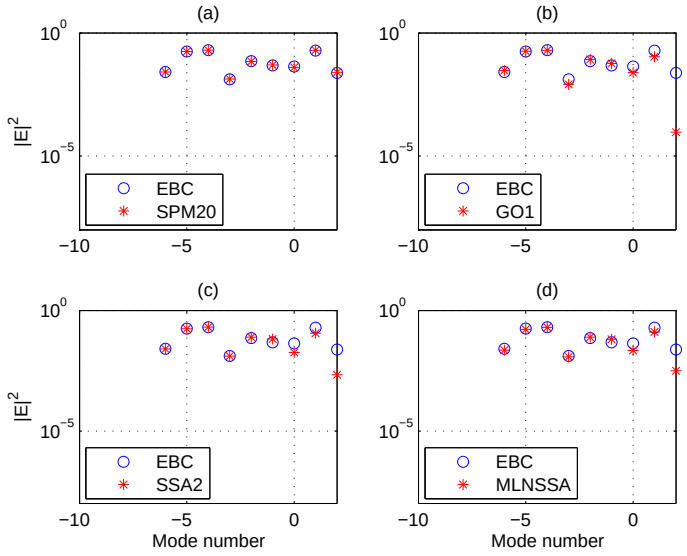

Figure 2.7: Medium height example: For $\theta_i = 20°$ incidence angle, the surface height is set to $A = 0.5\lambda$ and the period is assumed to be $P = 5\lambda$.(a)EBC-SPM20, (b)EBC-PO, (c)EBC-SSA2, (d)EBC-MNLSSA

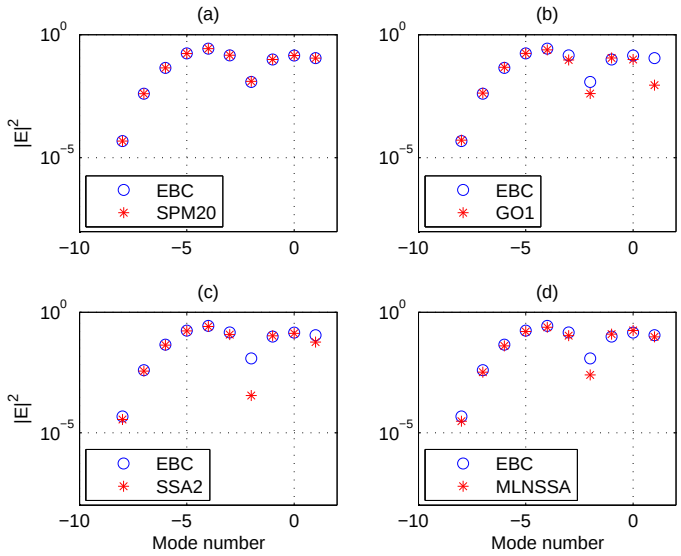

Figure 2.8: Medium height example: For $\theta_i = 45°$ incidence angle, the surface height is set to $A = 0.5\lambda$ and the period is assumed to be $P = 5\lambda$.(a)EBC-SPM20, (b)EBC-PO, (c)EBC-SSA2, (d)EBC-MNLSSA

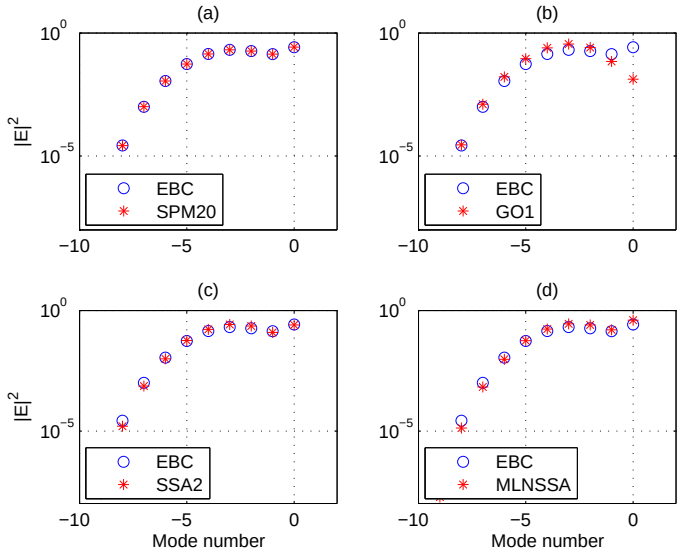

Figure 2.9: Medium height example: For $\theta_i = 70°$ incidence angle, the surface height is set to $A = 0.5\lambda$ and the period is assumed to be $P = 5\lambda$.(a)EBC-SPM20, (b)EBC-PO, (c)EBC-SSA2, (d)EBC-MNLSSA

2.5 Conclusion

In this chapter, several rough surface scattering formulations for the 1-D sinusoidal grating problem were presented. First, the arbitrary order SPM formulation was considered in detail, since the same model is utilized extensively in the rest of the chapter, for more complex cases. Then the SSA2 theory based on second order SPM kernels were presented for the identical problem. As an exact solution, the T-matrix method formulation was also included. The PO model solution was also included, as high frequency approximation. Finally, the MNLSSA as a more recent model was also introduced.

The final section of this chapter was devoted to the comparison of these models for several sinusoidal surface examples. The effect of surface slopes to the convergence of SPM series solution was highlighted. In addition, for several different incidence angles, the small, moderate and large height cases were investigated, utilizing all of these models, and in general, a good agreement between the models were observed.

CHAPTER 3

PERTURBATION THEORY OF 2D ROUGH LAYERED MEDIA: NUMERICAL SOLUTION

3.1 Introduction

In this chapter, the basic formulation for the two-layer problem is introduced. The two-layer problem implicitly means the electromagnetic scattering problem from an unbounded scatterer, consisting two 2D rough interfaces separated by a specified distance. Utilizing a perturbational approach, a complete (both TE and TM cases) solution is sought, under the assumption of the Rayleigh Hypothesis.

First the notational conventions for the rest of the dissertation are provided. Next, the boundary conditions are studied in a fashion similar with the previous chapter. Each boundary condition brings a so called forcing function, which can be utilized to express the solution of the problem as a set of two linear system of equations, for horizontal and vertical polarizations, respectively. The solution for these systems of equations is provided analytically. Later, a Fast Fourier Transform(FFT) based numerical solution is described. For validation purposes, the numerical perturbation solution is compared against an existing two and a half dimensional extended

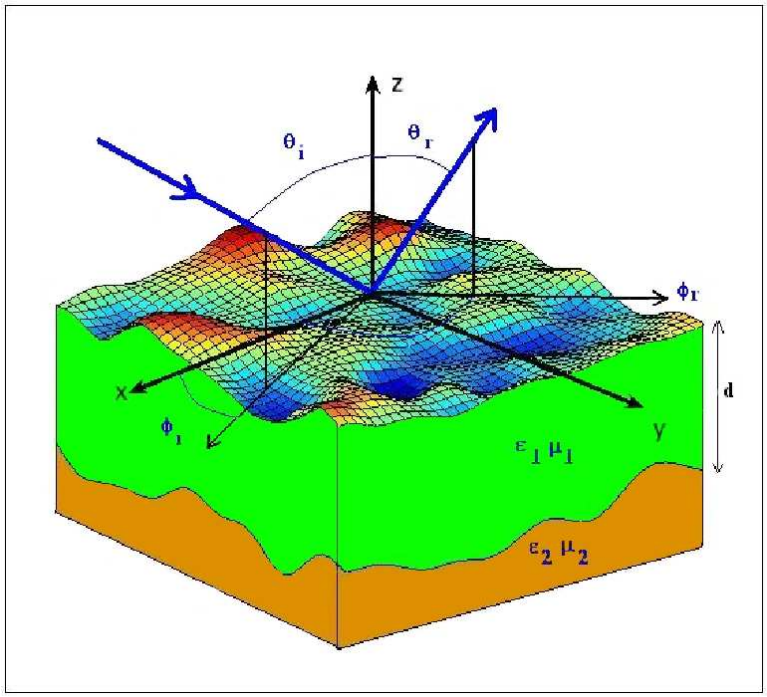

Figure 3.1: Problem Geometry

boundary condition(EBC) solution for two sine surfaces on top of each other, in the propagating modes, for several example cases.

Although only the two-layer case is considered analytically in subsequent chapters, an arbitrary number of layers is also considered as a final section in this chapter. This section can be considered as a generalization of the two-layer numerical SPM solution, which will be very useful in future work involving analytical arbitrary layer SPM solutions.

3.2 Basic Problem Setup

A two layer problem, as shown in Figure 3.1, has two rough interfaces $z = f_1(x, y)$ and $z = f_2(x, y) = -d + \bar{f}_2(x, y)$, which are both periodic. It will be assumed that

both functions have the same periods, P_x in $\hat{x}$ and P_y in $\hat{y}$ directions. We will also assume that distance parameter d between the mean planes of the surfaces, is larger then the sum of the maximum variations of each surface. The Fourier operator for the two dimensional case is given by:

$$\begin{aligned} f_i(x,y) &= \sum_{n=-\infty}^{+\infty}\sum_{m=-\infty}^{+\infty} h_{n,m}^{(i)} e^{j\left(\frac{2\pi n}{P_x}\right)x} e^{j\left(\frac{2\pi m}{P_y}\right)y} \\ h_{n,m}^{(i)} &= \mathcal{F}(f_i(x,y))_{n,m} \\ &= \frac{1}{P_x P_y}\int_0^{P_x}\int_0^{P_y} dxdy e^{-j\left(\frac{2\pi n}{P_x}\right)x} e^{-j\left(\frac{2\pi m}{P_y}\right)y} f_i(x,y) \end{aligned} \tag{3.1}$$

for $i = 1, 2$. In the rest of the derivations, vector notations: $\bar{n} = (n, m)$ and $\bar{x} = (x, y)$ will be used.

The regions are numbered (i.e. $q = 0, 1, 2$) and relevant parameters for each region are labeled accordingly: dielectric permittivity of region 2 is ϵ_2, wave impedance of region 1 is η_1, etc. Also a $+$ or $-$ sign is associated with each vector parameter, representing a $+\hat{z}$ or $-\hat{z}$ propagation direction of the associated waves.

First, define the propagation directions in each layer, both for up and down going waves:

$$\begin{aligned} \vec{k}_{\bar{0}}^{0-} &= k_{xi}\hat{x} + k_{yi}\hat{y} - k_{z0}^{\bar{0}}\hat{z} \\ \vec{k}_{\bar{n}}^{0+} &= k_{xn}\hat{x} + k_{ym}\hat{y} + k_{z0}^{\bar{n}}\hat{z} \\ \vec{k}_{\bar{n}}^{1-} &= k_{xn}\hat{x} + k_{ym}\hat{y} - k_{z1}^{\bar{n}}\hat{z} \\ \vec{k}_{\bar{n}}^{1+} &= k_{xn}\hat{x} + k_{ym}\hat{y} + k_{z1}^{\bar{n}}\hat{z} \\ \vec{k}_{\bar{n}}^{2-} &= k_{xn}\hat{x} + k_{ym}\hat{y} - k_{z2}^{\bar{n}}\hat{z} \end{aligned} \tag{3.2}$$

Here $k_{xi} = k_0 \sin(\theta_i)\cos(\phi_i)$ and $k_{yi} = k_0 \sin(\theta_i)\sin(\phi_i)$. θ_i and ϕ_i are the incidence angles. Other parameters are defined as:

$$\begin{aligned} k_{xn} &= k_{x(n)} = k_{xi} + \frac{2\pi n}{P_x} \\ k_{ym} &= k_{y(m)} = k_{yi} + \frac{2\pi m}{P_y} \\ k_\rho^{\bar{n}} &= \sqrt{k_{xn}^2 + k_{ym}^2} \\ k_{zq}^{\bar{n}} &= \sqrt{k_q^2 - (k_\rho^{\bar{n}})^2} \end{aligned} \tag{3.3}$$

Note that the first three parameters defined here are independent of the region, whereas the last parameter is defined separately for each region $q = 0, 1, 2$. Also for the $\bar{n} = \bar{0}$ case the following parameters are defined for convenience:

$$\begin{aligned} k_{\rho i} &= \sqrt{k_{xi}^2 + k_{yi}^2} \\ k_{zi} &= \sqrt{k_0^2 - (k_{\rho i})^2} \end{aligned} \tag{3.4}$$

Using an $e^{-j\omega t}$ time dependence, the fields in Region 0 can be expressed as:

$$\begin{aligned} \vec{E}_0^- &= \hat{e}_i e^{j\vec{k}_{\bar{0}}^{0-}.\vec{r}} \\ \vec{H}_0^- &= \frac{\hat{k}_{\bar{0}}^{0-} \times \hat{e}_i}{\eta_0} e^{j\vec{k}_{\bar{0}}^{0-}.\vec{r}} \\ \vec{E}_0^+ &= \sum_{\bar{n}} \left[\hat{h}_{\bar{n}}\alpha_{\bar{n}} + \hat{v}_{0+}^{\bar{n}}\beta_{\bar{n}}\right] e^{j\vec{k}_{\bar{n}}^{0+}.\vec{r}} \\ \vec{H}_0^+ &= \frac{1}{\eta_0}\sum_{\bar{n}} \left[-\hat{v}_{0+}^{\bar{n}}\alpha_{\bar{n}} + \hat{h}_{\bar{n}}\beta_{\bar{n}}\right] e^{j\vec{k}_{\bar{n}}^{0+}.\vec{r}} \end{aligned} \tag{3.5}$$

The incidence polarization vector $\hat{e}_i$ is equal to $\hat{h}_i$ or $\hat{v}_i$ for horizontal and vertical incidence respectively, which are given as follows:

$$\begin{aligned} \hat{h}_i &= \frac{k_{yi}}{k_\rho^{\bar{0}}}\hat{x} - \frac{k_{xi}}{k_\rho^{\bar{0}}}\hat{y} \\ \hat{v}_i &= \frac{k_{xi}k_{zi}}{k_0 k_\rho^{\bar{0}}}\hat{x} + \frac{k_{yi}k_{zi}}{k_0 k_\rho^{\bar{0}}}\hat{y} + \frac{k_\rho^{\bar{0}}}{k_0}\hat{z} \end{aligned} \tag{3.6}$$

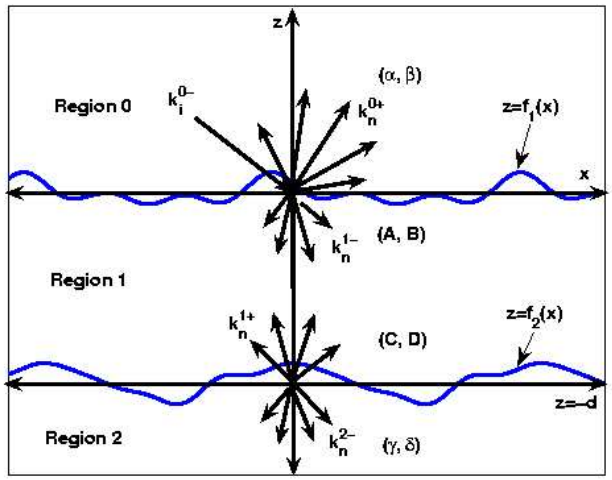

Figure 3.2: Two dimensional ($y = 0$) cross-section of the two-layer media. The unknown field coefficients $\{\alpha, \beta, A, B, C, D, \gamma, \delta\}$ are labeled in their domain of definition.

Note that, except the incident field, all field quantities have two unknown field amplitudes (i.e. $\alpha_{\bar{n}}$ and $\beta_{\bar{n}}$ for the reflected field) to take into account the depolarization effect of the rough surfaces. The unknown field amplitudes are defined in Figure 3.2

Fields in Regions 1 and 2 can also be expressed similarly as:

$$\begin{aligned}
\vec{E}_1^- &= \sum_{\bar{n}} \left[\hat{h}_{\bar{n}} A_{\bar{n}} + \hat{v}_{1-}^{\bar{n}} B_{\bar{n}}\right] e^{j\vec{k}_{\bar{n}}^{1-}.\vec{r}} \\
\vec{H}_1^- &= \frac{1}{\eta_1} \sum_{\bar{n}} \left[-\hat{v}_{1-}^{\bar{n}} A_{\bar{n}} + \hat{h}_{\bar{n}} B_{\bar{n}}\right] e^{j\vec{k}_{\bar{n}}^{1-}.\vec{r}} \\
\vec{E}_1^+ &= \sum_{\bar{n}} \left[\hat{h}_{\bar{n}} C_{\bar{n}} + \hat{v}_{1+}^{\bar{n}} D_{\bar{n}}\right] e^{j\vec{k}_{\bar{n}}^{1+}.\vec{r}} \\
\vec{H}_1^+ &= \frac{1}{\eta_1} \sum_{\bar{n}} \left[-\hat{v}_{1+}^{\bar{n}} C_{\bar{n}} + \hat{h}_{\bar{n}} D_{\bar{n}}\right] e^{j\vec{k}_{\bar{n}}^{1+}.\vec{r}} \\
\vec{E}_2^- &= \sum_{\bar{n}} \left[\hat{h}_{\bar{n}} \gamma_{\bar{n}} + \hat{v}_{2-}^{\bar{n}} \delta_{\bar{n}}\right] e^{j\vec{k}_{\bar{n}}^{2-}.\vec{r}} \\
\vec{H}_2^- &= \frac{1}{\eta_2} \sum_{\bar{n}} \left[-\hat{v}_{2-}^{\bar{n}} \gamma_{\bar{n}} + \hat{h}_{\bar{n}} \delta_{\bar{n}}\right] e^{j\vec{k}_{\bar{n}}^{2-}.\vec{r}}
\end{aligned} \tag{3.7}$$

Polarization vectors for these fields are:

$$\begin{aligned}
\hat{h}_{\bar{n}} &= \frac{1}{k_\rho^{\bar{n}}}\left(k_{ym}\hat{x} - k_{xn}\hat{y}\right) \\
\hat{v}_{0+}^{\bar{n}} &= -\frac{k_{z0}^{\bar{n}}}{k_0 k_\rho^{\bar{n}}}\left(k_{xn}\hat{x} + k_{ym}\hat{y}\right) + \frac{k_\rho^{\bar{n}}}{k_0}\hat{z} \\
\hat{v}_{1-}^{\bar{n}} &= +\frac{k_{z1}^{\bar{n}}}{k_1 k_\rho^{\bar{n}}}\left(k_{xn}\hat{x} + k_{ym}\hat{y}\right) + \frac{k_\rho^{\bar{n}}}{k_1}\hat{z} \\
\hat{v}_{1+}^{\bar{n}} &= -\frac{k_{z1}^{\bar{n}}}{k_1 k_\rho^{\bar{n}}}\left(k_{xn}\hat{x} + k_{ym}\hat{y}\right) + \frac{k_\rho^{\bar{n}}}{k_1}\hat{z} \\
\hat{v}_{2-}^{\bar{n}} &= +\frac{k_{z2}^{\bar{n}}}{k_2 k_\rho^{\bar{n}}}\left(k_{xn}\hat{x} + k_{ym}\hat{y}\right) + \frac{k_\rho^{\bar{n}}}{k_2}\hat{z}
\end{aligned} \tag{3.8}$$

Since the derivation involves several cross product terms, it will also be convenient to work them out here. The products of $\hat{z}$ can be given as:

$$\begin{aligned}
\hat{z}\times\hat{h}_i &= \hat{z}\times\hat{h}_{\bar{0}} = \frac{1}{k_{\rho i}}\left(k_{xi}\hat{x} + k_{yi}\hat{y}\right) \\
\hat{z}\times\hat{v}_i &= \hat{z}\times\hat{v}_{0-}^{\bar{0}} = \frac{-k_{zi}}{k_0}\hat{h}_i \\
\hat{z}\times\hat{h}_{\bar{n}} &= \frac{1}{k_\rho^{\bar{n}}}\left(k_{xn}\hat{x} + k_{ym}\hat{y}\right) \\
\hat{z}\times\hat{v}_{q\mp}^{\bar{n}} &= \mp\left(\frac{k_{zq}^{\bar{n}}}{k_q}\right)\hat{h}_{\bar{n}} \\
\hat{z}\times\hat{k}_i\times\hat{h}_i &= \left(\frac{k_{z0}^{\bar{0}}}{k_0}\right)\hat{h}_i \\
\hat{z}\times\hat{k}_i\times\hat{v}_i &= \hat{z}\times\hat{h}_i
\end{aligned} \tag{3.9}$$

Here, again $q = 1, 2$ represents the region number. Similarly, the products involving the gradients of the surfaces can be given as:

$$\begin{aligned}
\nabla_t f_{(i)}(\bar{x})\times\hat{h}_i &= (.....)\,\hat{z} \\
\nabla_t f_{(i)}(\bar{x})\times\hat{v}_i &= \frac{k_{\rho i}}{k_0}\left(\nabla_t f_{(i)}(\bar{x})\times\hat{z}\right) + (.....)\,\hat{z} \\
\nabla_t f_{(i)}(\bar{x})\times\hat{h}_{\bar{n}} &= (.....)\,\hat{z} \\
\nabla_t f_{(i)}(\bar{x})\times\hat{v}_{q\mp}^{\bar{n}} &= \frac{k_\rho^{\bar{n}}}{k_q}\left(\nabla_t f_{(i)}(\bar{x})\times\hat{z}\right) + (.....)\,\hat{z}
\end{aligned}$$

$$
\begin{aligned}
\nabla_t f_{(i)}(\bar{x}) \times \hat{z} &= \hat{x}\frac{\partial f_{(i)}}{\partial y} - \hat{y}\frac{\partial f_{(i)}}{\partial x} \\
\nabla_t f_{(i)}(\bar{x}) \times \hat{k}_i \times \hat{h}_i &= -\frac{k_{\rho i}}{k_0}\left(\nabla_t f_{(i)}(\bar{x}) \times \hat{z}\right) + (.....)\,\hat{z} \\
\nabla_t f_{(i)}(\bar{x}) \times \hat{k}_i \times \hat{v}_i &= (.....)\,\hat{z}
\end{aligned} \tag{3.10}
$$

Here, the subscript (i) is utilized with surface function f, indicating the number of the interface. Also the $\hat{z}$ components are described with (....) since we are not interested in them.

Expressions up-to this point conclude the basic notational conventions of the two layer rough interface scattering problem. The rest of the formulation involves algebraic manipulations of the boundary conditions.

3.3 Boundary Conditions

The boundary conditions considered in this problem are:

$$
\begin{aligned}
\vec{n}_1 \times \left[E_0^- + E_0^+\right] &= \vec{n}_1 \times \left[E_1^- + E_1^+\right]|_{z=f_1(\bar{x})} \\
\vec{n}_1 \times \left[H_0^- + H_0^+\right] &= \vec{n}_1 \times \left[H_1^- + H_1^+\right]|_{z=f_1(\bar{x})} \\
\vec{n}_2 \times \left[E_1^- + E_1^+\right] &= \vec{n}_2 \times \left[E_2^-\right]|_{z=f_2(\bar{x})} \\
\vec{n}_2 \times \left[H_1^- + H_1^+\right] &= \vec{n}_2 \times \left[H_2^-\right]|_{z=f_2(\bar{x})}
\end{aligned} \tag{3.11}
$$

Here $\vec{n}_1$ and $\vec{n}_2$ are the normals of surfaces $z = f_1(\bar{x})$ and $z = f_2(\bar{x})$ respectively, as follows:

$$
\begin{aligned}
\vec{n}_1 &= \hat{z} - \nabla_t f_1(\bar{x}) \\
\vec{n}_2 &= \hat{z} - \nabla_t f_2(\bar{x})
\end{aligned} \tag{3.12}
$$

These boundary conditions will be applied for both $\hat{x}$ and $\hat{y}$ field components. Plugging in the surface normals to the boundary conditions and after some rearranging,

we obtain:

$$\begin{aligned}
\hat{z}\times\left[E_0^+ - E_1^- - E_1^+\right] &= -\hat{z}\times E_0^- + \nabla_t f_1(\bar{x})\times E_0^- \\
&\quad +\nabla_t f_1(\bar{x})\times\left[E_0^+ - E_1^- - E_1^+\right]|_{z=f_1(\bar{x})} \\
\hat{z}\times\left[H_0^+ - H_1^- - H_1^+\right] &= -\hat{z}\times H_0^- + \nabla_t f_1(\bar{x})\times H_0^- \\
&\quad +\nabla_t f_1(\bar{x})\times\left[H_0^+ - H_1^- - H_1^+\right]|_{z=f_1(\bar{x})} \\
\hat{z}\times\left[E_1^- + E_1^+ - E_2^-\right] &= +\nabla_t f_2(\bar{x})\times\left[[E_1^- + E_1^+ - E_2^-\right]|_{z=f_2(\bar{x})} \\
\hat{z}\times\left[H_1^- + H_1^+ - H_2^-\right] &= +\nabla_t f_2(\bar{x})\times\left[[H_1^- + H_1^+ - H_2^-\right]|_{z=f_2(\bar{x})} \qquad (3.13)
\end{aligned}$$

Plugging in the field expressions and utilizing cross product relations provided in the previous section, an algebraic equation can be obtained for each boundary condition. These equations are:

First boundary condition:

$$\begin{aligned}
&\sum_{\bar{n}} e^{i\left(\frac{2\pi n}{P_x}\right)x + i\left(\frac{2\pi m}{P_y}\right)y}\left(\left(\hat{z}\times\hat{h}_{\bar{n}}\right)\left[\alpha_{\bar{n}}e^{+ik_{z0}^{\bar{n}}z} - A_{\bar{n}}e^{-ik_{z1}^{\bar{n}}z} - C_{\bar{n}}e^{+ik_{z1}^{\bar{n}}z}\right]\right. \\
&\qquad\left. +\left(\hat{h}_{\bar{n}}\right)\left[\frac{k_{z0}^{\bar{n}}}{k_0}\beta_{\bar{n}}e^{+ik_{z0}^{\bar{n}}z} + \frac{k_{z1}^{\bar{n}}}{k_1}B_{\bar{n}}e^{-ik_{z1}^{\bar{n}}z} - \frac{k_{z1}^{\bar{n}}}{k_1}D_{\bar{n}}e^{+ik_{z1}^{\bar{n}}z}\right]\right) \\
= &-\left(\hat{z}\times\hat{e}_i\right)e^{-ik_{zi}z} + \left(\nabla_t f_1(\bar{x})\times\hat{e}_i\right)e^{-ik_{zi}z} + \sum_{\bar{n}} e^{i\left(\frac{2\pi n}{P_x}\right)x + i\left(\frac{2\pi m}{P_y}\right)y}. \\
&.\left(\left(\nabla_t f_1(\bar{x})\times\hat{z}\right)\left(k_\rho^{\bar{n}}\right)\left[\frac{\beta_{\bar{n}}}{k_0}e^{+ik_{z0}^{\bar{n}}z} - \frac{B_{\bar{n}}}{k_1}e^{-ik_{z1}^{\bar{n}}z} - \frac{D_{\bar{n}}}{k_1}e^{+ik_{z1}^{\bar{n}}z}\right]\right) \qquad (3.14)
\end{aligned}$$

Second Boundary Condition:

$$\begin{aligned}
&\sum_{\bar{n}} e^{i\left(\frac{2\pi n}{P_x}\right)x + i\left(\frac{2\pi m}{P_y}\right)y}\left(\left(\hat{z}\times\hat{h}_{\bar{n}}\right)\left[\frac{\beta_{\bar{n}}}{\eta_0}e^{+ik_{z0}^{\bar{n}}z} - \frac{B_{\bar{n}}}{\eta_1}e^{-ik_{z1}^{\bar{n}}z} - \frac{D_{\bar{n}}}{\eta_1}e^{+ik_{z1}^{\bar{n}}z}\right]\right. \\
&\qquad\left. +\left(\hat{h}_{\bar{n}}\right)\left[-\frac{k_{z0}^{\bar{n}}}{k_0\eta_0}\alpha_{\bar{n}}e^{+ik_{z0}^{\bar{n}}z} - \frac{k_{z1}^{\bar{n}}}{k_1\eta_1}A_{\bar{n}}e^{-ik_{z1}^{\bar{n}}z} + \frac{k_{z1}^{\bar{n}}}{k_1\eta_1}C_{\bar{n}}e^{+ik_{z1}^{\bar{n}}z}\right]\right) \\
= &-\frac{1}{\eta_0}\left(\hat{z}\times\hat{k}_i\times\hat{e}_i\right)e^{-ik_{zi}z} + \frac{1}{\eta_0}\left(\nabla_t f_1(\bar{x})\times\hat{k}_i\times\hat{e}_i\right)e^{-ik_{zi}z} + \sum_{\bar{n}} e^{i\left(\frac{2\pi n}{P_x}\right)x + i\left(\frac{2\pi m}{P_y}\right)y}.
\end{aligned}$$

$$\cdot \left(\left(\nabla_t f_1(\bar{x}) \times \hat{z}\right)(k_\rho^{\bar{n}}) \left[-\frac{\alpha_{\bar{n}}}{k_0\eta_0} e^{+ik_{z0}^{\bar{n}} z} + \frac{A_{\bar{n}}}{k_1\eta_1} e^{-ik_{z1}^{\bar{n}} z} + \frac{C_{\bar{n}}}{k_1\eta_1} e^{+ik_{z1}^{\bar{n}} z} \right] \right) \tag{3.15}$$

Third Boundary Condition

$$\begin{aligned} & \sum_{\bar{n}} e^{i\left(\frac{2\pi n}{P_x}\right)x + i\left(\frac{2\pi m}{P_y}\right)y} \left(\left(\hat{z} \times \hat{h}_{\bar{n}}\right) \left[A_{\bar{n}} e^{-ik_{z1}^{\bar{n}} z} + C_{\bar{n}} e^{+ik_{z1}^{\bar{n}} z} - \gamma_{\bar{n}} e^{-ik_{z2}^{\bar{n}} z} \right] \right. \\ & \qquad \left. + \left(\hat{h}_{\bar{n}}\right) \left[-\frac{k_{z1}^{\bar{n}}}{k_1} B_{\bar{n}} e^{-ik_{z1}^{\bar{n}} z} + \frac{k_{z1}^{\bar{n}}}{k_1} D_{\bar{n}} e^{+ik_{z1}^{\bar{n}} z} + \frac{k_{z2}^{\bar{n}}}{k_2} \delta_{\bar{n}} e^{-ik_{z2}^{\bar{n}} z} \right] \right) \\ = \; & + \sum_{\bar{n}} e^{i\left(\frac{2\pi n}{P_x}\right)x + i\left(\frac{2\pi m}{P_y}\right)y} \left(\left(\nabla_t f_2(\bar{x}) \times \hat{z}\right)(k_\rho^{\bar{n}}). \right. \\ & \qquad \left. \cdot \left[\frac{B_{\bar{n}}}{k_1} e^{-ik_{z1}^{\bar{n}} z} + \frac{D_{\bar{n}}}{k_1} e^{+ik_{z1}^{\bar{n}} z} - \frac{\delta_{\bar{n}}}{k_2} e^{-ik_{z2}^{\bar{n}} z} \right] \right) \end{aligned} \tag{3.16}$$

Fourth Boundary Condition

$$\begin{aligned} & \sum_{\bar{n}} e^{i\left(\frac{2\pi n}{P_x}\right)x + i\left(\frac{2\pi m}{P_y}\right)y} \left(\left(\hat{z} \times \hat{h}_{\bar{n}}\right) \left[\frac{B_{\bar{n}}}{\eta_1} e^{-ik_{z1}^{\bar{n}} z} + \frac{D_{\bar{n}}}{\eta_1} e^{+ik_{z1}^{\bar{n}} z} - \frac{\delta_{\bar{n}}}{\eta_2} e^{-ik_{z2}^{\bar{n}} z} \right] \right. \\ & \qquad \left. + \left(\hat{h}_{\bar{n}}\right) \left[\frac{k_{z1}^{\bar{n}}}{k_1\eta_1} A_{\bar{n}} e^{-ik_{z1}^{\bar{n}} z} - \frac{k_{z1}^{\bar{n}}}{k_1\eta_1} C_{\bar{n}} e^{+ik_{z1}^{\bar{n}} z} - \frac{k_{z2}^{\bar{n}}}{k_2\eta_2} \gamma_{\bar{n}} e^{-ik_{z2}^{\bar{n}} z} \right] \right) \\ = \; & \sum_{\bar{n}} e^{i\left(\frac{2\pi n}{P_x}\right)x + i\left(\frac{2\pi m}{P_y}\right)y} \left(\left(\nabla_t f_1(\bar{x}) \times \hat{z}\right)(k_\rho^{\bar{n}}). \right. \\ & \qquad \left. \cdot \left[-\frac{A_{\bar{n}}}{k_1\eta_1} e^{-ik_{z1}^{\bar{n}} z} - \frac{C_{\bar{n}}}{k_1\eta_1} e^{+ik_{z1}^{\bar{n}} z} + \frac{\gamma_{\bar{n}}}{k_2\eta_2} e^{-ik_{z2}^{\bar{n}} z} \right] \right) \end{aligned} \tag{3.17}$$

3.4 Perturbative Development

As illustrated earlier in Chapter 1, the perturbative development involves an expansion of the unknown field amplitudes into perturbation series. The following series expansion is considered for all of the scattering coefficients ($\tau = \{\alpha, \beta, A, B, C, D, \gamma, \delta\}$).

$$\tau_{\bar{n}} = \sum_{m=0}^{+\infty} \tau_{\bar{n}}^{(m)} \tag{3.18}$$

The Taylor expansion of the upper surface at $z = 0$ is also necessary, which can be formulated as follows:

$$e^{jkz} = \sum_{q=0}^{+\infty} \frac{(jkz)^q}{q!} \tag{3.19}$$

For the lower surface, a Taylor expansion of the surface at its mean plane has to be considered. In this case, the Taylor expansion has to be expressed at $z = -d$, which can be given as follows:

$$e^{\mp jkz} = e^{\pm jkd} \sum_{q=0}^{+\infty} \frac{(\mp jk(z+d))^q}{q!} \tag{3.20}$$

Utilizing these series expansions, the forcing functions (i.e. $S(x)$ of Chapter 2) can be studied. In order to obtain the forcing functions, first step is to plug in the series expansion given by equations 3.18, 3.19 and 3.20 into boundary conditions. Then, the terms of the same order should be collected together. Considering only the N^{th} order terms and collecting the highest order unknowns on left side equation, the following forcing functions can be obtained.

$S_{E_1}^{(N)}(\bar{x})$ can be defined using the first boundary condition as:

$$\begin{aligned}
&\sum_{\bar{n}} e^{i\left(\frac{2\pi n}{P_x}\right)x + i\left(\frac{2\pi m}{P_y}\right)y} \Bigg(\left(\hat{z} \times \hat{h}_{\bar{n}}\right) \left[\alpha_{\bar{n}}^{(N)} - A_{\bar{n}}^{(N)} - C_{\bar{n}}^{(N)}\right] \\
&\qquad + \left(\hat{h}_{\bar{n}}\right) \left[\frac{k_{z0}^{\bar{n}}}{k_0}\beta_{\bar{n}}^{(N)} + \frac{k_{z1}^{\bar{n}}}{k_1}B_{\bar{n}}^{(N)} - \frac{k_{z1}^{\bar{n}}}{k_1}D_{\bar{n}}^{(N)}\right] \Bigg) \\
= \;& S_{E_1}^{(N)}(\bar{x}) \\
= \;& -\left(\hat{z} \times \hat{e}_i\right) \frac{(-ik_{zi}z)^N}{N!} + \left(\nabla_t f_1(\bar{x}) \times \hat{e}_i\right) \frac{(-ik_{zi}z)^{N-1}}{(N-1)!} \\
& - \sum_{l=0}^{N-1} \frac{(iz)^{N-l}}{(N-l)!} \Bigg(\sum_{\bar{n}} e^{i\left(\frac{2\pi n}{P_x}\right)x + i\left(\frac{2\pi m}{P_y}\right)y} \Bigg(\\
& \left(\hat{z} \times \hat{h}_{\bar{n}}\right) \left[\alpha_{\bar{n}}^{(l)}(k_{z0}^{\bar{n}})^{N-l} - A_{\bar{n}}^{(l)}(-k_{z1}^{\bar{n}})^{N-l} - C_{\bar{n}}^{(l)}(k_{z1}^{\bar{n}})^{N-l}\right]
\end{aligned}$$

$$+\left(\hat{h}_{\bar{n}}\right)\left[\frac{k_{z0}^{\bar{n}}}{k_0}\beta_{\bar{n}}^{(l)}(k_{z0}^{\bar{n}})^{N-l}+\frac{k_{z1}^{\bar{n}}}{k_1}B_{\bar{n}}^{(l)}(-k_{z1}^{\bar{n}})^{N-l}-\frac{k_{z1}^{\bar{n}}}{k_1}D_{\bar{n}}^{(l)}(k_{z1}^{\bar{n}})^{N-l}\right]\Bigg)\Bigg)$$

$$+\sum_{l=0}^{N-1}\frac{(iz)^{N-l-1}}{(N-l-1)!}\Bigg(\sum_{\bar{n}}e^{i\left(\frac{2\pi n}{P_x}\right)x+i\left(\frac{2\pi m}{P_y}\right)y}\Bigg(\left(\nabla_t f_1(\bar{x})\times\hat{z}\right)(k_\rho^{\bar{n}}).$$

$$\cdot\left[\frac{\beta_{\bar{n}}^{(l)}}{k_0}(k_{z0}^{\bar{n}})^{N-l-1}-\frac{B_{\bar{n}}^{(l)}}{k_1}(-k_{z1}^{\bar{n}})^{N-l-1}-\frac{D_{\bar{n}}^{(l)}}{k_1}(k_{z1}^{\bar{n}})^{N-l-1}\right]\Bigg)\Bigg) \tag{3.21}$$

$S_{H_1}^{(N)}(\bar{x})$ can be defined using the second boundary condition as:

$$\sum_{\bar{n}}e^{i\left(\frac{2\pi n}{P_x}\right)x+i\left(\frac{2\pi m}{P_y}\right)y}\Bigg(\left(\hat{z}\times\hat{h}_{\bar{n}}\right)\left[\frac{\beta_{\bar{n}}^{(N)}}{\eta_0}-\frac{B_{\bar{n}}^{(N)}}{\eta_1}-\frac{D_{\bar{n}}^{(N)}}{\eta_1}\right]$$

$$+\left(\hat{h}_{\bar{n}}\right)\left[-\frac{k_{z0}^{\bar{n}}}{k_0\eta_0}\alpha_{\bar{n}}^{(N)}-\frac{k_{z1}^{\bar{n}}}{k_1\eta_1}A_{\bar{n}}^{(N)}+\frac{k_{z1}^{\bar{n}}}{k_1\eta_1}C_{\bar{n}}^{(N)}\right]\Bigg)$$

$$=\quad S_{H_1}^{(N)}(\bar{x})$$

$$=\quad -\frac{1}{\eta_0}\left(\hat{z}\times\hat{k}_i\times\hat{e}_i\right)\frac{(-ik_{zi}z)^N}{N!}+\frac{1}{\eta_0}\left(\nabla_t f_1(\bar{x})\times\hat{k}_i\times\hat{e}_i\right)\frac{(-ik_{zi}z)^{N-1}}{(N-1)!}$$

$$-\sum_{l=0}^{N-1}\frac{(iz)^{N-l}}{(N-l)!}\Bigg(\sum_{\bar{n}}e^{i\left(\frac{2\pi n}{P_x}\right)x+i\left(\frac{2\pi m}{P_y}\right)y}\Bigg($$

$$\left(\hat{z}\times\hat{h}_{\bar{n}}\right)\left[\frac{\beta_{\bar{n}}^{(l)}}{\eta_0}(k_{z0}^{\bar{n}})^{N-l}-\frac{B_{\bar{n}}^{(l)}}{\eta_1}(-k_{z1}^{\bar{n}})^{N-l}-\frac{D_{\bar{n}}^{(l)}}{\eta_1}(k_{z1}^{\bar{n}})^{N-l}\right]$$

$$+\left(\hat{h}_{\bar{n}}\right)\left[-\frac{k_{z0}^{\bar{n}}}{k_0\eta_0}\alpha_{\bar{n}}^{(l)}(k_{z0}^{\bar{n}})^{N-l}-\frac{k_{z1}^{\bar{n}}}{k_1\eta_1}A_{\bar{n}}^{(l)}(-k_{z1}^{\bar{n}})^{N-l}+\frac{k_{z1}^{\bar{n}}}{k_1\eta_1}C_{\bar{n}}^{(l)}(k_{z1}^{\bar{n}})^{N-l}\right]\Bigg)\Bigg)$$

$$+\sum_{l=0}^{N-1}\frac{(iz)^{N-l-1}}{(N-l-1)!}\Bigg(\sum_{\bar{n}}e^{i\left(\frac{2\pi n}{P_x}\right)x+i\left(\frac{2\pi m}{P_y}\right)y}\Bigg(\left(\nabla_t f_1(\bar{x})\times\hat{z}\right)(k_\rho^{\bar{n}}).$$

$$\cdot\left[-\frac{\alpha_{\bar{n}}^{(l)}}{k_0\eta_0}(k_{z0}^{\bar{n}})^{N-l-1}+\frac{A_{\bar{n}}^{(l)}}{k_1\eta_1}(-k_{z1}^{\bar{n}})^{N-l-1}+\frac{C_{\bar{n}}^{(l)}}{k_1\eta_1}(k_{z1}^{\bar{n}})^{N-l-1}\right]\Bigg)\Bigg) \tag{3.22}$$

$S_{E_2}^{(N)}(\bar{x})$ can be defined using the third boundary condition as:

$$\sum_{\bar{n}} e^{i\left(\frac{2\pi n}{P_x}\right)x+i\left(\frac{2\pi m}{P_y}\right)y}\left(\left(\hat{z}\times\hat{h}_{\bar{n}}\right)\left[A_{\bar{n}}^{(N)}e^{+ik_{z1}^{\bar{n}}d}+C_{\bar{n}}^{(N)}e^{-ik_{z1}^{\bar{n}}d}-\gamma_{\bar{n}}^{(N)}e^{+ik_{z2}^{\bar{n}}d}\right]\right.$$
$$\left.+\left(\hat{h}_{\bar{n}}\right)\left[-\frac{k_{z1}^{\bar{n}}}{k_1}B_{\bar{n}}^{(N)}e^{+ik_{z1}^{\bar{n}}d}+\frac{k_{z1}^{\bar{n}}}{k_1}D_{\bar{n}}^{(N)}e^{-ik_{z1}^{\bar{n}}d}+\frac{k_{z2}^{\bar{n}}}{k_2}\delta_{\bar{n}}^{(N)}e^{+ik_{z2}^{\bar{n}}d}\right]\right)$$

$$= S_{E_2}^{(N)}(\bar{x})$$

$$= -\sum_{l=0}^{N-1}\frac{(i(z+d))^{N-l}}{(N-l)!}\left(\sum_{\bar{n}} e^{i\left(\frac{2\pi n}{P_x}\right)x+i\left(\frac{2\pi m}{P_y}\right)y}\left(\left(\hat{z}\times\hat{h}_{\bar{n}}\right)\left[A_{\bar{n}}^{(l)}(-k_{z1}^{\bar{n}})^{(N-l)}e^{+ik_{z1}^{\bar{n}}d}\right.\right.\right.$$
$$\left.+C_{\bar{n}}^{(l)}(+k_{z1}^{\bar{n}})^{(N-l)}e^{-ik_{z1}^{\bar{n}}d}-\gamma_{\bar{n}}^{(l)}(-k_{z2}^{\bar{n}})^{(N-l)}e^{+ik_{z2}^{\bar{n}}d}\right]$$
$$+\left(\hat{h}_{\bar{n}}\right)\left[-\frac{k_{z1}^{\bar{n}}}{k_1}B_{\bar{n}}^{(l)}(-k_{z1}^{\bar{n}})^{(N-l)}e^{+ik_{z1}^{\bar{n}}d}+\frac{k_{z1}^{\bar{n}}}{k_1}D_{\bar{n}}^{(l)}(+k_{z1}^{\bar{n}})^{(N-l)}e^{-ik_{z1}^{\bar{n}}d}\right.$$
$$\left.\left.\left.+\frac{k_{z2}^{\bar{n}}}{k_2}\delta_{\bar{n}}^{(l)}(-k_{z2}^{\bar{n}})^{(N-l)}e^{+ik_{z2}^{\bar{n}}d}\right]\right)\right)$$
$$+\sum_{l=0}^{N-1}\frac{(i(z+d))^{N-l-1}}{(N-l-1)!}\left(\sum_{\bar{n}} e^{i\left(\frac{2\pi n}{P_x}\right)x+i\left(\frac{2\pi m}{P_y}\right)y}\left(\left(\nabla_t f_2(\bar{x})\times\hat{z}\right)(k_\rho^{\bar{n}}).\right.\right.$$
$$\left.\left[\frac{B_{\bar{n}}^{(l)}}{k_1}(-k_{z1}^{\bar{n}})^{N-l-1}e^{+ik_{z1}^{\bar{n}}d}+\frac{D_{\bar{n}}^{(l)}}{k_1}(+k_{z1}^{\bar{n}})^{N-l-1}e^{-ik_{z1}^{\bar{n}}d}\right.\right.$$
$$\left.\left.\left.-\frac{\delta_{\bar{n}}^{(l)}}{k_2}(-k_{z2}^{\bar{n}})^{N-l-1}e^{+ik_{z2}^{\bar{n}}d}\right]\right)\right) \tag{3.23}$$

$S_{H_2}^{(N)}(\bar{x})$ can be defined using the fourth boundary condition as:

$$\sum_{\bar{n}} e^{i\left(\frac{2\pi n}{P_x}\right)x+i\left(\frac{2\pi m}{P_y}\right)y}\left(\left(\hat{z}\times\hat{h}_{\bar{n}}\right)\left[\frac{B_{\bar{n}}^{(N)}}{\eta_1}e^{+ik_{z1}^{\bar{n}}d}+\frac{D_{\bar{n}}^{(N)}}{\eta_1}e^{-ik_{z1}^{\bar{n}}d}-\frac{\delta_{\bar{n}}^{(N)}}{\eta_2}e^{+ik_{z2}^{\bar{n}}d}\right]\right.$$
$$\left.+\left(\hat{h}_{\bar{n}}\right)\left[\frac{k_{z1}^{\bar{n}}}{k_1\eta_1}A_{\bar{n}}^{(N)}e^{+ik_{z1}^{\bar{n}}d}-\frac{k_{z1}^{\bar{n}}}{k_1\eta_1}C_{\bar{n}}^{(N)}e^{-ik_{z1}^{\bar{n}}d}-\frac{k_{z2}^{\bar{n}}}{k_2\eta_2}\gamma_{\bar{n}}^{(N)}e^{+ik_{z2}^{\bar{n}}d}\right]\right)$$

$$= S_{H_2}^{(N)}(\bar{x})$$

$$= -\sum_{l=0}^{N-1}\frac{(i(z+d))^{N-l}}{(N-l)!}\left(\sum_{\bar{n}} e^{i\left(\frac{2\pi n}{P_x}\right)x+i\left(\frac{2\pi m}{P_y}\right)y}\left(\left(\hat{z}\times\hat{h}_{\bar{n}}\right)\left[\frac{B_{\bar{n}}^{(l)}}{\eta_1}(-k_{z1}^{\bar{n}})^{(N-l)}e^{+ik_{z1}^{\bar{n}}d}\right.\right.\right.$$

$$+\frac{D_{\bar{n}}^{(l)}}{\eta_1}(+k_{z1}^{\bar{n}})^{(N-l)}e^{-ik_{z1}^{\bar{n}}d}-\frac{\delta_{\bar{n}}^{(l)}}{\eta_2}(-k_{z2}^{\bar{n}})^{(N-l)}e^{+ik_{z2}^{\bar{n}}d}\Bigg]$$

$$+\left(\hat{h}_{\bar{n}}\right)\Bigg[\frac{k_{z1}^{\bar{n}}}{k_1\eta_1}A_{\bar{n}}^{(l)}(-k_{z1}^{\bar{n}})^{(N-l)}e^{+ik_{z1}^{\bar{n}}d}-\frac{k_{z1}^{\bar{n}}}{k_1\eta_1}C_{\bar{n}}^{(l)}(+k_{z1}^{\bar{n}})^{(N-l)}e^{-ik_{z1}^{\bar{n}}d}$$

$$-\frac{k_{z2}^{\bar{n}}}{k_2\eta_2}\gamma_{\bar{n}}^{(l)}(-k_{z2}^{\bar{n}})^{(N-l)}e^{+ik_{z2}^{\bar{n}}d}\Bigg]\Bigg)\Bigg)$$

$$+\sum_{l=0}^{N-1}\frac{(i(z+d))^{N-l-1}}{(N-l-1)!}\Bigg(\sum_{\bar{n}}e^{i\left(\frac{2\pi n}{P_x}\right)x+i\left(\frac{2\pi m}{P_y}\right)y}\Bigg((\nabla_t f_2(\bar{x})\times\hat{z})\,(k_\rho^{\bar{n}}).$$

$$\cdot\Bigg[-\frac{A_{\bar{n}}^{(l)}}{k_1\eta_1}(-k_{z1}^{\bar{n}})^{N-l-1}e^{+ik_{z1}^{\bar{n}}d}-\frac{C_{\bar{n}}^{(l)}}{k_1\eta_1}(+k_{z1}^{\bar{n}})^{N-l-1}e^{-ik_{z1}^{\bar{n}}d}$$

$$+\frac{\gamma_{\bar{n}}^{(l)}}{k_2\eta_2}(-k_{z2}^{\bar{n}})^{N-l-1}e^{+ik_{z2}^{\bar{n}}d}\Bigg]\Bigg)\Bigg) \tag{3.24}$$

3.5 Solution of the Unknowns

Applying the 2-D Fourier operator to the N^{th} order forcing functions, one obtains the following eight equations, each of which involves only three of the N^{th} order unknowns. These equations can grouped into two sets of four equations, involving horizontal and vertical polarized terms. For horizontal terms $\xi=\{\alpha,A,C,\gamma\}$:

$$\begin{aligned}
\left(\hat{z}\times\hat{h}_{\bar{n}'}\right)\cdot\mathcal{F}\left(S_{E_1}^{(N)}(\bar{x})\right)_{\bar{n}'} &= \alpha_{\bar{n}'}^{(N)}-A_{\bar{n}'}^{(N)}-C_{\bar{n}'}^{(N)}\\
\left(\hat{h}_{\bar{n}'}\right)\cdot\mathcal{F}\left(S_{H_1}^{(N)}(\bar{x})\right)_{\bar{n}'} &= -\frac{k_{z0}^{\bar{n}'}}{k_0\eta_0}\alpha_{\bar{n}'}^{(N)}-\frac{k_{z1}^{\bar{n}'}}{k_1\eta_1}A_{\bar{n}'}^{(N)}+\frac{k_{z1}^{\bar{n}'}}{k_1\eta_1}C_{\bar{n}'}^{(N)}\\
\left(\hat{z}\times\hat{h}_{\bar{n}'}\right)\cdot\mathcal{F}\left(S_{E_2}^{(N)}(\bar{x})\right)_{\bar{n}'} &= A_{\bar{n}'}^{(N)}e^{+ik_{z1}^{\bar{n}'}d}+C_{\bar{n}'}^{(N)}e^{-ik_{z1}^{\bar{n}'}d}-\gamma_{\bar{n}'}^{(N)}e^{+ik_{z2}^{\bar{n}'}d}\\
\left(\hat{h}_{\bar{n}'}\right)\cdot\mathcal{F}\left(S_{H_2}^{(N)}(\bar{x})\right)_{\bar{n}'} &= \frac{k_{z1}^{\bar{n}'}}{k_1\eta_1}A_{\bar{n}'}^{(N)}e^{+ik_{z1}^{\bar{n}'}d}-\frac{k_{z1}^{\bar{n}'}}{k_1\eta_1}C_{\bar{n}'}^{(N)}e^{-ik_{z1}^{\bar{n}'}d}\\
&\quad -\frac{k_{z2}^{\bar{n}'}}{k_2\eta_2}\gamma_{\bar{n}'}^{(N)}e^{+ik_{z2}^{\bar{n}'}d}
\end{aligned} \tag{3.25}$$

For vertical terms $\zeta = \{\beta, B, D, \delta\}$:

$$\begin{aligned}
\left(\hat{h}_{\bar{n}'}\right) \cdot \mathcal{F}\left(S_{E_1}^{(N)}(\bar{x})\right)_{\bar{n}'} &= \frac{k_{z0}^{\bar{n}'}}{k_0}\beta_{\bar{n}'}^{(N)} + \frac{k_{z1}^{\bar{n}'}}{k_1}B_{\bar{n}'}^{(N)} - \frac{k_{z1}^{\bar{n}'}}{k_1}D_{\bar{n}'}^{(N)} \\
\left(\hat{z} \times \hat{h}_{\bar{n}'}\right) \cdot \mathcal{F}\left(S_{H_1}^{(N)}(\bar{x})\right)_{\bar{n}'} &= \frac{\beta_{\bar{n}'}^{(N)}}{\eta_0} - \frac{B_{\bar{n}'}^{(N)}}{\eta_1} - \frac{D_{\bar{n}'}^{(N)}}{\eta_1} \\
\left(\hat{h}_{\bar{n}'}\right) \cdot \mathcal{F}\left(S_{E_2}^{(N)}(\bar{x})\right)_{\bar{n}'} &= -\frac{k_{z1}^{\bar{n}'}}{k_1}B_{\bar{n}'}^{(N)}e^{+ik_{z1}^{\bar{n}'}d} + \frac{k_{z1}^{\bar{n}'}}{k_1}D_{\bar{n}'}^{(N)}e^{-ik_{z1}^{\bar{n}'}d} + \frac{k_{z2}^{\bar{n}'}}{k_2}\delta_{\bar{n}'}^{(N)}e^{+ik_{z2}^{\bar{n}'}d} \\
\left(\hat{z} \times \hat{h}_{\bar{n}'}\right) \cdot \mathcal{F}\left(S_{H_2}^{(N)}(\bar{x})\right)_{\bar{n}'} &= \frac{B_{\bar{n}'}^{(N)}}{\eta_1}e^{+ik_{z1}^{\bar{n}'}d} + \frac{D_{\bar{n}'}^{(N)}}{\eta_1}e^{-ik_{z1}^{\bar{n}'}d} - \frac{\delta_{\bar{n}'}^{(N)}}{\eta_2}e^{+ik_{z2}^{\bar{n}'}d}
\end{aligned} \tag{3.26}$$

At this point, putting these equations into two 4×4 matrix form can be a logical approach to solve them. Leaving the Fourier transforms of the forcing functions on the right side, the following matrix representation can be considered.

$$M_\xi(\bar{n}') = \begin{bmatrix}
1 & -1 & -1 & 0 \\
\frac{-k_{z0}^{\bar{n}'}}{k_0\eta_0} & \frac{-k_{z1}^{\bar{n}'}}{k_1\eta_1} & \frac{k_{z1}^{\bar{n}'}}{k_1\eta_1} & 0 \\
0 & e^{+ik_{z1}^{\bar{n}'}d} & e^{-ik_{z1}^{\bar{n}'}d} & -e^{+ik_{z2}^{\bar{n}'}d} \\
0 & \frac{k_{z1}^{\bar{n}'}e^{+ik_{z1}^{\bar{n}'}d}}{k_1\eta_1} & \frac{-k_{z1}^{\bar{n}'}e^{-ik_{z1}^{\bar{n}'}d}}{k_1\eta_1} & \frac{-k_{z2}^{\bar{n}'}e^{+ik_{z2}^{\bar{n}'}d}}{k_2\eta_2}
\end{bmatrix} \tag{3.27}$$

$$M_\zeta(\bar{n}') = \begin{bmatrix}
\frac{k_{z0}^{\bar{n}'}}{k_0} & \frac{k_{z1}^{\bar{n}'}}{k_1} & \frac{-k_{z1}^{\bar{n}'}}{k_1} & 0 \\
\frac{1}{\eta_0} & \frac{-1}{\eta_1} & \frac{-1}{\eta_1} & 0 \\
0 & \frac{-k_{z1}^{\bar{n}'}e^{+ik_{z1}^{\bar{n}'}d}}{k_1} & \frac{k_{z1}^{\bar{n}'}e^{-ik_{z1}^{\bar{n}'}d}}{k_1} & \frac{k_{z2}^{\bar{n}'}e^{+ik_{z2}^{\bar{n}'}d}}{k_2} \\
0 & \frac{e^{+ik_{z1}^{\bar{n}'}d}}{\eta_1} & \frac{e^{-ik_{z1}^{\bar{n}'}d}}{\eta_1} & \frac{-e^{+ik_{z2}^{\bar{n}'}d}}{\eta_2}
\end{bmatrix} \tag{3.28}$$

The unknowns, or the scattered field amplitudes can be put in the following array form:

$$\bar{\xi}^{(N)}(\bar{n}') = \begin{bmatrix} \alpha_{\bar{n}'}^{(N)} \\ A_{\bar{n}'}^{(N)} \\ C_{\bar{n}'}^{(N)} \\ \gamma_{\bar{n}'}^{(N)} \end{bmatrix}, \qquad \bar{\zeta}^{(N)}(\bar{n}') = \begin{bmatrix} \beta_{\bar{n}'}^{(N)} \\ B_{\bar{n}'}^{(N)} \\ D_{\bar{n}'}^{(N)} \\ \delta_{\bar{n}'}^{(N)} \end{bmatrix} \tag{3.29}$$

Finally the right hand sides can also be put in the following array form:

$$\bar{b}_\xi(\bar{n}') = \begin{bmatrix}
\left(\hat{z} \times \hat{h}_{\bar{n}'}\right) . \mathcal{F}\left(S_{E_1}^{(N)}(\bar{x})\right)_{\bar{n}'} \\
\left(\hat{h}_{\bar{n}'}\right) . \mathcal{F}\left(S_{H_1}^{(N)}(\bar{x})\right)_{\bar{n}'} \\
\left(\hat{z} \times \hat{h}_{\bar{n}'}\right) . \mathcal{F}\left(S_{E_2}^{(N)}(\bar{x})\right)_{\bar{n}'} \\
\left(\hat{h}_{\bar{n}'}\right) . \mathcal{F}\left(S_{H_2}^{(N)}(\bar{x})\right)_{\bar{n}'}
\end{bmatrix}, \qquad \bar{b}_\zeta(\bar{n}') = \begin{bmatrix}
\left(\hat{h}_{\bar{n}'}\right) . \mathcal{F}\left(S_{E_1}^{(N)}(\bar{x})\right)_{\bar{n}'} \\
\left(\hat{z} \times \hat{h}_{\bar{n}'}\right) . \mathcal{F}\left(S_{H_1}^{(N)}(\bar{x})\right)_{\bar{n}'} \\
\left(\hat{h}_{\bar{n}'}\right) . \mathcal{F}\left(S_{E_2}^{(N)}(\bar{x})\right)_{\bar{n}'} \\
\left(\hat{z} \times \hat{h}_{\bar{n}'}\right) . \mathcal{F}\left(S_{H_2}^{(N)}(\bar{x})\right)_{\bar{n}'}
\end{bmatrix} \tag{3.30}$$

With these definitions, the solution of the N^{th} order unknowns reduces to the following matrix inversion problem:

$$\left.\begin{array}{l} M_\xi \bar{\xi} = \bar{b}_\xi \\ M_\zeta \bar{\zeta} = \bar{b}_\zeta \end{array}\right\} \qquad \Longrightarrow \qquad \begin{array}{l} \bar{\xi} = M_\xi^{-1} \bar{b}_\xi \\ \bar{\zeta} = M_\zeta^{-1} \bar{b}_\zeta \end{array} \tag{3.31}$$

The inverses of matrices M, can be given in the following convenient form:

$$M_\xi^{-1} = \begin{bmatrix} K_{E1}^{\alpha} & K_{H1}^{\alpha} & K_{E2}^{\alpha} & K_{H2}^{\alpha} \\ K_{E1}^{A} & K_{H1}^{A} & K_{E2}^{A} & K_{H2}^{A} \\ K_{E1}^{C} & K_{H1}^{C} & K_{E2}^{C} & K_{H2}^{C} \\ K_{E1}^{\gamma} & K_{H1}^{\gamma} & K_{E2}^{\gamma} & K_{H2}^{\gamma} \end{bmatrix}, \quad M_\zeta^{-1} = \begin{bmatrix} K_{E1}^{\beta} & K_{H1}^{\beta} & K_{E2}^{\beta} & K_{H2}^{\beta} \\ K_{E1}^{B} & K_{H1}^{B} & K_{E2}^{B} & K_{H2}^{B} \\ K_{E1}^{D} & K_{H1}^{D} & K_{E2}^{D} & K_{H2}^{D} \\ K_{E1}^{\delta} & K_{H1}^{\delta} & K_{E2}^{\delta} & K_{H2}^{\delta} \end{bmatrix} \tag{3.32}$$

We are going the define each individual term $K_{E,H}$ separately, later in the section. But for now, we can proceed to the solution in terms of these terms as follows: For horizontal terms $\xi = \{\alpha, A, C, \gamma\}$ we have:

$$\begin{aligned} \xi_{\bar{n}'}^{(N)} &= \left(\hat{z} \times \hat{h}_{\bar{n}'}\right) . \left[K_{E1}^{\xi}(\bar{n}') \mathcal{F}\left(S_{E_1}^{(N)}(\bar{x})\right)_{\bar{n}'} + K_{E2}^{\xi}(\bar{n}') \mathcal{F}\left(S_{E_2}^{(N)}(\bar{x})\right)_{\bar{n}'}\right] \\ &\quad \left(\hat{h}_{\bar{n}'}\right) . \left[K_{H1}^{\xi}(\bar{n}') \mathcal{F}\left(S_{H_1}^{(N)}(\bar{x})\right)_{\bar{n}'} + K_{H2}^{\xi}(\bar{n}') \mathcal{F}\left(S_{H_2}^{(N)}(\bar{x})\right)_{\bar{n}'}\right] \end{aligned} \tag{3.33}$$

and for vertical terms $\zeta = \{\beta, B, D, \delta\}$ we have:

$$\begin{aligned} \zeta_{\bar{n}'}^{(N)} &= \left(\hat{h}_{\bar{n}'}\right) . \left[K_{E1}^{\zeta}(\bar{n}') \mathcal{F}\left(S_{E_1}^{(N)}(\bar{x})\right)_{\bar{n}'} + K_{E2}^{\zeta}(\bar{n}') \mathcal{F}\left(S_{E_2}^{(N)}(\bar{x})\right)_{\bar{n}'}\right] \\ &\quad \left(\hat{z} \times \hat{h}_{\bar{n}'}\right) . \left[K_{H1}^{\zeta}(\bar{n}') \mathcal{F}\left(S_{H_1}^{(N)}(\bar{x})\right)_{\bar{n}'} + K_{H2}^{\zeta}(\bar{n}') \mathcal{F}\left(S_{H_2}^{(N)}(\bar{x})\right)_{\bar{n}'}\right] \end{aligned} \tag{3.34}$$

Before defining functions of type $K_{E,H}$, to reduce the complexity of the expressions, it will be convenient to define the following variables:

$$\begin{aligned} P_q^{\bar{n}'} &= \frac{k_{zq}^{\bar{n}'}}{k_q \eta_q}, \qquad R_q^{\bar{n}'} = e^{ik_{zq}^{\bar{n}'} d}, \qquad Q_{\bar{n}'}^{\mp} = 1 \mp e^{i2k_{z1}^{\bar{n}'} d} \\ D_H^{\bar{n}'} &= P_1^{\bar{n}'} \left(P_0^{\bar{n}'} + P_2^{\bar{n}'}\right) Q_{\bar{n}'}^{+} + \left((P_1^{\bar{n}'})^2 + P_0^{\bar{n}'} P_2^{\bar{n}'}\right) Q_{\bar{n}'}^{-} \\ D_V^{\bar{n}'} &= P_1^{\bar{n}'} \left(\frac{P_0^{\bar{n}'} \eta_0}{\eta_2} + \frac{P_2^{\bar{n}'} \eta_2}{\eta_0}\right) Q_{\bar{n}'}^{+} + \left(\frac{(P_1^{\bar{n}'} \eta_1)^2}{\eta_0 \eta_2} + \frac{P_0^{\bar{n}'} P_2^{\bar{n}'} \eta_0 \eta_2}{(\eta_1)^2}\right) Q_{\bar{n}'}^{-} \end{aligned} \tag{3.35}$$

In terms of these variables, $K_{E,H}$ functions(arguments $(\bar{n}')$ is dropped for convenience) can be expresed as follows:

For α:

$$\begin{aligned} K^{\alpha}_{E1} &= \frac{(P_1^{\bar{n}'})^2 Q^-_{\bar{n}'} + P_1^{\bar{n}'} P_2^{\bar{n}'} Q^+_{\bar{n}'}}{D_H^{\bar{n}'}} \\ K^{\alpha}_{H1} &= \frac{-\left(P_1^{\bar{n}'} Q^+_{\bar{n}'} + P_2^{\bar{n}'} Q^-_{\bar{n}'}\right)}{D_H^{\bar{n}'}} \\ K^{\alpha}_{E2} &= \frac{2P_1^{\bar{n}'} P_2^{\bar{n}'} R_1^{\bar{n}'}}{D_H^{\bar{n}'}} \\ K^{\alpha}_{H2} &= \frac{-2P_1^{\bar{n}'} R_1^{\bar{n}'}}{D_H^{\bar{n}'}} \end{aligned} \tag{3.36}$$

and for A:

$$\begin{aligned} K^{A}_{E1} &= \frac{-P_0^{\bar{n}'}\left(P_1^{\bar{n}'} + P_2^{\bar{n}'}\right)}{D_H^{\bar{n}'}} \\ K^{A}_{H1} &= \frac{-\left(P_1^{\bar{n}'} + P_2^{\bar{n}'}\right)}{D_H^{\bar{n}'}} \\ K^{A}_{E2} &= \frac{P_2^{\bar{n}'}\left(P_1^{\bar{n}'} - P_0^{\bar{n}'}\right) R_1^{\bar{n}'}}{D_H^{\bar{n}'}} \\ K^{A}_{H2} &= \frac{-\left(P_1^{\bar{n}'} - P_0^{\bar{n}'}\right) R_1^{\bar{n}'}}{D_H^{\bar{n}'}} \end{aligned} \tag{3.37}$$

and for C:

$$\begin{aligned} K^{C}_{E1} &= \frac{\left(P_2^{\bar{n}'} - P_1^{\bar{n}'}\right) P_0^{\bar{n}'} (R_1^{\bar{n}'})^2}{D_H^{\bar{n}'}} \\ K^{C}_{H1} &= \frac{\left(P_2^{\bar{n}'} - P_1^{\bar{n}'}\right) (R_1^{\bar{n}'})^2}{D_H^{\bar{n}'}} \\ K^{C}_{E2} &= \frac{\left(P_1^{\bar{n}'} + P_0^{\bar{n}'}\right) P_2^{\bar{n}'} R_1^{\bar{n}'}}{D_H^{\bar{n}'}} \\ K^{C}_{H2} &= \frac{-\left(P_1^{\bar{n}'} + P_0^{\bar{n}'}\right) R_1^{\bar{n}'}}{D_H^{\bar{n}'}} \end{aligned} \tag{3.38}$$

and for γ:

$$K^{\gamma}_{E1} = \frac{-2P_0^{\bar{n}'} P_1^{\bar{n}'} R_1^{\bar{n}'}}{D_H^{\bar{n}'} R_2^{\bar{n}'}}$$

$$
\begin{aligned}
K^{\gamma}_{H1} &= \frac{-2P_1^{\bar{n}'}R_1^{\bar{n}'}}{D_H^{\bar{n}'}R_2^{\bar{n}'}} \\
K^{\gamma}_{E2} &= \frac{-(P_1^{\bar{n}'})^2 Q^-_{\bar{n}'} + P_1^{\bar{n}'}P_0^{\bar{n}'}Q^+_{\bar{n}'}}{D_H^{\bar{n}'}R_2^{\bar{n}'}} \\
K^{\gamma}_{H2} &= \frac{-\left(P_1^{\bar{n}'}Q^+_{\bar{n}'} + P_0^{\bar{n}'}Q^-_{\bar{n}'}\right)}{D_H^{\bar{n}'}R_2^{\bar{n}'}}
\end{aligned} \tag{3.39}
$$

Similarly, for β we have:

$$
\begin{aligned}
K^{\beta}_{E1} &= \frac{\eta_2\left(\frac{P_1^{\bar{n}'}Q^+_{\bar{n}'}}{\eta_2^2} + \frac{P_2^{\bar{n}'}Q^-_{\bar{n}'}}{\eta_1^2}\right)}{D_V^{\bar{n}'}} \\
K^{\beta}_{H1} &= \frac{P_1^{\bar{n}'}\left(P_1^{\bar{n}'}Q^-_{\bar{n}'}\eta_1^2 + P_2^{\bar{n}'}Q^+_{\bar{n}'}\eta_2^2\right)}{\eta_2 D_V^{\bar{n}'}} \\
K^{\beta}_{E2} &= \frac{2P_1^{\bar{n}'}R_1^{\bar{n}'}}{\eta_2 D_V^{\bar{n}'}} \\
K^{\beta}_{H2} &= \frac{2P_1^{\bar{n}'}P_2^{\bar{n}'}R_1^{\bar{n}'}\eta_2}{D_V^{\bar{n}'}}
\end{aligned} \tag{3.40}
$$

for B:

$$
\begin{aligned}
K^{B}_{E1} &= \frac{P_1^{\bar{n}'}\frac{\eta_1}{\eta_2} + P_2^{\bar{n}'}\frac{\eta_2}{\eta_1}}{\eta_0 D_V^{\bar{n}'}} \\
K^{B}_{H1} &= \frac{-\left(P_0^{\bar{n}'}P_1^{\bar{n}'}\frac{\eta_0\eta_1}{\eta_2} + P_0^{\bar{n}'}P_2^{\bar{n}'}\frac{\eta_0\eta_2}{\eta_1}\right)}{D_V^{\bar{n}'}} \\
K^{B}_{E2} &= \frac{\left(P_1^{\bar{n}'}\frac{\eta_1}{\eta_0} - P_0^{\bar{n}'}\frac{\eta_0}{\eta_1}\right)R_1^{\bar{n}'}}{\eta_2 D_V^{\bar{n}'}} \\
K^{B}_{H2} &= \frac{\left(P_2^{\bar{n}'}P_1^{\bar{n}'}\frac{\eta_2\eta_1}{\eta 0} - P_0^{\bar{n}'}P_2^{\bar{n}'}\frac{\eta_0\eta_2}{\eta 1}\right)R_1^{\bar{n}'}}{D_V^{\bar{n}'}}
\end{aligned} \tag{3.41}
$$

for D:

$$
\begin{aligned}
K^{D}_{E1} &= \frac{\left(P_1^{\bar{n}'}\frac{\eta_1}{\eta_2} - P_2^{\bar{n}'}\frac{\eta_2}{\eta_1}\right)(R_1^{\bar{n}'})^2}{\eta_0 D_V^{\bar{n}'}} \\
K^{D}_{H1} &= \frac{\left(P_0^{\bar{n}'}P_2^{\bar{n}'}\frac{\eta_0\eta_2}{\eta_1} - P_0^{\bar{n}'}P_1^{\bar{n}'}\frac{\eta_0\eta_1}{\eta_2}\right)(R_1^{\bar{n}'})^2}{D_V^{\bar{n}'}} \\
K^{D}_{E2} &= \frac{\left(P_0^{\bar{n}'}\frac{\eta_0}{\eta_1} + P_1^{\bar{n}'}\frac{\eta_1}{\eta_0}\right)R_1^{\bar{n}'}}{\eta_2 D_V^{\bar{n}'}} \\
K^{D}_{H2} &= \frac{P_2^{\bar{n}'}\eta_2\left(P_0^{\bar{n}'}\frac{\eta_0}{\eta_1} + P_1^{\bar{n}'}\frac{\eta_1}{\eta_0}\right)R_1^{\bar{n}'}}{D_V^{\bar{n}'}}
\end{aligned} \tag{3.42}
$$

for δ:

$$\begin{aligned}
K^{\delta}_{E1} &= \frac{2P_1^{\bar{n}'}R_1^{\bar{n}'}}{\eta_0 D_V^{\bar{n}'}R_2^{\bar{n}'}} \\
K^{\delta}_{H1} &= \frac{-2P_0^{\bar{n}'}P_1^{\bar{n}'}R_1^{\bar{n}'}\eta_0}{D_V^{\bar{n}'}R_2^{\bar{n}'}} \\
K^{\delta}_{E2} &= \frac{P_0^{\bar{n}'}Q^{-}_{\bar{n}'}\frac{\eta_0}{\eta_1} + P_1^{\bar{n}'}Q^{+}_{\bar{n}'}\frac{\eta_1}{\eta_0}}{\eta_1 D_V^{\bar{n}'}R_2^{\bar{n}'}} \\
K^{\delta}_{H2} &= \frac{-P_1^{\bar{n}'}\eta_1\left(P_0^{\bar{n}'}Q^{+}_{\bar{n}'}\frac{\eta_0}{\eta_1} + P_1^{\bar{n}'}Q^{-}_{\bar{n}'}\frac{\eta_1}{\eta_0}\right)}{D_V^{\bar{n}'}R_2^{\bar{n}'}}
\end{aligned} \tag{3.43}$$

The derivations up to this point include all of the necessary ingredients to obtain a numerical solution for the two layer problem. Also known as a Fourier Rayleigh approach, Equation 3.33 can be easily implemented with an FFT based algorithm, which can solve the equations up to any order. Although we are mostly interested in an analytical solution procedure of arbitrary order, having a numerical solution is very helpful for verification purposes. In the next section, this numerical solution will be tested against an existing two and a half dimensional EBC solution for two sine surfaces on top of each other, for several example cases.

3.6 Verification

In order to verify the numerical SPM solution, described in the previous sections, a test setup, consisting of two sine waves for the lower and upper interfaces had been considered. The upper and lower interfaces are assumed to be in the following form:

$$\begin{aligned}
f_1(\bar{x}) &= A_1 \sin(\frac{2\pi}{P_x}x) \\
f_2(\bar{x}) &= -d + A_2 \sin(\frac{2\pi}{P_x}x)
\end{aligned} \tag{3.44}$$

so that the Fourier coefficients can be given as:

$$h^{(1)}_{\bar{n}} = \frac{A_1}{2j}\delta_m\delta_{n-1} - \frac{A_1}{2j}\delta_m\delta_{n+1}$$

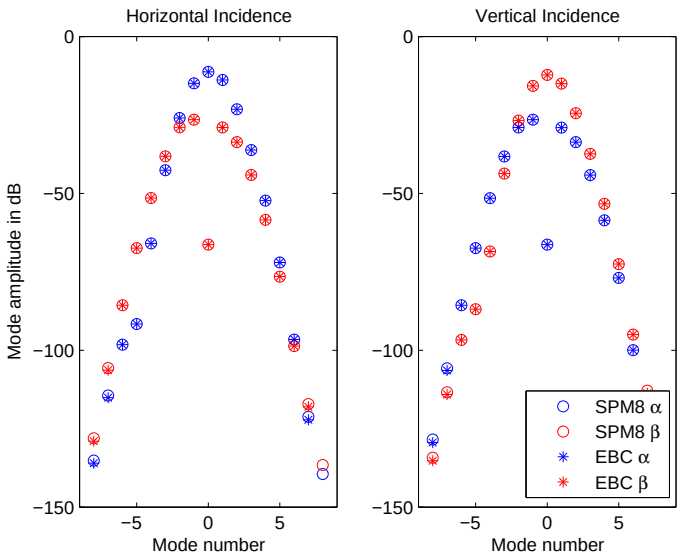

Figure 3.3: Comparison against EBC: Amplitude of the scattering coefficients α and β (in dB) plotted versus mode number: $\theta_i = 20, \phi_i = 45, \epsilon_1 = 9, \epsilon_2 = 4, d = 2\lambda, A_1 = A_2 = 0.1\lambda, P_x = 10\lambda$

$$h_{\bar{n}}^{(2)} = \frac{A_2}{2j}\delta_m\delta_{n-1} - \frac{A_2}{2j}\delta_m\delta_{n+1} \tag{3.45}$$

where δ is Kronecker's' delta function, which should not be confused with the scattering coefficient δ.

For several experimental setups, numerical SPM solution at 8^{th} order is compared against an existing two and a half dimensional EBC code [74]. The comparison is done in the propagating modes, in a similar fashion with the previous chapter. The horizontal axis is reserved for the mode number, while the vertical axis presents the amplitudes of the reflected field scattering coefficients in dB. Each figure has two subfigures, for horizontal and vertical incidence cases respectively. The electromagnetic radiation wavelength is assumed to be $1m$ for all of the results.

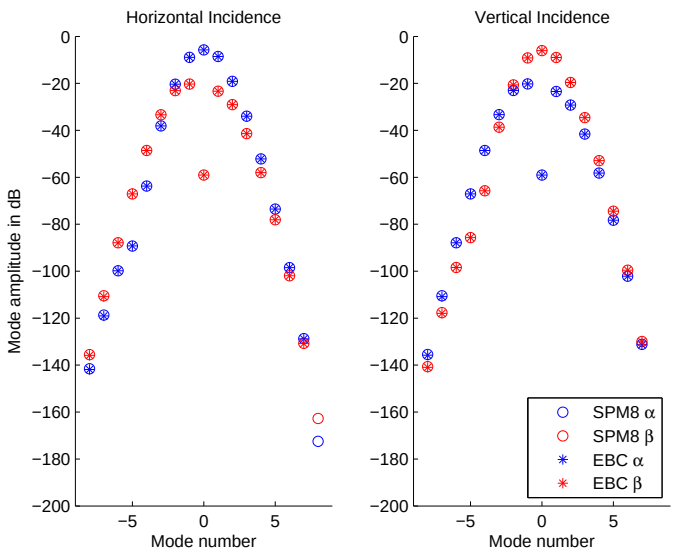

Figure 3.4: Comparison against EBC: Amplitude of the scattering coefficients α and β (in dB) plotted versus mode number: $\theta_i = 20, \phi_i = 45, \epsilon_1 = 3+i25, \epsilon_2 = 32+i9, d = 2\lambda, A_1 = A_2 = 0.1\lambda, P_x = 10\lambda$

First result considered here, given in Figure 3.3, is a lossless media example, with dielectric permittivities: $\epsilon_0 = 1$ for top region, $\epsilon_1 = 9$ for intermediate region and $\epsilon_2 = 4$ for the bottom region. All the three regions are assumed to be non-magnetic. The period of the sinusoidal surfaces is assumed to be $P_x = 10\lambda$. The amplitudes of both upper and lower interfaces is assumed to be $A_1 = A_2 = 0.1\lambda$ and the separation between the interfaces is set to $d = 2\lambda$. The incidence angles are assumed to be $\theta_i = 20°$ and $\phi_i = 45°$. Especially for the lower order modes a perfect match is observed between the methods. For the higher order modes, slight differences can be observed, which is due to the number of contributions to the corresponding mode. For the second result, given in Figure 3.4, parameters of the first result other than the dielectric permittivities are kept unchanged. Instead, a lossy case is considered

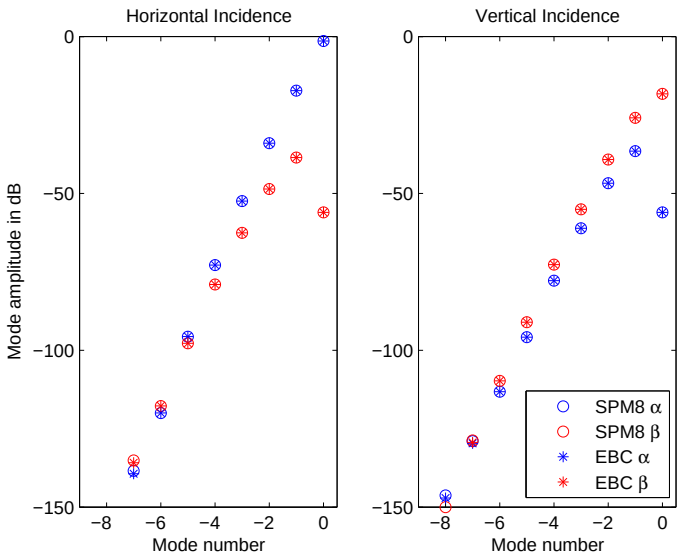

Figure 3.5: Comparison against EBC: Amplitude of the scattering coefficients α and β (in dB) plotted versus mode number: $\theta_i = 75, \phi_i = 30, \epsilon_1 = 9, \epsilon_2 = 4, d = 2\lambda, A_1 = A_2 = 0.1\lambda, P_x = 10\lambda$

with: $\epsilon_1 = 3 + i25$ for the intermediate region and $\epsilon_2 = 32 + i9$ for the bottom region. And again, close to perfect agreement is observed as in the previous case.

Next in Figure 3.5, again using the same lossless parameters as in the first case: ie. dielectric permittivities: $\epsilon_0 = 1$ for top region, $\epsilon_1 = 9$ for intermediate region and $\epsilon_2 = 4$, the periods of the sinusoidal surfaces are assumed to be $P_x = 10\lambda$, the amplitudes of both upper and lower interfaces are assumed to be $A_1 = A_2 = 0.1\lambda$ and the separation between the interfaces is set to $d = 2\lambda$. The incidence angles are assumed to be $\theta_i = 75°$ and $\phi_i = 30°$ here, which is smaller grazing angle value. As observed in Figure 3.5, no positive mode is propagating, and the models are in almost perfect agreement, especially in smaller modes.

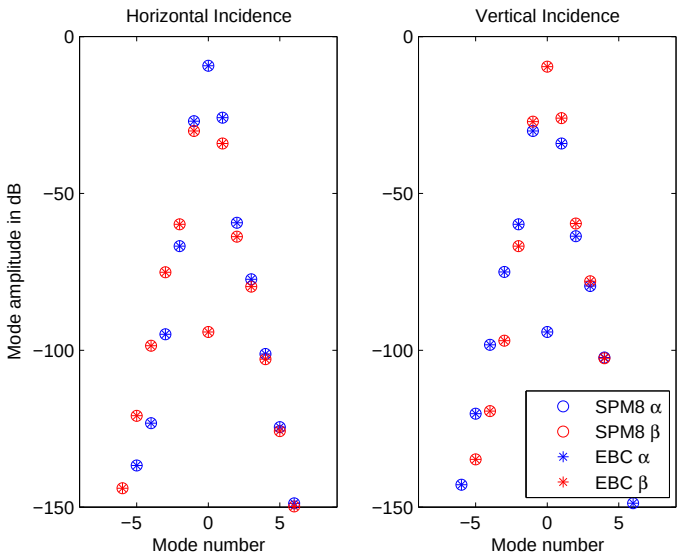

Figure 3.6: Comparison against EBC: Amplitude of the scattering coefficients α and β (in dB) plotted versus mode number: $\theta_i = 10, \phi_i = 60, \epsilon_1 = 9, \epsilon_2 = 4, d = 2\lambda, A_1 = 0.01\lambda, A_2 = 0.0001\lambda, P_x = 10\lambda$

Next two results, given Figures 3.6 and 3.7, are an investigation of the upper and lower surface amplitude effects. Again for the lossless media of the first result: dielectric permittivities: $\epsilon_0 = 1$ for top region, $\epsilon_1 = 9$ for intermediate region and $\epsilon_2 = 4$, periods of the sinusoidal surfaces are assumed to be $P_x = 10\lambda$, and the separation between the interfaces is set to $d = 2\lambda$. For incidence angles of $\theta_i = 10°$ and $\phi_i = 60°$, in Figure 3.6, the amplitude of the upper surface is set to $A_1 = 0.01\lambda$, while the amplitude of the lower surface is set to $A_2 = 0.0001\lambda$. Conversely in Figure 3.7, the surface amplitude values are switched: $A_1 = 0.0001\lambda$ and $A_2 = 0.01\lambda$. As the plots indicate, both methods agree well, in each case. It is also true that, the amplitudes are really small values here. An investigation of the convergence of the SPM solution for the higher surface amplitudes will considered in the next chapter.

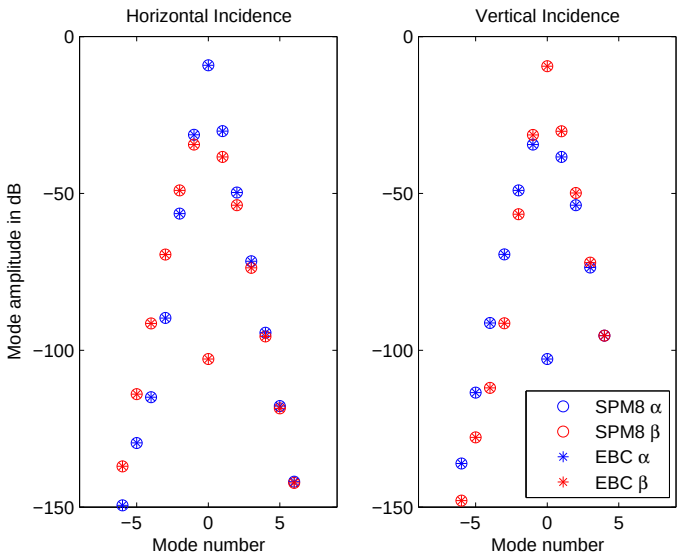

Figure 3.7: Comparison against EBC: Amplitude of the scattering coefficients α and β (in dB) plotted versus mode number: $\theta_i = 10, \phi_i = 60, \epsilon_1 = 9, \epsilon_2 = 4, d = 2\lambda, A_1 = 0.0001\lambda, A_2 = 0.01\lambda, P_x = 10\lambda$

Final two results, given in Figures 3.8 and 3.9, are a study of the effect of the separation of the surfaces. Here, the media of the first result is assumed: dielectric permittivities: $\epsilon_0 = 1$ for top region, $\epsilon_1 = 9$ for intermediate region and $\epsilon_2 = 4$, periods of the sinusoidal surfaces are assumed to be $P_x = 10\lambda$. The incidence angles are assumed to be normal: $\theta_i = 0^\circ$ and $\phi_i = 0^\circ$. In Figure 3.8, the separation parameter is assumed to be $d = 5\lambda$, and both methods are in good agreement, as in Figure 3.3. But in Figure 3.9, the separation parameter is assumed to be $d = 25\lambda$, and disagreement in higher mode numbers and in the cross pol. zeroth order modes can clearly be observed. Clearly this is an indication of the importance of the separation parameter d for the convergence of the overall SPM solutions.

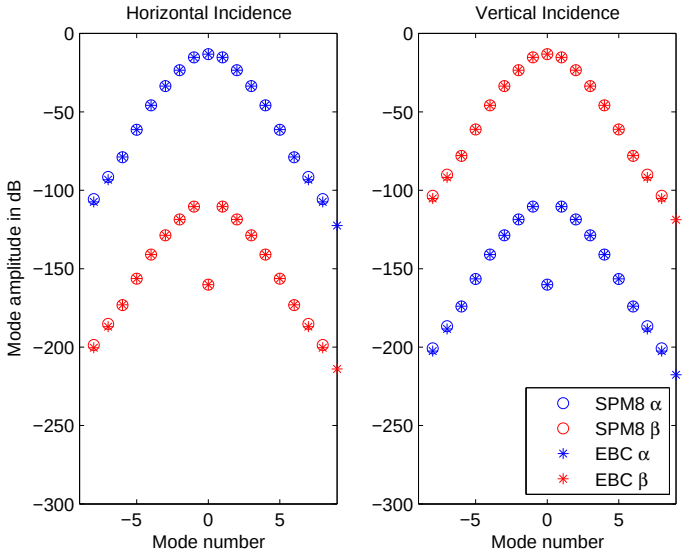

Figure 3.8: Comparison against EBC: Amplitude of the scattering coefficients α and β (in dB) plotted versus mode number: $\theta_i = 0, \phi_i = 0, \epsilon_1 = 9, \epsilon_2 = 4, d = 5\lambda, A_1 = A_2 = 0.1\lambda, P_x = 10\lambda$

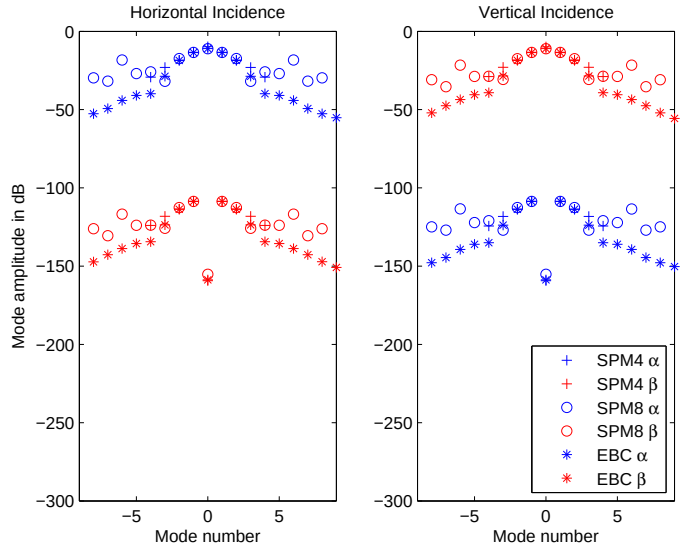

Figure 3.9: Comparison against EBC: Amplitude of the scattering coefficients α and β (in dB) plotted versus mode number: $\theta_i = 0, \phi_i = 0, \epsilon_1 = 9, \epsilon_2 = 4, d = 25\lambda, A_1 = A_2 = 0.1\lambda, P_x = 10\lambda$

3.7 Extension to arbitrary number of layers

In this section, the procedure followed in the previous sections for the two layer problem is generalized for the arbitrary number of layers case. First, the basic notational conventions are introduced. Later, without the derivation details, the forcing functions for each layer: (the top layer, the repeating intermediate layers and finally the bottom layer) are provided. Although, the arbitrary number of layers case is not considered in the rest of the dissertation, Equations of the form (3.25-3.26) are also included, which are sufficient for an arbitrary order, arbitrary layer, numerical solution. Such a solution is very useful for further studies on the subject.

An N-layer problem has N rough interfaces $z = -d_{(i)} + f_{(i)}(x, y)$, $i = 1, 2, ..., N$. It will be assumed that all of the surface functions are periodic with the same periods, P_x in $\hat{x}$ and P_y in $\hat{y}$ directions. We will also assume that the mean planes of the surfaces are located at $d_{(i)}$, with $d_{(1)} = 0$ and $d_{(i)} < d_{(i+1)}$ for all i. Distances between the mean planes of the surfaces are larger then the sum of maximum variations of each surface. A descriptive sketch of the problem is provided in Figure 3.10. The Fourier operator is defined as usual as given in Equation 3.1. Also the standard vector notation is also assumed: i.e. $\bar{n} = (n, m)$ and $\bar{x} = (x, y)$.

The regions are numbered (i.e. $q = 0, 1, 2, ..., N$) and relevant parameters for each region are labeled accordingly: dielectric permittivity of region 7 is ϵ_7, wave impedance of region 4 is η_4, etc. Also a $+$ or $-$ sign is associated with each vector parameter, representing a $+\hat{z}$ or $-\hat{z}$ propagation direction of the associated waves. The propagation directions in each layer, both for up and down going waves are defined as:

$$\vec{k}_{\bar{n}}^{q\pm} = k_{xn}\hat{x} + k_{ym}\hat{y} \pm k_{zq}^{\bar{n}}\hat{z} \tag{3.46}$$

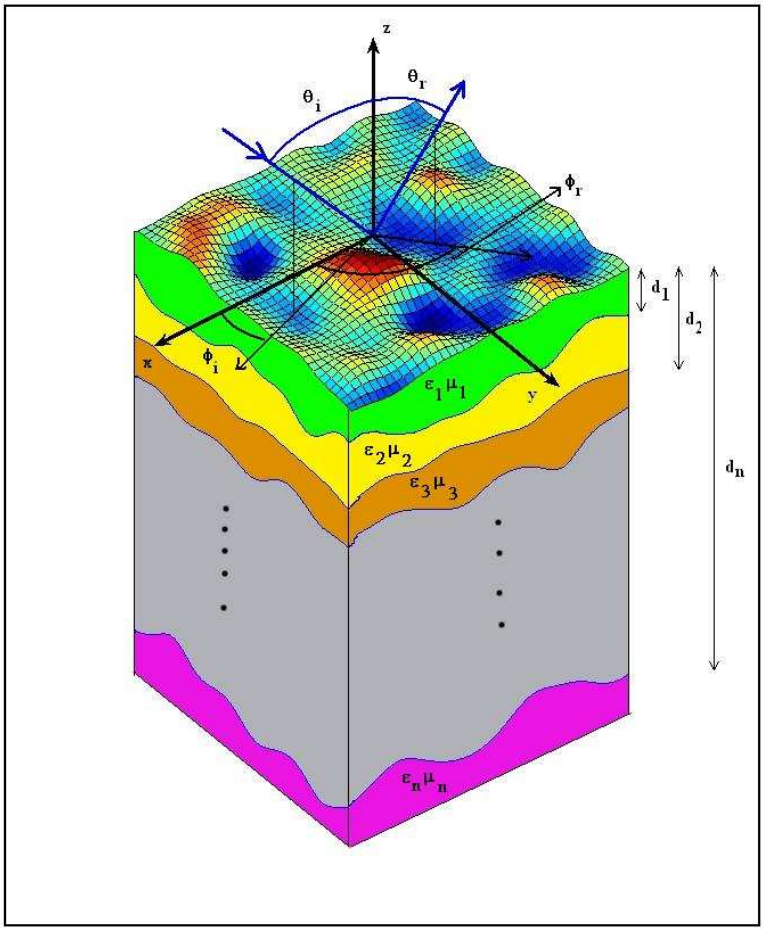

Figure 3.10: Problem Geometry of N-layer case

Here, as for the two layer case: $k_{xi} = k_0 \sin(\theta_i)\cos(\phi_i)$ and $k_{yi} = k_0 \sin(\theta_i)\sin(\phi_i)$. θ_i and ϕ_i are the incidence angles. Also, $k_{xn} = k_{x(n)} = k_{xi} + \frac{2\pi n}{P_x}$, $k_{ym} = k_{y(m)} = k_{yi} + \frac{2\pi m}{P_y}$ and $k_\rho^{\bar{n}} = \sqrt{k_{xn}^2 + k_{ym}^2}$, and for each layer we have $k_{zq}^{\bar{n}} = \sqrt{k_q^2 - (k_\rho^{\bar{n}})^2}$.

Using the same time dependence ($e^{-j\omega t}$), the incidence polarization vector $\hat{e}_i$ and the fields in Region 0 are identical to the expressions given in Equations 3.5 and 3.6: The fields in the intermediate regions can also be expressed: for Region q, $q = 1, 2, ..., N-1$:

$$\begin{aligned}
\vec{E}_q^- &= \sum_{\bar{n}} \left[\hat{h}_{\bar{n}} A_{q,\bar{n}} + \hat{v}_{q-}^{\bar{n}} B_{q,\bar{n}}\right] e^{j\vec{k}_{\bar{n}}^{q-}\cdot\vec{r}} \\
\vec{H}_q^- &= \frac{1}{\eta_q} \sum_{\bar{n}} \left[-\hat{v}_{q-}^{\bar{n}} A_{q,\bar{n}} + \hat{h}_{\bar{n}} B_{q,\bar{n}}\right] e^{j\vec{k}_{\bar{n}}^{q-}\cdot\vec{r}} \\
\vec{E}_q^+ &= \sum_{\bar{n}} \left[\hat{h}_{\bar{n}} C_{q,\bar{n}} + \hat{v}_{q+}^{\bar{n}} D_{q,\bar{n}}\right] e^{j\vec{k}_{\bar{n}}^{q+}\cdot\vec{r}} \\
\vec{H}_q^+ &= \frac{1}{\eta_q} \sum_{\bar{n}} \left[-\hat{v}_{q+}^{\bar{n}} C_{q,\bar{n}} + \hat{h}_{\bar{n}} D_{q,\bar{n}}\right] e^{j\vec{k}_{\bar{n}}^{q+}\cdot\vec{r}}
\end{aligned} \tag{3.47}$$

Fields of the lowest region are:

$$\begin{aligned}
\vec{E}_N^- &= \sum_{\bar{n}} \left[\hat{h}_{\bar{n}} \gamma_{\bar{n}} + \hat{v}_{N-}^{\bar{n}} \delta_{\bar{n}}\right] e^{j\vec{k}_{\bar{n}}^{N-}\cdot\vec{r}} \\
\vec{H}_N^- &= \frac{1}{\eta_N} \sum_{\bar{n}} \left[-\hat{v}_{N-}^{\bar{n}} \gamma_{\bar{n}} + \hat{h}_{\bar{n}} \delta_{\bar{n}}\right] e^{j\vec{k}_{\bar{n}}^{N-}\cdot\vec{r}}
\end{aligned} \tag{3.48}$$

Note that the reflected and transmitted field unknown scattering coefficients are named α, β, γ and δ as usual. The intermediate field coefficients of the two layer problem A, B, C and D are also utilized here with region index q. These coefficients are described in Figure 3.11. Polarization vectors for each region q are given by:

$$\begin{aligned}
\hat{h}_{\bar{n}} &= \frac{1}{k_\rho^{\bar{n}}} \left(k_{ym}\hat{x} - k_{xn}\hat{y}\right) \\
\hat{v}_{q\pm}^{\bar{n}} &= \mp \frac{k_{zq}^{\bar{n}}}{k_q k_\rho^{\bar{n}}} \left(k_{xn}\hat{x} + k_{ym}\hat{y}\right) + \frac{k_\rho^{\bar{n}}}{k_q}\hat{z}
\end{aligned} \tag{3.49}$$

The boundary conditions considered for the top and intermediate interfaces are:

$$\vec{n}_{(i)} \times \left[E_{(i-1)}^- + E_{(i-1)}^+\right] = \vec{n}_{(i)} \times \left[E_{(i)}^- + E_{(i)}^+\right] |_{z=f_{(i)}(\bar{x})}$$

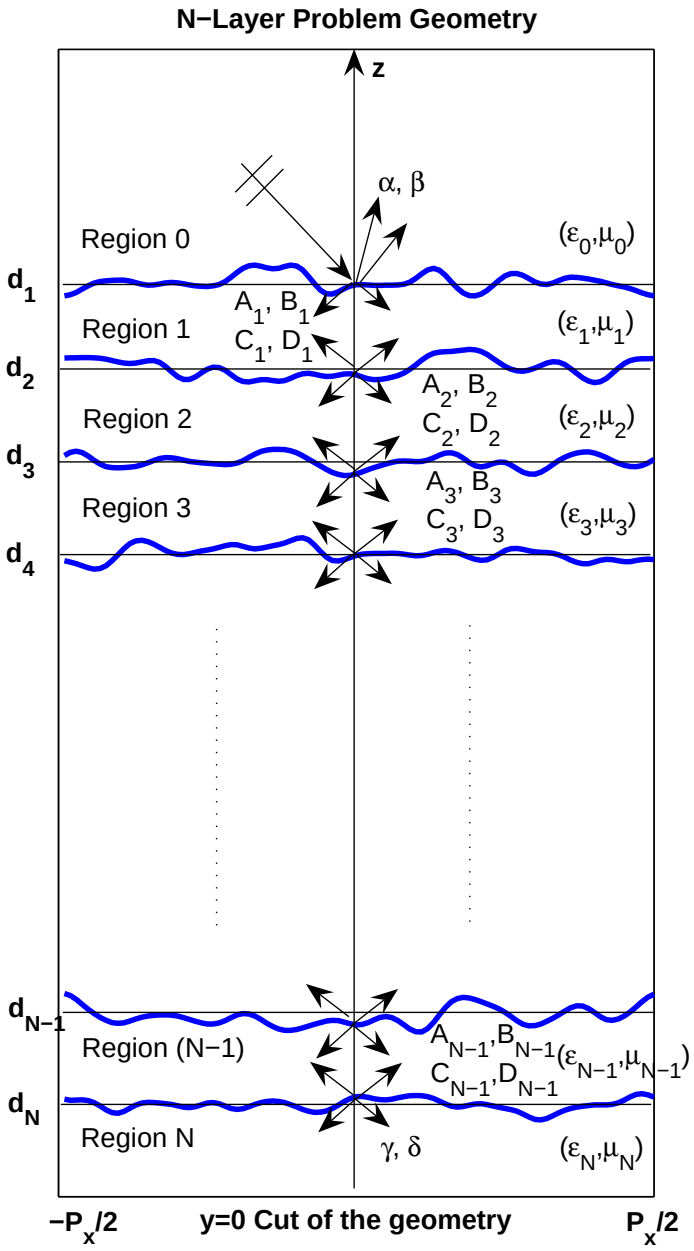

Figure 3.11: Two dimensional ($y = 0$) cross-section of the N-layer media. The unknown field coefficients are labeled in their domain of definition.

$$\vec{n}_{(i)} \times \left[H^{-}_{(i-1)} + H^{+}_{(i-1)}\right] \;=\; \vec{n}_{(i)} \times \left[H^{-}_{(i)} + H^{+}_{(i)}\right] |_{z=f_{(i)}(\bar{x})} \tag{3.50}$$

for $i = 1, 2, ..., (N-1)$, and for the last boundary we have:

$$\begin{aligned} \vec{n}_{(N)} \times \left[E^{-}_{(N-1)} + E^{+}_{(N-1)}\right] &= \vec{n}_{(N)} \times \left[E^{-}_{(N)}\right] |_{z=f_{(N)}(\bar{x})} \\ \vec{n}_{(N)} \times \left[H^{-}_{(N-1)} + H^{+}_{(N-1)}\right] &= \vec{n}_{(N)} \times \left[H^{-}_{(N)}\right] |_{z=f_{(N)}(\bar{x})} \end{aligned} \tag{3.51}$$

Here $\vec{n}_{(i)}$ is the normal of the surface $z = f_{(i)}(\bar{x})$, which is defined as follows:

$$\vec{n}_{(i)} = \hat{z} - \nabla_t f_{(i)}(\bar{x}) \tag{3.52}$$

Note that these boundary conditions are enforced for the $\hat{x}$ and $\hat{y}$ field components only.

There are a total of $2N$ forcing functions for the N-layer problem. In the two layer case, we have already studied 4 forcing functions, obtained from the top and the bottom interfaces. Those forcing functions are directly modified for the N-layer problem. In order to avoid confusion, the forcing functions are given for a solution of order M. According to the new formulation, the first forcing function is transformed into the following form:

$$\begin{aligned} S^{(M)}_{E_1}(\bar{x}) = &- \left(\hat{z} \times \hat{e}_i\right) \frac{(-ik_{zi}z)^M}{M!} + \left(\nabla_t f_1(\bar{x}) \times \hat{e}_i\right) \frac{(-ik_{zi}z)^{M-1}}{(M-1)!} \\ &- \sum_{l=0}^{M-1} \frac{(iz)^{M-l}}{(M-l)!} \left(\sum_{\bar{n}} e^{i\left(\frac{2\pi n}{P_x}\right)x + i\left(\frac{2\pi m}{P_y}\right)y} \left(\right.\right. \\ &\left(\hat{z} \times \hat{h}_{\bar{n}}\right) \left[\alpha^{(l)}_{\bar{n}} (k^{\bar{n}}_{z0})^{M-l} - A^{(l)}_{1,\bar{n}} (-k^{\bar{n}}_{z1})^{M-l} - C^{(l)}_{1,\bar{n}} (k^{\bar{n}}_{z1})^{M-l}\right] \\ &+ \left(\hat{h}_{\bar{n}}\right) \left[\frac{\beta^{(l)}_{\bar{n}}}{k_0} (k^{\bar{n}}_{z0})^{M-l+1} - \frac{B^{(l)}_{1,\bar{n}}}{k_1} (-k^{\bar{n}}_{z1})^{M-l+1} - \frac{D^{(l)}_{1,\bar{n}}}{k_1} (k^{\bar{n}}_{z1})^{M-l+1}\right] \left.\left.\right)\right) \\ &+ \sum_{l=0}^{M-1} \frac{(iz)^{M-l-1}}{(M-l-1)!} \left(\sum_{\bar{n}} e^{i\left(\frac{2\pi n}{P_x}\right)x + i\left(\frac{2\pi m}{P_y}\right)y} \left(\left(\nabla_t f_1(\bar{x}) \times \hat{z}\right) (k^{\bar{n}}_{\rho}). \right.\right. \end{aligned}$$

$$\cdot \left[\frac{\beta_{\bar{n}}^{(l)}}{k_0} (k_{z0}^{\bar{n}})^{M-l-1} - \frac{B_{1,\bar{n}}^{(l)}}{k_1} (-k_{z1}^{\bar{n}})^{M-l-1} - \frac{D_{1,\bar{n}}^{(l)}}{k_1} (k_{z1}^{\bar{n}})^{M-l-1} \right] \Bigg) \Bigg) \tag{3.53}$$

Similarly, the second one has the following form:

$$\begin{aligned}
S_{H_1}^{(M)}(\bar{x}) &= -\frac{1}{\eta_0} \left(\hat{z} \times \hat{k}_i \times \hat{e}_i \right) \frac{(-ik_{zi}z)^M}{M!} + \frac{1}{\eta_0} \left(\nabla_t f_1(\bar{x}) \times \hat{k}_i \times \hat{e}_i \right) \frac{(-ik_{zi}z)^{M-1}}{(M-1)!} \\
&- \sum_{l=0}^{M-1} \frac{(iz)^{M-l}}{(M-l)!} \Bigg(\sum_{\bar{n}} e^{i\left(\frac{2\pi n}{P_x}\right)x + i\left(\frac{2\pi m}{P_y}\right)y} \Bigg(\\
&\left(\hat{z} \times \hat{h}_{\bar{n}} \right) \left[\frac{\beta_{\bar{n}}^{(l)}}{\eta_0} (k_{z0}^{\bar{n}})^{M-l} - \frac{B_{1,\bar{n}}^{(l)}}{\eta_1} (-k_{z1}^{\bar{n}})^{M-l} - \frac{D_{1,\bar{n}}^{(l)}}{\eta_1} (k_{z1}^{\bar{n}})^{M-l} \right] \\
&+ \left(\hat{h}_{\bar{n}} \right) \left[-\frac{\alpha_{\bar{n}}^{(l)}}{k_0\eta_0} (k_{z0}^{\bar{n}})^{M-l+1} + \frac{A_{1,\bar{n}}^{(l)}}{k_1\eta_1} (-k_{z1}^{\bar{n}})^{M-l+1} + \frac{C_{1,\bar{n}}^{(l)}}{k_1\eta_1} (k_{z1}^{\bar{n}})^{M-l+1} \right] \Bigg) \Bigg) \\
&+ \sum_{l=0}^{M-1} \frac{(iz)^{M-l-1}}{(M-l-1)!} \Bigg(\sum_{\bar{n}} e^{i\left(\frac{2\pi n}{P_x}\right)x + i\left(\frac{2\pi m}{P_y}\right)y} \Bigg(\left(\nabla_t f_1(\bar{x}) \times \hat{z} \right) (k_\rho^{\bar{n}}). \\
&\cdot \left[-\frac{\alpha_{\bar{n}}^{(l)}}{k_0\eta_0} (k_{z0}^{\bar{n}})^{M-l-1} + \frac{A_{1,\bar{n}}^{(l)}}{k_1\eta_1} (-k_{z1}^{\bar{n}})^{M-l-1} + \frac{C_{1,\bar{n}}^{(l)}}{k_1\eta_1} (k_{z1}^{\bar{n}})^{M-l-1} \right] \Bigg) \Bigg)
\end{aligned} \tag{3.54}$$

The last two forcing functions are also modified: For the $(2N-1)^{th}$ forcing function:

$$\begin{aligned}
S_{E_N}^{(M)}(\bar{x}) &= -\sum_{l=0}^{M-1} \frac{(i(z+d_N))^{M-l}}{(M-l)!} \Bigg(\sum_{\bar{n}} e^{i\left(\frac{2\pi n}{P_x}\right)x + i\left(\frac{2\pi m}{P_y}\right)y} \Bigg(\\
&\left(\hat{z} \times \hat{h}_{\bar{n}} \right) \Bigg[A_{N-1,\bar{n}}^{(l)} (-k_{z(N-1)}^{\bar{n}})^{(M-l)} e^{+ik_{z(N-1)}^{\bar{n}} d_N} \\
&\qquad + C_{N-1,\bar{n}}^{(l)} (+k_{z(N-1)}^{\bar{n}})^{(M-l)} e^{-ik_{z(N-1)}^{\bar{n}} d_N} - \gamma_{\bar{n}}^{(l)} (-k_{zN}^{\bar{n}})^{(M-l)} e^{+ik_{zN}^{\bar{n}} d_N} \Bigg] \\
&+ \left(\hat{h}_{\bar{n}} \right) \Bigg[\frac{B_{N-1,\bar{n}}^{(l)}}{k_{N-1}} (-k_{z(N-1)}^{\bar{n}})^{(M-l+1)} e^{+ik_{z(N-1)}^{\bar{n}} d_N}
\end{aligned}$$

$$+\frac{D^{(l)}_{N-1,\bar{n}}}{k_{N-1}}(+k^{\bar{n}}_{z(N-1)})^{(M-l+1)}e^{-ik^{\bar{n}}_{z(N-1)}d_N}-\frac{\delta^{(l)}_{\bar{n}}}{k_N}(-k^{\bar{n}}_{zN})^{(M-l+1)}e^{+ik^{\bar{n}}_{zN}d_N}\Bigg]\Bigg)\Bigg)$$

$$+\sum_{l=0}^{M-1}\frac{(i(z+d_N))^{M-l-1}}{(M-l-1)!}\Bigg(\sum_{\bar{n}}e^{i\left(\frac{2\pi n}{P_x}\right)x+i\left(\frac{2\pi m}{P_y}\right)y}\Bigg((\nabla_t f_N(\bar{x})\times\hat{z})\,(k^{\bar{n}}_{\rho}).$$

$$\cdot\Bigg[\frac{B^{(l)}_{N-1,\bar{n}}}{k_{N-1}}(-k^{\bar{n}}_{z(N-1)})^{M-l-1}e^{+ik^{\bar{n}}_{z(N-1)}d_N}+\frac{D^{(l)}_{N-1,\bar{n}}}{k_{N-1}}(+k^{\bar{n}}_{z(N-1)})^{M-l-1}e^{-ik^{\bar{n}}_{z(N-1)}d_N}$$

$$-\frac{\delta^{(l)}_{\bar{n}}}{k_N}(-k^{\bar{n}}_{zN})^{M-l-1}e^{+ik^{\bar{n}}_{zN}d_N}\Bigg]\Bigg)\Bigg) \tag{3.55}$$

And for the $(2N)^{th}$ case:

$$S^{(M)}_{H_N}(\bar{x})=-\sum_{l=0}^{M-1}\frac{(i(z+d_N))^{M-l}}{(M-l)!}\Bigg(\sum_{\bar{n}}e^{i\left(\frac{2\pi n}{P_x}\right)x+i\left(\frac{2\pi m}{P_y}\right)y}\Bigg($$

$$\left(\hat{z}\times\hat{h}_{\bar{n}}\right)\Bigg[\frac{B^{(l)}_{N-1,\bar{n}}}{\eta_{N-1}}(-k^{\bar{n}}_{z(N-1)})^{(M-l)}e^{+ik^{\bar{n}}_{z(N-1)}d_N}$$

$$+\frac{D^{(l)}_{N-1,\bar{n}}}{\eta_{N-1}}(+k^{\bar{n}}_{z(N-1)})^{(M-l)}e^{-ik^{\bar{n}}_{z(N-1)}d_N}-\frac{\delta^{(l)}_{\bar{n}}}{\eta_N}(-k^{\bar{n}}_{zN})^{(M-l)}e^{+ik^{\bar{n}}_{zN}d_N}\Bigg]$$

$$+\left(\hat{h}_{\bar{n}}\right)\Bigg[-\frac{A^{(l)}_{N-1,\bar{n}}}{k_{N-1}\eta_{N-1}}(-k^{\bar{n}}_{z(N-1)})^{(M-l+1)}e^{+ik^{\bar{n}}_{z(N-1)}d_N}$$

$$-\frac{C^{(l)}_{N-1,\bar{n}}}{k_{N-1}\eta_{N-1}}(+k^{\bar{n}}_{z(N-1)})^{(M-l+1)}e^{-ik^{\bar{n}}_{z(N-1)}d_N}+\frac{\gamma^{(l)}_{\bar{n}}}{k_N\eta_N}(-k^{\bar{n}}_{zN})^{(M-l+1)}e^{+ik^{\bar{n}}_{zN}d_N}\Bigg]\Bigg)\Bigg)$$

$$+\sum_{l=0}^{M-1}\frac{(i(z+d_N))^{M-l-1}}{(M-l-1)!}\Bigg(\sum_{\bar{n}}e^{i\left(\frac{2\pi n}{P_x}\right)x+i\left(\frac{2\pi m}{P_y}\right)y}\Bigg((\nabla_t f_N(\bar{x})\times\hat{z})\,(k^{\bar{n}}_{\rho}).$$

$$\cdot\Bigg[-\frac{A^{(l)}_{N-1,\bar{n}}}{k_{N-1}\eta_{N-1}}(-k^{\bar{n}}_{z(N-1)})^{M-l-1}e^{+ik^{\bar{n}}_{z(N-1)}d_N}$$

$$-\frac{C^{(l)}_{N-1,\bar{n}}}{k_{N-1}\eta_{N-1}}(k^{\bar{n}}_{z(N-1)})^{M-l-1}e^{-ik^{\bar{n}}_{z(N-1)}d_N}+\frac{\gamma^{(l)}_{\bar{n}}}{k_N\eta_N}(-k^{\bar{n}}_{zN})^{M-l-1}e^{+ik^{\bar{n}}_{zN}d_N}\Bigg]\Bigg)\Bigg) \tag{3.56}$$

For each intermediate interface, we have two forcing functions, with identical forms. These forcing functions are:

$$
\begin{aligned}
S_{E_i}^{(M)}(\bar{x}) = &- \sum_{l=0}^{M-1} \frac{(i(z+d_i))^{M-l}}{(M-l)!} \left(\sum_{\bar{n}} e^{i\left(\frac{2\pi n}{P_x}\right)x + i\left(\frac{2\pi m}{P_y}\right)y} \left(\left(\hat{z} \times \hat{h}_{\bar{n}}\right) \right.\right. \\
&\left[A_{(i-1),\bar{n}}^{(l)} (-k_{z(i-1)}^{\bar{n}})^{(M-l)} e^{+ik_{z(i-1)}^{\bar{n}} d_i} + C_{(i-1),\bar{n}}^{(l)} (+k_{z(i-1)}^{\bar{n}})^{(M-l)} e^{-ik_{z(i-1)}^{\bar{n}} d_i} \right. \\
&\left. - A_{(i),\bar{n}}^{(l)} (-k_{z(i)}^{\bar{n}})^{(M-l)} e^{+ik_{z(i)}^{\bar{n}} d_i} - C_{(i),\bar{n}}^{(l)} (+k_{z(i)}^{\bar{n}})^{(M-l)} e^{-ik_{z(i)}^{\bar{n}} d_i} \right] \\
&+ \left(\hat{h}_{\bar{n}}\right) \left[\frac{B_{(i-1),\bar{n}}^{(l)}}{k_{(i-1)}} (-k_{z(i-1)}^{\bar{n}})^{(M-l+1)} e^{+ik_{z(i-1)}^{\bar{n}} d_i} + \frac{D_{(i-1),\bar{n}}^{(l)}}{k_{(i-1)}} (k_{z(i-1)}^{\bar{n}})^{(M-l+1)} e^{-ik_{z(i-1)}^{\bar{n}} d_i} \right. \\
&\left.\left. \left. - \frac{B_{(i),\bar{n}}^{(l)}}{k_{(i)}} (-k_{z(i)}^{\bar{n}})^{(M-l+1)} e^{+ik_{z(i)}^{\bar{n}} d_i} - \frac{D_{(i),\bar{n}}^{(l)}}{k_{(i)}} (k_{z(i)}^{\bar{n}})^{(M-l+1)} e^{-ik_{z(i)}^{\bar{n}} d_i} \right] \right) \right) \\
&+ \sum_{l=0}^{M-1} \frac{(i(z+d_i))^{M-l-1}}{(M-l-1)!} \left(\sum_{\bar{n}} e^{i\left(\frac{2\pi n}{P_x}\right)x + i\left(\frac{2\pi m}{P_y}\right)y} \left(\left(\nabla_t f_{(i)}(\bar{x}) \times \hat{z}\right)(k_\rho^{\bar{n}}). \right.\right. \\
&\cdot \left[\frac{B_{(i-1),\bar{n}}^{(l)}}{k_{(i-1)}} (-k_{z(i-1)}^{\bar{n}})^{(M-l-1)} e^{+ik_{z(i-1)}^{\bar{n}} d_i} + \frac{D_{(i-1),\bar{n}}^{(l)}}{k_{(i-1)}} (k_{z(i-1)}^{\bar{n}})^{(M-l-1)} e^{-ik_{z(i-1)}^{\bar{n}} d_i} \right. \\
&\left.\left. \left. - \frac{B_{(i),\bar{n}}^{(l)}}{k_{(i)}} (-k_{z(i)}^{\bar{n}})^{(M-l-1)} e^{+ik_{z(i)}^{\bar{n}} d_i} - \frac{D_{(i),\bar{n}}^{(l)}}{k_{(i)}} (k_{z(i)}^{\bar{n}})^{(M-l-1)} e^{-ik_{z(i)}^{\bar{n}} d_i} \right] \right) \right)
\end{aligned}
\tag{3.57}
$$

and

$$
\begin{aligned}
S_{H_i}^{(M)}(\bar{x}) = &- \sum_{l=0}^{M-1} \frac{(i(z+d_i))^{M-l}}{(M-l)!} \left(\sum_{\bar{n}} e^{i\left(\frac{2\pi n}{P_x}\right)x + i\left(\frac{2\pi m}{P_y}\right)y} \left(\left(\hat{z} \times \hat{h}_{\bar{n}}\right) \right.\right. \\
&\left[\frac{B_{(i-1),\bar{n}}^{(l)}}{\eta_{(i-1)}} (-k_{z(i-1)}^{\bar{n}})^{(M-l)} e^{+ik_{z(i-1)}^{\bar{n}} d_i} + \frac{D_{(i-1),\bar{n}}^{(l)}}{\eta_{(1-1)}} (k_{z(i-1)}^{\bar{n}})^{(M-l)} e^{-ik_{z(i-1)}^{\bar{n}} d_i} \right. \\
&\left. - \frac{B_{(i),\bar{n}}^{(l)}}{\eta_{(i)}} (-k_{z(i)}^{\bar{n}})^{(M-l)} e^{+ik_{z(i)}^{\bar{n}} d_i} - \frac{D_{(i),\bar{n}}^{(l)}}{\eta_{(i)}} (k_{z(i)}^{\bar{n}})^{(M-l)} e^{-ik_{z(i)}^{\bar{n}} d_i} \right] \\
&+ \left(\hat{h}_{\bar{n}}\right) \left[- \frac{A_{(i-1),\bar{n}}^{(l)}}{k_{(i-1)}\eta_{(i-1)}} (-k_{z(i-1)}^{\bar{n}})^{(M-l+1)} e^{+ik_{z(i-1)}^{\bar{n}} d_i} \right. \\
&\left. - \frac{C_{(i-1),\bar{n}}^{(l)}}{k_{(i-1)}\eta_{(i-1)}} (k_{z(i-1)}^{\bar{n}})^{(M-l+1)} e^{-ik_{z(i-1)}^{\bar{n}} d_i} \right.
\end{aligned}
$$

$$+\frac{A^{(l)}_{(i),\bar{n}}}{k_{(i)}\eta_{(i)}}(-k^{\bar{n}}_{z(i)})^{(M-l-1)}e^{+ik^{\bar{n}}_{z(i)}d_i}+\frac{C^{(l)}_{(i),\bar{n}}}{k_{(i)}\eta_{(i)}}(k^{\bar{n}}_{z(i)})^{(M-l-1)}e^{-ik^{\bar{n}}_{z(i)}d_i}\Bigg]\Bigg)\Bigg)$$

$$+\sum_{l=0}^{M-1}\frac{(i(z+d_i))^{M-l-1}}{(M-l-1)!}\Bigg(\sum_{\bar{n}}e^{i\left(\frac{2\pi n}{P_x}\right)x+i\left(\frac{2\pi m}{P_y}\right)y}\Bigg(\left(\nabla_t f_{(i)}(\bar{x})\times\hat{z}\right)(k^{\bar{n}}_{\rho}).$$

$$.\Bigg[-\frac{A^{(l)}_{(i-1),\bar{n}}}{k_{(i-1)}\eta_{(i-1)}}(-k^{\bar{n}}_{z(i-1)})^{(M-l-1)}e^{+ik^{\bar{n}}_{z(i-1)}d_i}-\frac{C^{(l)}_{(i-1),\bar{n}}}{k_{(i-1)}\eta_{(i-1)}}(k^{\bar{n}}_{z(i-1)})^{(M-l-1)}e^{-ik^{\bar{n}}_{z(i-1)}d_i}$$

$$+\frac{A^{(l)}_{(i),\bar{n}}}{k_{(i)}\eta_{(i)}}(-k^{\bar{n}}_{z(i)})^{(M-l-1)}e^{+ik^{\bar{n}}_{z(i)}d_i}+\frac{C^{(l)}_{(i),\bar{n}}}{k_{(i)}\eta_{(i)}}(k^{\bar{n}}_{z(i)})^{(M-l-1)}e^{-ik^{\bar{n}}_{z(i)}d_i}\Bigg]\Bigg)\Bigg) \tag{3.58}$$

Applying the 2-D Fourier operator to the N^{th} order forcing functions, the following $(4N)$ equations are obtained. These equations are (for the top boundary):

$$\begin{aligned}
\left(\hat{z}\times\hat{h}_{\bar{n}'}\right).\mathcal{F}\left(S^{(M)}_{E_1}(\bar{x})\right)_{\bar{n}'} &= \alpha^{(M)}_{\bar{n}'}-A^{(M)}_{(1),\bar{n}'}-C^{(M)}_{(1),\bar{n}'}\\
\left(\hat{h}_{\bar{n}'}\right).\mathcal{F}\left(S^{(M)}_{E_1}(\bar{x})\right)_{\bar{n}'} &= \frac{k^{\bar{n}'}_{z0}}{k_0}\beta^{(M)}_{\bar{n}'}+\frac{k^{\bar{n}'}_{z1}}{k_1}B^{(M)}_{(1),\bar{n}'}-\frac{k^{\bar{n}'}_{z1}}{k_1}D^{(M)}_{(1),\bar{n}'}\\
\left(\hat{z}\times\hat{h}_{\bar{n}'}\right).\mathcal{F}\left(S^{(M)}_{H_1}(\bar{x})\right)_{\bar{n}'} &= \frac{\beta^{(M)}_{\bar{n}'}}{\eta_0}-\frac{B^{(M)}_{(1),\bar{n}'}}{\eta_1}-\frac{D^{(M)}_{(1),\bar{n}'}}{\eta_1}\\
\left(\hat{h}_{\bar{n}'}\right).\mathcal{F}\left(S^{(M)}_{H_1}(\bar{x})\right)_{\bar{n}'} &= -\frac{k^{\bar{n}'}_{z0}}{k_0\eta_0}\alpha^{(M)}_{\bar{n}'}-\frac{k^{\bar{n}'}_{z1}}{k_1\eta_1}A^{(M)}_{(1),\bar{n}'}+\frac{k^{\bar{n}'}_{z1}}{k_1\eta_1}C^{(M)}_{(1),\bar{n}'}
\end{aligned} \tag{3.59}$$

For $i=2,3,....,N-1$ we have:

$$\begin{aligned}
\left(\hat{z}\times\hat{h}_{\bar{n}'}\right).\mathcal{F}\left(S^{(M)}_{E_{(i)}}(\bar{x})\right)_{\bar{n}'} &= A^{(M)}_{(i-1),\bar{n}}e^{+ik^{\bar{n}}_{z(i-1)}d_i}+C^{(M)}_{(i-1),\bar{n}}e^{-ik^{\bar{n}}_{z(i-1)}d_i}\\
&\quad -A^{(M)}_{(i),\bar{n}}e^{+ik^{\bar{n}}_{z(i)}d_i}-C^{(M)}_{(i),\bar{n}}e^{-ik^{\bar{n}}_{z(i)}d_i}\\
\left(\hat{h}_{\bar{n}'}\right).\mathcal{F}\left(S^{(M)}_{E_{(i)}}(\bar{x})\right)_{\bar{n}'} &= -\frac{k^{\bar{n}}_{z(i-1)}}{k_{i-1}}B^{(M)}_{(i-1),\bar{n}}e^{+ik^{\bar{n}}_{z(i-1)}d_i}+\frac{k^{\bar{n}}_{z(i-1)}}{k_{i-1}}D^{(M)}_{(i-1),\bar{n}}e^{-ik^{\bar{n}}_{z(i-1)}d_i}\\
&\quad +\frac{k^{\bar{n}}_{z(i)}}{k_i}B^{(M)}_{(i),\bar{n}}e^{+ik^{\bar{n}}_{z(i)}d_i}-\frac{k^{\bar{n}}_{z(i)}}{k_i}D^{(M)}_{(i),\bar{n}}e^{-ik^{\bar{n}}_{z(i)}d_i}\\
\left(\hat{z}\times\hat{h}_{\bar{n}'}\right).\mathcal{F}\left(S^{(M)}_{H_{(i)}}(\bar{x})\right)_{\bar{n}'} &= \frac{B^{(M)}_{(i-1),\bar{n}}}{\eta_{i-1}}e^{+ik^{\bar{n}}_{z(i-1)}d_i}+\frac{D^{(M)}_{(i-1),\bar{n}}}{\eta_{i-1}}e^{-ik^{\bar{n}}_{z(i-1)}d_i}\\
&\quad -\frac{B^{(M)}_{(i),\bar{n}}}{\eta_i}e^{+ik^{\bar{n}}_{z(i)}d_i}-\frac{D^{(M)}_{(i),\bar{n}}}{\eta_i}e^{-ik^{\bar{n}}_{z(i)}d_i}
\end{aligned}$$

$$\begin{aligned}
\left(\hat{h}_{\bar{n}'}\right).\mathcal{F}\left(S^{(M)}_{H_{(i)}}(\bar{x})\right)_{\bar{n}'} &= +\frac{k^{\bar{n}}_{z(i-1)}}{k_{i-1}\eta_{i-1}}A^{(M)}_{(i-1),\bar{n}}e^{+ik^{\bar{n}}_{z(i-1)}d_i} \\
-\frac{k^{\bar{n}}_{z(i-1)}}{k_{i-1}\eta_{i-1}}C^{(M)}_{(i-1),\bar{n}}e^{-ik^{\bar{n}}_{z(i-1)}d_i} &- \frac{k^{\bar{n}}_{z(i)}}{k_i\eta_i}A^{(M)}_{(i),\bar{n}}e^{+ik^{\bar{n}}_{z(i)}d_i} + \frac{k^{\bar{n}}_{z(i)}}{k_i\eta_i}C^{(M)}_{(i),\bar{n}}e^{-ik^{\bar{n}}_{z(i)}d_i} \qquad (3.60)
\end{aligned}$$

And for the last boundary:

$$\begin{aligned}
\left(\hat{z}\times\hat{h}_{\bar{n}'}\right).\mathcal{F}\left(S^{(M)}_{E_N}(\bar{x})\right)_{\bar{n}'} &= A^{(M)}_{(N-1),\bar{n}'}e^{+ik^{\bar{n}'}_{z(N-1)}d_N} + C^{(M)}_{(N-1),\bar{n}'}e^{-ik^{\bar{n}'}_{z(N-1)}d_N} \\
&\quad -\gamma^{(M)}_{\bar{n}'}e^{+ik^{\bar{n}'}_{zN}d_N} \\
\left(\hat{h}_{\bar{n}'}\right).\mathcal{F}\left(S^{(M)}_{E_N}(\bar{x})\right)_{\bar{n}'} &= -\frac{k^{\bar{n}'}_{z(N-1)}}{k_{N-1}}B^{(M)}_{(N-1),\bar{n}'}e^{+ik^{\bar{n}'}_{z(N-1)}d_N} \\
&\quad +\frac{k^{\bar{n}'}_{z(N-1)}}{k_{N-1}}D^{(M)}_{(N-1),\bar{n}'}e^{-ik^{\bar{n}'}_{z(N-1)}d_N} + \frac{k^{\bar{n}'}_{zN}}{k_N}\delta^{(M)}_{\bar{n}'}e^{+ik^{\bar{n}'}_{zN}d_N} \\
\left(\hat{z}\times\hat{h}_{\bar{n}'}\right).\mathcal{F}\left(S^{(M)}_{H_N}(\bar{x})\right)_{\bar{n}'} &= \frac{B^{(M)}_{(N-1),\bar{n}'}}{\eta_{N-1}}e^{+ik^{\bar{n}'}_{z(N-1)}d_N} + \frac{D^{(M)}_{(N-1),\bar{n}'}}{\eta_{N-1}}e^{-ik^{\bar{n}'}_{z(N-1)}d_N} \\
&\quad -\frac{\delta^{(M)}_{\bar{n}'}}{\eta_N}e^{+ik^{\bar{n}'}_{zN}d_N} \\
\left(\hat{h}_{\bar{n}'}\right).\mathcal{F}\left(S^{(M)}_{H_N}(\bar{x})\right)_{\bar{n}'} &= \frac{k^{\bar{n}'}_{z(N-1)}}{k_{N-1}\eta_{N-1}}A^{(M)}_{(N-1),\bar{n}'}e^{+ik^{\bar{n}'}_{z(N-1)}d_N} \\
&\quad -\frac{k^{\bar{n}'}_{z(N-1)}}{k_{N-1}\eta_{N-1}}C^{(M)}_{(N-1),\bar{n}'}e^{-ik^{\bar{n}'}_{z(N-1)}d_N} - \frac{k^{\bar{n}'}_{z2}}{k_N\eta_N}\gamma^{(M)}_{\bar{n}'}e^{+ik^{\bar{n}'}_{zN}d_N} \qquad (3.61)
\end{aligned}$$

Similar to the two layer case, these equations can be grouped into two sets of $(2N)$ equations, involving horizontal and vertical polarized terms. Putting these equations into matrix form, matrices similar to $M_\xi(\bar{n}')$ and $M_\zeta(\bar{n}')$ (both are of size $(2N\times 2N)$ here) for the N-layer Problem can be easily obtained. Also, using a numerical FFT based approach for the Fourier transform operators, an arbitrary order, arbitrary number of layer solution can be obtained. As mentioned before, such a code will be very useful, especially for verification purposes in an analytical study of the N-layer problem, or for deterministic problems.

3.8 Conclusion

In this chapter, first the notational conventions for the rest of the dissertation were provided. Next, the boundary conditions were studied, each boundary condition brought a so called forcing function. These functions were utilized to express the solution of the problem as a set of two linear system of equations, for horizontal and vertical polarizations, respectively. The solution for these systems of equations was provided analytically. Later, a Fast Fourier Transform(FFT) based numerical solution was described. The numerical perturbation solution was validated against an existing two and a half dimensional extended boundary condition(EBC) solution for two sine surfaces on top of each other, in the propagating modes.

Although only the two-layer case will be considered analytically in following chapters, the arbitrary number of layers case was also considered only numerically, and the numerical solution was provided in this chapter as a final section. This section can be considered as a generalization of the two-layer numerical SPM solution, which will be very useful in future work involving analytical arbitrary layer SPM solutions.

CHAPTER 4

TWO LAYER SPM THEORY: ANALYTICAL SOLUTION

4.1 Introduction

In this chapter, an analytical solution procedure for the two-layer problem is presented. The basic steps for obtaining the analytical SPM solution directly follow from the second chapter, where the 1-D Dirichlet problem was considered. First, the zeroth, first, and second order explicit solutions are considered. Later, a tensor based iterative arbitrary order solution procedure is presented.

In the next sections, the zeroth order solution will first be provided in terms of the $K_{E,H}$ functions, defined in Chapter 3. The zeroth and arbitrary order contributions to the general N^{th} order solution will be studied from the forcing functions provided in Chapter 3. Zeroth order contribution terms are studied separately for horizontal and vertical incidence cases, while the arbitrary order contributions are identical for both incidence cases. Next, partial SPM solutions for the zeroth and lower order contribution terms are obtained. Later, these partial solutions are utilized to obtain the complete first and second order solutions. Then, general form of higher order solutions is studied, and based on this generalization, a new tensor based notation

is introduced. The tensor notation is applied to the partial SPM solutions, and the arbitrary order SPM solution procedure is constructed with them.

4.2 Zeroth order solution

This section provides the zeroth order solution to the two layer problem. The zeroth order (unperturbed) solution is equivalent to a flat interface solution, and can be directly obtained from Equations 3.33 and 3.34 by plugging in the zeroth order forcing functions to the right hand side array b of Equation 3.30.

The zeroth order forcing functions are very simple:

$$\begin{aligned} S_{E_1}^{(N)}(\bar{x}) &= -(\hat{z}\times\hat{e}_i), \qquad S_{H_1}^{(N)}(\bar{x}) = -\frac{1}{\eta_0}(\hat{z}\times\hat{k}_i\times\hat{e}_i) \\ S_{E_2}^{(N)}(\bar{x}) &= 0, \qquad S_{H_2}^{(N)}(\bar{x}) = 0 \end{aligned} \tag{4.1}$$

The Fourier transforms of these functions are utilized to obtain b in Equation 3.30 as:

$$\bar{b}_\xi(\bar{n}') = \begin{bmatrix} -(\hat{z}\times\hat{h}_i).(\hat{z}\times\hat{e}_i) \\ -\frac{1}{\eta_0}(\hat{h}_i).(\hat{z}\times\hat{k}_i\times\hat{e}_i) \\ 0 \\ 0 \end{bmatrix}\delta_{\bar{n}'}, \qquad \bar{b}_\zeta(\bar{n}') = \begin{bmatrix} -(\hat{h}_i).(\hat{z}\times\hat{e}_i) \\ -\frac{1}{\eta_0}(\hat{z}\times\hat{h}_i).(\hat{z}\times\hat{k}_i\times\hat{e}_i) \\ 0 \\ 0 \end{bmatrix}\delta_{\bar{n}'} \tag{4.2}$$

Here, $\xi = \{\alpha, A, C, \gamma\}$ and $\zeta = \{\beta, B, D, \delta\}$ as usual.

Working out the cross products for each incidence polarization and multiplying the resulting arrays with the inverses of the corresponding M matrices, the zeroth solution is obtained. The resulting expressions are for the horizontal incidence case (i.e. $\hat{e}_i = \hat{h}_i$):

$$\begin{aligned} \xi_{\bar{n}'}^{(0)} &= \Gamma_\xi = -\left(K_{E1}^{\xi}(\bar{0}) + \frac{k_{z0}^{\bar{0}}}{k_0\eta_0}K_{H1}^{\xi}(\bar{0})\right)\delta(\bar{n}') \\ \zeta_{\bar{n}'}^{(0)} &= 0 \end{aligned} \tag{4.3}$$

and for the vertical incidence case (i.e. $\hat{e}_i = \hat{v}_i$):

$$\begin{aligned} \xi_{\bar{n}'}^{(0)} &= 0 \\ \zeta_{\bar{n}'}^{(0)} &= \Gamma_\zeta = \left(\frac{k_{z0}^{\bar{0}}}{k_0} K_{E1}^{\zeta}(\bar{0}) - \frac{1}{\eta_0} K_{H1}^{\zeta}(\bar{0}) \right) \delta(\bar{n}') \end{aligned} \tag{4.4}$$

Although the flat interface solution is well known, the Γ_ξ and Γ_ζ terms defined here will be very useful simplifying the higher order solutions.

4.3 Study of the forcing functions

In this section, four forcing functions given in Equations 3.21 through 3.24 are separated into zeroth and lower order contribution terms in a fashion similar to that described in Section 2.2.1. In order to obtain a arbitrary order SPM solution, such a treatment of the forcing functions is necessary.

Each forcing function at N^{th} order(i.e. $S^{(N)}(\bar{x})$) is written as a sum of zeroth and lower order contribution terms as follows:

$$S^{(N)}(\bar{x}) = S^{(N,0)}(\bar{x}) + \sum_{r=1}^{N-1} S^{(N,r)}(\bar{x}) \tag{4.5}$$

such that $S^{(N,r)}(\bar{x})$ is part of the forcing function that contains only the terms involving the r^{th} order scattering coefficients. The zeroth order contribution term $S^{(N,0)}(\bar{x})$ has to be studied separately for each incidence polarization, but the term $S^{(N,r)}(\bar{x})$ has a unique representation for both incidence polarizations.

In the following subsections, first, several intermediate functionals and operators are defined to reduce the complexity of the expressions. Later, using these intermediate functionals and operators, the zeroth and lower order contribution terms of the forcing functions are presented.

4.3.1 Notational conventions

Due to the highly complex nature of the SPM expressions, several intermediate functionals and operators must be defined. These intermediate expressions can be grouped into two basic categories. In the first group, there a total of eight expressions involving the zeroth order solution. They are given as follows:

$$R_{E_1,h}^{(N)} = \Gamma_\alpha (k_{z0}^{\bar{0}})^N - \Gamma_A (-k_{z1}^{\bar{0}})^N - \Gamma_C (k_{z1}^{\bar{0}})^N \tag{4.6}$$

$$R_{H_1,h}^{(N)} = -\Gamma_\alpha \frac{(k_{z0}^{\bar{0}})^N}{k_0\eta_0} + \Gamma_A \frac{(-k_{z1}^{\bar{0}})^N}{k_1\eta_1} + \Gamma_C \frac{(k_{z1}^{\bar{0}})^N}{k_1\eta_1} \tag{4.7}$$

$$R_{E_2,h}^{(N)} = \Gamma_A (-k_{z1}^{\bar{0}})^N e^{+ik_{z1}^{\bar{0}}d} + \Gamma_C (+k_{z1}^{\bar{0}})^N e^{-ik_{z1}^{\bar{0}}d} - \Gamma_\gamma (-k_{z2}^{\bar{0}})^N e^{+ik_{z2}^{\bar{0}}d} \tag{4.8}$$

$$R_{H_2,h}^{(N)} = -\Gamma_A \frac{(-k_{z1}^{\bar{0}})^N}{k_1\eta_1} e^{+ik_{z1}^{\bar{0}}d} - \Gamma_C \frac{(+k_{z1}^{\bar{0}})^N}{k_1\eta_1} e^{-ik_{z1}^{\bar{0}}d} + \Gamma_\gamma \frac{(-k_{z2}^{\bar{0}})^N}{k_2\eta_2} e^{+ik_{z2}^{\bar{0}}d} \tag{4.9}$$

$$R_{E_1,v}^{(N)} = \Gamma_\beta \frac{(k_{z0}^{\bar{0}})^N}{k_0} - \Gamma_B \frac{(-k_{z1}^{\bar{0}})^N}{k_1} - \Gamma_D \frac{(k_{z1}^{\bar{0}})^N}{k_1} \tag{4.10}$$

$$R_{H_1,v}^{(N)} = \Gamma_\beta \frac{(k_{z0}^{\bar{0}})^N}{\eta_0} - \Gamma_B \frac{(-k_{z1}^{\bar{0}})^N}{\eta_1} - \Gamma_D \frac{(k_{z1}^{\bar{0}})^N}{\eta_1} \tag{4.11}$$

$$R_{E_2,v}^{(N)} = \Gamma_B \frac{(-k_{z1}^{\bar{0}})^N}{k_1} e^{+ik_{z1}^{\bar{0}}d} + \Gamma_D \frac{(+k_{z1}^{\bar{0}})^N}{k_1} e^{-ik_{z1}^{\bar{0}}d} - \Gamma_\delta \frac{(-k_{z2}^{\bar{0}})^N}{k_2} e^{+ik_{z2}^{\bar{0}}d} \tag{4.12}$$

$$R_{H_2,v}^{(N)} = \Gamma_B \frac{(-k_{z1}^{\bar{0}})^N}{\eta_1} e^{+ik_{z1}^{\bar{0}}d} + \Gamma_D \frac{(+k_{z1}^{\bar{0}})^N}{\eta_1} e^{-ik_{z1}^{\bar{0}}d} - \Gamma_\delta \frac{(-k_{z2}^{\bar{0}})^N}{\eta_2} e^{+ik_{z2}^{\bar{0}}d} \tag{4.13}$$

The next group also has eight expressions which involve the lower order (r^{th} order) SPM solutions. They are given as:

$$\mathcal{A}_{E1}^{(N,r)}(\bar{n}) = \left[\alpha_{\bar{n}}^{(r)} (k_{z0}^{\bar{n}})^{N-r} - A_{\bar{n}}^{(r)} (-k_{z1}^{\bar{n}})^{N-r} - C_{\bar{n}}^{(r)} (k_{z1}^{\bar{n}})^{N-r}\right] \tag{4.14}$$

$$\mathcal{B}_{E1}^{(N,r)}(\bar{n}) = \left[\frac{\beta_{\bar{n}}^{(r)}}{k_0} (k_{z0}^{\bar{n}})^{N-r} - \frac{B_{\bar{n}}^{(r)}}{k_1} (-k_{z1}^{\bar{n}})^{N-r} - \frac{D_{\bar{n}}^{(r)}}{k_1} (k_{z1}^{\bar{n}})^{N-r}\right] \tag{4.15}$$

$$\mathcal{A}_{H1}^{(N,r)}(\bar{n}) = \left[-\frac{\alpha_{\bar{n}}^{(r)}}{k_0\eta_0} (k_{z0}^{\bar{n}})^{N-r} + \frac{A_{\bar{n}}^{(r)}}{k_1\eta_1} (-k_{z1}^{\bar{n}})^{N-r} + \frac{C_{\bar{n}}^{(r)}}{k_1\eta_1} (k_{z1}^{\bar{n}})^{N-r}\right] \tag{4.16}$$

$$\mathcal{B}_{H1}^{(N,r)}(\bar{n}) = \left[\frac{\beta_{\bar{n}}^{(r)}}{\eta_0}(k_{z0}^{\bar{n}})^{N-r} - \frac{B_{\bar{n}}^{(r)}}{\eta_1}(-k_{z1}^{\bar{n}})^{N-r} - \frac{D_{\bar{n}}^{(r)}}{\eta_1}(k_{z1}^{\bar{n}})^{N-r} \right] \tag{4.17}$$

$$\begin{aligned} \mathcal{A}_{E2}^{(N,r)}(\bar{n}) &= \Bigg[A_{\bar{n}}^{(r)}(-k_{z1}^{\bar{n}})^{N-r} e^{+ik_{z1}^{\bar{n}}d} + C_{\bar{n}}^{(r)}(+k_{z1}^{\bar{n}})^{N-r} e^{-ik_{z1}^{\bar{n}}d} \\ &\quad - \gamma_{\bar{n}}^{(r)}(-k_{z2}^{\bar{n}})^{N-r} e^{+ik_{z2}^{\bar{n}}d} \Bigg] \end{aligned} \tag{4.18}$$

$$\begin{aligned} \mathcal{B}_{E2}^{(N,r)}(\bar{n}) &= \Bigg[\frac{(-k_{z1}^{\bar{n}})^{N-r}}{k_1} e^{+ik_{z1}^{\bar{n}}d} B_{\bar{n}}^{(r)} + \frac{(+k_{z1}^{\bar{n}})^{N-r}}{k_1} e^{-ik_{z1}^{\bar{n}}d} D_{\bar{n}}^{(r)} \\ &\quad - \frac{(-k_{z2}^{\bar{n}})^{N-r}}{k_2} e^{+ik_{z2}^{\bar{n}}d} \delta_{\bar{n}}^{(r)} \Bigg] \end{aligned} \tag{4.19}$$

$$\begin{aligned} \mathcal{A}_{H2}^{(N,r)}(\bar{n}) &= \Bigg[- \frac{(-k_{z1}^{\bar{n}})^{N-r}}{k_1\eta_1} e^{+ik_{z1}^{\bar{n}}d} A_{\bar{n}}^{(r)} - \frac{(+k_{z1}^{\bar{n}})^{N-r}}{k_1\eta_1} e^{-ik_{z1}^{\bar{n}}d} C_{\bar{n}}^{(r)} \\ &\quad + \frac{(-k_{z2}^{\bar{n}})^{N-r}}{k_2\eta_2} e^{+ik_{z2}^{\bar{n}}d} \gamma_{\bar{n}}^{(r)} \Bigg] \end{aligned} \tag{4.20}$$

$$\begin{aligned} \mathcal{B}_{H2}^{(N,r)}(\bar{n}) &= \Bigg[\frac{(-k_{z1}^{\bar{n}})^{N-r}}{\eta_1} e^{+ik_{z1}^{\bar{n}}d} B_{\bar{n}}^{(r)} + \frac{(+k_{z1}^{\bar{n}})^{N-r}}{\eta_1} e^{-ik_{z1}^{\bar{n}}d} D_{\bar{n}}^{(r)} \\ &\quad - \frac{(-k_{z2}^{\bar{n}})^{N-r}}{\eta_2} e^{+ik_{z2}^{\bar{n}}d} \delta_{\bar{n}}^{(r)} \Bigg] \end{aligned} \tag{4.21}$$

With these definitions, we can proceed to the zeroth and lower order forcing function components.

4.3.2 Components of the forcing functions

The zeroth order components of the forcing functions can be expressed in terms of the intermediate functionals ($R^{(N)}$) defined in the previous subsection in the following simple form:

For horizontal incidence:

$$S_{E_1}^{(N,0),h}(\bar{x}) = -\left(\hat{z} \times \hat{h}_i\right) z_1^N \left(\frac{(-i)^N}{N!} k_{zi}^N + \frac{(i)^N}{N!} R_{E_1}^{(N),h}(\bar{0}) \right) \tag{4.22}$$

$$S_{H_1}^{(N,0),h}(\bar{x}) = -\left(\hat{h}_i\right) z_1^N \left(\frac{k_{z0}^{\bar{0}}}{k_0\eta_0}\frac{(-i)^N}{N!}k_{zi}^N + \frac{(i)^N}{N!}R_{H_1}^{(N+1),h}(\bar{0})\right)$$
$$-\left(\nabla_t f_1(\bar{x})\times\hat{z}\right) z_1^{N-1}\left(\frac{k_{\rho i}}{k_0\eta_0}\frac{(-i)^{N-1}}{(N-1)!}k_{zi}^{N-1} - \frac{(i)^{N-1}}{(N-1)!}k_\rho^{\bar{0}}R_{H_1}^{(N-1),h}(\bar{0})\right) \quad (4.23)$$

$$S_{E_2}^{(N,0),h} = -\left(\hat{z}\times\hat{h}_i\right) z_2^N\left(\frac{(i)^N}{N!}R_{E_2}^{(N),h}(\bar{0})\right) \quad (4.24)$$

$$S_{H_2}^{(N,0),h}(\bar{x}) = -\left(\hat{h}_i\right) z_2^N\left(\frac{(i)^N}{N!}R_{H_2}^{(N+1),h}(\bar{0})\right)$$
$$+\left(\nabla_t f_2(\bar{x})\times\hat{z}\right) z_2^{N-1}\left(\frac{(i)^{N-1}}{(N-1)!}k_\rho^{\bar{0}}R_{H_2}^{(N-1),h}(\bar{0})\right) \quad (4.25)$$

For vertical incidence:

$$S_{E_1}^{(N,0),v}(\bar{x}) = \left(\hat{h}_i\right) z_1^N\left(\frac{k_{zi}}{k_0}\frac{(-i)^N}{N!}k_{zi}^N - \frac{(i)^N}{N!}R_{E_1}^{(N+1),v}(\bar{0})\right)$$
$$+\left(\nabla_t f_1(\bar{x})\times\hat{z}\right) z_1^{N-1}\left(\frac{k_{\rho i}}{k_0}\frac{(-i)^{N-1}}{(N-1)!}k_{zi}^{N-1} + \frac{(i)^{N-1}}{(N-1)!}k_\rho^{\bar{0}}R_{E_1}^{(N-1),v}(\bar{0})\right) \quad (4.26)$$

$$S_{H_1}^{(N,0),v}(\bar{x}) = -\left(\hat{z}\times\hat{h}_i\right) z_1^N\left(\frac{1}{\eta_0}\frac{(-i)^N}{N!}k_{zi}^N + \frac{(i)^N}{N!}R_{H_1}^{(N),v}(\bar{0})\right) \quad (4.27)$$

$$S_{E_2}^{(N,0),v} = -\left(\hat{h}_i\right) z_2^N\left(\frac{(i)^N}{(N)!}R_{E_2}^{(N+1),v}(\bar{0})\right)$$
$$+\left(\nabla_t f_2(\bar{x})\times\hat{z}\right) z_2^{N-1}\left(\frac{(i)^{N-1}}{(N-1)!}k_\rho^{\bar{0}}R_{E_2}^{(N-1),v}(\bar{0})\right) \quad (4.28)$$

$$S_{H_2}^{(N,0),v}(\bar{x}) = -\left(\hat{z}\times\hat{h}_i\right) z_2^N\left(\frac{(i)^N}{N!}R_{H_2}^{(N),v}(\bar{0})\right) \quad (4.29)$$

Also note that a superscript: h or v is added to the forcing functions to indicate the incidence polarization. In addition, two new variables z_1 and z_2 are defined in the following way:

$$z_1 = f_1(\bar{x}), \qquad z_2 = \bar{f}_2(\bar{x}) \quad (4.30)$$

to identify the surface on which the forcing functions are defined.

The lower order components of the forcing functions can be expressed in terms of the operators $\mathcal{A}$ and $\mathcal{B}$: The first forcing function becomes:

$$\begin{aligned} S_{E_1}^{(N,r)}(\bar{x}) &= -\frac{(iz_1)^{N-r}}{(N-r)!}\Bigg(\sum_{\bar{n}} e^{i\left(\frac{2\pi n}{P_x}\right)x+i\left(\frac{2\pi m}{P_y}\right)y}\Bigg(\\ &\quad \left(\hat{z}\times\hat{h}_{\bar{n}}\right)\mathcal{A}_{E1}^{(N,r)}(\bar{n})+\left(\hat{h}_{\bar{n}}\right)\mathcal{B}_{E1}^{(N+1,r)}(\bar{n})\Bigg)\Bigg) \\ &\quad +\frac{(iz_1)^{N-r-1}}{(N-r-1)!}\Bigg(\sum_{\bar{n}} e^{i\left(\frac{2\pi n}{P_x}\right)x+i\left(\frac{2\pi m}{P_y}\right)y} \\ &\quad \Bigg(\left(\nabla_t f_1(\bar{x})\times\hat{z}\right)(k_\rho^{\bar{n}})\mathcal{B}_{E1}^{(N-1,r)}(\bar{n})\Bigg)\Bigg) \end{aligned} \tag{4.31}$$

The second forcing function becomes:

$$\begin{aligned} S_{H_1}^{(N,r)}(\bar{x}) &= -\frac{(iz_1)^{N-r}}{(N-r)!}\Bigg(\sum_{\bar{n}} e^{i\left(\frac{2\pi n}{P_x}\right)x+i\left(\frac{2\pi m}{P_y}\right)y}\Bigg(\\ &\quad \left(\hat{z}\times\hat{h}_{\bar{n}}\right)\mathcal{B}_{H1}^{(N,r)}(\bar{n})+\left(\hat{h}_{\bar{n}}\right)\mathcal{A}_{H1}^{(N+1,r)}(\bar{n})\Bigg)\Bigg) \\ &\quad +\frac{(iz_1)^{N-r-1}}{(N-r-1)!}\Bigg(\sum_{\bar{n}} e^{i\left(\frac{2\pi n}{P_x}\right)x+i\left(\frac{2\pi m}{P_y}\right)y} \\ &\quad \Bigg(\left(\nabla_t f_1(\bar{x})\times\hat{z}\right)(k_\rho^{\bar{n}})\mathcal{A}_{H1}^{(N-1,r)}(\bar{n})\Bigg)\Bigg) \end{aligned} \tag{4.32}$$

The third forcing function becomes:

$$\begin{aligned} S_{E_2}^{(N,r)} &= -\frac{(iz_2)^{N-r}}{(N-r)!}\Bigg(\sum_{\bar{n}} e^{i\left(\frac{2\pi n}{P_x}\right)x+i\left(\frac{2\pi m}{P_y}\right)y}\Bigg(\\ &\quad \left(\hat{z}\times\hat{h}_{\bar{n}}\right)\mathcal{A}_{E2}^{(N,r)}(\bar{n})+\left(\hat{h}_{\bar{n}}\right)\mathcal{B}_{E2}^{(N+1,r)}(\bar{n})\Bigg)\Bigg) \end{aligned}$$

$$+\frac{(iz_2)^{N-r-1}}{(N-r-1)!}\left(\sum_{\bar{n}} e^{i\left(\frac{2\pi n}{P_x}\right)x+i\left(\frac{2\pi m}{P_y}\right)y}\right.$$

$$\left.\left((\nabla_t f_2(\bar{x})\times\hat{z})\,(k_\rho^{\bar{n}})\mathcal{B}_{E2}^{(N-1,r)}(\bar{n})\right)\right) \tag{4.33}$$

Finally the fourth forcing function becomes:

$$\begin{aligned} S_{H_2}^{(N,r)}(\bar{x}) &= -\frac{(iz_2)^{N-r}}{(N-r)!}\left(\sum_{\bar{n}} e^{i\left(\frac{2\pi n}{P_x}\right)x+i\left(\frac{2\pi m}{P_y}\right)y}\left(\right.\right. \\ &\left.\left.\left(\hat{z}\times\hat{h}_{\bar{n}}\right)\mathcal{B}_{H2}^{(N,r)}(\bar{n})+\left(\hat{h}_{\bar{n}}\right)\mathcal{A}_{H2}^{(N+1,r)}(\bar{n})\right)\right) \\ &+\frac{(iz_2)^{N-r-1}}{(N-r-1)!}\left(\sum_{\bar{n}} e^{i\left(\frac{2\pi n}{P_x}\right)x+i\left(\frac{2\pi m}{P_y}\right)y}\right. \\ &\left.\left((\nabla_t f_2(\bar{x})\times\hat{z})\,(k_\rho^{\bar{n}})\mathcal{A}_{H2}^{(N-1,r)}(\bar{n})\right)\right) \end{aligned} \tag{4.34}$$

In the next section, the solution procedure of Section 3.5 is applied to the zeroth and lower order components of the forcing functions.

4.4 General zeroth and lower order contributions to N^{th} order solution

In Section 3.5, a solution procedure for SPM scattering coefficients was described in terms of (four) forcing functions through a matrix inversion process. Going through those steps analytically for only the zeroth or the lower order contributions of the forcing functions, the corresponding components of the scattering coefficients are obtained. Mathematically speaking, let $\tau^{(N)} = \{\xi^{(N)}, \zeta^{(N)}\}$ be any horizontal $\xi^{(N)} = \{\alpha^{(N)}, A^{(N)}, C^{(N)}, \gamma^{(N)}\}$ or vertical $\zeta^{(N)} = \{\beta^{(N)}, B^{(N)}, D^{(N)}, \delta^{(N)}\}$ scattering coefficient of order N. Then, the zeroth $\tau^{(N,0)}$ and the lower order $\tau^{(N,r)}$ components of

the scattering coefficients can be defined such that:

$$\left.\begin{matrix} S_{E_1}^{(N,0)}(\bar{x}) \\ S_{H_1}^{(N,0)}(\bar{x}) \\ S_{E_2}^{(N,0)}(\bar{x}) \\ S_{H_2}^{(N,0)}(\bar{x}) \end{matrix}\right\} \xrightarrow{\text{Eq.3.33, 3.34}} \tau^{(N,0)} \qquad \left.\begin{matrix} S_{E_1}^{(N,r)}(\bar{x}) \\ S_{H_1}^{(N,r)}(\bar{x}) \\ S_{E_2}^{(N,r)}(\bar{x}) \\ S_{H_2}^{(N,r)}(\bar{x}) \end{matrix}\right\} \xrightarrow{\text{Eq.3.33, 3.34}} \tau^{(N,r)} \tag{4.35}$$

Later, we can construct the scattering coefficients, by simply adding them in the following form:

$$\tau^{(N)} = \tau^{(N,0)} + \sum_{r=1}^{N-1} \tau^{(N,r)} \tag{4.36}$$

As an example, suppose we want to obtain the third order horizontally polarized reflected field scattering coefficient $\alpha^{(3)}$ in the case of vertically incident plane wave. Then we need to study the zeroth, first and second order contributions of all four forcing functions:

$$\left.\begin{matrix} S_{E_1}^{(3,0),v}(\bar{x}) \\ S_{H_1}^{(3,0),v}(\bar{x}) \\ S_{E_2}^{(3,0),v}(\bar{x}) \\ S_{H_2}^{(3,0),v}(\bar{x}) \end{matrix}\right\} \rightarrow \alpha^{(3,0)} \qquad \left.\begin{matrix} S_{E_1}^{(3,1)}(\bar{x}) \\ S_{H_1}^{(3,1)}(\bar{x}) \\ S_{E_2}^{(3,1)}(\bar{x}) \\ S_{H_2}^{(3,1)}(\bar{x}) \end{matrix}\right\} \rightarrow \alpha^{(3,1)} \qquad \left.\begin{matrix} S_{E_1}^{(3,2)}(\bar{x}) \\ S_{H_1}^{(3,2)}(\bar{x}) \\ S_{E_2}^{(3,2)}(\bar{x}) \\ S_{H_2}^{(3,2)}(\bar{x}) \end{matrix}\right\} \rightarrow \alpha^{(3,2)} \tag{4.37}$$

noting that the superscript v is added to the zeroth order contribution term, indicating incidence polarization. Then the total scattering coefficient can be expressed as:

$$\alpha^{(3)} = \alpha^{(3,0)} + \alpha^{(3,1)} + \alpha^{(3,2)} \tag{4.38}$$

In this section, first, general expressions for the zeroth order contributions to the scattering coefficients ($\tau^{(N,0)}$) are derived in terms of forcing function components $S^{(N,0)}(\bar{x})$. Later, general expressions for the lower order contributions to the scattering coefficients ($\tau^{(N,r)}$) are derived in terms of forcing function components $S^{(N,r)}(\bar{x})$.

First of all, the solution for the zeroth or lower order contributions is given by:
For $\xi = \{\alpha, A, C, \gamma\}$,

$$\xi_{\bar{n}'}^{(N,s)} \quad = \quad \left(\hat{z} \times \hat{h}_{\bar{n}'}\right) . K_{E1}^{\xi}(\bar{n}') \mathcal{F}\left(S_{E_1}^{(N,s)}(\bar{x})\right)_{\bar{n}'}$$

$$+\left(\hat{z}\times\hat{h}_{\bar{n}'}\right).K^{\xi}_{E2}(\bar{n}')\mathcal{F}\left(S^{(N,s)}_{E_2}(\bar{x})\right)_{\bar{n}'}$$
$$+\left(\hat{h}_{\bar{n}'}\right).K^{\xi}_{H1}(\bar{n}')\mathcal{F}\left(S^{(N,s)}_{H_1}(\bar{x})\right)_{\bar{n}'}$$
$$+\left(\hat{h}_{\bar{n}'}\right).K^{\xi}_{H2}(\bar{n}')\mathcal{F}\left(S^{(N,s)}_{H_2}(\bar{x})\right)_{\bar{n}'} \tag{4.39}$$

For $\zeta=\{\beta,B,D,\delta\}$.

$$\begin{aligned}\zeta^{(N,s)}_{\bar{n}'} &= \left(\hat{h}_{\bar{n}'}\right).K^{\zeta}_{E1}(\bar{n}')\mathcal{F}\left(S^{(N,s)}_{E_1}(\bar{x})\right)_{\bar{n}'}\\ &+\left(\hat{h}_{\bar{n}'}\right).K^{\zeta}_{E2}(\bar{n}')\mathcal{F}\left(S^{(N,s)}_{E_2}(\bar{x})\right)_{\bar{n}'}\\ &+\left(\hat{z}\times\hat{h}_{\bar{n}'}\right).K^{\zeta}_{H1}(\bar{n}')\mathcal{F}\left(S^{(N,s)}_{H_1}(\bar{x})\right)_{\bar{n}'}\\ &+\left(\hat{z}\times\hat{h}_{\bar{n}'}\right).K^{\zeta}_{H2}(\bar{n}')\mathcal{F}\left(S^{(N,s)}_{H_2}(\bar{x})\right)_{\bar{n}'}\end{aligned} \tag{4.40}$$

where $s=0,1,...,(N-1)$.

These equations require several dot products of either $\hat{z}\times\hat{h}_{\bar{n}'}$ or $\hat{h}_{\bar{n}'}$ with the Fourier transforms of the forcing functions. In order to work out these products, the following functions are defined for convenience(basically representing sine and cosine functions.)

$$c_{\bar{n}_1,\bar{n}_2}=\frac{k_{xn_1}k_{xn_2}+k_{ym_1}k_{ym_2}}{k^{\bar{n}_1}_{\rho}k^{\bar{n}_2}_{\rho}} \tag{4.41}$$

$$s_{\bar{n}_1,\bar{n}_2}=\frac{k_{xn_1}k_{ym_2}-k_{ym_1}k_{xn_2}}{k^{\bar{n}_1}_{\rho}k^{\bar{n}_2}_{\rho}} \tag{4.42}$$

noting that $c_{\bar{n}_1,\bar{n}_2}=c_{\bar{n}_2,\bar{n}_1}$ and $s_{\bar{n}_1,\bar{n}_2}=-s_{\bar{n}_2,\bar{n}_1}$. With these definitions, the following dot products can be conveniently written as:

$$\begin{aligned}\left(\hat{z}\times\hat{h}_{\bar{n}'}\right).\left(\hat{h}_{\bar{n}}\right) &= s_{\bar{n}',\bar{n}}\\ \left(\hat{z}\times\hat{h}_{\bar{n}'}\right).\left(\hat{z}\times\hat{h}_{\bar{n}}\right) &= c_{\bar{n}',\bar{n}}\\ \left(\hat{h}_{\bar{n}'}\right).\left(\hat{h}_{\bar{n}}\right) &= c_{\bar{n}',\bar{n}}\\ \left(\hat{h}_{\bar{n}'}\right).\left(\hat{z}\times\hat{h}_{\bar{n}}\right) &= s_{\bar{n},\bar{n}'}\end{aligned} \tag{4.43}$$

In the case of the zeroth order contributions, the following dot products are most useful:

$$\begin{aligned}
\left(\hat{z}\times\hat{h}_{\bar{n}'}\right).\left(\hat{h}_i\right) &= s_{\bar{n}',\bar{0}} = s_{\bar{n}',i} \\
\left(\hat{z}\times\hat{h}_{\bar{n}'}\right).\left(\hat{z}\times\hat{h}_i\right) &= c_{\bar{n}',\bar{0}} = c_{\bar{n}',i} \\
\left(\hat{h}_{\bar{n}'}\right).\left(\hat{h}_i\right) &= c_{\bar{n}',\bar{0}} = c_{\bar{n}',i} \\
\left(\hat{h}_{\bar{n}'}\right).\left(\hat{z}\times\hat{h}_i\right) &= s_{\bar{0},\bar{n}'} = s_{i,\bar{n}'}
\end{aligned} \tag{4.44}$$

Similarly, for the dot the products involving the gradient of the interfaces; we have the following:

$$\begin{aligned}
\left(\hat{z}\times\hat{h}_{\bar{n}'}\right).\left(\nabla_t f_i(\bar{x})\times\hat{z}\right) &= \frac{k_{xn'}}{k_\rho^{\bar{n}'}}\partial_y f_i - \frac{k_{ym'}}{k_\rho^{\bar{n}'}}\partial_x f_i \\
\left(\hat{h}_{\bar{n}'}\right).\left(\nabla_t f_i(\bar{x})\times\hat{z}\right) &= \frac{k_{xn'}}{k_\rho^{\bar{n}'}}\partial_x f_i + \frac{k_{ym'}}{k_\rho^{\bar{n}'}}\partial_y f_i
\end{aligned} \tag{4.45}$$

where

$$\left(\nabla_t f_i(\bar{x})\right) = \partial_x f_i\hat{x} + \partial_y f_i\hat{y} \tag{4.46}$$

Plugging in the components of the forcing functions into the solutions given in Equations 4.39 and 4.40, contributions to the scattering coefficients at any order can be easily obtained. For a more general (arbitrary order) formulation, the following definitions are necessary. First, as a reminder, the Fourier transform of the p^{th} power of the surface profile is given as:

$$\mathcal{F}\left\{z^p\right\}_{\bar{n}'} = \sum_{\bar{n}_1}...\sum_{\bar{n}_{p-1}} h_{\bar{n}_1}....h_{\bar{n}_{p-1}}\; h_{\bar{n}'-\sum_{i=1}^{p-1}\bar{n}_i} \tag{4.47}$$

In addition, for the case when the gradients of the surfaces are involved, terms with the first partial derivative of the surface, multiplied with the $(p-1)^{th}$ power of the surface profile are obtained. These terms can be expressed as:

$$\mathcal{F}\left\{\partial_x f_{(i)} z_{(i)}^{p-1}\right\}_{\bar{n}'} = \sum_{\bar{n}_1}...\sum_{\bar{n}_{p-1}} h_{\bar{n}_1}^{(i)}....h_{\bar{n}_{p-1}}^{(i)}\; h_{\bar{n}'-\sum_{i=1}^{p-1}\bar{n}_i}^{(i)}\left(\frac{2\pi i}{P_x}(n'-\sum_{i=1}^{p-1}n_i)\right) \tag{4.48}$$

and

$$\mathcal{F}\left\{\partial_y f_{(i)} z_{(i)}^{p-1}\right\}_{\bar{n}'} = \sum_{\bar{n}_1} ... \sum_{\bar{n}_{p-1}} h_{\bar{n}_1}^{(i)} .... h_{\bar{n}_{p-1}}^{(i)} \; h_{\bar{n}'-\sum_{i=1}^{p-1}\bar{n}_i}^{(i)} \left(\frac{2\pi i}{P_y}(m' - \sum_{i=1}^{p-1} m_i)\right) \tag{4.49}$$

where, $(i) = 1$ for the upper surface and $(i) = 2$ for the lower surface.

Similar to the Dirichlet treatment given in Chapter 2, the following index terms are defined for convenience:

$$\bar{n}^* = \sum_{i=1}^{N-1} \bar{n}_i, \qquad \bar{n}^{r*} = \bar{n} + \sum_{i=1}^{N-r-1} \bar{n}_i \tag{4.50}$$

Finally, it should be noted that expressions of the following form:

$$\begin{aligned} &\left(\frac{k_{xn'}}{k_\rho^{\bar{n}'}}\mathcal{F}\left\{\partial_x f_i \; (z_i)^{N-1}\right\}_{\bar{n}'} + \frac{k_{ym'}}{k_\rho^{\bar{n}'}}\mathcal{F}\left\{\partial_y f_i \; (z_i)^{N-1}\right\}_{\bar{n}'}\right) \\ &\left(\frac{k_{xn'}}{k_\rho^{\bar{n}'}}\mathcal{F}\left\{\partial_y f_i \; (z_i)^{N-1}\right\}_{\bar{n}'} - \frac{k_{ym'}}{k_\rho^{\bar{n}'}}\mathcal{F}\left\{\partial_x f_i \; (z_i)^{N-1}\right\}_{\bar{n}'}\right) \end{aligned} \tag{4.51}$$

are obtained in several steps of the derivations. Using the formulation defined above, these expressions can be reduced to:

$$\begin{aligned} &i\left(k_\rho^{\bar{n}'} - k_\rho^{\bar{n}^*} c_{\bar{n}^*,\bar{n}'}\right)\mathcal{F}\left\{(z_i)^N\right\}_{\bar{n}'} \\ &i\left(k_\rho^{\bar{n}^*} \; s_{\bar{n}^*,\bar{n}'}\right)\mathcal{F}\left\{(z_i)^N\right\}_{\bar{n}'} \end{aligned} \tag{4.52}$$

respectively. After these clarifications, solutions are provided in the following subsections.

4.4.1 Zeroth order contribution to N^{th} order solution: Horizontal Incidence Case

In case of horizontal incidence, the zeroth order contribution to the general N^{th} order solution can be expressed for horizontally polarized scattering coefficients: $\xi =$

$\{\alpha, A, C, \gamma\}$,

$$\begin{aligned}
\xi_{\bar{n}'}^{(N,0)} &= \mathcal{F}\left\{z_1^N\right\}_{\bar{n}'}\Bigg[- c_{\bar{n}',\bar{0}} K_{E1}^{\xi}(\bar{n}')\left(\frac{(-i)^N}{N!}k_{zi}^N + \frac{(i)^N}{N!}R_{E_1}^{(N),h}(\bar{0})\right) \\
&\quad - c_{\bar{n}',\bar{0}}\, K_{H1}^{\xi}(\bar{n}')\left(\frac{k_{z0}^{\bar{0}}}{k_0\eta_0}\frac{(-i)^N}{N!}k_{zi}^N + \frac{(i)^N}{N!}R_{H_1}^{(N+1),h}(\bar{0})\right) \\
&\quad - i\left(k_\rho^{\bar{n}'} - k_\rho^{\bar{n}^*}c_{\bar{n}^*,\bar{n}'}\right)K_{H1}^{\xi}(\bar{n}')\left(\frac{k_{\rho i}}{k_0\eta_0}\frac{(-i)^{N-1}}{(N-1)!}k_{zi}^{N-1} - \frac{(i)^{N-1}}{(N-1)!}k_\rho^{\bar{0}}R_{H_1}^{(N-1),h}(\bar{0})\right)\Bigg] \\
&\quad + \mathcal{F}\left\{z_2^N\right\}_{\bar{n}'}\Bigg[- c_{\bar{n}',\bar{0}}\, K_{E2}^{\xi}(\bar{n}')\left(\frac{(i)^N}{N!}R_{E_2}^{(N),h}(\bar{0})\right) \\
&\quad - c_{\bar{n}',\bar{0}}\, K_{H2}^{\xi}(\bar{n}')\left(\frac{(i)^N}{N!}R_{H_2}^{(N+1),h}(\bar{0})\right) \\
&\quad + i\left(k_\rho^{\bar{n}'} - k_\rho^{\bar{n}^*}c_{\bar{n}^*,\bar{n}'}\right)K_{H2}^{\xi}(\bar{n}')\left(\frac{(i)^{N-1}}{(N-1)!}k_\rho^{\bar{0}}R_{H_2}^{(N-1),h}(\bar{0})\right)\Bigg] \qquad (4.53)
\end{aligned}$$

And for vertically polarized scattering coefficients:$\zeta = \{\beta, B, D, \delta\}$:

$$\begin{aligned}
\zeta_{\bar{n}'}^{(N,0)} &= \mathcal{F}\left\{z_1^N\right\}_{\bar{n}'}\Bigg[- s_{\bar{0},\bar{n}'} K_{E1}^{\zeta}(\bar{n}')\left(\frac{(-i)^N}{N!}k_{zi}^N + \frac{(i)^N}{N!}R_{E_1}^{(N),h}(\bar{0})\right) \\
&\quad - s_{\bar{n}',\bar{0}}\, K_{H1}^{\zeta}(\bar{n}')\left(\frac{k_{z0}^{\bar{0}}}{k_0\eta_0}\frac{(-i)^N}{N!}k_{zi}^N + \frac{(i)^N}{N!}R_{H_1}^{(N+1),h}(\bar{0})\right) \\
&\quad - i\left(k_\rho^{\bar{n}^*}\, s_{\bar{n}^*,\bar{n}'}\right)K_{H1}^{\zeta}(\bar{n}')\left(\frac{k_{\rho i}}{k_0\eta_0}\frac{(-i)^{N-1}}{(N-1)!}k_{zi}^{N-1} - \frac{(i)^{N-1}}{(N-1)!}k_\rho^{\bar{0}}R_{H_1}^{(N-1),h}(\bar{0})\right)\Bigg] \\
&\quad + \mathcal{F}\left\{z_2^N\right\}_{\bar{n}'}\Bigg[- s_{\bar{0},\bar{n}'}\, K_{E2}^{\zeta}(\bar{n}')\left(\frac{(i)^N}{N!}R_{E_2}^{(N),h}(\bar{0})\right) \\
&\quad - s_{\bar{n}',\bar{0}}\, K_{H2}^{\zeta}(\bar{n}')\left(\frac{(i)^N}{N!}R_{H_2}^{(N+1),h}(\bar{0})\right) \\
&\quad + i\left(k_\rho^{\bar{n}^*}\, s_{\bar{n}^*,\bar{n}'}\right)K_{H2}^{\zeta}(\bar{n}')\left(\frac{(i)^{N-1}}{(N-1)!}k_\rho^{\bar{0}}R_{H_2}^{(N-1),h}(\bar{0})\right)\Bigg] \qquad (4.54)
\end{aligned}$$

4.4.2 Zeroth order contribution to N^{th} order solution: Vertical Incidence Case

In case of vertical incidence, the zeroth order contribution to the general N^{th} order solution can be expressed for horizontally polarized scattering coefficients as :

$\xi = \{\alpha, A, C, \gamma\}$,

$$\begin{aligned}
\xi_{\bar{n}'}^{(N,0)} &= \mathcal{F}\left\{z_1^N\right\}_{\bar{n}'}\Bigg[s_{\bar{n}',\bar{0}}\; K_{E1}^{\xi}(\bar{n}')\left(\frac{k_{zi}}{k_0}\frac{(-i)^N}{N!}k_{zi}^N - \frac{(i)^N}{N!}R_{E_1}^{(N+1),v}(\bar{0})\right) \\
&\quad + i\left(k_\rho^{\bar{n}^*}\; s_{\bar{n}^*,\bar{n}'}\right)K_{E1}^{\xi}(\bar{n}')\left(\frac{k_{\rho i}}{k_0}\frac{(-i)^{N-1}}{(N-1)!}k_{zi}^{N-1} + \frac{(i)^{N-1}}{(N-1)!}k_\rho^{\bar{0}}R_{E_1}^{(N-1),v}(\bar{0})\right) \\
&\quad - s_{\bar{0},\bar{n}'}K_{H1}^{\xi}(\bar{n}')\left(\frac{1}{\eta_0}\frac{(-i)^N}{N!}k_{zi}^N + \frac{(i)^N}{N!}R_{H_1}^{(N),v}(\bar{0})\right)\Bigg] \\
&\quad + \mathcal{F}\left\{z_2^N\right\}_{\bar{n}'}\Bigg[- s_{\bar{n}',\bar{0}}\; K_{E2}^{\xi}(\bar{n}')\left(\frac{(i)^N}{(N)!}R_{E_2}^{(N+1),v}(\bar{0})\right) \\
&\quad + i\left(k_\rho^{\bar{n}^*}\; s_{\bar{n}^*,\bar{n}'}\right)K_{E2}^{\xi}(\bar{n}')\left(\frac{(i)^{N-1}}{(N-1)!}k_\rho^{\bar{0}}R_{E_2}^{(N-1),v}(\bar{0})\right) \\
&\quad - s_{\bar{0},\bar{n}'}\; K_{H2}^{\xi}(\bar{n}')\left(\frac{(i)^N}{N!}R_{H_2}^{(N),v}(\bar{0})\right)\Bigg] \qquad (4.55)
\end{aligned}$$

and for vertically polarized scattering coefficients: $\zeta = \{\beta, B, D, \delta\}$.

$$\begin{aligned}
\zeta_{\bar{n}'}^{(N,0)} &= \mathcal{F}\left\{z_1^N\right\}_{\bar{n}'}\Bigg[c_{\bar{n}',\bar{0}}\; K_{E1}^{\zeta}(\bar{n}')\left(\frac{k_{zi}}{k_0}\frac{(-i)^N}{N!}k_{zi}^N - \frac{(i)^N}{N!}R_{E_1}^{(N+1),v}(\bar{0})\right) \\
&\quad + i\left(k_\rho^{\bar{n}'} - k_\rho^{\bar{n}^*}c_{\bar{n}^*,\bar{n}'}\right)K_{E1}^{\zeta}(\bar{n}')\left(\frac{k_{\rho i}}{k_0}\frac{(-i)^{N-1}}{(N-1)!}k_{zi}^{N-1} + \frac{(i)^{N-1}}{(N-1)!}k_\rho^{\bar{0}}R_{E_1}^{(N-1),v}(\bar{0})\right) \\
&\quad - c_{\bar{n}',\bar{0}}K_{H1}^{\zeta}(\bar{n}')\left(\frac{1}{\eta_0}\frac{(-i)^N}{N!}k_{zi}^N + \frac{(i)^N}{N!}R_{H_1}^{(N),v}(\bar{0})\right)\Bigg] \\
&\quad + \mathcal{F}\left\{z_2^N\right\}_{\bar{n}'}\Bigg[- c_{\bar{n}',\bar{0}}\; K_{E2}^{\zeta}(\bar{n}')\left(\frac{(i)^N}{(N)!}R_{E_2}^{(N+1),v}(\bar{0})\right) \\
&\quad + i\left(k_\rho^{\bar{n}'} - k_\rho^{\bar{n}^*}c_{\bar{n}^*,\bar{n}'}\right)K_{E2}^{\zeta}(\bar{n}')\left(\frac{(i)^{N-1}}{(N-1)!}k_\rho^{\bar{0}}R_{E_2}^{(N-1),v}(\bar{0})\right) \\
&\quad - c_{\bar{n}',\bar{0}}\; K_{H2}^{\zeta}(\bar{n}')\left(\frac{(i)^N}{N!}R_{H_2}^{(N),v}(\bar{0})\right)\Bigg] \qquad (4.56)
\end{aligned}$$

4.4.3 Lower order contributions to N^{th} order solution:

The lower(r^{th}) order contribution to the general N^{th} order solution has the same representation for both horizontal and vertical incidence cases. These solutions can

be expressed in the following compact form: For horizontally polarized scattering coefficients: $\xi = \{\alpha, A, C, \gamma\}$,

$$\begin{aligned}
\xi_{\bar{n}'}^{(N,r)} &= -\frac{(i)^{N-r}}{(N-r)!}\sum_{\bar{n}}\mathcal{F}\left\{z_1^{N-r}\right\}_{\bar{n}'-\bar{n}} \\
&\left(c_{\bar{n}',\bar{n}}\left(K_{E1}^{\xi}(\bar{n}')\mathcal{A}_{E1}^{(N,r)}(\bar{n}) + K_{H1}^{\xi}(\bar{n}')\mathcal{A}_{H1}^{(N+1,r)}(\bar{n})\right)\right. \\
&+s_{\bar{n}',\bar{n}}\left(K_{E1}^{\xi}(\bar{n}')\mathcal{B}_{E1}^{(N+1,r)}(\bar{n}) - K_{H1}^{\xi}(\bar{n}')\mathcal{B}_{H1}^{(N,r)}(\bar{n})\right) \\
&-(N-r)(k_\rho^{\bar{n}})\left(\left(k_\rho^{\bar{n}^{r*}}s_{\bar{n}^{r*},\bar{n}'}\right)K_{E1}^{\xi}(\bar{n}')\mathcal{B}_{E1}^{(N-1,r)}(\bar{n})\right. \\
&\qquad\left.\left.+\left(k_\rho^{\bar{n}'} - k_\rho^{\bar{n}^{r*}}c_{\bar{n}^{r*},\bar{n}'}\right)K_{H1}^{\xi}(\bar{n}')\mathcal{A}_{H1}^{(N-1,r)}(\bar{n})\right)\right) \\
&-\frac{(i)^{N-r}}{(N-r)!}\sum_{\bar{n}}\mathcal{F}\left\{z_2^{N-r}\right\}_{\bar{n}'-\bar{n}} \\
&\left(c_{\bar{n}',\bar{n}}\left(K_{E2}^{\xi}(\bar{n}')\mathcal{A}_{E2}^{(N,r)}(\bar{n}) + K_{H2}^{\xi}(\bar{n}')\mathcal{A}_{H2}^{(N+1,r)}(\bar{n})\right)\right. \\
&+s_{\bar{n}',\bar{n}}\left(K_{E2}^{\xi}(\bar{n}')\mathcal{B}_{E2}^{(N+1,r)}(\bar{n}) - K_{H2}^{\xi}(\bar{n}')\mathcal{B}_{H2}^{(N,r)}(\bar{n})\right) \\
&-(N-r)(k_\rho^{\bar{n}})\left(\left(k_\rho^{\bar{n}^{r*}}s_{\bar{n}^{r*},\bar{n}'}\right)K_{E2}^{\xi}(\bar{n}')\mathcal{B}_{E2}^{(N-1,r)}(\bar{n})\right. \\
&\qquad\left.\left.+\left(k_\rho^{\bar{n}'} - k_\rho^{\bar{n}^{r*}}c_{\bar{n}^{r*},\bar{n}'}\right)K_{H2}^{\xi}(\bar{n}')\mathcal{A}_{H2}^{(N-1,r)}(\bar{n})\right)\right) \qquad (4.57)
\end{aligned}$$

and for vertically polarized scattering coefficients: $\zeta = \{\beta, B, D, \delta\}$:

$$\begin{aligned}
\zeta_{\bar{n}'}^{(N,r)} &= -\frac{(i)^{N-r}}{(N-r)!}\sum_{\bar{n}}\mathcal{F}\left\{z_1^{N-r}\right\}_{\bar{n}'-\bar{n}} \\
&\left(s_{\bar{n}',\bar{n}}\left(K_{H1}^{\zeta}(\bar{n}')\mathcal{A}_{H1}^{(N+1,r)}(\bar{n}) - K_{E1}^{\zeta}(\bar{n}')\mathcal{A}_{E1}^{(N,r)}(\bar{n})\right)\right. \\
&+c_{\bar{n}',\bar{n}}\left(K_{E1}^{\zeta}(\bar{n}')\mathcal{B}_{E1}^{(N+1,r)}(\bar{n}) + K_{H1}^{\zeta}(\bar{n}')\mathcal{B}_{H1}^{(N,r)}(\bar{n})\right) \\
&-(N-r)(k_\rho^{\bar{n}})\left(\left(k_\rho^{\bar{n}^{r*}}s_{\bar{n}^{r*},\bar{n}'}\right)K_{H1}^{\zeta}(\bar{n}')\mathcal{A}_{H1}^{(N-1,r)}(\bar{n})\right. \\
&\qquad\left.\left.+\left(k_\rho^{\bar{n}'} - k_\rho^{\bar{n}^{r*}}c_{\bar{n}^{r*},\bar{n}'}\right)K_{E1}^{\zeta}(\bar{n}')\mathcal{B}_{E1}^{(N-1,r)}(\bar{n})\right)\right)
\end{aligned}$$

$$
\begin{aligned}
&-\frac{(i)^{N-r}}{(N-r)!}\sum_{\bar{n}}\mathcal{F}\left\{z_2^{N-r}\right\}_{\bar{n}'-\bar{n}} \\
&\Bigg(s_{\bar{n}',\bar{n}}\left(K_{H2}^{\zeta}(\bar{n}')\mathcal{A}_{H2}^{(N+1,r)}(\bar{n})-K_{E2}^{\zeta}(\bar{n}')\mathcal{A}_{E2}^{(N,r)}(\bar{n})\right) \\
&+c_{\bar{n}',\bar{n}}\left(K_{E2}^{\zeta}(\bar{n}')\mathcal{B}_{E2}^{(N+1,r)}(\bar{n})+K_{H2}^{\zeta}(\bar{n}')\mathcal{B}_{H2}^{(N,r)}(\bar{n})\right) \\
&-(N-r)(k_\rho^{\bar{n}})\Bigg(\left(k_\rho^{\bar{n}^{r*}}s_{\bar{n}^{r*},\bar{n}'}\right)K_{H2}^{\zeta}(\bar{n}')\mathcal{A}_{H2}^{(N-1,r)}(\bar{n}) \\
&\qquad\qquad+\left(k_\rho^{\bar{n}'}-k_\rho^{\bar{n}^{r*}}c_{\bar{n}^{r*},\bar{n}'}\right)K_{E2}^{\zeta}(\bar{n}')\mathcal{B}_{E2}^{(N-1,r)}(\bar{n})\Bigg)\Bigg)
\end{aligned}
\tag{4.58}
$$

With these general form of solutions, we can proceed to the first, second, and then the arbitrary order solutions. In the next section, a complete first order solution will be considered, where only the zeroth order contribution terms are relevant.

4.5 First Order Solution

In this section the first order complete solution is provided. The first order solution requires the study of only the zeroth order components of the forcing functions. By directly plugging in the value of $N = 1$ to the Equations 4.53 through 4.56, the following general form is obtained.

$$
\tau_{\bar{n}'}^{(1)} = h_{\bar{n}'}^{(1)}\, g_\tau^{(1,0)}(\bar{n}') + h_{\bar{n}'}^{(2)}\, g_\tau^{(0,1)}(\bar{n}') \tag{4.59}
$$

Here, $h_{\bar{n}'}^{(1)}$ and $h_{\bar{n}'}^{(2)}$ are the Fourier coefficients of the upper and lower surfaces respectively. The terms $g_\tau^{(1,0)}(\bar{n}')$ and $g_\tau^{(0,1)}(\bar{n}')$ are the so called "SPM kernels" at the first order. General indexing of $g_\tau^{(p,q)}$ is used for the SPM kernels of order $(p+q)$ throughout the rest of the dissertation, where p and q are integers, representing the number of Fourier coefficients necessary to obtain the scattering coefficients of the upper and lower surface respectively. As an example, when an SPM kernel, say $g^{3,2}$

is given, then a term that is of fifth order is understood, which requires three Fourier coefficients from the upper surface and two Fourier coefficients from the lower surface. This representation will be discuss in more detail in the following chapter. For now, we will proceed to explicit expressions of the first order SPM kernels, starting with horizontal incidence.

The first order SPM kernels for a horizontally polarized incident plane wave can be expressed as follows: For horizontally polarized scattering coefficients: $\xi = \{\alpha, A, C, \gamma\}$,

$$\begin{aligned} g_{\xi}^{(1,0)}(\bar{n}') &= \Bigg[ic_{\bar{n}',\bar{0}} K_{E1}^{\xi}(\bar{n}') \left(k_{zi} - R_{E_1}^{(1),h}(\bar{0})\right) \\ &\quad + ic_{\bar{n}',\bar{0}}\, K_{H1}^{\xi}(\bar{n}') \left(\frac{k_{zi}^2}{k_0\eta_0} - R_{H_1}^{(2),h}(\bar{0})\right) \\ &\quad - i\left(k_{\rho}^{\bar{n}'} - k_{\rho i} c_{\bar{n}',\bar{0}}\right) k_{\rho i} K_{H1}^{\xi}(\bar{n}') \left(\frac{1}{k_0\eta_0} - R_{H_1}^{(0),h}(\bar{0})\right) \Bigg] \end{aligned} \tag{4.60}$$

and

$$\begin{aligned} g_{\xi}^{(0,1)}(\bar{n}') &= \Bigg[- ic_{\bar{n}',\bar{0}}\, K_{E2}^{\xi}(\bar{n}') \left(R_{E_2}^{(1),h}(\bar{0})\right) \\ &\quad - ic_{\bar{n}',\bar{0}}\, K_{H2}^{\xi}(\bar{n}') \left(R_{H_2}^{(2),h}(\bar{0})\right) \\ &\quad + i\left(k_{\rho}^{\bar{n}'} - k_{\rho i} c_{\bar{n}',\bar{0}}\right) k_{\rho i} K_{H2}^{\xi}(\bar{n}') \left(R_{H_2}^{(0),h}(\bar{0})\right) \Bigg] \end{aligned} \tag{4.61}$$

and for vertically polarized scattering coefficients: $\zeta = \{\beta, B, D, \delta\}$:

$$\begin{aligned} g_{\zeta}^{(1,0)}(\bar{n}') &= \Bigg[+ is_{\bar{0},\bar{n}'} K_{E1}^{\zeta}(\bar{n}') \left(k_{zi} - R_{E_1}^{(1),h}(\bar{0})\right) \\ &\quad + is_{\bar{n}',\bar{0}}\, K_{H1}^{\zeta}(\bar{n}') \left(\frac{k_{zi}^2}{k_0\eta_0} - R_{H_1}^{(2),h}(\bar{0})\right) \\ &\quad - i\left(k_{\rho i}^2\, s_{\bar{0},\bar{n}'}\right) K_{H1}^{\zeta}(\bar{n}') \left(\frac{1}{k_0\eta_0} - R_{H_1}^{(0),h}(\bar{0})\right) \Bigg] \end{aligned} \tag{4.62}$$

and

$$g_{\zeta}^{(0,1)}(\bar{n}') = \Bigg[-is_{\bar{0},\bar{n}'}\, K_{E2}^{\zeta}(\bar{n}') \left(R_{E_2}^{(1),h}(\bar{0})\right) - is_{\bar{n}',\bar{0}}\, K_{H2}^{\zeta}(\bar{n}') \left(R_{H_2}^{(2),h}(\bar{0})\right) + i\left(k_{\rho i}^2\, s_{\bar{0},\bar{n}'}\right) K_{H2}^{\zeta}(\bar{n}') \left(R_{H_2}^{(0),h}(\bar{0})\right) \Bigg] \tag{4.63}$$

The first order SPM kernels for a vertically polarized incident plane wave can be expressed as follows: For horizontally polarized scattering coefficients: $\xi = \{\alpha, A, C, \gamma\}$,

$$g_{\xi}^{(1,0)}(\bar{n}') = \Bigg[-is_{\bar{n}',\bar{0}}\, K_{E1}^{\xi}(\bar{n}') \left(\frac{k_{zi}^2}{k_0} + R_{E_1}^{(2),v}(\bar{0})\right) + i\left(k_{\rho i}^2\, s_{\bar{0},\bar{n}'}\right) K_{E1}^{\xi}(\bar{n}') \left(\frac{1}{k_0} + R_{E_1}^{(0),v}(\bar{0})\right) + is_{\bar{0},\bar{n}'} K_{H1}^{\xi}(\bar{n}') \left(\frac{1}{\eta_0} k_{zi} - R_{H_1}^{(1),v}(\bar{0})\right) \Bigg] \tag{4.64}$$

$$g_{\xi}^{(0,1)}(\bar{n}') = \Bigg[-is_{\bar{n}',\bar{0}}\, K_{E2}^{\xi}(\bar{n}') \left(R_{E_2}^{(2),v}(\bar{0})\right) + i\left(k_{\rho i}^2\, s_{\bar{0},\bar{n}'}\right) K_{E2}^{\xi}(\bar{n}') \left(R_{E_2}^{(0),v}(\bar{0})\right) - is_{\bar{0},\bar{n}'}\, K_{H2}^{\xi}(\bar{n}') \left(R_{H_2}^{(1),v}(\bar{0})\right) \Bigg] \tag{4.65}$$

and for vertically polarized scattering coefficients: $\zeta = \{\beta, B, D, \delta\}$:

$$g_{\zeta}^{(1,0)}(\bar{n}') = \Bigg[-ic_{\bar{n}',\bar{0}}\, K_{E1}^{\zeta}(\bar{n}') \left(\frac{k_{zi}^2}{k_0} + R_{E_1}^{(2),v}(\bar{0})\right) + i\left(k_{\rho}^{\bar{n}'} - k_{\rho i} c_{\bar{0},\bar{n}'}\right) k_{\rho i} K_{E1}^{\zeta}(\bar{n}') \left(\frac{1}{k_0} + R_{E_1}^{(0),v}(\bar{0})\right) + ic_{\bar{n}',\bar{0}} K_{H1}^{\zeta}(\bar{n}') \left(\frac{1}{\eta_0} k_{zi} - R_{H_1}^{(1),v}(\bar{0})\right) \Bigg] \tag{4.66}$$

$$g_{\zeta}^{(0,1)}(\bar{n}') = \Bigg[-ic_{\bar{n}',\bar{0}}\, K_{E2}^{\zeta}(\bar{n}') \left(R_{E_2}^{(2),v}(\bar{0})\right)$$

$$+i\left(k_{\rho}^{\bar{n}'}-k_{\rho i}c_{\bar{0},\bar{n}'}\right)k_{\rho i}K_{E2}^{\zeta}(\bar{n}')\left(R_{E_2}^{(0),v}(\bar{0})\right)$$
$$-ic_{\bar{n}',\bar{0}}\;K_{H2}^{\zeta}(\bar{n}')\left(R_{H_2}^{(1),v}(\bar{0})\right)\Bigg] \tag{4.67}$$

The expressions up to this point complete the first order solution. Next, the second order solution is considered.

4.6 Second Order Solution

The second order solution can be obtained by studying the zeroth order contribution expressions given by Equations 4.53 through 4.56 for $N = 2$, together with the lower order contribution expressions given by Equations 4.57 and 4.58 for $N = 2$ and $r = 1$. Following these steps, the following general form for the second order solution is obtained:

$$\begin{aligned}\tau_{\bar{n}'}^{(2)} \;=\; \sum_{\bar{n}_1}\Bigg(& h_{\bar{n}_1}^{(1)}\;h_{\bar{n}'-\bar{n}_1}^{(1)}g_{\tau}^{(2,0)}(\bar{n}',\bar{n}_1)\\ & +h_{\bar{n}_1}^{(2)}\;h_{\bar{n}'-\bar{n}_1}^{(1)}g_{\tau}^{(1,1)}(\bar{n}',\bar{n}_1)\\ & +h_{\bar{n}_1}^{(2)}\;h_{\bar{n}'-\bar{n}_1}^{(2)}g_{\tau}^{(0,2)}(\bar{n}',\bar{n}_1)\Bigg)\end{aligned} \tag{4.68}$$

It should be noted here that the zeroth order contribution terms contribute only to the kernels $g_{\tau}^{(2,0)}$ and $g_{\tau}^{(0,2)}$. However, the first order contribution formulation ($r = 1$) contributes to all three kernels. In addition, for a compact notation, a new operator ($\{....\}_{\{p,q\}}$) is defined for the lower order functionals $\mathcal{A}$ and $\mathcal{B}$. A demonstration of this operator is presented here for $\mathcal{A}_{E1}^{(N,1)}$, and similar ideas directly follow to the other functionals; First, recall that the $\mathcal{A}_{E1}^{(N,r)}$ functional was defined as:

$$\mathcal{A}_{E1}^{(N,r)}(\bar{n}) = \left[\alpha_{\bar{n}}^{(r)}(k_{z0}^{\bar{n}})^{N-r} - A_{\bar{n}}^{(r)}(-k_{z1}^{\bar{n}})^{N-r} - C_{\bar{n}}^{(r)}(k_{z1}^{\bar{n}})^{N-r}\right] \tag{4.69}$$

Plugging in $r = 1$ gives:

$$\mathcal{A}_{E1}^{(N,1)}(\bar{n}) = \left[\alpha_{\bar{n}}^{(1)}(k_{z0}^{\bar{n}})^{N-1} - A_{\bar{n}}^{(1)}(-k_{z1}^{\bar{n}})^{N-1} - C_{\bar{n}}^{(1)}(k_{z1}^{\bar{n}})^{N-1}\right] \tag{4.70}$$

It is also known that the first order solution has the following general form:

$$\tau_{\bar{n}'}^{(1)} = h_{\bar{n}'}^{(1)}\ g_{\tau}^{(1,0)}(\bar{n}') + h_{\bar{n}'}^{(2)}\ g_{\tau}^{(0,1)}(\bar{n}') \tag{4.71}$$

Here, we define the $(\{....\}_{\{p,q\}})$ operator as follows:

$$\begin{aligned}
\{\mathcal{A}_{E1}^{(N,1)}(\bar{n})\}_{\{1,0\}} &= \left[g_{\alpha}^{(1,0)}(n)(k_{z0}^{\bar{n}})^{N-1} - g_{A}^{(1,0)}(n)(-k_{z1}^{\bar{n}})^{N-1} - g_{C}^{(1,0)}(n)(k_{z1}^{\bar{n}})^{N-1}\right] \\
\{\mathcal{A}_{E1}^{(N,1)}(\bar{n})\}_{\{0,1\}} &= \left[g_{\alpha}^{(0,1)}(n)(k_{z0}^{\bar{n}})^{N-1} - g_{A}^{(0,1)}(n)(-k_{z1}^{\bar{n}})^{N-1} - g_{C}^{(0,1)}(n)(k_{z1}^{\bar{n}})^{N-1}\right]
\end{aligned} \tag{4.72}$$

so that the original functional $\mathcal{A}_{E1}^{(N,1)}(\bar{n})$ can be expressed as:

$$\mathcal{A}_{E1}^{(N,1)}(\bar{n}) = h_{\bar{n}}^{(1)}\{\mathcal{A}_{E1}^{(N,1)}(\bar{n})\}_{\{1,0\}} + h_{\bar{n}}^{(2)}\{\mathcal{A}_{E1}^{(N,1)}(\bar{n})\}_{\{0,1\}} \tag{4.73}$$

Using the notation described above, the second order SPM kernels can be simplified: First, the formulation for the horizontally polarized scattering coefficients is considered: The $g_{\xi}^{(2,0)}$ kernels for horizontal incidence can expressed as:

$$\begin{aligned}
g_{\xi}^{(2,0)}(\bar{n}', \bar{n}_1) &= \Bigg[+ \frac{1}{2} c_{\bar{n}',\bar{0}} K_{E1}^{\xi}(\bar{n}') \left(k_{zi}^2 + R_{E_1}^{(2),h}(\bar{0})\right) \\
&\quad + \frac{1}{2} c_{\bar{n}',\bar{0}}\ K_{H1}^{\xi}(\bar{n}') \left(\frac{k_{zi}^3}{k_0\eta_0} + R_{H_1}^{(3),h}(\bar{0})\right) \\
&\quad - \left(k_{\rho}^{\bar{n}'} - k_{\rho}^{\bar{n}_1} c_{\bar{n}_1,\bar{n}'}\right) k_{\rho i} K_{H1}^{\xi}(\bar{n}') \left(\frac{k_{zi}}{k_0\eta_0} + R_{H_1}^{(1),h}(\bar{0})\right) \\
&\quad - (i) \Bigg\{ c_{\bar{n}',\bar{n}_1} \left(K_{E1}^{\xi}(\bar{n}')\{\mathcal{A}_{E1}^{(2,1)}(\bar{n}_1)\}_{\{1,0\}} + K_{H1}^{\xi}(\bar{n}')\{\mathcal{A}_{H1}^{(3,1)}(\bar{n}_1)\}_{\{1,0\}}\right) \\
&\quad + s_{\bar{n}',\bar{n}_1} \left(K_{E1}^{\xi}(\bar{n}')\{\mathcal{B}_{E1}^{(3,1)}(\bar{n}_1)\}_{\{1,0\}} - K_{H1}^{\xi}(\bar{n}')\{\mathcal{B}_{H1}^{(2,1)}(\bar{n}_1)\}_{\{1,0\}}\right) \\
&\quad - (k_{\rho}^{\bar{n}_1}) \Bigg(\left(k_{\rho}^{\bar{n}_1} s_{\bar{n}_1,\bar{n}'}\right) K_{E1}^{\xi}(\bar{n}')\{\mathcal{B}_{E1}^{(1,1)}(\bar{n}_1)\}_{\{1,0\}} \\
&\quad + \left(k_{\rho}^{\bar{n}'} - k_{\rho}^{\bar{n}_1} c_{\bar{n}_1,\bar{n}'}\right) K_{H1}^{\xi}(\bar{n}')\{\mathcal{A}_{H1}^{(1,1)}(\bar{n}_1)\}_{\{1,0\}} \Bigg) \Bigg\} \Bigg]
\end{aligned} \tag{4.74}$$

And for vertical incidence:

$$
\begin{aligned}
g_{\xi}^{(2,0)}(\bar{n}',\bar{n}_1) \;=\; & \Bigg[-\frac{1}{2} s_{\bar{n}',\bar{0}}\; K_{E1}^{\xi}(\bar{n}') \left(\frac{k_{zi}^3}{k_0} - R_{E_1}^{(3),v}(\bar{0}) \right) \\
& + \left(k_{\rho}^{\bar{n}_1}\; s_{\bar{n}_1,\bar{n}'} \right) k_{\rho i} K_{E1}^{\xi}(\bar{n}') \left(\frac{k_{zi}}{k_0} - R_{E_1}^{(1),v}(\bar{0}) \right) \\
& + \frac{1}{2} s_{\bar{0},\bar{n}'} K_{H1}^{\xi}(\bar{n}') \left(\frac{k_{zi}^2}{\eta_0} + R_{H_1}^{(2),v}(\bar{0}) \right) \\
& - (i) \Bigg\{ c_{\bar{n}',\bar{n}_1} \left(K_{E1}^{\xi}(\bar{n}') \{ \mathcal{A}_{E1}^{(2,1)}(\bar{n}_1) \}_{\{1,0\}} + K_{H1}^{\xi}(\bar{n}') \{ \mathcal{A}_{H1}^{(3,1)}(\bar{n}_1) \}_{\{1,0\}} \right) \\
& + s_{\bar{n}',\bar{n}_1} \left(K_{E1}^{\xi}(\bar{n}') \{ \mathcal{B}_{E1}^{(3,1)}(\bar{n}_1) \}_{\{1,0\}} - K_{H1}^{\xi}(\bar{n}') \{ \mathcal{B}_{H1}^{(2,1)}(\bar{n}_1) \}_{\{1,0\}} \right) \\
& - (k_{\rho}^{\bar{n}_1}) \Bigg(\left(k_{\rho}^{\bar{n}_1} s_{\bar{n}_1,\bar{n}'} \right) K_{E1}^{\xi}(\bar{n}') \{ \mathcal{B}_{E1}^{(1,1)}(\bar{n}_1) \}_{\{1,0\}} \\
& + \left(k_{\rho}^{\bar{n}'} - k_{\rho}^{\bar{n}_1} c_{\bar{n}_1,\bar{n}'} \right) K_{H1}^{\xi}(\bar{n}') \{ \mathcal{A}_{H1}^{(1,1)}(\bar{n}_1) \}_{\{1,0\}} \Bigg) \Bigg\} \Bigg]
\end{aligned}
\tag{4.75}
$$

For both horizontal and vertical polarizations, the $g_{\xi}^{(1,1)}$ kernel has the following unique representation:

$$
\begin{aligned}
g_{\xi}^{(1,1)}(\bar{n}',\bar{n}_1) \;=\; & -(i) \left(c_{\bar{n}',\bar{n}_1} \left(K_{E1}^{\xi}(\bar{n}') \{ \mathcal{A}_{E1}^{(2,1)}(\bar{n}_1) \}_{\{0,1\}} + K_{H1}^{\xi}(\bar{n}') \{ \mathcal{A}_{H1}^{(3,1)}(\bar{n}_1) \}_{\{0,1\}} \right) \right. \\
& + s_{\bar{n}',\bar{n}_1} \left(K_{E1}^{\xi}(\bar{n}') \{ \mathcal{B}_{E1}^{(3,1)}(\bar{n}_1) \}_{\{0,1\}} - K_{H1}^{\xi}(\bar{n}') \{ \mathcal{B}_{H1}^{(2,1)}(\bar{n}_1) \}_{\{0,1\}} \right) \\
& - (k_{\rho}^{\bar{n}_1}) \Bigg(\left(k_{\rho}^{\bar{n}_1} s_{\bar{n}_1,\bar{n}'} \right) K_{E1}^{\xi}(\bar{n}') \{ \mathcal{B}_{E1}^{(1,1)}(\bar{n}_1) \}_{\{0,1\}} \\
& + \left(k_{\rho}^{\bar{n}'} - k_{\rho}^{\bar{n}_1} c_{\bar{n}_1,\bar{n}'} \right) K_{H1}^{\xi}(\bar{n}') \{ \mathcal{A}_{H1}^{(1,1)}(\bar{n}_1) \}_{\{0,1\}} \Bigg) \\
& + c_{\bar{n}',\bar{n}'-\bar{n}_1} \left(K_{E2}^{\xi}(\bar{n}') \{ \mathcal{A}_{E2}^{(2,1)}(\bar{n}'-\bar{n}_1) \}_{\{1,0\}} + K_{H2}^{\xi}(\bar{n}') \{ \mathcal{A}_{H2}^{(3,1)}(\bar{n}'-\bar{n}_1) \}_{\{1,0\}} \right) \\
& + s_{\bar{n}',\bar{n}'-\bar{n}_1} \left(K_{E2}^{\xi}(\bar{n}') \{ \mathcal{B}_{E2}^{(3,1)}(\bar{n}'-\bar{n}_1) \}_{\{1,0\}} - K_{H2}^{\xi}(\bar{n}') \{ \mathcal{B}_{H2}^{(2,1)}(\bar{n}'-\bar{n}_1) \}_{\{1,0\}} \right) \\
& - (k_{\rho}^{\bar{n}'-\bar{n}_1}) \Bigg(\left(k_{\rho}^{\bar{n}'-\bar{n}_1} s_{\bar{n}'-\bar{n}_1,\bar{n}'} \right) K_{E2}^{\xi}(\bar{n}') \{ \mathcal{B}_{E2}^{(1,1)}(\bar{n}'-\bar{n}_1) \}_{\{1,0\}}
\end{aligned}
$$

$$+\left(k_\rho^{\bar{n}'}-k_\rho^{\bar{n}'-\bar{n}_1}c_{\bar{n}'-\bar{n}_1,\bar{n}'}\right)K^\xi_{H2}(\bar{n}')\{\mathcal{A}^{(1,1)}_{H2}(\bar{n}'-\bar{n}_1)\}_{\{1,0\}}\Bigg)\Bigg) \tag{4.76}$$

The $g_\xi^{(0,2)}$ kernels for horizontal incidence can expressed as:

$$\begin{aligned}
g_\xi^{(0,2)}(\bar{n}',\bar{n}_1) &= \Bigg[\frac{1}{2}c_{\bar{n}',\bar{0}}\;K^\xi_{E2}(\bar{n}')\left(R^{(2),h}_{E_2}(\bar{0})\right)\\
&+\frac{1}{2}c_{\bar{n}',\bar{0}}\;K^\xi_{H2}(\bar{n}')\left(R^{(3),h}_{H_2}(\bar{0})\right)\\
&-\left(k_\rho^{\bar{n}'}-k_\rho^{\bar{n}_1}c_{\bar{n}_1,\bar{n}'}\right)K^\xi_{H2}(\bar{n}')\left(k_{\rho i}R^{(1),h}_{H_2}(\bar{0})\right)\\
&-(i)\Bigg\{c_{\bar{n}',\bar{n}_1}\left(K^\xi_{E2}(\bar{n}')\{\mathcal{A}^{(2,1)}_{E2}(\bar{n}_1)\}_{\{0,1\}}+K^\xi_{H2}(\bar{n}')\{\mathcal{A}^{(3,1)}_{H2}(\bar{n}_1)\}_{\{0,1\}}\right)\\
&+s_{\bar{n}',\bar{n}_1}\left(K^\xi_{E2}(\bar{n}')\{\mathcal{B}^{(3,1)}_{E2}(\bar{n}_1)\}_{\{0,1\}}-K^\xi_{H2}(\bar{n}')\{\mathcal{B}^{(2,1)}_{H2}(\bar{n}_1)\}_{\{0,1\}}\right)\\
&-(k_\rho^{\bar{n}_1})\Bigg(\left(k_\rho^{\bar{n}_1}s_{\bar{n}_1,\bar{n}'}\right)K^\xi_{E2}(\bar{n}')\{\mathcal{B}^{(1,1)}_{E2}(\bar{n}_1)\}_{\{0,1\}}\\
&+\left(k_\rho^{\bar{n}'}-k_\rho^{\bar{n}_1}c_{\bar{n}_1,\bar{n}'}\right)K^\xi_{H2}(\bar{n}')\{\mathcal{A}^{(1,1)}_{H2}(\bar{n}_1)\}_{\{0,1\}}\Bigg)\Bigg\}\Bigg]
\end{aligned} \tag{4.77}$$

and for vertical incidence:

$$\begin{aligned}
g_\xi^{(0,2)}(\bar{n}',\bar{n}_1) &= \Bigg[\frac{1}{2}s_{\bar{n}',\bar{0}}\;K^\xi_{E2}(\bar{n}')\left(R^{(3),v}_{E_2}(\bar{0})\right)\\
&-\left(k_\rho^{\bar{n}_1}\;s_{\bar{n}_1,\bar{n}'}\right)K^\xi_{E2}(\bar{n}')\left(k_{\rho i}R^{(1),v}_{E_2}(\bar{0})\right)\\
&+\frac{1}{2}s_{\bar{0},\bar{n}'}\;K^\xi_{H2}(\bar{n}')\left(R^{(2),v}_{H_2}(\bar{0})\right)\\
&-(i)\Bigg\{c_{\bar{n}',\bar{n}_1}\left(K^\xi_{E2}(\bar{n}')\{\mathcal{A}^{(2,1)}_{E2}(\bar{n}_1)\}_{\{0,1\}}+K^\xi_{H2}(\bar{n}')\{\mathcal{A}^{(3,1)}_{H2}(\bar{n}_1)\}_{\{0,1\}}\right)\\
&+s_{\bar{n}',\bar{n}_1}\left(K^\xi_{E2}(\bar{n}')\{\mathcal{B}^{(3,1)}_{E2}(\bar{n}_1)\}_{\{0,1\}}-K^\xi_{H2}(\bar{n}')\{\mathcal{B}^{(2,1)}_{H2}(\bar{n}_1)\}_{\{0,1\}}\right)\\
&-(k_\rho^{\bar{n}_1})\Bigg(\left(k_\rho^{\bar{n}_1}s_{\bar{n}_1,\bar{n}'}\right)K^\xi_{E2}(\bar{n}')\{\mathcal{B}^{(1,1)}_{E2}(\bar{n}_1)\}_{\{0,1\}}\\
&+\left(k_\rho^{\bar{n}'}-k_\rho^{\bar{n}_1}c_{\bar{n}_1,\bar{n}'}\right)K^\xi_{H2}(\bar{n}')\{\mathcal{A}^{(1,1)}_{H2}(\bar{n}_1)\}_{\{0,1\}}\Bigg)\Bigg\}\Bigg]
\end{aligned} \tag{4.78}$$

The formulation for the vertically polarized scattering coefficients: The $g_\zeta^{(2,0)}$ kernels for horizontal incidence can expressed as:

$$
\begin{aligned}
g_\zeta^{(2,0)}(\bar{n}', \bar{n}_1) \;=\; & \Bigg[\frac{1}{2} s_{\bar{0},\bar{n}'} K_{E1}^{\zeta}(\bar{n}') \left(k_{zi}^2 + R_{E_1}^{(2),h}(\bar{0}) \right) \\
& + \frac{1}{2} s_{\bar{n}',\bar{0}} \; K_{H1}^{\zeta}(\bar{n}') \left(\frac{k_{zi}^3}{k_0 \eta_0} + R_{H_1}^{(3),h}(\bar{0}) \right) \\
& - \left(k_\rho^{\bar{n}_1} \; s_{\bar{n}_1,\bar{n}'} \right) K_{H1}^{\zeta}(\bar{n}') k_{\rho i} \left(\frac{k_{zi}}{k_0 \eta_0} + R_{H_1}^{(1),h}(\bar{0}) \right) \\
& - (i) \left(s_{\bar{n}',\bar{n}_1} \left(K_{H1}^{\zeta}(\bar{n}') \{ \mathcal{A}_{H1}^{(3,1)}(\bar{n}_1) \}_{(1,0)} - K_{E1}^{\zeta}(\bar{n}') \{ \mathcal{A}_{E1}^{(2,1)}(\bar{n}_1) \}_{(1,0)} \right) \right. \\
& + c_{\bar{n}',\bar{n}_1} \left(K_{E1}^{\zeta}(\bar{n}') \{ \mathcal{B}_{E1}^{(3,1)}(\bar{n}_1) \}_{(1,0)} + K_{H1}^{\zeta}(\bar{n}') \{ \mathcal{B}_{H1}^{(2,1)}(\bar{n}_1) \}_{(1,0)} \right) \\
& - (k_\rho^{\bar{n}_1}) \left(\left(k_\rho^{\bar{n}_1} s_{\bar{n}_1,\bar{n}'} \right) K_{H1}^{\zeta}(\bar{n}') \{ \mathcal{A}_{H1}^{(1,1)}(\bar{n}_1) \}_{(1,0)} \right. \\
& \left. \left. + \left(k_\rho^{\bar{n}'} - k_\rho^{\bar{n}_1} c_{\bar{n}_1,\bar{n}'} \right) K_{E1}^{\zeta}(\bar{n}') \{ \mathcal{B}_{E1}^{(1,1)}(\bar{n}_1) \}_{(1,0)} \right) \right) \Bigg]
\end{aligned}
\tag{4.79}
$$

And, for vertical incidence:

$$
\begin{aligned}
g_\zeta^{(2,0)}(\bar{n}', \bar{n}_1) \;=\; & \Bigg[- \frac{1}{2} c_{\bar{n}',\bar{0}} \; K_{E1}^{\zeta}(\bar{n}') \left(\frac{k_{zi}^3}{k_0} - R_{E_1}^{(3),v}(\bar{0}) \right) \\
& + \left(k_\rho^{\bar{n}'} - k_\rho^{\bar{n}_1} c_{\bar{n}_1,\bar{n}'} \right) k_{\rho i} K_{E1}^{\zeta}(\bar{n}') \left(\frac{k_{zi}}{k_0} - R_{E_1}^{(1),v}(\bar{0}) \right) \\
& + \frac{1}{2} c_{\bar{n}',\bar{0}} K_{H1}^{\zeta}(\bar{n}') \left(\frac{1}{\eta_0} k_{zi}^2 + R_{H_1}^{(2),v}(\bar{0}) \right) \\
& - (i) \left(s_{\bar{n}',\bar{n}_1} \left(K_{H1}^{\zeta}(\bar{n}') \{ \mathcal{A}_{H1}^{(3,1)}(\bar{n}_1) \}_{(1,0)} - K_{E1}^{\zeta}(\bar{n}') \{ \mathcal{A}_{E1}^{(2,1)}(\bar{n}_1) \}_{(1,0)} \right) \right. \\
& + c_{\bar{n}',\bar{n}_1} \left(K_{E1}^{\zeta}(\bar{n}') \{ \mathcal{B}_{E1}^{(3,1)}(\bar{n}_1) \}_{(1,0)} + K_{H1}^{\zeta}(\bar{n}') \{ \mathcal{B}_{H1}^{(2,1)}(\bar{n}_1) \}_{(1,0)} \right) \\
& - (k_\rho^{\bar{n}_1}) \left(\left(k_\rho^{\bar{n}_1} s_{\bar{n}_1,\bar{n}'} \right) K_{H1}^{\zeta}(\bar{n}') \{ \mathcal{A}_{H1}^{(1,1)}(\bar{n}_1) \}_{(1,0)} \right.
\end{aligned}
$$

$$+\left(k_\rho^{\bar{n}'}-k_\rho^{\bar{n}_1}c_{\bar{n}_1,\bar{n}'}\right)K_{E1}^{\zeta}(\bar{n}')\{\mathcal{B}_{E1}^{(1,1)}(\bar{n}_1)\}_{(1,0)}\Bigg)\Bigg)\Bigg] \tag{4.80}$$

For both horizontal and vertical polarizations, the $g_\zeta^{(1,1)}$ kernels have the following unique representation:

$$\begin{aligned}
g_\zeta^{(1,1)}(\bar{n}',\bar{n}_1) &= -(i)\Bigg(s_{\bar{n}',\bar{n}_1}\left(K_{H1}^{\zeta}(\bar{n}')\{\mathcal{A}_{H1}^{(3,1)}(\bar{n}_1)\}_{(0,1)}-K_{E1}^{\zeta}(\bar{n}')\{\mathcal{A}_{E1}^{(2,1)}(\bar{n}_1)\}_{(0,1)}\right)\\
&+c_{\bar{n}',\bar{n}}\left(K_{E1}^{\zeta}(\bar{n}')\{\mathcal{B}_{E1}^{(3,1)}(\bar{n}_1)\}_{(0,1)}+K_{H1}^{\zeta}(\bar{n}')\{\mathcal{B}_{H1}^{(2,1)}(\bar{n}_1)\}_{(0,1)}\right)\\
&-(k_\rho^{\bar{n}_1})\Bigg(\left(k_\rho^{\bar{n}_1}s_{\bar{n}_1,\bar{n}'}\right)K_{H1}^{\zeta}(\bar{n}')\{\mathcal{A}_{H1}^{(1,1)}(\bar{n}_1)\}_{(0,1)}\\
&+\left(k_\rho^{\bar{n}'}-k_\rho^{\bar{n}_1}c_{\bar{n}_1,\bar{n}'}\right)K_{E1}^{\zeta}(\bar{n}')\{\mathcal{B}_{E1}^{(1,1)}(\bar{n}_1)\}_{(0,1)}\Bigg)\\
&+s_{\bar{n}',\bar{n}'-\bar{n}_1}\left(K_{H2}^{\zeta}(\bar{n}')\{\mathcal{A}_{H2}^{(3,1)}(\bar{n}'-\bar{n}_1)\}_{(1,0)}-K_{E2}^{\zeta}(\bar{n}')\{\mathcal{A}_{E2}^{(2,1)}(\bar{n}'-\bar{n}_1)\}_{(1,0)}\right)\\
&+c_{\bar{n}',\bar{n}'-\bar{n}_1}\left(K_{E2}^{\zeta}(\bar{n}')\{\mathcal{B}_{E2}^{(3,1)}(\bar{n}'-\bar{n}_1)\}_{(1,0)}+K_{H2}^{\zeta}(\bar{n}')\{\mathcal{B}_{H2}^{(2,1)}(\bar{n}'-\bar{n}_1)\}_{(1,0)}\right)\\
&-(k_\rho^{\bar{n}'-\bar{n}_1})\Bigg(\left(k_\rho^{\bar{n}'-\bar{n}_1}s_{\bar{n}'-\bar{n}_1,\bar{n}'}\right)K_{H2}^{\zeta}(\bar{n}')\{\mathcal{A}_{H2}^{(1,1)}(\bar{n}'-\bar{n}_1)\}_{(1,0)}\\
&+\left(k_\rho^{\bar{n}'}-k_\rho^{\bar{n}'-\bar{n}_1}c_{\bar{n}'-\bar{n}_1,\bar{n}'}\right)K_{E2}^{\zeta}(\bar{n}')\{\mathcal{B}_{E2}^{(1,1)}(\bar{n}'-\bar{n}_1)\}_{(1,0)}\Bigg)\Bigg)
\end{aligned} \tag{4.81}$$

Finally, the $g_\zeta^{(0,2)}$ kernels for horizontal incidence can expressed as:

$$\begin{aligned}
g_\zeta^{(0,2)}(\bar{n}',\bar{n}_1) &= \Bigg[\frac{1}{2}s_{\bar{0},\bar{n}'}\;K_{E2}^{\zeta}(\bar{n}')\left(R_{E_2}^{(2),h}(\bar{0})\right)\\
&+\frac{1}{2}s_{\bar{n}',\bar{0}}\;K_{H2}^{\zeta}(\bar{n}')\left(R_{H_2}^{(3),h}(\bar{0})\right)\\
&-\left(k_\rho^{\bar{n}_1}\;s_{\bar{n}_1,\bar{n}'}\right)K_{H2}^{\zeta}(\bar{n}')\left(k_{\rho i}R_{H_2}^{(1),h}(\bar{0})\right)\\
&-(i)\left(s_{\bar{n}',\bar{n}_1}\left(K_{H2}^{\zeta}(\bar{n}')\{\mathcal{A}_{H2}^{(3,1)}(\bar{n}_1)\}_{(0,1)}-K_{E2}^{\zeta}(\bar{n}')\{\mathcal{A}_{E2}^{(2,1)}(\bar{n}_1)\}_{(0,1)}\right)\right.\\
&+c_{\bar{n}',\bar{n}}\left(K_{E2}^{\zeta}(\bar{n}')\{\mathcal{B}_{E2}^{(3,1)}(\bar{n}_1)\}_{(0,1)}+K_{H2}^{\zeta}(\bar{n}')\{\mathcal{B}_{H2}^{(2,1)}(\bar{n}_1)\}_{(0,1)}\right)
\end{aligned}$$

$$
\begin{aligned}
&-(k_\rho^{\bar{n}_1})\Bigg(\left(k_\rho^{\bar{n}_1}s_{\bar{n}_1,\bar{n}'}\right)K_{H2}^{\zeta}(\bar{n}')\{\mathcal{A}_{H2}^{(1,1)}(\bar{n}_1)\}_{(0,1)} \\
&+\left(k_\rho^{\bar{n}'}-k_\rho^{\bar{n}_1}c_{\bar{n}_1,\bar{n}'}\right)K_{E2}^{\zeta}(\bar{n}')\{\mathcal{B}_{E2}^{(1,1)}(\bar{n}_1)\}_{(0,1)}\Bigg)\Bigg] \qquad (4.82)
\end{aligned}
$$

for the vertical incidence case:

$$
\begin{aligned}
g_\zeta^{(0,2)}(\bar{n}',\bar{n}_1) \;=\; &\Bigg[\frac{1}{2}c_{\bar{n}',\bar{0}}\,K_{E2}^{\zeta}(\bar{n}')\left(R_{E_2}^{(3),v}(\bar{0})\right) \\
&-\left(k_\rho^{\bar{n}'}-k_\rho^{\bar{n}_1}c_{\bar{n}_1,\bar{n}'}\right)k_{\rho i}K_{E2}^{\zeta}(\bar{n}')\left(R_{E_2}^{(1),v}(\bar{0})\right) \\
&+\frac{1}{2}c_{\bar{n}',\bar{0}}\,K_{H2}^{\zeta}(\bar{n}')\left(R_{H_2}^{(2),v}(\bar{0})\right) \\
&-(i)\Bigg(s_{\bar{n}',\bar{n}_1}\left(K_{H2}^{\zeta}(\bar{n}')\{\mathcal{A}_{H2}^{(3,1)}(\bar{n}_1)\}_{(0,1)}-K_{E2}^{\zeta}(\bar{n}')\{\mathcal{A}_{E2}^{(2,1)}(\bar{n}_1)\}_{(0,1)}\right) \\
&+c_{\bar{n}',\bar{n}}\left(K_{E2}^{\zeta}(\bar{n}')\{\mathcal{B}_{E2}^{(3,1)}(\bar{n}_1)\}_{(0,1)}+K_{H2}^{\zeta}(\bar{n}')\{\mathcal{B}_{H2}^{(2,1)}(\bar{n}_1)\}_{(0,1)}\right) \\
&-(k_\rho^{\bar{n}_1})\Bigg(\left(k_\rho^{\bar{n}_1}s_{\bar{n}_1,\bar{n}'}\right)K_{H2}^{\zeta}(\bar{n}')\{\mathcal{A}_{H2}^{(1,1)}(\bar{n}_1)\}_{(0,1)} \\
&+\left(k_\rho^{\bar{n}'}-k_\rho^{\bar{n}_1}c_{\bar{n}_1,\bar{n}'}\right)K_{E2}^{\zeta}(\bar{n}')\{\mathcal{B}_{E2}^{(1,1)}(\bar{n}_1)\}_{(0,1)}\Bigg)\Bigg] \qquad (4.83)
\end{aligned}
$$

The formulation presented up to this point concludes the complete second order SPM solution. In the following sections, instead of studying the higher order kernels one by one, a more general form of the solution is considered.

4.7 Higher order solutions

Previously, the SPM kernels up to second order were derived explicitly. The general form of solution was given for "τ" denoting any of the scattering coefficients $\{\alpha, A, C, \gamma, \beta, B, D, \delta\}$. The zeroth order solution was:

$$
\tau_{\bar{n}'}^{(0)} = \Gamma_\tau\,\delta_{\bar{n}'} \qquad (4.84)
$$

and the first order solution was:

$$\tau_{\bar{n}'}^{(1)} = h_{\bar{n}'}^{(1)}\ g_{\tau}^{(1,0)}(\bar{n}') + h_{\bar{n}'}^{(2)}\ g_{\tau}^{(0,1)}(\bar{n}') \tag{4.85}$$

while the second order solution was:

$$\begin{aligned}\tau_{\bar{n}'}^{(2)} \;=\; \sum_{\bar{n}_1}\Bigg(& h_{\bar{n}_1}^{(1)}\ h_{\bar{n}'-\bar{n}_1}^{(1)} g_{\tau}^{(2,0)}(\bar{n}', \bar{n}_1) \\ & + h_{\bar{n}_1}^{(2)}\ h_{\bar{n}'-\bar{n}_1}^{(1)} g_{\tau}^{(1,1)}(\bar{n}', \bar{n}_1) \\ & + h_{\bar{n}_1}^{(2)}\ h_{\bar{n}'-\bar{n}_1}^{(2)} g_{\tau}^{(0,2)}(\bar{n}', \bar{n}_1) \Bigg)\end{aligned} \tag{4.86}$$

Simply by inspection, we can express the third order solution in the following form:

$$\begin{aligned}\tau_{\bar{n}'}^{(3)} \;=\; \sum_{\bar{n}_1}\sum_{\bar{n}_2}\Bigg(& h_{\bar{n}_1}^{(1)}\ h_{\bar{n}_2}^{(1)}\ h_{\bar{n}'-\bar{n}_1-\bar{n}_2}^{(1)} g_{\tau}^{(3,0)}(\bar{n}', \bar{n}_1, \bar{n}_2) \\ & + h_{\bar{n}_1}^{(2)}\ h_{\bar{n}_2}^{(1)}\ h_{\bar{n}'-\bar{n}_1-\bar{n}_2}^{(1)} g_{\tau}^{(2,1)}(\bar{n}', \bar{n}_1, \bar{n}_2) \\ & + h_{\bar{n}_1}^{(2)}\ h_{\bar{n}_2}^{(2)}\ h_{\bar{n}'-\bar{n}_1-\bar{n}_2}^{(1)} g_{\tau}^{(1,2)}(\bar{n}', \bar{n}_1, \bar{n}_2) \\ & + h_{\bar{n}_1}^{(2)}\ h_{\bar{n}_2}^{(2)}\ h_{\bar{n}'-\bar{n}_1-\bar{n}_2}^{(2)} g_{\tau}^{(0,3)}(\bar{n}', \bar{n}_1, \bar{n}_2) \Bigg)\end{aligned} \tag{4.87}$$

When higher order solutions are considered, the explicit kernel equations can be quite cumbersome. In general, there are a total of $(N+1)$ SPM kernels that have be considered in order to express the (N^{th}) order SPM solution, a more general and compact form of formulation can be obtained, if a notation based on tensors and vectors, is assumed and the summation over the kernels is expressed as a dot product. In this section, the basic notational conventions for such a compact formulation are described.

First, all of the unknown N^{th} order SPM scattering coefficients are put in a single array of size (1×8) in the following form:

$$\bar{\tau}_{\bar{n}'}^{(N)} = \left[\alpha_{\bar{n}'}^{(N)}, \beta_{\bar{n}'}^{(N)}, A_{\bar{n}'}^{(N)}, B_{\bar{n}'}^{(N)}, C_{\bar{n}'}^{(N)}, D_{\bar{n}'}^{(N)}, \gamma_{\bar{n}'}^{(N)}, \delta_{\bar{n}'}^{(N)}\right] \tag{4.88}$$

A similar treatment can be done for the Fourier coefficient combinations, that multiply the SPM kernels. In this way, a general Fourier array can be defined as $\bar{\chi}^{(N)}_{\bar{n}'}$ with size $(1 \times (N+1))$, where the i^{th} element$(i = 0, 1, ..., N)$ is given by:

$$\chi^{(N)}_{\bar{n}',i} = h^{(2)}_{\bar{n}_1} h^{(2)}_{\bar{n}_2} ... h^{(2)}_{\bar{n}_i} h^{(1)}_{\bar{n}_{i+1}} .... h^{(1)}_{\bar{n}_{N-1}} h^{(1)}_{\bar{n}' - \sum_{t=1}^{N-1} \bar{n}_t} \tag{4.89}$$

so that $\bar{\chi}^{(N)}_{\bar{n}'}$ can be expressed as:

$$\bar{\chi}^{(N)}_{\bar{n}'}(\bar{n}_1, ..., \bar{n}_{N-1}) = \begin{bmatrix} h^{(1)}_{\bar{n}_1} h^{(1)}_{\bar{n}_2} .... h^{(1)}_{\bar{n}_{N-1}} h^{(1)}_{\bar{n}' - \sum_{t=1}^{N-1} \bar{n}_t} \\ h^{(2)}_{\bar{n}_1} h^{(1)}_{\bar{n}_2} .... h^{(1)}_{\bar{n}_{N-1}} h^{(1)}_{\bar{n}' - \sum_{t=1}^{N-1} \bar{n}_t} \\ h^{(2)}_{\bar{n}_1} h^{(2)}_{\bar{n}_2} .... h^{(1)}_{\bar{n}_{N-1}} h^{(1)}_{\bar{n}' - \sum_{t=1}^{N-1} \bar{n}_t} \\ \vdots \\ h^{(2)}_{\bar{n}_1} h^{(2)}_{\bar{n}_2} .... h^{(2)}_{\bar{n}_{N-1}} h^{(1)}_{\bar{n}' - \sum_{t=1}^{N-1} \bar{n}_t} \\ h^{(2)}_{\bar{n}_1} h^{(2)}_{\bar{n}_2} .... h^{(2)}_{\bar{n}_{N-1}} h^{(2)}_{\bar{n}' - \sum_{t=1}^{N-1} \bar{n}_t} \end{bmatrix}^T \tag{4.90}$$

Finally by defining the following two dimensional $((N+1) \times 8)$ tensor for the N^{th} order SPM kernel:

$$\bar{\bar{g}}^{(N)}(\bar{n}', \bar{n}_1, .., \bar{n}_{N-1}) = \begin{bmatrix} g^{(N,0)}_{\alpha} & g^{(N,0)}_{\beta} & \cdots & g^{(N,0)}_{\delta} \\ g^{(N-1,1)}_{\alpha} & g^{(N-1,1)}_{\beta} & & g^{(N-1,1)}_{\delta} \\ \vdots & & \ddots & \vdots \\ g^{(0,N)}_{\alpha} & g^{(0,N)}_{\beta} & \cdots & g^{(0,N)}_{\delta} \end{bmatrix} \tag{4.91}$$

with arguments of the tensor elements dropped for convenience, the solution can be given in following compact form:

$$\bar{\tau}^{(N)}_{\bar{n}'} = \sum_{\bar{n}_1} \sum_{\bar{n}_2} ... \sum_{\bar{n}_{N-1}} \bar{\chi}^{(N)}_{\bar{n}'} . \bar{\bar{g}}^{(N)}(\bar{n}', \bar{n}_1, .., \bar{n}_{N-1}) \tag{4.92}$$

In the following section, based on the tensor notation of the scattering coefficients and the corresponding kernels, an arbitrary order iterative solution procedure for SPM kernels will be introduced. First, the arbitrary order solution procedure will be described in an iterative fashion with several tensor definitions. Later, these tensors will be derived separately by studying the zeroth and lower order partial solutions given by Equations 4.53 through 4.58.

4.8 Arbitrary order solution: Tensor Notation

In this section, similar to the arbitrary order iterative solution for the 1-D Dirichlet problem presented in Chapter 2, the two layer SPM kernels are expressed as an iterative sum: higher order solutions in terms of lower order ones. First, the the complete solution is presented with several tensor definitions, derived from Equations 4.53 through 4.58. Then, each tensor will be provided explicitly.

The arbitrary order (N^{th} order) SPM kernel for the two layer problem is given in the following compact form:

$$\bar{\bar{g}}^{(N)}(\bar{n}', \bar{n}_1, .., \bar{n}_{N-1}) = \bar{\bar{u}}_0 . \bar{\bar{g}}_0^{(N)}(\bar{n}', s_{N-1}) + \sum_{l=1}^{2} \sum_{r=1}^{N-1} \bar{\bar{u}}_l^{(N,r)} . \bar{\bar{g}}_l^{(r)} . \bar{\bar{v}}_l^{(N,r)} \tag{4.93}$$

with

$$\bar{\bar{g}}_l^{(r)} = \begin{cases} \bar{\bar{g}}^{(r)}(\bar{s}_r, \bar{n}_1, .., \bar{n}_{r-1}) & l = 1 \\ \bar{\bar{g}}^{(r)}(\bar{n}' - \bar{s}_{N-r}, \bar{n}_{N-r+1}, .., \bar{n}_{N-1}) & l = 2 \end{cases} \tag{4.94}$$

and

$$\bar{\bar{v}}_l^{(N,r)} = \begin{cases} \bar{\bar{v}}_1^{(N,r)}(\bar{n}', \bar{s}_r, \bar{s}_{N-1}) & l = 1 \\ \bar{\bar{v}}_2^{(N,r)}(\bar{n}', \bar{n}' - \bar{s}_{N-r}, \bar{n}' - \bar{n}_{N-r}) & l = 2 \end{cases} \tag{4.95}$$

Here, we have:

$$\bar{n}^{r*} = \bar{n} + \sum_{i=1}^{N-r-1} \bar{n}_i, \qquad \bar{n}^* = \sum_{i=1}^{N-1} \bar{n}_i \tag{4.96}$$

as before and also we define a partial sum term:

$$\bar{s}_p = \sum_{k=1}^{p} \bar{n}_k \tag{4.97}$$

for convenience.The $\bar{\bar{u}}_0$ tensor is defined as:

$$\bar{\bar{u}}_0^{(N)} = \begin{bmatrix} 1 & 0 \\ 0 & 0 \\ \vdots & \vdots \\ 0 & 0 \\ 0 & 1 \end{bmatrix}_{(N+1)\times 2} \tag{4.98}$$

and the $\bar{\bar{u}}$ tensors of size $((N+1)\times(r+1))$ are defined as:

$$\bar{\bar{u}}_1^{(N,r)} = \begin{bmatrix} I_{(r+1)\times(r+1)} \\ ..... \\ 0_{(N-r)\times(r+1)} \end{bmatrix}, \quad \bar{\bar{u}}_2^{(N,r)} = \begin{bmatrix} 0_{(N-r)\times(r+1)} \\ ..... \\ I_{(r+1)\times(r+1)} \end{bmatrix} \tag{4.99}$$

In the following subsections, first the zeroth order contribution tensor $\bar{\bar{g}}_0^{(N)}$ will be introduced. Next, the lower order contribution kernels $\bar{\bar{v}}_l^{(N,r)}$, $l = 1, 2$ will be derived.

4.8.1 Zeroth order contribution tensor: $\bar{\bar{g}}_0^{(N)}$

The zeroth order contribution tensor is directly obtained from Equations 4.53 through 4.56. Note that the surface profiles were defined as $z_1 = f_1(\bar{x})$ and $z_2 = \bar{f}_2(\bar{x})$ with their p^{th} power Fourier coefficients given by:

$$\mathcal{F}\left\{z^p\right\}_{\bar{n}'} = \sum_{\bar{n}_1} ... \sum_{\bar{n}_{p-1}} h_{\bar{n}_1} .... h_{\bar{n}_{p-1}}\ h_{\bar{n}'-\sum_{i=1}^{p-1}\bar{n}_i} \tag{4.100}$$

With the new tensor notation we will have:

$$\mathcal{F}\left\{z_1^p\right\}_{\bar{n}'} = \sum_{\bar{n}_1} ... \sum_{\bar{n}_{p-1}} \chi^{(p)}_{\bar{n}',0}, \qquad \mathcal{F}\left\{z_2^p\right\}_{\bar{n}'} = \sum_{\bar{n}_1} ... \sum_{\bar{n}_{p-1}} \chi^{(p)}_{\bar{n}',p} \tag{4.101}$$

If these expressions plugged into Equations 4.53 through 4.56, these equations simplify to the following form:

$$\tau^{(N,0)}_{\bar{n}'} = \sum_{\bar{n}_1} ... \sum_{\bar{n}_{N-1}} \left(\chi^{(N)}_{\bar{n}',0}\ g^{(N)}_{0\tau 1}(\bar{n}', \bar{n}^*) + \chi^{(N)}_{\bar{n}',N}\ g^{(N)}_{0\tau 2}(\bar{n}', \bar{n}^*)\right) \tag{4.102}$$

Notice that the zeroth order contribution solution of the scattering coefficients only contribute to the SPM kernels $g^{(N,0)}$ and $g^{(0,N)}$. So, with the help of the tensor u_0, these contributions can be mapped into the corresponding SPM kernels. The $\bar{\bar{g}}_0^{(N)}$ tensor can be expressed in terms of these $g^{(N)}_{0\tau 1,2}(\bar{n}', \bar{n}^*)$ functions as:

$$\bar{\bar{g}}_0^{(N)} = \begin{bmatrix} g^{(N)}_{0\alpha 1} & g^{(N)}_{0\beta 1} & g^{(N)}_{0A1} & g^{(N)}_{0B1} & g^{(N)}_{0C1} & g^{(N)}_{0D1} & g^{(N)}_{0\gamma 1} & g^{(N)}_{0\delta 1} \\ g^{(N)}_{0\alpha 2} & g^{(N)}_{0\beta 2} & g^{(N)}_{0A2} & g^{(N)}_{0B2} & g^{(N)}_{0C2} & g^{(N)}_{0D2} & g^{(N)}_{0\gamma 2} & g^{(N)}_{0\delta 2} \end{bmatrix} \tag{4.103}$$

with the elements related to the upper surface given in the first row and the the elements of the lower surface, in the second row.

With the following newly defined variables:

$$\kappa_c(\bar{n}', \bar{n}^*) = \left(k_\rho^{\bar{n}'} - k_\rho^{\bar{n}^*} c_{\bar{n}^*,\bar{n}'}\right), \qquad \kappa_s(\bar{n}', \bar{n}^*) = \left(k_\rho^{\bar{n}^*}\, s_{\bar{n}^*,\bar{n}'}\right) \tag{4.104}$$

and slightly modified versions of the $R^{(N)}$ functionals given in Section 4.3.1, Equations 4.6 through 4.13:

$$\mathcal{R}^{(N)}_{E_1,h} = (-k^{\bar{0}}_{z0})^N + \Gamma_\alpha (k^{\bar{0}}_{z0})^N - \Gamma_A (-k^{\bar{0}}_{z1})^N - \Gamma_C (k^{\bar{0}}_{z1})^N \tag{4.105}$$

$$\mathcal{R}^{(N)}_{H_1,h} = -\frac{(-k^{\bar{0}}_{z0})^N}{k_0\eta_0} - \Gamma_\alpha \frac{(k^{\bar{0}}_{z0})^N}{k_0\eta_0} + \Gamma_A \frac{(-k^{\bar{0}}_{z1})^N}{k_1\eta_1} + \Gamma_C \frac{(k^{\bar{0}}_{z1})^N}{k_1\eta_1} \tag{4.106}$$

$$\mathcal{R}^{(N)}_{E_2,h} = \Gamma_A (-k^{\bar{0}}_{z1})^N e^{+ik^{\bar{0}}_{z1}d} + \Gamma_C (+k^{\bar{0}}_{z1})^N e^{-ik^{\bar{0}}_{z1}d} - \Gamma_\gamma (-k^{\bar{0}}_{z2})^N e^{+ik^{\bar{0}}_{z2}d} \tag{4.107}$$

$$\mathcal{R}^{(N)}_{H_2,h} = -\Gamma_A \frac{(-k^{\bar{0}}_{z1})^N}{k_1\eta_1} e^{+ik^{\bar{0}}_{z1}d} - \Gamma_C \frac{(+k^{\bar{0}}_{z1})^N}{k_1\eta_1} e^{-ik^{\bar{0}}_{z1}d} + \Gamma_\gamma \frac{(-k^{\bar{0}}_{z2})^N}{k_2\eta_2} e^{+ik^{\bar{0}}_{z2}d} \tag{4.108}$$

$$\mathcal{R}^{(N)}_{E_1,v} = \frac{(-k^{\bar{0}}_{z0})^N}{k_0} + \Gamma_\beta \frac{(k^{\bar{0}}_{z0})^N}{k_0} - \Gamma_B \frac{(-k^{\bar{0}}_{z1})^N}{k_1} - \Gamma_D \frac{(k^{\bar{0}}_{z1})^N}{k_1} \tag{4.109}$$

$$\mathcal{R}^{(N)}_{H_1,v} = \frac{(-k^{\bar{0}}_{z0})^N}{\eta_0} + \Gamma_\beta \frac{(k^{\bar{0}}_{z0})^N}{\eta_0} - \Gamma_B \frac{(-k^{\bar{0}}_{z1})^N}{\eta_1} - \Gamma_D \frac{(k^{\bar{0}}_{z1})^N}{\eta_1} \tag{4.110}$$

$$\mathcal{R}^{(N)}_{E_2,v} = \Gamma_B \frac{(-k^{\bar{0}}_{z1})^N}{k_1} e^{+ik^{\bar{0}}_{z1}d} + \Gamma_D \frac{(+k^{\bar{0}}_{z1})^N}{k_1} e^{-ik^{\bar{0}}_{z1}d} - \Gamma_\delta \frac{(-k^{\bar{0}}_{z2})^N}{k_2} e^{+ik^{\bar{0}}_{z2}d} \tag{4.111}$$

$$\mathcal{R}^{(N)}_{H_2,v} = \Gamma_B \frac{(-k^{\bar{0}}_{z1})^N}{\eta_1} e^{+ik^{\bar{0}}_{z1}d} + \Gamma_D \frac{(+k^{\bar{0}}_{z1})^N}{\eta_1} e^{-ik^{\bar{0}}_{z1}d} - \Gamma_\delta \frac{(-k^{\bar{0}}_{z2})^N}{\eta_2} e^{+ik^{\bar{0}}_{z2}d} \tag{4.112}$$

the elements of the zeroth order contribution kernel $\bar{\bar{g}}_0^{(N)}(\bar{n}', s_{N-1})$ can be given in a compact form; For horizontal polarization we have:

$$\begin{aligned} g^{(N),h}_{0\{\xi,\zeta\}l}(\bar{n}', \bar{n}^*) \;=\; & -\frac{(i)^N}{N!} \Bigg[K^{\{\xi,\zeta\}}_{El}(\bar{n}') \{c, s\}_{\bar{0},\bar{n}'} \mathcal{R}^{(N)}_{E_l,h} \\ & + K^{\{\xi,\zeta\}}_{Hl}(\bar{n}') \left(\{c, s\}_{\bar{n}',\bar{0}}\, \mathcal{R}^{(N+1)}_{H_l,h} - N \kappa_{\{c,s\}}(\bar{n}', \bar{n}^*) k_{\rho i} \mathcal{R}^{(N-1)}_{H_l,h} \right) \Bigg] \end{aligned} \tag{4.113}$$

and for vertical polarization:

$$g^{(N),v}_{0\{\xi,\zeta\}l}(\bar{n}',\bar{n}^*) = -\frac{(i)^N}{N!}\Bigg[K^{\{\xi,\zeta\}}_{Hl}(\bar{n}')\{s,c\}_{\bar{0},\bar{n}'}\mathcal{R}^{(N)}_{H_l,v} + K^{\{\xi,\zeta\}}_{El}(\bar{n}')\left(\{s,c\}_{\bar{n}',\bar{0}}\mathcal{R}^{(N+1)}_{E_l,v} - N\kappa_{\{s,c\}}(\bar{n}',\bar{n}^*)k_{\rho i}\mathcal{R}^{(N-1)}_{E_l,v}\right)\Bigg] \quad (4.114)$$

Note that ξ denotes $\{\alpha, A, C, \gamma\}$ and ζ denotes $\{\beta, B, D, \delta\}$ here and $l = 1, 2$. Also, a new notation of the form: $\{\xi, \zeta\}$ with either $\{c, s\}$ or $\{s, c\}$ is used in these equations, simply indicating an index change. For example, in Equation 4.113, if a horizontal scattering coefficient (and element of ξ) is intended, then c should be used either as a subscript or as a function in the rest of the expression.

4.8.2 Lower order contribution tensors: $\bar{\bar{v}}^{(N,r)}_l$

In this section , the procedure for obtaining the $\bar{\bar{v}}^{(N,r)}_l$ tensors is described. The first step is to study the $\mathcal{A}$ and $\mathcal{B}$ operators defined in Section 4.3.1 in tensor notation. Consider $\mathcal{A}^{(N,r)}_{E1}(\bar{n})$ for an example and the steps must be repeated for the others. In tensor notation $\mathcal{A}^{(N,r)}_{E1}$ can be given as:

$$\mathcal{A}^{(N,r)}_{E1}(\bar{n}) = \sum_{\bar{m}_1}\sum_{\bar{m}_2}...\sum_{\bar{m}_{r-1}} \bar{\chi}^{(r)}_{\bar{n}}(\bar{m}_1,...,\bar{m}_{r-1}).\bar{\bar{g}}^{(r)}(\bar{n},\bar{m}_1,..,\bar{m}_{r-1}).\begin{bmatrix} (k^{\bar{n}}_{z0})^{N-r} \\ 0 \\ -(-k^{\bar{n}}_{z1})^{N-r} \\ 0 \\ -(k^{\bar{n}}_{z1})^{N-r} \\ 0 \\ 0 \\ 0 \end{bmatrix} \quad (4.115)$$

Notice that $\mathcal{A}^{(N,r)}_{E1}$ can be represented by a simple column vector.

After studying all of the operators from $\mathcal{A}_{E1}^{(N,r)}$ to $\mathcal{B}_{H2}^{(N,r)}$, the next step is to put these column vectors into the lower order partial solution expressions given in Equations 4.57 and 4.58. In tensor notation, these equations can rewritten as:

$$\begin{aligned}\bar{\tau}_{\bar{n}'}^{(N,r)} &= \sum_{\bar{n}} \left(\sum_{\bar{n}_1} ... \sum_{\bar{n}_{N-r-1}} \right) \left(\sum_{\bar{m}_1} ... \sum_{\bar{m}_{r-1}} \right) \\ &\Bigg(\chi_{\bar{n}'-\bar{n},0}^{(N-r)}(\bar{n}_1,...,\bar{n}_{N-r-1}) \bar{\chi}_{\bar{n}}^{(r)}(\bar{m}_1,...,\bar{m}_{r-1}). \\ &\qquad .\bar{\bar{g}}^{(N)}(\bar{n}',\bar{m}_1,..,\bar{m}_{r-1}) \bar{\bar{v}}_1^{(N,r)}(\bar{n}',\bar{n},\bar{n}_1,...,\bar{n}_{N-r-1}) \\ &+ \chi_{\bar{n}'-\bar{n},N-r}^{(N-r)}(\bar{n}_1,...,\bar{n}_{N-r-1}) \bar{\chi}_{\bar{n}}^{(r)}(\bar{m}_1,...,\bar{m}_{r-1}). \\ &\qquad .\bar{\bar{g}}^{(N)}(\bar{n}',\bar{m}_1,..,\bar{m}_{r-1}) \bar{\bar{v}}_2^{(N,r)}(\bar{n}',\bar{n},\bar{n}_1,...,\bar{n}_{N-r-1}) \Bigg) \end{aligned} \quad (4.116)$$

Here, the $\bar{\bar{v}}_l^{(N,r)}$ tensors ($l = 1, 2$) are of size (8×8), and in fact, they are functions of only $\bar{n}'$, $\bar{n}$ and $\bar{n}^{r*}$. Their general form can be given as:

$$\bar{\bar{v}}_l^{(N,r)}(\bar{n}',\bar{n},\bar{n}^{r*}) = \begin{bmatrix} \vdots & \vdots & \vdots & \vdots & \vdots & \vdots & \vdots & \vdots \\ \bar{v}_{\alpha l} & \bar{v}_{\beta l} & \bar{v}_{Al} & \bar{v}_{Bl} & \bar{v}_{Cl} & \bar{v}_{Dl} & \bar{v}_{\gamma l} & \bar{v}_{\delta l} \\ \vdots & \vdots & \vdots & \vdots & \vdots & \vdots & \vdots & \vdots \end{bmatrix} \quad (4.117)$$

Each column here corresponds to a single scattering coefficient and can be expressed in terms of four special column vectors and their duals, in the following compact form:

$$\begin{aligned} \bar{v}_{\xi l}^{(N,r)}(\bar{n}',\bar{n},\bar{n}^{r*}) &= -\frac{(i)^{N-r}}{(N-r)!} \left(K_{El}^{\xi}(\bar{n}') \bar{v}_{El} + K_{Hl}^{\xi}(\bar{n}') \bar{v}_{Hl}^{(d)} \right) \\ \bar{v}_{\zeta l}^{(N,r)}(\bar{n}',\bar{n},\bar{n}^{r*}) &= -\frac{(i)^{N-r}}{(N-r)!} \left(K_{El}^{\zeta}(\bar{n}') \bar{v}_{El}^{(d)} + K_{Hl}^{\zeta}(\bar{n}') \bar{v}_{Hl} \right) \end{aligned} \quad (4.118)$$

These four special column vectors ($\bar{v}_{E1}$, $\bar{v}_{H1}$, $\bar{v}_{E2}$ and $\bar{v}_{H2}$) are given as::

$$\bar{v}_{E1}(\bar{n}', \bar{n}, \bar{n}^{r*}) = \begin{bmatrix} c_{\bar{n}',\bar{n}}(k_{z0}^{\bar{n}})^{N-r} \\ s_{\bar{n}',\bar{n}}\frac{(k_{z0}^{\bar{n}})^{N-r+1}}{k_0} - (N-r)k_\rho^{\bar{n}}\kappa_s(\bar{n}', \bar{n}^{r*})\frac{(k_{z0}^{\bar{n}})^{N-r-1}}{k_0} \\ -c_{\bar{n}',\bar{n}}(-k_{z1}^{\bar{n}})^{N-r} \\ -s_{\bar{n}',\bar{n}}\frac{(-k_{z1}^{\bar{n}})^{N-r+1}}{k_1} + (N-r)k_\rho^{\bar{n}}\kappa_s(\bar{n}', \bar{n}^{r*})\frac{(-k_{z1}^{\bar{n}})^{N-r-1}}{k_1} \\ -c_{\bar{n}',\bar{n}}(k_{z1}^{\bar{n}})^{N-r} \\ -s_{\bar{n}',\bar{n}}\frac{(k_{z1}^{\bar{n}})^{N-r+1}}{k_1} + (N-r)k_\rho^{\bar{n}}\kappa_s(\bar{n}', \bar{n}^{r*})\frac{(k_{z1}^{\bar{n}})^{N-r-1}}{k_1} \\ 0 \\ 0 \end{bmatrix} \tag{4.119}$$

$$\bar{v}_{H1}(\bar{n}', \bar{n}, \bar{n}^{r*}) = \begin{bmatrix} -s_{\bar{n}',\bar{n}}\frac{(k_{z0}^{\bar{n}})^{N-r+1}}{k_0\eta_0} + (N-r)(k_\rho^{\bar{n}})\kappa_s(\bar{n}', \bar{n}^{r*})\frac{(k_{z0}^{\bar{n}})^{N-r-1}}{k_0\eta_0} \\ c_{\bar{n}',\bar{n}}\frac{(k_{z0}^{\bar{n}})^{N-r}}{\eta_0} \\ s_{\bar{n}',\bar{n}}\frac{(-k_{z1}^{\bar{n}})^{N-r+1}}{k_1\eta_1} - (N-r)(k_\rho^{\bar{n}})\kappa_s(\bar{n}', \bar{n}^{r*})\frac{(-k_{z1}^{\bar{n}})^{N-r-1}}{k_1\eta_1} \\ -c_{\bar{n}',\bar{n}}\frac{(-k_{z1}^{\bar{n}})^{N-r}}{\eta_1} \\ s_{\bar{n}',\bar{n}}\frac{(k_{z1}^{\bar{n}})^{N-r+1}}{k_1\eta_1} - (N-r)(k_\rho^{\bar{n}})\kappa_s(\bar{n}', \bar{n}^{r*})\frac{(k_{z1}^{\bar{n}})^{N-r-1}}{k_1\eta_1} \\ -c_{\bar{n}',\bar{n}}\frac{(k_{z1}^{\bar{n}})^{N-r}}{\eta_1} \\ 0 \\ 0 \end{bmatrix} \tag{4.120}$$

$$\bar{v}_{E2}(\bar{n}', \bar{n}, \bar{n}^{r*}) = \begin{bmatrix} 0 \\ 0 \\ c_{\bar{n}',\bar{n}}(-k_{z1}^{\bar{n}})^{N-r}e^{+ik_{z1}^{\bar{n}}d} \\ \left(s_{\bar{n}',\bar{n}}(k_{z1}^{\bar{n}})^2 - (N-r)(k_\rho^{\bar{n}})\kappa_s(\bar{n}', \bar{n}^{r*})\right)\frac{(-k_{z1}^{\bar{n}})^{N-r-1}}{k_1}e^{+ik_{z1}^{\bar{n}}d} \\ c_{\bar{n}',\bar{n}}(+k_{z1}^{\bar{n}})^{N-r}e^{-ik_{z1}^{\bar{n}}d} \\ \left(s_{\bar{n}',\bar{n}}(k_{z1}^{\bar{n}})^2 - (N-r)(k_\rho^{\bar{n}})\kappa_s(\bar{n}', \bar{n}^{r*})\right)\frac{(+k_{z1}^{\bar{n}})^{N-r-1}}{k_1}e^{-ik_{z1}^{\bar{n}}d} \\ -c_{\bar{n}',\bar{n}}(-k_{z2}^{\bar{n}})^{N-r}e^{+ik_{z2}^{\bar{n}}d} \\ \left(-s_{\bar{n}',\bar{n}}(k_{z2}^{\bar{n}})^2 + (N-r)(k_\rho^{\bar{n}})\kappa_s(\bar{n}', \bar{n}^{r*})\right)\frac{(-k_{z2}^{\bar{n}})^{N-r-1}}{k_2}e^{+ik_{z2}^{\bar{n}}d} \end{bmatrix} \tag{4.121}$$

$$\bar{v}_{H2}(\bar{n}', \bar{n}, \bar{n}^{r*}) = \begin{bmatrix} 0 \\ 0 \\ \left(-s_{\bar{n}',\bar{n}}(k_{z1}^{\bar{n}})^2 + (N-r)(k_\rho^{\bar{n}})\kappa_s(\bar{n}', \bar{n}^{r*})\right)\frac{(-k_{z1}^{\bar{n}})^{N-r-1}}{k_1\eta_1}e^{+ik_{z1}^{\bar{n}}d} \\ c_{\bar{n}',\bar{n}}\frac{(-k_{z1}^{\bar{n}})^{N-r}}{\eta_1}e^{+ik_{z1}^{\bar{n}}d} \\ \left(-s_{\bar{n}',\bar{n}}(k_{z1}^{\bar{n}})^2 + (N-r)(k_\rho^{\bar{n}})\kappa_s(\bar{n}', \bar{n}^{r*})\right)\frac{(+k_{z1}^{\bar{n}})^{N-r-1}}{k_1\eta_1}e^{-ik_{z1}^{\bar{n}}d} \\ c_{\bar{n}',\bar{n}}\frac{(+k_{z1}^{\bar{n}})^{N-r}}{\eta_1}e^{-ik_{z1}^{\bar{n}}d} \\ \left(s_{\bar{n}',\bar{n}}(k_{z2}^{\bar{n}})^2 - (N-r)(k_\rho^{\bar{n}})\kappa_s(\bar{n}', \bar{n}^{r*})\right)\frac{(-k_{z2}^{\bar{n}})^{N-r-1}}{k_2\eta_2}e^{+ik_{z2}^{\bar{n}}d} \\ -c_{\bar{n}',\bar{n}}\frac{(-k_{z2}^{\bar{n}})^{N-r}}{\eta_2}e^{+ik_{z2}^{\bar{n}}d} \end{bmatrix} \tag{4.122}$$

The duals of these column vectors (i.e. $\bar{v}^{(d)}$) can be obtained by replacing the $c_{\bar{n}',\bar{n}}$ with $-s_{\bar{n}',\bar{n}}$ and replacing $s_{\bar{n}',\bar{n}}$ with $c_{\bar{n}',\bar{n}}$ and finally replacing $\kappa_s(\bar{n}', \bar{n}^{r*})$ with $\kappa_c(\bar{n}', \bar{n}^{r*})$.

The rest of the derivation involves finding the correct indexes of the $\bar{\bar{v}}$ tensors, which are already given in Equations 4.94 and 4.95 and the shifting tensors $\bar{\bar{u}}_1$ and $\bar{\bar{u}}_2$ given in Equation 4.99. These indexing are obtained by finding mappings that satisfy the following transforms:

$$\begin{aligned} \chi^{(N-r)}_{\bar{n}'-\bar{n},0}(\bar{n}_1, ..., \bar{n}_{N-r-1})\bar{\chi}^{(r)}_{\bar{n}}(\bar{m}_1, ..., \bar{m}_{r-1}) &= \bar{\chi}^{(N)}_{\bar{n}}(\bar{n}_1, ..., \bar{n}_{N-1}).\bar{\bar{u}}_1 \\ \chi^{(N-r)}_{\bar{n}'-\bar{n},N-r}(\bar{n}_1, ..., \bar{n}_{N-r-1})\bar{\chi}^{(r)}_{\bar{n}}(\bar{m}_1, ..., \bar{m}_{r-1}) &= \bar{\chi}^{(N)}_{\bar{n}}(\bar{n}_1, ..., \bar{n}_{N-1}).\bar{\bar{u}}_2 \end{aligned} \quad (4.123)$$

that come up in Equation 4.116.

This concludes the complete SPM solution for the two layer problem. The SPM solution is obtained in a total of three different methods, the numerical solution described in Chapter 3, the explicit analytical solution up to second order given in Sections 4.5 and 4.6 and finally the arbitrary order tensor solution described in this section. Each solution method has been implemented, and a perfect match has been observed between them. Because the arbitrary order tensor solution is the most efficient of all and has the flexibility to go up to any order, it will be assumed as the primary SPM solution in the rest of the dissertation.

4.9 Conclusion

In this chapter, the analytical arbitrary order solution procedure, described in Chapter 2 was applied to the two layer problem. The zeroth, first, and second order explicit solutions were considered. Once the general form of solutions were determined, a tensor based formulation was introduced. Utilizing this new formulation, the arbitrary order SPM solution for the two layer problem was obtained. Such a

form is very useful, because it allows evaluation of the field statistical moments in a direct manner, when considering stochastic surfaces.

Writing the arbitrary order solution in the iterative form has several advantages such as modular programing and faster computations, as discussed in the second chapter for the one dimensional Dirichlet formulation. In the two layer problem case, considering the two dimensional nature of the solutions with two layers, the expressions are far more complex and consequently, the advantages of iterative solution become more appreciable. In fact, this solution will be utilized in the next chapter to do an extensive power analysis of the two layer problem.

CHAPTER 5

APPLICATIONS: CALCULATION OF POWER FOR TWO-LAYER PROBLEM

5.1 Introduction

In this chapter, both coherent and incoherent power analysis of the two-layer problem is provided for both periodic and non-periodic cases. The derivations are valid for for any scattering coefficient, i.e. reflected, intermediate and transmitted powers. In the following sections, first, a general discussion on the power calculations is provided. Assumptions involving the statistical surface properties are highlighted. Then, under the assumption of Gaussian Random Process (GRP), the zeroth and the second order coherent reflectivity and the second and the fourth order incoherent bi-static Radar Cross Sections (RCS) are derived. For the case when the two surfaces are uncorrelated, the bi-static RCS term is studied throughly and the effects of upper and lower roughness and the interaction of roughness effects are identified. A special term is defined as the ratio of the interaction effect to the overall RCS, as a measure of the importance of the interaction effects.

Later in the chapter, the derived power quantities are examined extensively for uncorrelated GRPs. First the second order correction to the coherent reflectivity is

studied. Next, the bi-static RCS is studied for lossless, air-ice-rock type interface for all possible scattering angles. Then, RCS quantities are examined for backscattering for the effects of surface correlation lengths, thickness of the intermediate layer, incidence angle and dielectric contrasts of the media.

As a reminder, "ς" denoting any of the scattering coefficients:

$$\varsigma = \{\alpha, A, C, \gamma, \beta, B, D, \delta\}, \tag{5.1}$$

then the zeroth order solution was given with:

$$\varsigma_{\bar{n}'}^{(0)} = \Gamma_\varsigma \; \delta_{\bar{n}'} \tag{5.2}$$

and the first order solution:

$$\varsigma_{\bar{n}'}^{(1)} = h_{\bar{n}'}^{(1)} \; g_\varsigma^{(1,0)}(\bar{n}') + h_{\bar{n}'}^{(2)} \; g_\varsigma^{(0,1)}(\bar{n}') \tag{5.3}$$

and the second order solution was:

$$\begin{aligned} \varsigma_{\bar{n}'}^{(2)} \;=\; \sum_{\bar{n}_1} \Bigg(& h_{\bar{n}_1}^{(1)} \; h_{\bar{n}'-\bar{n}_1}^{(1)} g_\varsigma^{(2,0)}(\bar{n}', \bar{n}_1) \\ & + h_{\bar{n}_1}^{(2)} \; h_{\bar{n}'-\bar{n}_1}^{(1)} g_\varsigma^{(1,1)}(\bar{n}', \bar{n}_1) \\ & + h_{\bar{n}_1}^{(2)} \; h_{\bar{n}'-\bar{n}_1}^{(2)} g_\varsigma^{(0,2)}(\bar{n}', \bar{n}_1) \Bigg) \end{aligned} \tag{5.4}$$

and finally the third order solution was:

$$\begin{aligned} \varsigma_{\bar{n}'}^{(3)} \;=\; \sum_{\bar{n}_1} \sum_{\bar{n}_2} \Bigg(& h_{\bar{n}_1}^{(1)} \; h_{\bar{n}_2}^{(1)} \; h_{\bar{n}'-\bar{n}_1-\bar{n}_2}^{(1)} g_\varsigma^{(3,0)}(\bar{n}', \bar{n}_1, \bar{n}_2) \\ & + h_{\bar{n}_1}^{(2)} \; h_{\bar{n}_2}^{(1)} \; h_{\bar{n}'-\bar{n}_1-\bar{n}_2}^{(1)} g_\varsigma^{(2,1)}(\bar{n}', \bar{n}_1, \bar{n}_2) \\ & + h_{\bar{n}_1}^{(2)} \; h_{\bar{n}_2}^{(2)} \; h_{\bar{n}'-\bar{n}_1-\bar{n}_2}^{(1)} g_\varsigma^{(1,2)}(\bar{n}', \bar{n}_1, \bar{n}_2) \\ & + h_{\bar{n}_1}^{(2)} \; h_{\bar{n}_2}^{(2)} \; h_{\bar{n}'-\bar{n}_1-\bar{n}_2}^{(2)} g_\varsigma^{(0,3)}(\bar{n}', \bar{n}_1, \bar{n}_2) \Bigg) \end{aligned} \tag{5.5}$$

Given the field solution to the third order in surface height, reflected and transmitted powers can also be derived to third order. Next, power calculations will be discussed for the periodic case.

5.2 Calculation of the power terms for periodic surfaces

In this section, calculation of the coherent reflectivity and the incoherent power are discussed under the periodicity assumption. Since the power in particular Floquet mode is directly proportional to its amplitude squared, and since the distinct polarizations are orthogonal, the relevant quantities to consider are:

$$\left|\varsigma_{\bar{n}'}\right|^2 = \left|\varsigma_{\bar{n}'}^{(0)} + \varsigma_{\bar{n}'}^{(1)} + \varsigma_{\bar{n}'}^{(2)} + \varsigma_{\bar{n}'}^{(3)} + ...\right|^2 \tag{5.6}$$

Collecting the terms of identical order yields:

$$\begin{aligned}
\left|\varsigma_{\bar{n}'}\right|^2 \;=\; & \left[\left|\varsigma_{\bar{n}'}^{(0)}\right|^2\right] + \left[2Re\left\{\varsigma_{\bar{n}'}^{(0)*}\varsigma_{\bar{n}'}^{(1)}\right\}\right] \\
& + \left[\left|\varsigma_{\bar{n}'}^{(1)}\right|^2 + 2Re\left\{\varsigma_{\bar{n}'}^{(0)*}\varsigma_{\bar{n}'}^{(2)}\right\}\right] \\
& + \left[2Re\left\{\varsigma_{\bar{n}'}^{(1)*}\varsigma_{\bar{n}'}^{(2)}\right\} + 2Re\left\{\varsigma_{\bar{n}'}^{(0)*}\varsigma_{\bar{n}'}^{(3)}\right\}\right] \\
& + \left[\left|\varsigma_{\bar{n}'}^{(2)}\right|^2 + 2Re\left\{\varsigma_{\bar{n}'}^{(1)*}\varsigma_{\bar{n}'}^{(3)}\right\} + 2Re\left\{\varsigma_{\bar{n}'}^{(0)*}\varsigma_{\bar{n}'}^{(4)}\right\}\right] + ...
\end{aligned} \tag{5.7}$$

where individual orders are grouped inside parenthesis, and a fourth order term has been included as well, even though the fourth order solution is not considered in this chapter. Immediately it can be recognized that the zeroth order term represents the reflectivity of a flat surface, and also that terms multiplying $\varsigma_{\bar{n}'}^{(0)}$ are evaluated only with $\bar{n}' = \bar{0}$ since $\varsigma_{\bar{n}'}^{(0)}$ vanishes for all other indices; these terms represent corrections to the flat surface reflectivity. If it is assumed that the surfaces have a zero spatial average value (i.e. $h_{\bar{0}}^{(1,2)} = \bar{0}$) then the first order term vanishes since it is directly proportional to $h_{\bar{0}}$. All other terms exist in the general case and contribute to reflected and transmitted powers. Fractions of the incident power reflected into a specific polarization of a Floquet mode ($\bar{n}'$) can be shown to be

$$\mathrm{Re}\left\{\frac{k_{z0}^{\bar{n}'}}{k_{zi}}\right\}\left|\varsigma\right|^2, \tag{5.8}$$

where $\varsigma = \alpha$ or β, while the fraction of power transmitted into a specific polarization of Floquet mode ($\bar{n}'$) in a lossless medium can be shown to be

$$\mathrm{Re}\left\{\frac{k_{z2}^{\bar{n}'}}{k_{zi}}\right\}|\varsigma|^2, \tag{5.9}$$

where $\varsigma = \gamma$ or δ. And finally, the the fraction of intermediate power in a specific polarization of Floquet mode ($\bar{n}'$) in a lossless medium can be shown to be

$$\mathrm{Re}\left\{\frac{k_{z1}^{\bar{n}'}}{k_{zi}}\right\}|\varsigma|^2, \tag{5.10}$$

where $\varsigma = A$, B, C or D.

5.2.1 Coherent Reflectivity

Since the small perturbation method is frequently applied in the analysis of stochastic surfaces, it is also of interest to consider scattered and transmitted coherent and incoherent powers. In this case, the results are considerably simplified by assuming that each point on the surface profiles $z_1(x,y)$ and $z_2(x,y)$ is a zero mean random variable (i.e. $< z_1(x,y) >= 0$ and $< z_2(x,y) >= 0$) so that $< h_{\bar{0}}^{(1,2)} >= \bar{0}$.

In this case, the coherent reflectivity,

$$|< \varsigma >|^2 \;=\; \left|< \Gamma_\varsigma^{eff} >\right|^2 \tag{5.11}$$

with $\varsigma = \alpha$ or β is found to exist only in the specular direction $\bar{n}' = \bar{0}$ up to third order, and the effective reflection coefficient $< \Gamma_\varsigma^{eff} >$ is given by

$$\begin{aligned} < \Gamma_\varsigma^{eff} > \;&=\; \Gamma_\varsigma \\ &\quad + \sum_{\bar{n}_1} < \left|h_{\bar{n}_1}^{(1)}\right|^2 > g_\varsigma^{(2,0)}(\bar{0}, \bar{n1}) \\ &\quad + \sum_{\bar{n}_1} < \left|h_{\bar{n}_1}^{(2)} h_{\bar{n}_1}^{(1)}\right| > g_\varsigma^{(1,1)}(\bar{0}, \bar{n1}) \end{aligned}$$

$$
\begin{aligned}
&+\sum_{\bar{n}_1} < \left|h_{\bar{n}_1}^{(2)}\right|^2 > g_{\varsigma}^{(0,2)}(\bar{0},\bar{n1}) \\
&+\sum_{\bar{n}_1}\sum_{\bar{n}_2} < h_{\bar{n}_1}^{(1)} h_{\bar{n}_2}^{(1)} h_{-\bar{n}_1-\bar{n}_2}^{(1)} > g_{\zeta}^{(3,0)}(\bar{0},\bar{n}_1,\bar{n}_2) \\
&+\sum_{\bar{n}_1}\sum_{\bar{n}_2} < h_{\bar{n}_1}^{(2)} h_{\bar{n}_2}^{(1)} h_{-\bar{n}_1-\bar{n}_2}^{(1)} > g_{\zeta}^{(2,1)}(\bar{0},\bar{n}_1,\bar{n}_2) \\
&+\sum_{\bar{n}_1}\sum_{\bar{n}_2} < h_{\bar{n}_1}^{(2)} h_{\bar{n}_2}^{(2)} h_{-\bar{n}_1-\bar{n}_2}^{(1)} > g_{\zeta}^{(1,2)}(\bar{0},\bar{n}_1,\bar{n}_2) \\
&+\sum_{\bar{n}_1}\sum_{\bar{n}_2} < h_{\bar{n}_1}^{(2)} h_{\bar{n}_2}^{(2)} h_{-\bar{n}_1-\bar{n}_2}^{(2)} > g_{\zeta}^{(0,3)}(\bar{0},\bar{n}_1,\bar{n}_2) \qquad (5.12)
\end{aligned}
$$

to third order in surface height. A corresponding equation can be derived for the effective transmission coefficient in a lossless medium. Note an expansion of the coherent power $\left|< \Gamma_{\varsigma}^{eff} >\right|^2$ similar to equation (5.7) is required to group coherent power terms to third order consistently. If it is further assumed that the surfaces are Gaussian random processes and there is no correlation between the surfaces (i.e. $< \left|h_{\bar{n}_1}^{(2)} h_{\bar{n}_1}^{(1)}\right| >= 0$), the bi-spectrum like terms (i.e.$< h_{\bar{n}}^{(1,2)} h_{\bar{n}_1}^{(1,2)} h_{-\bar{n}-\bar{n}_1}^{(1,2)} >$) all vanish and the following simpler form is obtained:

$$
\begin{aligned}
< \Gamma_{\varsigma}^{eff} > \;&=\; \Gamma_{\varsigma} + \sum_{\bar{n}_1} < \left|h_{\bar{n}_1}^{(1)}\right|^2 > g_{\varsigma}^{(2,0)}(\bar{0},\bar{n1}) \\
&\quad + \sum_{\bar{n}_1} < \left|h_{\bar{n}_1}^{(2)}\right|^2 > g_{\varsigma}^{(0,2)}(\bar{0},\bar{n1}) \qquad (5.13)
\end{aligned}
$$

This expression is valid for the periodic case. The non-periodic, (continuous spectrum) case expressions are derived later in the chapter. Next, the incoherent power terms will be considered again for the periodic case.

5.2.2 Incoherent Powers

The expansion for incoherent powers produces

$$
\begin{aligned}
< \left|\varsigma_{\bar{n}'} - < \varsigma_{\bar{n}'} >\right|^2 > \;&=\; < \left|\varsigma_{\bar{n}'}^{(1)}\right|^2 > + 2\mathrm{Re}\left\{ < \varsigma_{\bar{n}'}^{(1)*} \varsigma_{\bar{n}'}^{(2)} > \right\} + \\
&\quad < \left|\varsigma_{\bar{n}'}^{(2)} - < \varsigma_{\bar{n}'}^{(2)} >\right|^2 > + 2\mathrm{Re}\left\{ < \varsigma_{\bar{n}'}^{(1)*} \varsigma_{\bar{n}'}^{(3)} > \right\} \qquad (5.14)
\end{aligned}
$$

to fourth order; note that the third order solution for fields is sufficient to determine incoherent scattered and transmitted powers to fourth order. The above expression under the uncorrelated surfaces assumption can be rewritten as:

$$
\begin{aligned}
< |\varsigma_{\bar{n}'} - <\varsigma_{\bar{n}'}>|^2 > \;\; = \;\; & < \left|h^{(1)}_{\bar{n}'}\right|^2 > \left|g^{(1,0)}_{\varsigma}(\bar{n}')\right|^2 + < \left|h^{(2)}_{\bar{n}'}\right|^2 > \left|g^{(0,1)}_{\varsigma}(\bar{n}')\right|^2 \\
& + 2\mathrm{Re}\left\{ \sum_{\bar{n}_1} \Big(< h^{(1)*}_{\bar{n}'} h^{(1)}_{\bar{n}_1} h^{(1)}_{\bar{n}'-\bar{n}_1} > g^{(1,0)*}_{\varsigma}(\bar{n}') g^{(2,0)}_{\varsigma}(\bar{n}', \bar{n}_1) \right. \\
& \qquad + < h^{(1)*}_{\bar{n}'} h^{(2)}_{\bar{n}_1} h^{(1)}_{\bar{n}'-\bar{n}_1} > g^{(1,0)*}_{\varsigma}(\bar{n}') g^{(1,1)}_{\varsigma}(\bar{n}', \bar{n}_1) \\
& \qquad + < h^{(1)*}_{\bar{n}'} h^{(2)}_{\bar{n}_1} h^{(2)}_{\bar{n}'-\bar{n}_1} > g^{(1,0)*}_{\varsigma}(\bar{n}') g^{(0,2)}_{\varsigma}(\bar{n}', \bar{n}_1) \\
& \qquad + < h^{(2)*}_{\bar{n}'} h^{(1)}_{\bar{n}_1} h^{(1)}_{\bar{n}'-\bar{n}_1} > g^{(0,1)*}_{\varsigma}(\bar{n}') g^{(2,0)}_{\varsigma}(\bar{n}', \bar{n}_1) \\
& \qquad + < h^{(2)*}_{\bar{n}'} h^{(2)}_{\bar{n}_1} h^{(1)}_{\bar{n}'-\bar{n}_1} > g^{(0,1)*}_{\varsigma}(\bar{n}') g^{(1,1)}_{\varsigma}(\bar{n}', \bar{n}_1) \\
& \qquad \left. + < h^{(2)*}_{\bar{n}'} h^{(2)}_{\bar{n}_1} h^{(2)}_{\bar{n}'-\bar{n}_1} > g^{(0,1)*}_{\varsigma}(\bar{n}') g^{(0,2)}_{\varsigma}(\bar{n}', \bar{n}_1) \Big) \right\} \\
& + \sum_{\bar{n}_1} \sum_{\bar{n}_2} \Big[\Big(< h^{(1)}_{\bar{n}_1} h^{(1)}_{\bar{n}'-\bar{n}_1} h^{(1)*}_{\bar{n}_2} h^{(1)*}_{\bar{n}'-\bar{n}_2} > \\
& \qquad - < h^{(1)}_{\bar{n}_1} h^{(1)}_{\bar{n}'-\bar{n}_1} >< h^{(1)*}_{\bar{n}_2} h^{(1)*}_{\bar{n}'-\bar{n}_2} > \Big) g^{(2,0)}_{\varsigma}(\bar{n}', \bar{n}_1) g^{(2,0)*}_{\varsigma}(\bar{n}', \bar{n}_2) \\
& \qquad + \Big(< h^{(2)}_{\bar{n}_1} h^{(1)}_{\bar{n}'-\bar{n}_1} h^{(2)*}_{\bar{n}_2} h^{(1)*}_{\bar{n}'-\bar{n}_2} > \Big) g^{(1,1)}_{\varsigma}(\bar{n}', \bar{n}_1) g^{(1,1)*}_{\varsigma}(\bar{n}', \bar{n}_2) \\
& \qquad + \Big(< h^{(2)}_{\bar{n}_1} h^{(2)}_{\bar{n}'-\bar{n}_1} h^{(2)*}_{\bar{n}_2} h^{(2)*}_{\bar{n}'-\bar{n}_2} > \\
& \qquad - < h^{(2)}_{\bar{n}_1} h^{(2)}_{\bar{n}'-\bar{n}_1} >< h^{(2)*}_{\bar{n}_2} h^{(2)*}_{\bar{n}'-\bar{n}_2} > \Big) g^{(0,2)}_{\varsigma}(\bar{n}', \bar{n}_1) g^{(0,2)*}_{\varsigma}(\bar{n}', \bar{n}_2) \Big] \\
& + 2\mathrm{Re}\left\{ \sum_{\bar{n}_1} \sum_{\bar{n}_2} \Big[< h^{(1)*}_{\bar{n}'} h^{(1)}_{\bar{n}_1} h^{(1)}_{\bar{n}_2} h^{(1)}_{\bar{n}'-\bar{n}_1-\bar{n}_2} > g^{(1,0)*}_{\varsigma}(\bar{n}') g^{(3,0)}_{\varsigma}(\bar{n}', \bar{n}_1, \bar{n}_2) \right. \\
& \qquad < h^{(1)*}_{\bar{n}'} h^{(2)}_{\bar{n}_1} h^{(1)}_{\bar{n}_2} h^{(1)}_{\bar{n}'-\bar{n}_1-\bar{n}_2} > g^{(1,0)*}_{\varsigma}(\bar{n}') g^{(2,1)}_{\varsigma}(\bar{n}', \bar{n}_1, \bar{n}_2) \\
& \qquad < h^{(1)*}_{\bar{n}'} h^{(2)}_{\bar{n}_1} h^{(2)}_{\bar{n}_2} h^{(1)}_{\bar{n}'-\bar{n}_1-\bar{n}_2} > g^{(1,0)*}_{\varsigma}(\bar{n}') g^{(1,2)}_{\varsigma}(\bar{n}', \bar{n}_1, \bar{n}_2) \\
& \qquad < h^{(1)*}_{\bar{n}'} h^{(2)}_{\bar{n}_1} h^{(2)}_{\bar{n}_2} h^{(2)}_{\bar{n}'-\bar{n}_1-\bar{n}_2} > g^{(1,0)*}_{\varsigma}(\bar{n}') g^{(0,3)}_{\varsigma}(\bar{n}', \bar{n}_1, \bar{n}_2) \\
& \qquad < h^{(2)*}_{\bar{n}'} h^{(1)}_{\bar{n}_1} h^{(1)}_{\bar{n}_2} h^{(1)}_{\bar{n}'-\bar{n}_1-\bar{n}_2} > g^{(0,1)*}_{\varsigma}(\bar{n}') g^{(3,0)}_{\varsigma}(\bar{n}', \bar{n}_1, \bar{n}_2) \\
& \qquad \left. < h^{(2)*}_{\bar{n}'} h^{(2)}_{\bar{n}_1} h^{(1)}_{\bar{n}_2} h^{(1)}_{\bar{n}'-\bar{n}_1-\bar{n}_2} > g^{(0,1)*}_{\varsigma}(\bar{n}') g^{(2,1)}_{\varsigma}(\bar{n}', \bar{n}_1, \bar{n}_2) \right.
\end{aligned}
$$

$$< h^{(2)*}_{\bar{n}'} h^{(2)}_{\bar{n}_1} h^{(2)}_{\bar{n}_2} h^{(1)}_{\bar{n}'-\bar{n}_1-\bar{n}_2} > g^{(0,1)*}_{\varsigma}(\bar{n}') g^{(1,2)}_{\varsigma}(\bar{n}', \bar{n}_1, \bar{n}_2)$$
$$< h^{(2)*}_{\bar{n}'} h^{(2)}_{\bar{n}_1} h^{(2)}_{\bar{n}_2} h^{(2)}_{\bar{n}'-\bar{n}_1-\bar{n}_2} > g^{(0,1)*}_{\varsigma}(\bar{n}') g^{(0,3)}_{\varsigma}(\bar{n}', \bar{n}_1, \bar{n}_2) \;] \Big\} \quad (5.15)$$

showing the dependencies of incoherent power at second order on the surface spectra, at third order on the surface bi-spectra, and at fourth order on quantities which can be related to the surface tri-spectra, power spectra, and correlations between Fourier coefficients. Again for a Gaussian random process the bi-spectra and third order power terms vanish, while the fourth order power term can be expressed in terms of the surface power spectra only [23].

Under the assumption of a GRP, Equation 5.15 becomes:

$$\begin{aligned}
< |\varsigma_{\bar{n}'} - < \varsigma_{\bar{n}'} >|^2 > \; &= \; < \left| h^{(1)}_{\bar{n}'} \right|^2 > \left| g^{(1,0)}_{\varsigma}(\bar{n}') \right|^2 + < \left| h^{(2)}_{\bar{n}'} \right|^2 > \left| g^{(0,1)}_{\varsigma}(\bar{n}') \right|^2 \\
&+ \sum_{\bar{n}_1} \sum_{\bar{n}_2} \Bigg[\Big(< h^{(1)}_{\bar{n}_1} h^{(1)}_{\bar{n}'-\bar{n}_1} h^{(1)*}_{\bar{n}_2} h^{(1)*}_{\bar{n}'-\bar{n}_2} > \\
&\quad - < h^{(1)}_{\bar{n}_1} h^{(1)}_{\bar{n}'-\bar{n}_1} >< h^{(1)*}_{\bar{n}_2} h^{(1)*}_{\bar{n}'-\bar{n}_2} > \Big) g^{(2,0)}_{\varsigma}(\bar{n}', \bar{n}_1) g^{(2,0)*}_{\varsigma}(\bar{n}', \bar{n}_2) \\
&\quad + \Big(< h^{(2)}_{\bar{n}_1} h^{(1)}_{\bar{n}'-\bar{n}_1} h^{(2)*}_{\bar{n}_2} h^{(1)*}_{\bar{n}'-\bar{n}_2} > \Big) g^{(1,1)}_{\varsigma}(\bar{n}', \bar{n}_1) g^{(1,1)*}_{\varsigma}(\bar{n}', \bar{n}_2) \\
&\quad + \Big(< h^{(2)}_{\bar{n}_1} h^{(2)}_{\bar{n}'-\bar{n}_1} h^{(2)*}_{\bar{n}_2} h^{(2)*}_{\bar{n}'-\bar{n}_2} > \\
&\quad - < h^{(2)}_{\bar{n}_1} h^{(2)}_{\bar{n}'-\bar{n}_1} >< h^{(2)*}_{\bar{n}_2} h^{(2)*}_{\bar{n}'-\bar{n}_2} > \Big) g^{(0,2)}_{\varsigma}(\bar{n}', \bar{n}_1) g^{(0,2)*}_{\varsigma}(\bar{n}', \bar{n}_2) \Bigg] \\
&+ 2\mathrm{Re} \Bigg\{ \sum_{\bar{n}_1} \sum_{\bar{n}_2} \Big[< h^{(1)*}_{\bar{n}'} h^{(1)}_{\bar{n}_1} h^{(1)}_{\bar{n}_2} h^{(1)}_{\bar{n}'-\bar{n}_1-\bar{n}_2} > g^{(1,0)*}_{\varsigma}(\bar{n}') g^{(3,0)}_{\varsigma}(\bar{n}', \bar{n}_1, \bar{n}_2) \\
&\quad < h^{(1)*}_{\bar{n}'} h^{(2)}_{\bar{n}_1} h^{(2)}_{\bar{n}_2} h^{(1)}_{\bar{n}'-\bar{n}_1-\bar{n}_2} > g^{(1,0)*}_{\varsigma}(\bar{n}') g^{(1,2)}_{\varsigma}(\bar{n}', \bar{n}_1, \bar{n}_2) \\
&\quad < h^{(2)*}_{\bar{n}'} h^{(2)}_{\bar{n}_1} h^{(1)}_{\bar{n}_2} h^{(1)}_{\bar{n}'-\bar{n}_1-\bar{n}_2} > g^{(0,1)*}_{\varsigma}(\bar{n}') g^{(2,1)}_{\varsigma}(\bar{n}', \bar{n}_1, \bar{n}_2) \\
&\quad < h^{(2)*}_{\bar{n}'} h^{(2)}_{\bar{n}_1} h^{(2)}_{\bar{n}_2} h^{(2)}_{\bar{n}'-\bar{n}_1-\bar{n}_2} > g^{(0,1)*}_{\varsigma}(\bar{n}') g^{(0,3)}_{\varsigma}(\bar{n}', \bar{n}_1, \bar{n}_2) \;] \Bigg\} \quad (5.16)
\end{aligned}$$

5.3 Derivations for non-periodic surfaces

Scattering cross sections per unit area for a non-periodic surface (whose dimensions must be large compared to the electromagnetic wavelength and any surface features, and neglecting edge scattering effects) can also be derived from these results by considering the limit as the surface periods approach infinity following [23]. The scattering cross section per unit area at a particular scattering angle (related to ($\bar{n}'$)) and in a particular polarization can be shown to be

$$\sigma_{\varsigma} = 4\pi k_0^2 \frac{\cos^2\theta_s}{\cos\theta_i} \frac{<|\varsigma|^2>}{\delta k_x \delta k_y} \tag{5.17}$$

where $\delta k_x = \frac{2\pi}{P_x}$ and $\delta k_y = \frac{2\pi}{P_y}$ are differential quantities which cancel when $h_{\bar{n}'}$ terms are related to their continuous counterparts.

The definitions

$$\mathbf{k}_{\bar{n}_1} = (\delta k_x n_1, \delta k_y m_1) \tag{5.18}$$

$$\frac{<|h_{\bar{n}'}|^2>}{\delta k_x \delta k_y} = W(\mathbf{k}_{\bar{n}'}) \tag{5.19}$$

$$\frac{<h_{\bar{n}'} h_{\bar{n}_1} h_{-\bar{n}'-\bar{n}_1}>}{(\delta k_x)^2 (\delta k_y)^2} = B(\mathbf{k}_{\bar{n}'}, \mathbf{k}_{\bar{n}_1}) \tag{5.20}$$

and

$$\frac{<h_{\bar{n}'} h_{\bar{n}_1} h_{\bar{n}_2} h_{-\bar{n}'-\bar{n}_1-\bar{n}_2}>}{(\delta k_x)^3 (\delta k_y)^3} = T(\mathbf{k}_{\bar{n}'}, \mathbf{k}_{\bar{n}_1}, \mathbf{k}_{\bar{n}_2}) \tag{5.21}$$

where W, B, and T represent the continuous surface power spectrum, bi-spectrum, and a quantity which can be related to the tri-spectrum, respectively, enable the sums over $\bar{n}$ variable in the coherent and incoherent power expressions to be converted into integrals over the corresponding wavenumber.

First, consider the coherent reflectivity term, given in Equation 5.13, in the case of continuous GRP surface. In that case, the expression can be rewritten as an integral

in the following form:

$$< \Gamma_{\varsigma}^{eff} >= \Gamma_{\varsigma}^{(0)} + \Gamma_{\varsigma}^{(2)} + ... \tag{5.22}$$

where $\Gamma^{(0)}$ is the corresponding zeroth order solution and $\Gamma^{(2)}$ is given by:

$$\Gamma_{\varsigma}^{(2)} = \int d\mathbf{k}' \left[W^{(1)}(\mathbf{k}') g_{\varsigma}^{(2,0)}(\bar{0}, \mathbf{k}') + W^{(2)}(\mathbf{k}') g_{\varsigma}^{(0,2)}(\bar{0}, \mathbf{k}') \right] \tag{5.23}$$

where $\mathbf{k}'$ is a dummy variable and the superscript ((1) or (2)) of the power spectrum indicates the corresponding (upper or lower) surface.

Similarly, for a continuous GRP, the bi-static RCS σ_{ς} up to fourth order per unit area at a particular scattering wavenumber (related to $(\mathbf{k}_{\bar{n}'})$ now) and in a particular polarization can be expressed as sum of several terms that are given as integrals over the corresponding wavenumber. Each term is labeled according to the SPM kernels involved.

The terms due to $< \left| \varsigma_{\bar{n}'}^{(1)} \right|^2 >$ in Equation 5.14 are given as:

$$\sigma_{\varsigma}^{10-10} = 4\pi k_0^2 \cos^2\theta_s W^{(1)}(\mathbf{k}_{\bar{n}'}) \left| g_{\varsigma}^{(1,0)}(\mathbf{k}_{\bar{n}'}) \right|^2 \tag{5.24}$$

$$\sigma_{\varsigma}^{01-01} = 4\pi k_0^2 \cos^2\theta_s W^{(2)}(\mathbf{k}_{\bar{n}'}) \left| g_{\varsigma}^{(0,1)}(\mathbf{k}_{\bar{n}'}) \right|^2 \tag{5.25}$$

and do not involve any integrations. The first order SPM kernels are absolute squared and multiplied by the corresponding surface power spectra. The sum of these two terms gives the total second order RCS, which is the first term in the expansion. It very clear here that $\sigma_{\varsigma}^{10-10}$ is associated with the upper surface roughness, while $\sigma_{\varsigma}^{01-01}$ is associated with the lower surface roughness. This identification is important, since identifying the upper, lower and interaction of roughness effects is one of the main purposes of this study.

Similarly, three terms are obtained from $< \left|\varsigma_{\bar{n}'}^{(2)} - < \varsigma_{\bar{n}'}^{(2)} >\right|^2 >$ in Equation 5.14, given as:

$$\begin{aligned}\sigma_{\varsigma}^{20-20} &= 4\pi k_0^2 \cos^2\theta_s \int\int d\mathbf{k}_{\bar{n}_1} W^{(1)}(\mathbf{k}_{\bar{n}_1}) W^{(1)}(\mathbf{k}_{\bar{n}'-\bar{n}_1}) \\ &\quad \left(\left|g_{\varsigma}^{(2,0)}(\mathbf{k}_{\bar{n}'}, \mathbf{k}_{\bar{n}_1})\right|^2 + g_{\varsigma}^{(2,0)*}(\mathbf{k}_{\bar{n}'}, \mathbf{k}_{\bar{n}'-\bar{n}_1}) g_{\varsigma}^{(2,0)}(\mathbf{k}_{\bar{n}'}, \mathbf{k}_{\bar{n}_1})\right) \end{aligned} \tag{5.26}$$

$$\sigma_{\varsigma}^{11-11} = 4\pi k_0^2 \cos^2\theta_s \int\int d\mathbf{k}_{\bar{n}_1} W^{(2)}(\mathbf{k}_{\bar{n}_1}) W^{(1)}(\mathbf{k}_{\bar{n}'-\bar{n}_1}) \left|g_{\varsigma}^{(1,1)}(\mathbf{k}_{\bar{n}'}, \mathbf{k}_{\bar{n}_1})\right|^2 \tag{5.27}$$

$$\begin{aligned}\sigma_{\varsigma}^{02-02} &= 4\pi k_0^2 \cos^2\theta_s \int\int d\mathbf{k}_{\bar{n}_1} W^{(2)}(\mathbf{k}_{\bar{n}_1}) W^{(2)}(\mathbf{k}_{\bar{n}'-\bar{n}_1}) \\ &\quad \left(\left|g_{\varsigma}^{(0,2)}(\mathbf{k}_{\bar{n}'}, \mathbf{k}_{\bar{n}_1})\right|^2 + g_{\varsigma}^{(0,2)*}(\mathbf{k}_{\bar{n}'}, \mathbf{k}_{\bar{n}'-\bar{n}_1}) g_{\varsigma}^{(0,2)}(\mathbf{k}_{\bar{n}'}, \mathbf{k}_{\bar{n}_1})\right) \end{aligned} \tag{5.28}$$

each involving double integrals over the dummy variable $\mathbf{k}_{\bar{n}_1}$. Again, due to involving surface power spectra, the first term $\sigma_{\varsigma}^{20-20}$ is related only to the upper surface roughness and the last term $\sigma_{\varsigma}^{02-02}$ is related only to the lower surface roughness. The middle term $\sigma_{\varsigma}^{11-11}$ involves both spectra, so is an interaction term.

Finally, four extra terms are obtained from the $2\mathrm{Re}\left\{< \varsigma_{\bar{n}'}^{(1)*} \varsigma_{\bar{n}'}^{(3)} >\right\}$ term in Equation 5.14, given as:

$$\begin{aligned}\sigma_{\varsigma}^{10-30} &= \left(4\pi k_0^2 \cos^2\theta_s\right) .2\mathrm{Re}\left\{ W^{(1)}(\mathbf{k}_{\bar{n}'}) g_{\varsigma}^{(1,0)*}(\mathbf{k}_{\bar{n}'}) \int\int d\mathbf{k}_{\bar{n}_1} W^{(1)}(\mathbf{k}_{\bar{n}_1}) . \right. \\ &\quad \left. . \left(g_{\varsigma}^{(3,0)}(\mathbf{k}_{\bar{n}'}, \mathbf{k}_{\bar{n}'}, \mathbf{k}_{\bar{n}_1}) + g_{\varsigma}^{(3,0)}(\mathbf{k}_{\bar{n}'}, \mathbf{k}_{\bar{n}_1}, \mathbf{k}_{\bar{n}'}) + g_{\varsigma}^{(3,0)}(\mathbf{k}_{\bar{n}'}, \mathbf{k}_{\bar{n}_1}, -\mathbf{k}_{\bar{n}_1})\right) \right\} \end{aligned} \tag{5.29}$$

$$\begin{aligned}\sigma_{\varsigma}^{10-12} &= \left(4\pi k_0^2 \cos^2\theta_s\right) .2\mathrm{Re}\left\{ W^{(1)}(\mathbf{k}_{\bar{n}'}) g_{\varsigma}^{(1,0)*}(\mathbf{k}_{\bar{n}'}) \int\int d\mathbf{k}_{\bar{n}_1} W^{(2)}(\mathbf{k}_{\bar{n}_1}) . \right. \\ &\quad \left. . g_{\varsigma}^{(1,2)}(\mathbf{k}_{\bar{n}'}, \mathbf{k}_{\bar{n}_1}, \mathbf{k}_{\bar{n}'}) \right\} \end{aligned} \tag{5.30}$$

$$\begin{aligned}\sigma_{\varsigma}^{01-21} &= \left(4\pi k_0^2 \cos^2\theta_s\right) .2\mathrm{Re}\left\{ W^{(2)}(\mathbf{k}_{\bar{n}'}) g_{\varsigma}^{(0,1)*}(\mathbf{k}_{\bar{n}'}) \int\int d\mathbf{k}_{\bar{n}_1} W^{(1)}(\mathbf{k}_{\bar{n}_1}) . \right. \\ &\quad \left. . g_{\varsigma}^{(2,1)}(\mathbf{k}_{\bar{n}'}, \mathbf{k}_{\bar{n}_1}, \mathbf{k}_{\bar{n}'}) \right\} \end{aligned} \tag{5.31}$$

$$\sigma_{\varsigma}^{01-03} = \left(4\pi k_0^2 \cos^2\theta_s\right).2\mathrm{Re}\left\{ W^{(2)}(\mathbf{k}_{\bar{n}'}) g_{\varsigma}^{(0,1)*}(\mathbf{k}_{\bar{n}'}) \int\int d\mathbf{k}_{\bar{n}_1} W^{(2)}(\mathbf{k}_{\bar{n}_1}). \right.$$
$$\left. . \left(g_{\varsigma}^{(0,3)}(\mathbf{k}_{\bar{n}'}, \mathbf{k}_{\bar{n}'}, \mathbf{k}_{\bar{n}_1}) + g_{\varsigma}^{(0,3)}(\mathbf{k}_{\bar{n}'}, \mathbf{k}_{\bar{n}_1}, \mathbf{k}_{\bar{n}'}) + g_{\varsigma}^{(0,3)}(\mathbf{k}_{\bar{n}'}, \mathbf{k}_{\bar{n}_1}, -\mathbf{k}_{\bar{n}_1}) \right) \right\} \quad (5.32)$$

and similarly, the first term $\sigma_{\varsigma}^{10-30}$ and the last term $\sigma_{\varsigma}^{01-03}$ are upper and lower roughness only terms respectively. The two terms in the middle, $\sigma_{\varsigma}^{10-12}$ and $\sigma_{\varsigma}^{01-21}$ are the other interaction terms.

Although, the integrals involved in Equations 5.26 through 5.32 are defined on the whole 2-D space, the integration domain is truncated to the circle centered at the origin, with radius $4k_0$, since kernels evaluated outside of this circle did not contribute to the integrals. The integration is done numerically in cylindrical coordinates, first in ρ rigorously, then in ϕ. The ρ integration is evaluated with adaptive integration algorithm, enforcing several convergence criteria. Then the integration on ϕ is evaluated by a simple Gaussian quadrature rule.

With the definitions above, the total fourth order bi-static cross section term is obtained as a sum of three roughness effects, which can be given as:

$$\sigma_{\varsigma}^{incoh} = \sigma_{\varsigma}^{upper} + \sigma_{\varsigma}^{lower} + \sigma_{\varsigma}^{inter} \quad (5.33)$$

where each roughness effect is given by:

$$\begin{aligned} \sigma_{\varsigma}^{upper} &= \sigma_{\varsigma}^{10-10} + \sigma_{\varsigma}^{20-20} + \sigma_{\varsigma}^{10-30} \\ \sigma_{\varsigma}^{lower} &= \sigma_{\varsigma}^{01-01} + \sigma_{\varsigma}^{02-02} + \sigma_{\varsigma}^{01-03} \\ \sigma_{\varsigma}^{inter} &= \sigma_{\varsigma}^{11-11} + \sigma_{\varsigma}^{10-12} + \sigma_{\varsigma}^{01-21} \end{aligned} \quad (5.34)$$

in terms of the individual expressions defined above.

A final quantity of interest is also defined:

$$r^{int} = \frac{\sigma_{\varsigma}^{inter}}{\sigma_{\varsigma}^{incoh}} \quad (5.35)$$

and called "interaction ratio", since it is the ratio of interaction effect to the total cross section at the fourth order. Such a unitless quantity is very useful as a measure of the importance of surface interactions.

In the next section, using an isotropic Gaussian spectrum for both surfaces, the coherent reflectivity, bi-static RCS and the interaction ratio are investigated in detail for several example cases.

5.4 Sample Results

In this section, example results from the power calculations of the non-periodic surfaces are presented. In the following subsections, first the coherent reflection coefficient is studied at zeroth and second order for a few example cases. Then an incoherent scattering analysis is provided. The bi-static RCS is studied as a function of scattering angles for lossless and a lossy examples. In the rest of the study, the backscattering RCS is considered. The effects of correlation lengths of the surfaces, the separation distance, the scattering angle, and the dielectric contrast of the medium on the backscattering RCS together with the interaction ratio are investigated.

A incident wave frequency of $f = 300MHz$ is assumed so that the upper medium wave number is $\lambda_0 = 1m$. Both upper and lower surfaces are assumed to be GRP's, with an isotropic Gaussian power spectral density, which is given by:

$$W^{(i)}(k_\rho) = \frac{h_{(i)}^2 l_{(i)}^2}{4\pi} \exp\left(-\frac{k_\rho^2 l_{(i)}^2}{4}\right), \qquad i = 1, 2 \tag{5.36}$$

where h refers to surface rms height and l is the surface correlation length. Since the rms height parameter factors out from the spectrum, its dependence is assumed to be obvious. By defining the slope variables of the surfaces:

$$s_{(i)} = h_{(i)}/l_{(i)}, \qquad i = 1, 2 \tag{5.37}$$

and setting the surface slopes to a reasonable value of $s_{(i)} = 0.1$, the surface rms height dependence of the spectrum is suppressed in the rest of the chapter.

Air-ice-rock type interfaces are assumed in most of the following examples (i.e. The media are assumed to be non-magnetic, with relative dielectric permitivities: $\epsilon_0 = 1$, $\epsilon_1 = 3$ and $\epsilon_2 = 9$.) While, the imaginary components should also be considered for a more realistic analysis, introducing loss to the media will clearly result in attenuation of the fields, so that the lossless case is more interesting in terms of highlighting interaction effects.

5.4.1 Coherent Reflectivity Study

The coherent reflectivity of two layer media is considered in this section. Coherent reflection only occurs in the specular direction, and is calculated for both horizontal incidence - horizontal scattering and vertical incidence - vertical scattering cases up to second order. The general air-ice-rock interface is considered here, not only because it is a realistic example but also, because the dielectric permitivities: $\epsilon_0 = 1$, $\epsilon_1 = 3$ and $\epsilon_2 = 9$ satisfy: $(\epsilon_1 = \sqrt{\epsilon_0.\epsilon_2})$, so that the zeroth order reflection coefficient vanishes at normal incidence, when the thickness of the intermediate medium is an odd multiple of $\frac{\lambda_1}{4}$, where λ_1 is the electromagnetic radiation wavelength in the intermediate medium.

Introducing roughness to the layers, the first correction to the unperturbed solution comes at the second order. The second order correction term is investigated for the following numerical example: For the air-ice-rock interface, both upper and lower surfaces are assumed to have same slope values and same correlation lengths. The results are given in Figures 5.1 and 5.2. In Figure 5.1, a small correlation length $(l_{1,2} = 0.1\lambda_0)$ value, and in Figure 5.2, a larger correlation length value $(l_{1,2} = 0.5\lambda_0)$

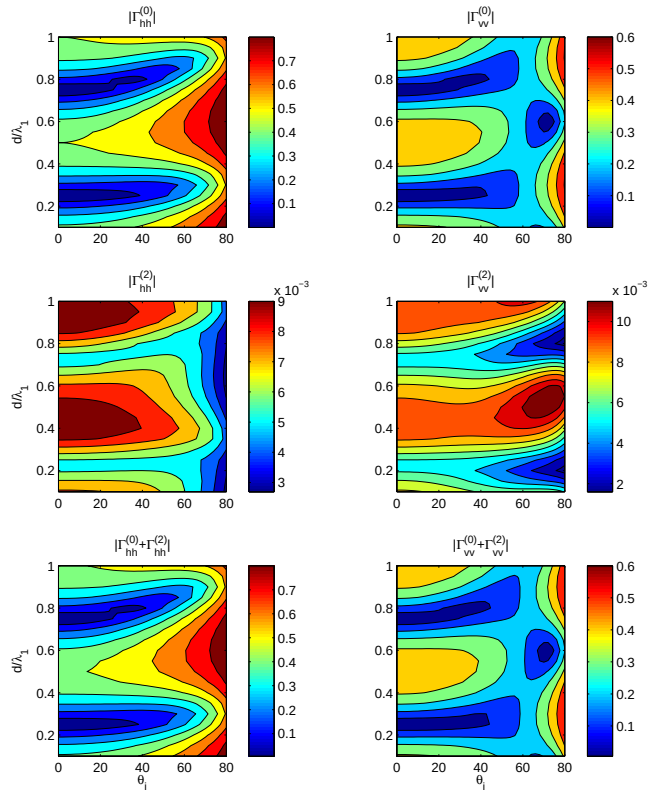

Figure 5.1: Coherent Reflectivity Study: for $\bar{\epsilon}_r = [1, 3, 9]$, $\bar{\mu}_r = [1, 1, 1]$, $\phi_i = 0$, slopes of both upper and lower surfaces are fixed to $s_{1,2} = 0.1$. The correlation lengths are fixed to $l_{1,2} = 0.1\lambda_0$.

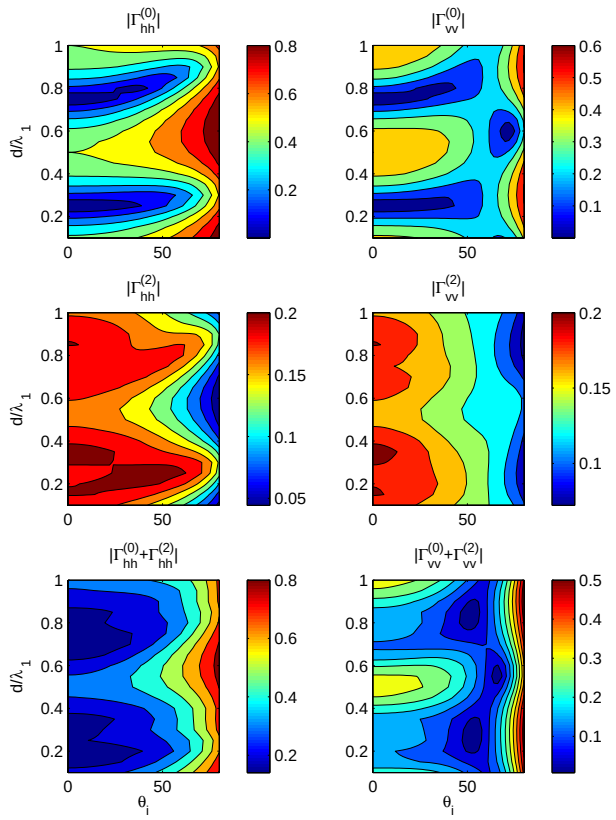

Figure 5.2: Coherent Reflectivity Study: for $\bar{\epsilon}_r = [1, 3, 9]$, $\bar{\mu}_r = [1, 1, 1]$, $\phi_i = 0$, slopes of both upper and lower surfaces are fixed to $s_{1,2} = 0.1$. The correlation lengths are fixed to $l_{1,2} = 0.5\lambda_0$.

is considered. The slopes are set to $s_{1,2} = 0.1$ and the azimuthal angle ϕ is set to 0 degrees in both figures. In these figures, the horizontal axis is reserved for the incidence (also scattering) angle θ, and the vertical axis represents the thickness of the intermediate medium, normalized by the corresponding wavelength. Each figure has three rows, first one shows the unperturbed reflection coefficient, the second row presents the the second order coefficient, and the last row presents the total coefficient. In both figures, the zeroth order solutions are identical and the reflection coefficient at normal incidence at $d = \frac{\lambda_1}{4}$ and $d = \frac{3\lambda_1}{4}$ vanishes, as expected. Moreover, at lower incidence angles, the reflection coefficient has minimum points for thickness values close to normal incidence zeros. As the angle increases, the minima tend to curve upwards, meaning that the minimum points occur periodically, at larger thickness values.

When the second order corrections to the effective coherent reflection coefficient are considered, in Figure 5.1, where a small correlation length ($l_{1,2} = 0.1\lambda_0$) value is considered, clearly very small corrections are observed, while in Figure 5.2, where a larger correlation length value ($l_{1,2} = 0.5\lambda_0$) is considered, the corrections become appreciable. Notice that between the two cases, the surface heights increased by a factor of five and the maximum value of the second order reflection coefficient increased by a factor of 200. The total reflection coefficient subplots also highlight these effects. These results clearly indicate that roughness might have important effects on coherent scattering (i.e. for optical applications, such as thin film fabrication, a detailed coherent scattering analysis is important for determination of limits of roughness that occur in the fabrication process). Next, the bi-static radar cross section will be studied for the two layer problem.

5.4.2 Bi-static RCS Study

In this section, the bi-static RCS derived in Section 5.3 is investigated for the two layer problem. In this study, the scattering angle θ_s is varied from 0 to π, and the azimuth angle ϕ_s is varied from 0 to 2π. For a fixed incidence angle $\theta_i = 20$ and $\phi_i = 30$. Again, the air-ice-rock type interface is assumed. (i.e. non-magnetic medium, with relative dielectric permitivities: $\epsilon_0 = 1$, $\epsilon_0 = 3$ and $\epsilon_2 = 9$.) The slopes of both upper and lower surfaces are fixed to $s_{1,2} = 0.1$ and the correlation lengths are fixed to $l_{1,2} = 0.1\lambda_0$. The thickness parameter is assumed to be $d = 1\lambda_0$. Each figure is divided into four subplots as a 2×2 array, where the first and the second row represents the horizontally and vertically polarized scattering, respectively. Similarly, the columns are reserved for the incidence polarization (i.e. first column is horizontal incidence, while the second is vertical.)

First, in Figures 5.3 through 5.5, the upper, lower and interaction terms, defined in Equation 5.34, are plotted respectively. As the results indicate for co-pol cross sections, all of the surface components (upper, lower and interaction) of the total RCS obtains their in the plane of incidence. On the other hand, the cross-pol components maximize when the scattering angle is orthogonal to angle of incidence.

Then, in Figures 5.6 through 5.8, the total second order, the fourth order only and the total fourth order RCS values are plotted, again for each possible polarization. The co-pol and cross-pol distinction observed in the previous case is still valid here. Moreover, it is also clear that, the second order results are the dominant ones here. Next, in Figure 5.9, the interaction ratio term is plotted with the same configuration. This plot indicates that the effects of interactions are more important for the cross-pol terms then for the co-pol terms. Also, for co-pol scattering, maximum interaction

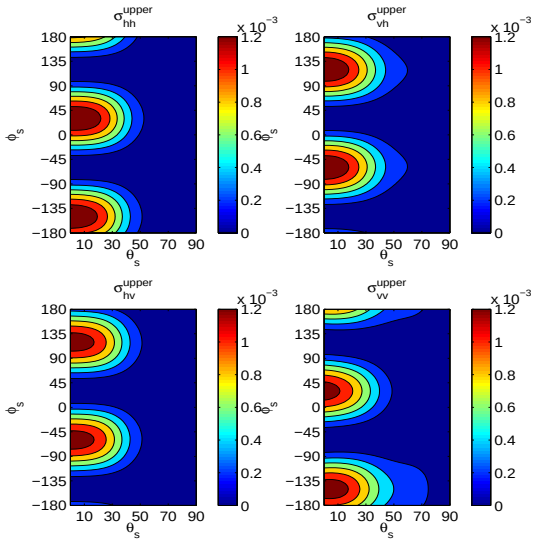

Figure 5.3: Bi-static RCS Study: σ^{upper} for $\bar{\epsilon}_r = [1, 3, 9]$, $\bar{\mu}_r = [1, 1, 1]$, $\theta_i = 20$, $\phi_i = 30$, slopes of both upper and lower surfaces are fixed to $s_{1,2} = 0.1$. The correlation lengths are fixed to $l_{1,2} = 0.1\lambda_0$. The thickness parameter is assumed to be $d = 1\lambda_0$.

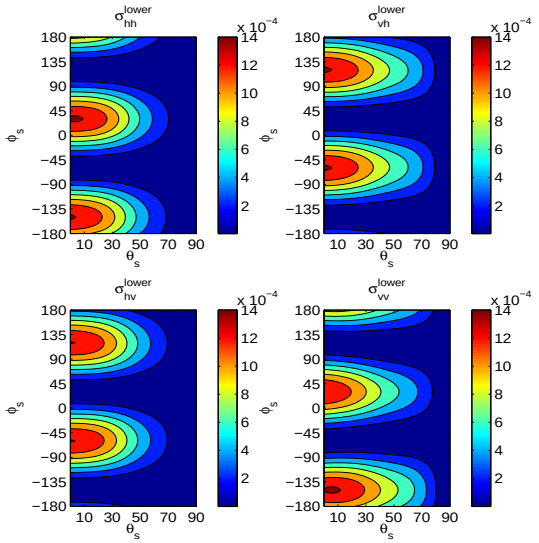

Figure 5.4: Bi-static RCS Study: σ^{lower} for $\bar{\epsilon}_r = [1, 3, 9]$, $\bar{\mu}_r = [1, 1, 1]$, $\theta_i = 20$, $\phi_i = 30$, slopes of both upper and lower surfaces are fixed to $s_{1,2} = 0.1$. The correlation lengths are fixed to $l_{1,2} = 0.1\lambda_0$. The thickness parameter is assumed to be $d = 1\lambda_0$.

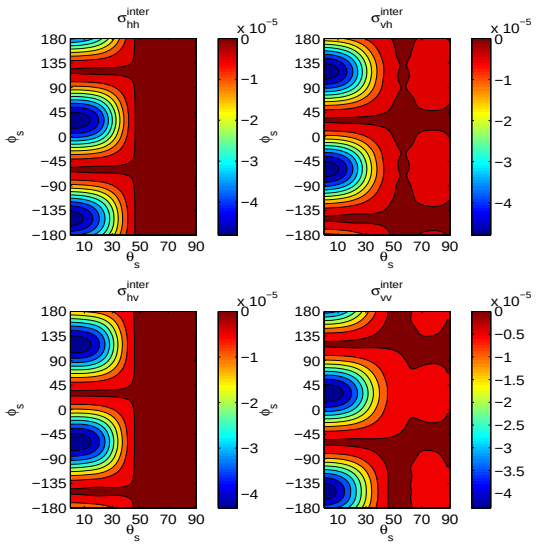

Figure 5.5: Bi-static RCS Study: σ^{inter} for $\bar{\epsilon}_r = [1, 3, 9]$, $\bar{\mu}_r = [1, 1, 1]$, $\theta_i = 20$, $\phi_i = 30$, slopes of both upper and lower surfaces are fixed to $s_{1,2} = 0.1$. The correlation lengths are fixed to $l_{1,2} = 0.1\lambda_0$. The thickness parameter is assumed to be $d = 1\lambda_0$.

ratio occurs at observation angles, orthogonal to the incidence angle and for cross-pol scattering, the maximum of the intersection ratio occurs at either backscattering or specular scattering angles.

In order to highlight the effect of loss to the cross sections, one final numerical study is also included here, given in Figures 5.10 and 5.11, as analogs of Figures 5.8 and 5.9, respectively. The dielectric properties of the media is redefined with small loss as: non-magnetic medium, with the dielectric permitivities: $\epsilon_0 = 1$, $\epsilon_0 = 3 + i$ and $\epsilon_2 = 9 + 0.1i$. The other parameters of the previous study is kept unchanged. In Figure 5.10, the effect of loss of the media can be clearly identified as attenuation of the fields and the cross sections. The maximum values of the cross sections are decreased by approximately 14dB. In Figure 5.11, the interaction ratios are given,

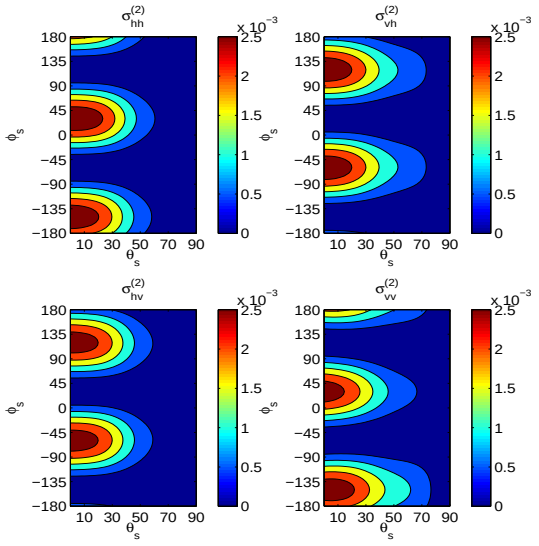

Figure 5.6: Bi-static RCS Study: $\sigma^{(2)}$ for $\bar{\epsilon}_r = [1, 3, 9]$, $\bar{\mu}_r = [1, 1, 1]$, $\theta_i = 20$, $\phi_i = 30$, slopes of both upper and lower surfaces are fixed to $s_{1,2} = 0.1$. The correlation lengths are fixed to $l_{1,2} = 0.1\lambda_0$. The thickness parameter is assumed to be $d = 1\lambda_0$.

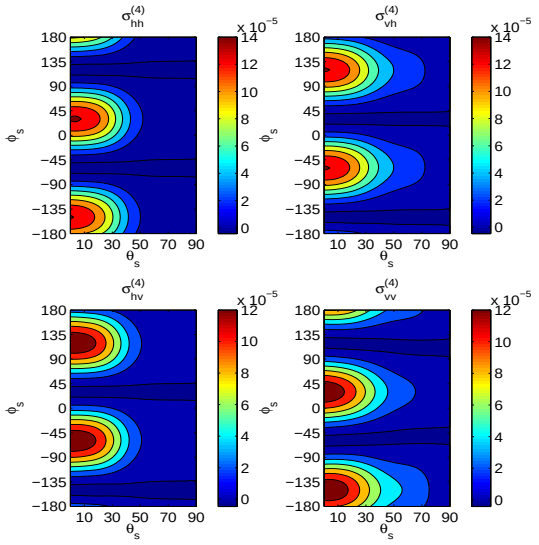

Figure 5.7: Bi-static RCS Study: $\sigma^{(4)}$ for $\bar{\epsilon}_r = [1, 3, 9]$, $\bar{\mu}_r = [1, 1, 1]$, $\theta_i = 20$, $\phi_i = 30$, slopes of both upper and lower surfaces are fixed to $s_{1,2} = 0.1$. The correlation lengths are fixed to $l_{1,2} = 0.1\lambda_0$. The thickness parameter is assumed to be $d = 1\lambda_0$.

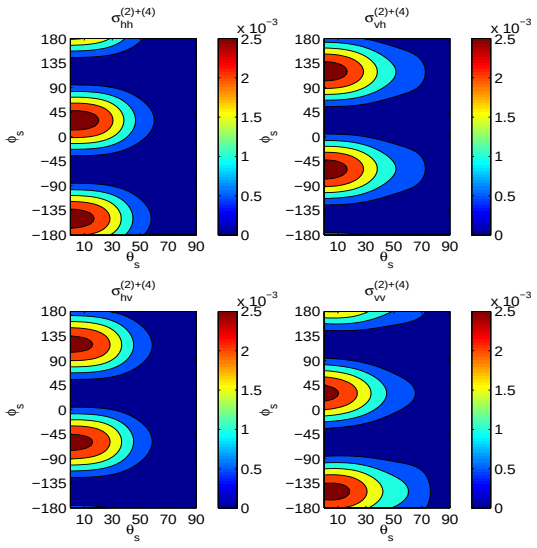

Figure 5.8: Bi-static RCS Study: σ^{incoh} for $\bar{\epsilon}_r = [1, 3, 9]$, $\bar{\mu}_r = [1, 1, 1]$, $\theta_i = 20$, $\phi_i = 30$, slopes of both upper and lower surfaces are fixed to $s_{1,2} = 0.1$. The correlation lengths are fixed to $l_{1,2} = 0.1\lambda_0$. The thickness parameter is assumed to be $d = 1\lambda_0$.

which reduced significantly. Although, some of the characteristics, like the locations of the maximums (in the absolute sense), have similarities, due to complete changes in the kernels, specific differences can be observed especially for vertical scattering cross sections.

5.4.3 Backscattering Study: Effects of correlation lengths

In this section, the bi-static RCS derived in Section 5.3 is investigated for backscattering. Again a lossless, non-magnetic medium, described by the dielectric permitivities $\epsilon_0 = 1$, $\epsilon_1 = 3$ and $\epsilon_2 = 9$ is considered here. Two different incidence angles are investigated in this section: ($\theta_i = 15$ and $\phi_i = 0$) as a low angle example, and ($\theta_i = 75$ and $\phi_i = 0$) as a large angle example. The slopes of both upper and lower surfaces are fixed to $s_{1,2} = 0.1$. The thickness parameter is assumed to be $d = 1\lambda_0$.

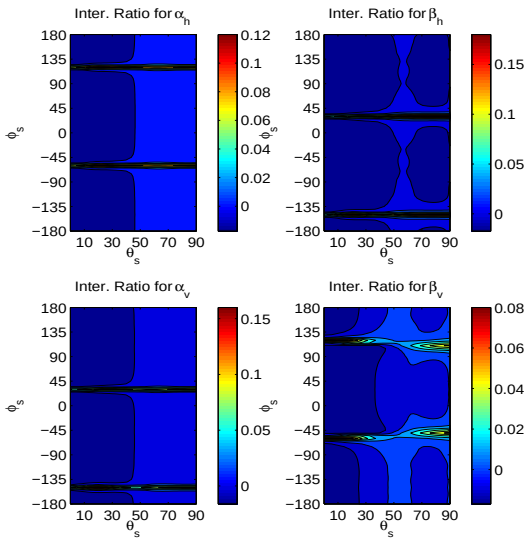

Figure 5.9: Bi-static RCS Study: Interaction ratio for $\bar{\epsilon}_r = [1, 3, 9]$, $\bar{\mu}_r = [1, 1, 1]$, $\theta_i = 20$, $\phi_i = 30$, slopes of both upper and lower surfaces are fixed to $s_{1,2} = 0.1$. The correlation lengths are fixed to $l_{1,2} = 0.1\lambda_0$. The thickness parameter is assumed to be $d = 1\lambda_0$.

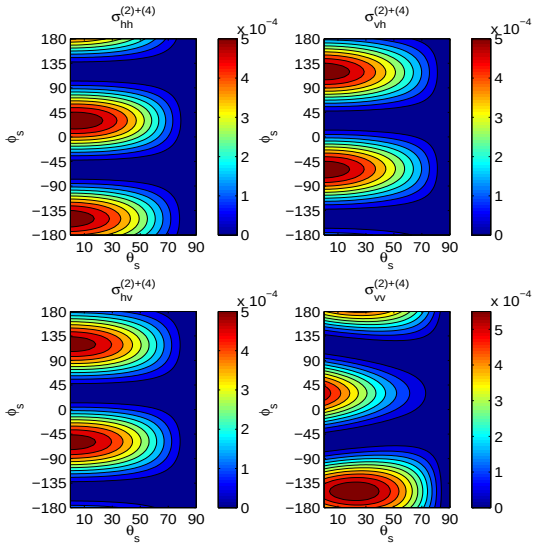

Figure 5.10: Bi-static RCS Study: σ^{incoh} for lossy case, $\bar{\epsilon}_r = [1, 3 + i, 9 + 0.1i]$, $\bar{\mu}_r = [1, 1, 1]$, $\theta_i = 20$, $\phi_i = 30$, slopes of both upper and lower surfaces are fixed to $s_{1,2} = 0.1$. The correlation lengths are fixed to $l_{1,2} = 0.1\lambda_0$. The thickness parameter is assumed to be $d = 1\lambda_0$.

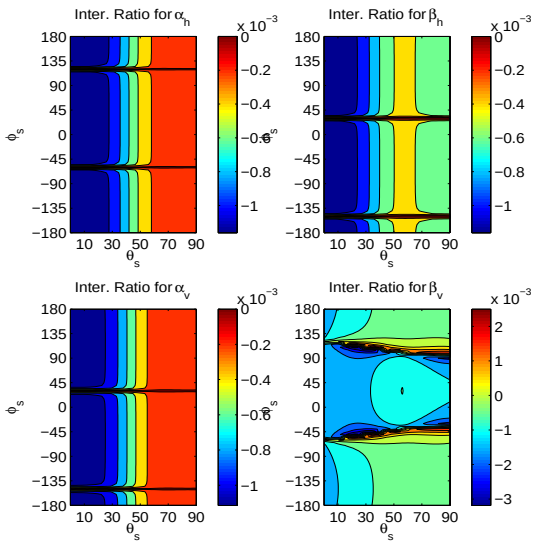

Figure 5.11: Bi-static RCS Study: Interaction ratio for lossy case, $\bar{\epsilon}_r = [1, 3+i, 9+0.1i]$, $\bar{\mu}_r = [1, 1, 1]$, $\theta_i = 20$, $\phi_i = 30$, slopes of both upper and lower surfaces are fixed to $s_{1,2} = 0.1$. The correlation lengths are fixed to $l_{1,2} = 0.1\lambda_0$. The thickness parameter is assumed to be $d = 1\lambda_0$.

The correlation lengths of both upper and lower surfaces are varied from $0.01\lambda_0$ to $1\lambda_0$. For each incidence angle case, two plots are given, first for the cross sections, and second for the interaction ratio.

In Figures 5.12 and 5.13, results from the ($\theta_i = 15$ and $\phi_i = 0$) case are presented. In Figure 5.12, the backscattering cross sections are provided: second order co-pol terms, given in the first row and the fourth order terms for all polarizations, given in the second and third rows, as labeled. It is a low incidence angle characteristic for isotropic spectrum that the horizontal-horizontal and vertical-vertical results, and also two cross-pol results are very close to each other. In the case of normal incidence, they are identical. It should also be noted that these results are Gaussian spectrum specific. The Gaussian spectrum highlights a specific part of the kernel, and these regions are

clearly observed. Typically, increasing correlation length causes an increase of the cross sections in the absolute sense. In Figure 5.13, the interaction ratio is investigated in the total fourth order. The logarithm of the absolute interaction ratio is plotted for convenience, for all four polarizations. These results indicate that the interaction term is more important for the cross-pol rather than the co-pol cross sections for lower correlation lengths. This ratio could be as much as ± 0.1 for this example. For co-pol results, the interpretation is slightly different. The co-pol fourth order kernels have resonance (rapidly changing) behavior for some parts of the integration domain, and when these regions are highlighted by the spectra, rapid changes in the cross sections occur. For this example, these changes occur for the correlation length values of $l_{1,2} \approx 1\lambda_0$. And for these special resonance regions, the interaction term becomes very important, even having values as much as ± 10.

In Figures 5.14 and 5.15, results from the ($\theta_i = 75$ and $\phi_i = 0$) case are presented as a close to grazing incidence example. In Figure 5.14, similar to Figure 5.12, the second and fourth order cross sections are provided. Typically, the co-pol cross sections reduced significantly in amplitude. The cross-pol cross sections are still comparable to previous case. Increasing cross sections with the increasing correlation length is still true here at least up to the resonance region. Although the cross sections tend to drop after the resonance region, they start to increase again, with increasing correlation lengths. Also, the resonance effects occur in smaller correlation lengths here, which is due to the incidence angle dependence of the cross section kernels. In Figure 5.15, the interaction ratios, again in absolute logarithm are provided for each polarization. In this case, the interaction of surfaces effect becomes extremely important for the cross

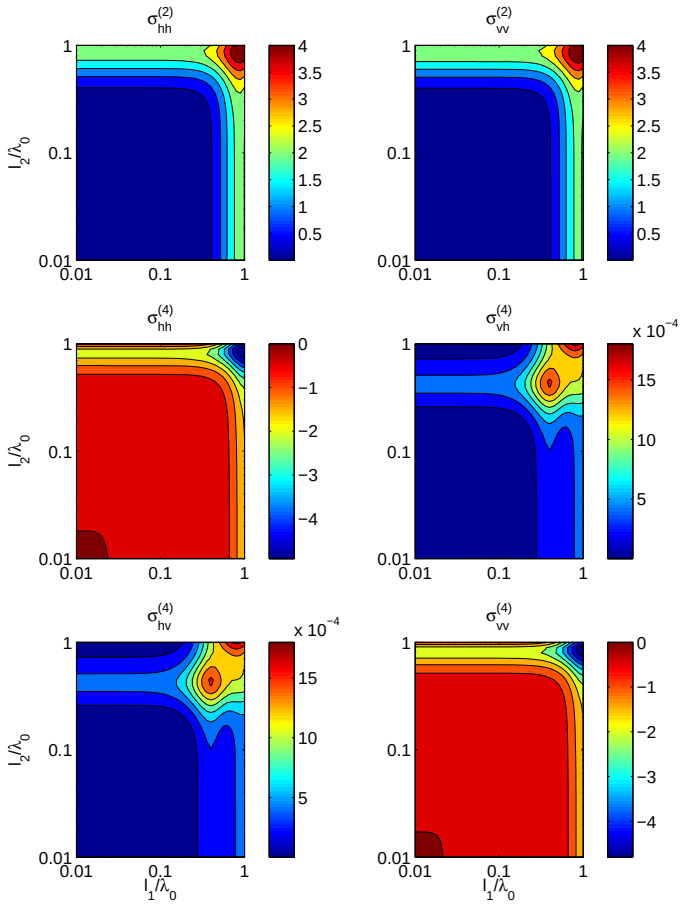

Figure 5.12: Backscattering Study: Effects of correlation lengths for $\bar{\epsilon}_r = [1, 3, 9]$, $\bar{\mu}_r = [1, 1, 1]$, $\theta_i = 15$, $\phi_i = 0$, slopes of both upper and lower surfaces are fixed to $s_{1,2} = 0.1$. The thickness parameter is assumed to be $d = 1\lambda_0$.

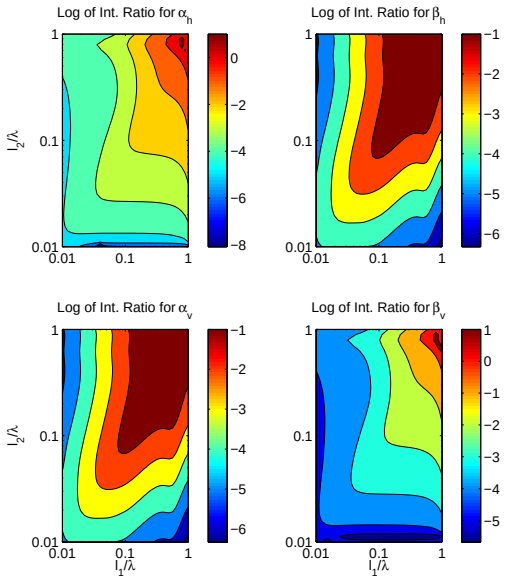

Figure 5.13: Backscattering Study: Effects of correlation lengths for $\bar{\epsilon}_r = [1, 3, 9]$, $\bar{\mu}_r = [1, 1, 1]$, $\theta_i = 15$, $\phi_i = 0$, slopes of both upper and lower surfaces are fixed to $s_{1,2} = 0.1$. The thickness parameter is assumed to be $d = 1\lambda_0$.

polarized cross sections. Unlike the previous case, the co-pol ratios are significantly reduced.

5.4.4 Backscattering Study: Effect of thickness

In this section, the bi-static RCS derived in Section 5.3 is investigated for backscattering, for the effects of thicknesses and correlation lengths. Again a lossless, non-magnetic medium, described by the dielectric permitivities: $\epsilon_0 = 1$, $\epsilon_1 = 3$ and $\epsilon_2 = 9$ is considered here. The correlation lengths of the upper and lower medium are assumed to be equal and varied from from $0.01\lambda_0$ to $1\lambda_0$, on logarithmic scale. The thickness of the intermediate media is varied from $0.1\lambda_0$ to $1\lambda_0$, on linear scale. The incidence (and also the observation) angle is fixed to ($\theta_i = 45$ and $\phi_i = 0$) degrees.

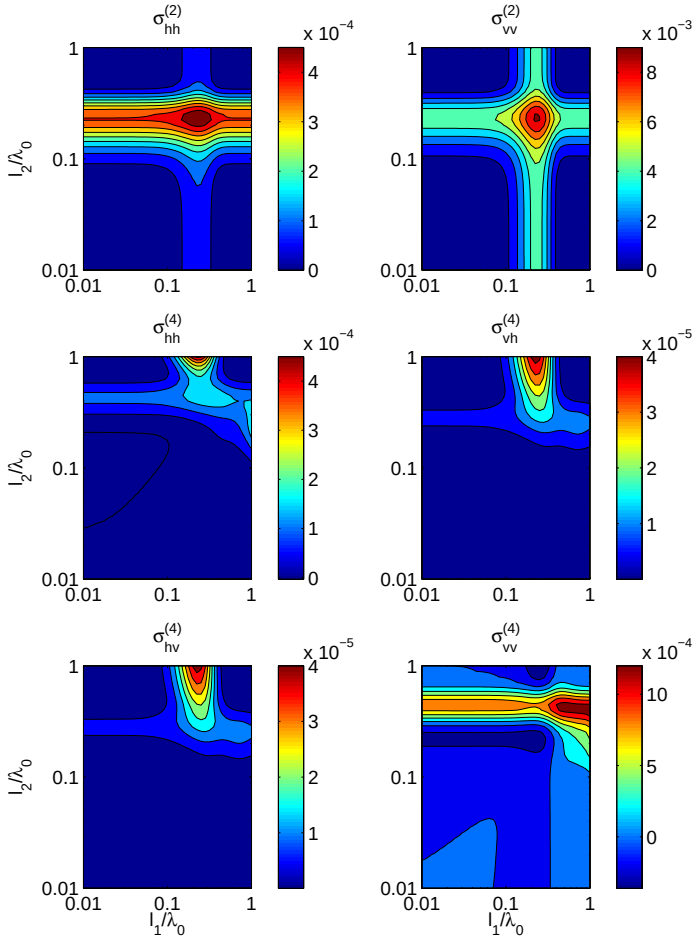

Figure 5.14: Backscattering Study: Effects of correlation lengths for $\bar{\epsilon}_r = [1, 3, 9]$, $\bar{\mu}_r = [1, 1, 1]$, $\theta_i = 75$, $\phi_i = 0$, slopes of both upper and lower surfaces are fixed to $s_{1,2} = 0.1$. The thickness parameter is assumed to be $d = 1\lambda_0$.

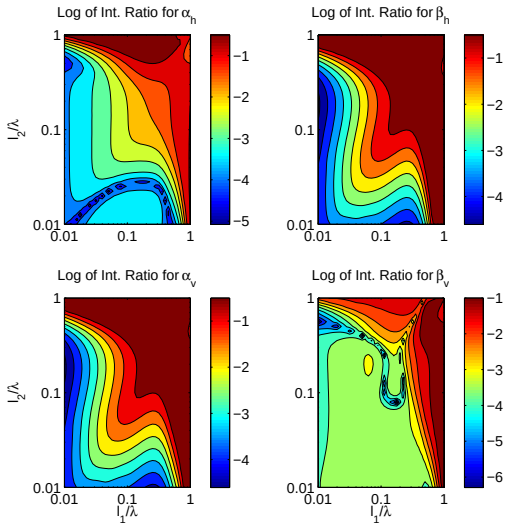

Figure 5.15: Backscattering Study: Effects of correlation lengths for $\bar{\epsilon}_r = [1, 3, 9]$, $\bar{\mu}_r = [1, 1, 1]$, $\theta_i = 75$, $\phi_i = 0$, slopes of both upper and lower surfaces are fixed to $s_{1,2} = 0.1$. The thickness parameter is assumed to be $d = 1\lambda_0$.

The slopes of both upper and lower surfaces are fixed to $s_{1,2} = 0.1$. The results are presented in Figures 5.16 and 5.17 , for cross sections and interaction ratios, respectively.

In Figure 5.16, the second and fourth order cross sections are provided. A resonance occurs around the correlation value of $l_{1,2} \approx 0.3\lambda_0$, for this incidence angle, at the second order. The fourth order terms also have the resonance effects, but for a slightly larger correlation length value. This is due to the fact that the two spectra terms involved in fourth order expressions and the combination of two spectra highlights a different region of the kernels. Also, in the co-pol results, the rapid sign change in the cross section with the correlation parameter is observed as a typical resonance effect. Clearly, the periodic nature of the cross sections are observed with the separation d. In addition, the separation of the surfaces effects the cross-pol cross

section kernels in a way that lower thickness values result in higher cross sections. In Figure 5.17, interaction ratios are investigated, based on the cross sections provided in Figure 5.16 for all polarizations. For cross-pol results, the interaction effect can reach values up to 1, especially with increasing correlation length. Again the periodicity with thickness can be observed, as expected. The co-pol ratios are smaller, taking values up to 0.3 in the resonance regions. Generally speaking, outside the resonance regions, the interaction effect is small for co-pol cross sections. Next, the effect of incidence angle is investigated, with respect to varying thickness of the intermediate medium.

5.4.5 Backscattering Study: Effect of incidence angle

In this section, the bi-static RCS derived in Section 5.3 is investigated for backscattering for the effects of incidence (also observation) angle and thickness of the intermediate medium. Again a lossless, non-magnetic medium, described by the dielectric permitivities: $\epsilon_0 = 1$, $\epsilon_1 = 3$ and $\epsilon_2 = 9$ is considered here. The azimuthal incidence angle is set to $\phi_i = 0$, and the slopes of both upper and lower surfaces are fixed to $s_{1,2} = 0.1$. The calculations are done for a fixed correlation length of $l_{1,2} = 0.1\lambda_0$, for both upper and lower surfaces so that no resonance effect can occur for any of these incidence angles. The thickness parameter d is varied, again from $0.1\lambda_0$ to $1\lambda_0$, on a linear scale , and the incidence angle is varied from 0 to 80 degrees, linearly. The results are given in Figures 5.18 and 5.19, again for the cross sections and interaction ratios, respectively.

In Figure 5.18, the second and fourth order cross sections are plotted in a similar format with the previous cross section results. Typically, the cross sections are larger

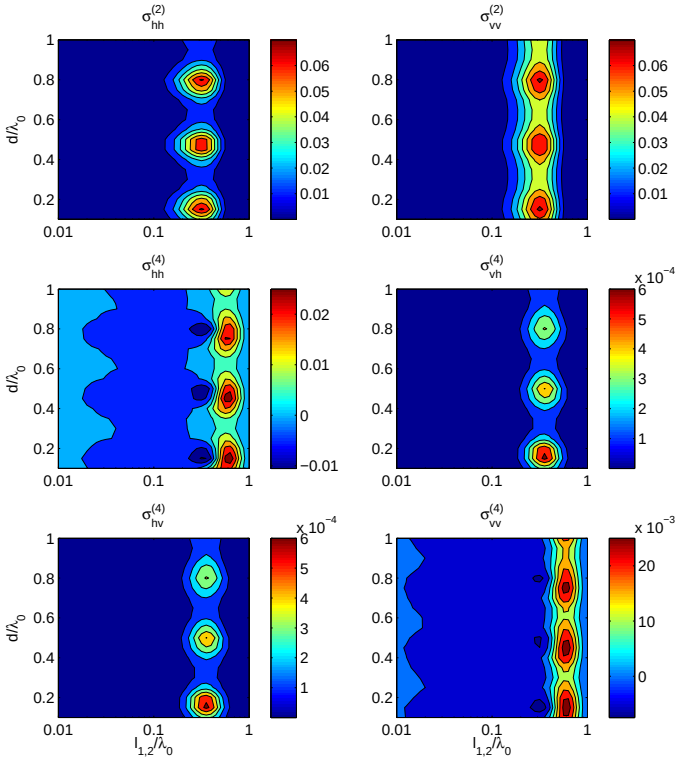

Figure 5.16: Backscattering Study: Effect of thickness: for $\bar{\epsilon}_r = [1, 3, 9]$, $\bar{\mu}_r = [1, 1, 1]$, $\theta_i = 45$, $\phi_i = 0$, slopes of both upper and lower surfaces are fixed to $s_{1,2} = 0.1$.

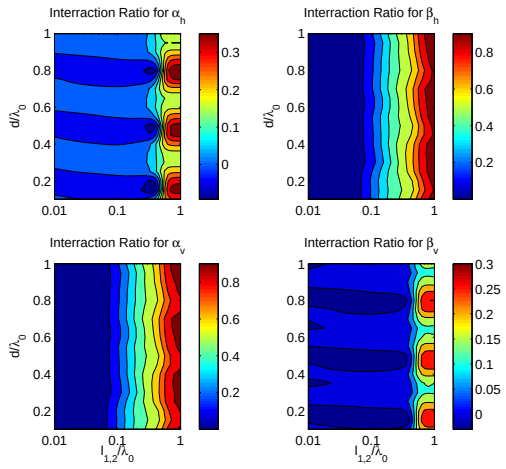

Figure 5.17: Backscattering Study: Effect of thickness: for $\bar{\epsilon}_r = [1, 3, 9]$, $\bar{\mu}_r = [1, 1, 1]$, $\theta_i = 45$, $\phi_i = 0$, slopes of both upper and lower surfaces are fixed to $s_{1,2} = 0.1$.

in the absolute sense for close to normal incidence angles. The fourth order co-pol cross sections are negative, while all other cross sections are positive. The periodicity in thickness parameter d is still observed here as in the coherent case.

In Figure 5.19, the interaction ratio is plotted for each polarization. Due to the periodicity of the cross sections in the thickness parameter d, the interaction ratios are also periodic. Since the resonance effects are not involved, the interaction ratio is negligible for co-pol cross sections. But still, it is possible to conclude that for horizontal-horizontal polarization, the interaction term is more important at larger incidence angles, while for vertical-vertical polarization, the interaction ratio reaches a minimum in between. This point for this example is around 60 degrees. This point is directly related to the Brewster angle of the first interface, where almost zero reflection occurs. For the cross-pol cross sections, interaction of roughness effects is very important. The interaction ratio for this case typically increases as the incidence

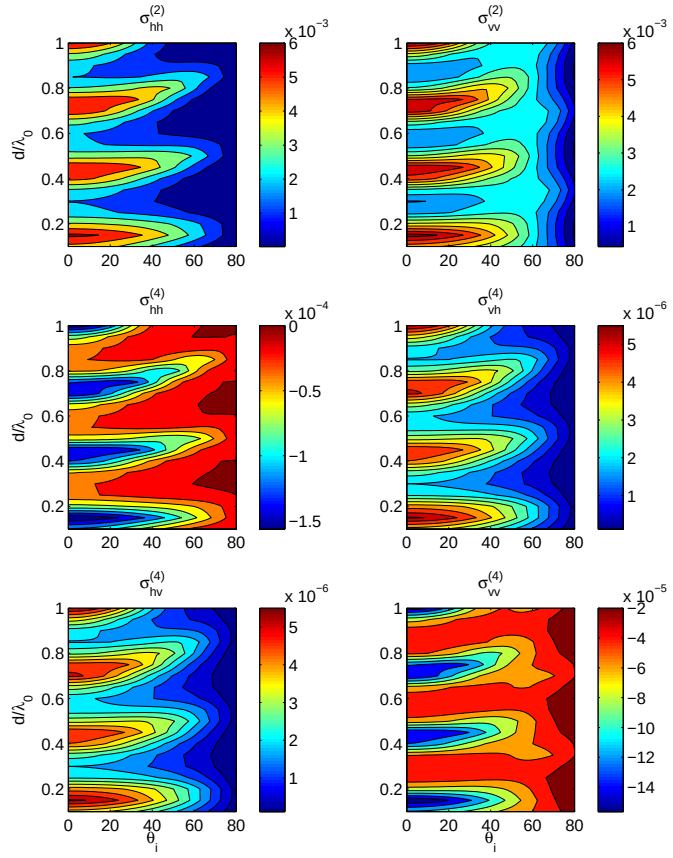

Figure 5.18: Backscattering Study: Effect of incidence angle: for $\bar{\epsilon}_r = [1, 3, 9]$, $\bar{\mu}_r = [1, 1, 1]$, $\phi_i = 0$, slopes of both upper and lower surfaces are fixed to $s_{1,2} = 0.1$. Correlation lengths are fixed to $l_{1,2} = 0.1\lambda_0$.

angle increases, and as the thickness decreases. In other words, the interaction term contributes most to the backscattering cross-pol cross sections when surfaces are close to each other at near grazing incidence.

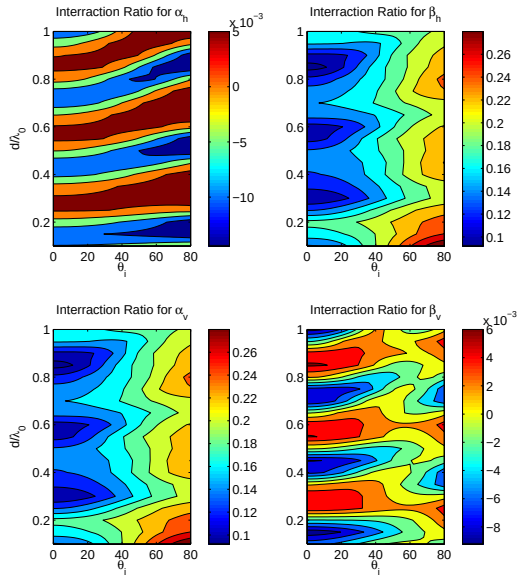

Figure 5.19: Backscattering Study: Effect of incidence angle: for $\bar{\epsilon}_r = [1, 3, 9]$, $\bar{\mu}_r = [1, 1, 1]$, $\phi_i = 0$, slopes of both upper and lower surfaces are fixed to $s_{1,2} = 0.1$. Correlation lengths are fixed to $l_{1,2} = 0.1\lambda_0$.

5.4.6 Backscattering Study: Effect of dielectric contrasts

In this section, the backscattering RCS is investigated for the effects of upper and lower surface dielectric contrasts. Again a lossless and non-magnetic medium is considered. The azimuthal component of the incidence angle is set to $\phi_i = 0$. The slopes of both upper and lower surfaces are fixed to $s_{1,2} = 0.1$ and the correlation lengths are fixed to $l_{1,2} = 0.1\lambda_0$, to avoid any resonance effect. The thickness parameter is assumed to be $d = 1\lambda_0$. The results are presented in Figures 5.20 and 5.21, for incidence angles of $\theta_i = 0$ and $\theta_i = 45$ degrees, respectively. Only the interaction ratios are provided. Figure 5.20 only has two sub-figures, one is for the co-pol and the other is for the cross-pol ratios, since at normal incidence, there is no horizontal or

vertical polarization distinction. But ,the $\theta_i = 45$ degree result has the same standard sub-figure format as the previous ratio results. On each sub-figure of these plots, the horizontal axis represents the upper interface contrast, defined by $\frac{\epsilon_1}{\epsilon_0}$, which is varied from 1 to 10, and the vertical axis represents the lower surface dielectric contrast, defined similarly as $\frac{\epsilon_2}{\epsilon_1}$, varying from 0.1 to 10. Triangular regions at the lower left corner of these sub-figures, defined by the points $(1, 1)$, $(1, 0.1)$ and $(10, 0.1)$, are manually set to zero, since any point in these regions would mean a dielectric permittivity less than 1 for the lower region.

In Figure 5.20, interaction ratios for the $\theta_i = 0$ degrees case are presented for co-pol and cross-pol cross sections. The behavior of interaction ratio on two specific lines are very important in this study. The first line is defined by its two end points: $(1, 1)$ and $(10, 1)$, corresponds to the case when the lower region has the same dielectric permittivity with the intermediate region. In other words, this line is the one layer limit. On this line, the term σ^{upper} is the only term that contributes to total cross section and the interaction ratio vanishes, as expected, for all polarizations. The second important line is defined, again by its end points: $(1, 1)$ and $(10, 0.1)$, corresponding to an air-substrate-air type of media. This is the case when the strongest interaction effects are observed. This oscillation is in fact the exact same phenomena that we observed in the previous section while we were varying the thickness parameter d. As the dielectric permittivity of the intermediate medium changes, the thickness of the substrate changes with respect to changing wavelength of the substrate. And as we move vertically from any point on this line, the interaction ratio decreases, and eventually vanishes as we pass through the first line. The points above the first line correspond to media similar to the air-ice-rock interface, with increasing dielectric

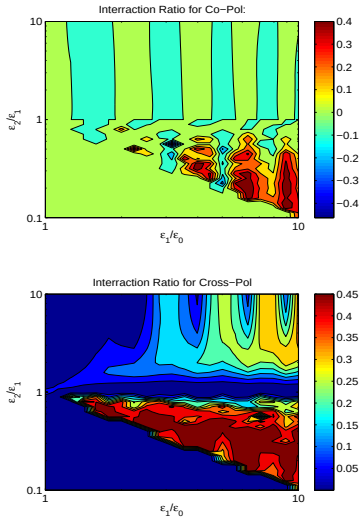

Figure 5.20: Backscattering Study: Effect of dielectric contrasts: for $\theta_i = 0$, $\phi_i = 0$, slopes of both upper and lower surfaces are fixed to $s_{1,2} = 0.1$. Correlation lengths are fixed to $l_{1,2} = 0.1\lambda_0$. The thickness parameter is assumed to be $d = 1\lambda_0$.

permittivity downwards. The cross-pol ratios are slightly higher, and since the correlation lengths are chosen to avoid any resonance effect, co-pol ratios are almost negligible. In fact, small periodicity with the upper interface contrast can be observed, again can be explained with thickness changes relative to the intermediate medium wavelength.

Finally, in figure 5.21, the $\theta_i = 45$ degrees case is presented for all polarizations. Most of the characteristics of this plot are similar to the previous result. The important point here to note is the rapid increase of the interaction ratios for cross-pol cross sections. As mentioned in the section about the effects of incidence angle to backscattering RCS, increasing incidence angle should produce larger interaction ratios, which can clearly be observed.

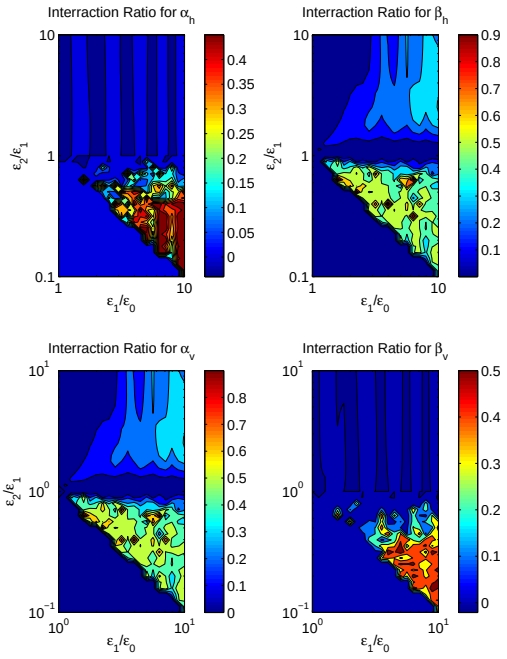

Figure 5.21: Backscattering Study: Effect of dielectric contrasts: for $\theta_i = 45$, $\phi_i = 0$, slopes of both upper and lower surfaces are fixed to $s_{1,2} = 0.1$. Correlation lengths are fixed to $l_{1,2} = 0.1\lambda_0$. The thickness parameter is assumed to be $d = 1\lambda_0$.

5.5 Conclusion

In this chapter, first, a general discussion on the power calculations was provided. Assumptions on the statistical surface properties were highlighted. Then, under the assumption of Gaussian Random Process (GRP), the zeroth and the second order coherent reflectivity and the second and the fourth order incoherent bi-static Radar Cross Sections (RCS) were derived. For the case, when the two surfaces are uncorrelated, the bi-static RCS term was studied thoroughly and the effects of upper and lower roughness and the interaction of roughness effects were identified. A special term was defined as the ratio of the interaction effect to the overall RCS.

Later, the derived power quantities were examined extensively for uncorrelated GRPs. The results presented in this chapter provide the most extensive study of the two layer SPM cross sections to date. First, the second order correction to the coherent reflectivity was considered and an the effects of incidence angle and mid-layer thickness were analyzed. Next, the bi-static RCS was studied for a lossless air-ice-rock type interface for all possible scattering angles. In the rest of the study, only backscattering cross sections were considered. The effects of surface correlation lengths, thickness of the intermediate layer with respect to both the incidence angle and the correlation lengths, and the dielectric contrasts of the media were presented. The key deductions from these studies can be summarized as follows:

- The second order correction to the coherent reflectivity is very sensitive to the surface correlation lengths: although small correlation lengths result in negligible contributions, even moderate values can cause appreciable corrections.

- The bi-static RCS study revealed that the plane of incidence and the orthogonal plane include the scattering angles where maximum interaction between the surfaces occur, for co-pol and cross-pol, respectively.

- The dominant effect of introducing loss to the media is rapid attenuation of the lower layer scattered fields and consequent drop in the lower layer cross sections.

- Increasing correlation length typically increases the interaction ratio at least for the lower correlation lengths.

- Specific correlation lengths cause resonance like effects mostly in co-pol cross sections: rapid changes in the cross sections result in large interaction ratios. This effect is likely Gaussian spectrum specific.

- For correlation lengths that do not cause resonances, the interaction effects are more dominant in cross-pol cross sections.

- Variation of the thickness parameter clearly causes periodic changes in both cross sections and the interaction ratios. In addition, an attenuation of cross-pol cross sections is observed with increasing thickness.

- Cross-pol interactions are weakly dependent on the thickness, while the co-pol interactions have a strong periodic dependence.

- The interaction term contributes most to the backscattering cross-pol cross sections when surfaces are close to each other at near grazing incidence.

- The interaction effects are more dominant for air-substrate-air type or thin layer like media.

Briefly, the results confirm that surface interactions are important for the two layer problem, and consequently, higher order solutions are necessary for analyzing layered roughness effects.

CHAPTER 6

EMISSION THEORY OF ROUGH SURFACES BASED ON SINGLE LAYER SPM

6.1 Introduction

In this chapter, the SPM scattering solution of [69] is applied in Kirchhoff's Law of thermal emission [10] to derive the fourth order correction in the small slope emission theory. Section 6.2 briefly reviews the SPM scattering solution from [69] and introduces the notation to be utilized. These scattered field solutions are then applied in Section 6.3 with Kirchhoff's Law to derive the fourth order SSA emission term; it is shown that this term has the form of an integration over a product of two spectra for a Gaussian random process sea. In Section 6.4, the analysis of [78] is extended to fourth order to demonstrate again that the SSA theory continues to match a slope expanded PO theory for large-scale surface emission contributions.

Numerical evaluation of the four-fold SSA4 integral for computing "long-short" wave interactions is discussed in Section 6.5, and an approximation for computing such interactions is presented in Section 6.6. The form of the approximation obtained allows a sea spectrum independent comparison with the two-scale theory of long-short wave tilting effects to be performed in terms of a set of weighting functions;

these functions are found to be similar but not identical between the two theories. To provide more concrete illustrations, Section 6.7 presents azimuthal harmonic coefficients of emitted brightnesses obtained from a numerical four-fold SSA4 integration and compares results with predictions of the approximation from Section 6.6 as well as the two-scale theory. Results show the SSA4 expansion to perform well for computing long-short wave interactions, and that SSA4 and two-scale model predictions remain similar but not identical. Final discussions and conclusions are provided in Chapter 7.

6.2 Review of single layer SPM scattered field solution

The basic notation introduced in [68]-[69] is used below unless otherwise notated. Consider a periodic rough interface $z = f(x, y)$ separating free space ($z > f(x, y)$) from a dielectric region with relative permittivity ϵ. A plane wave is incident from free space upon this interface; the resulting scattered and transmitted fields can be completely described in terms of the polarization complex amplitudes of a set of Floquet modes. Horizontally and vertically polarized scattered mode complex amplitudes are denoted by $\alpha_{\overline{n}'}$ and $\beta_{\overline{n}'}$, respectively, while $\gamma_{\overline{n}'}$ and $\delta_{\overline{n}'}$ refer to transmitted horizontally and vertically polarized complex amplitudes, respectively. Here $\overline{n}' = (n', m')$ provides indexes to a particular Floquet mode, thus describing the direction of propagation of the corresponding scattered or transmitted field. Note the requirement for a periodic interface can be removed after the solution is completed by allowing the periods to approach infinity, as in [22].

Following the process in [68] but shifting some of the indices appropriately allows the multiple terms in [68] to be combined. Scattering and transmission coefficients,

all united in a vector quantity, $\bar{\zeta} = [\alpha, \beta, \gamma, \delta]^T$ at Nth order ($N \geq 2$) can then be expressed as [69]:

$$\begin{aligned} \bar{\zeta}_{\overline{n}'}^{(N)} &= \sum_{\overline{n}_1} \sum_{\overline{n}_2} \cdots \sum_{\overline{n}_{N-1}} h_{\overline{n}_1} h_{\overline{n}_2} \ldots h_{\overline{n}_{N-1}} h_{\overline{n}'-\overline{n}_1-\cdots\overline{n}_{N-1}} \\ &\qquad \cdot \bar{g}^{(N)}\left(\overline{n}', \overline{n}_1, \ldots, \overline{n}_{N-1}\right) \end{aligned} \tag{6.1}$$

where $h_{\overline{n}}$ refers to the Fourier coefficients of the surface; note N of these are included so that the overall term is Nth order in surface height. The Nth order SPM "kernel" is expressed in terms of lower order kernels as follows [69]:

$$\begin{aligned} \bar{g}^{(N)}\left(\overline{n}', \overline{n}_1, \ldots, \overline{n}_{N-1}\right) &= \bar{g}^{(N,\,0)}\left(\overline{n}', \overline{n}_1, \ldots, \overline{n}_{N-1}\right) \\ &\quad + \sum_{l=1}^{N-1} \left[\bar{\bar{\nu}}^{(N-l)}\left(\overline{n}', \overline{n}_s^{(l)}, \overline{n}_{l+1}, \ldots, \overline{n}_{N-1}\right) \right. \\ &\qquad \left. \cdot \bar{g}^{(l)}\left(\overline{n}_s^{(l)}, \overline{n}_2, \ldots, \overline{n}_l\right) \right] \end{aligned} \tag{6.2}$$

where $\overline{n}_s^{(l)}$ is

$$\overline{n}_s^{(l)} = \sum_{i=1}^{l} \overline{n}_i \tag{6.3}$$

The $\bar{\bar{\nu}}^{(N-l)}(\overline{n}', \overline{n}, \overline{n}_1, \ldots, \overline{n}_{N-l-1})$ quantity above is a four-by-four tensor with elements ν_{ij} at row i and column j, while the kernel function vector $\bar{g}^{(l)}$ for $l = 1$ to N is a 4 element column vector defined analogously to $\bar{\zeta}$. Elements of the $\bar{\bar{\nu}}^{N-l}$ tensor, the $\bar{g}^{(N,\,0)}$ quantity, and other details are given in [69]. The above formulation provides a recursive solution that is easily programmed for determining the SPM kernel at a specific argument and at arbitrary order.

Note that ultimately the transmission coefficients (γ, δ) of $\bar{\zeta}$ are not needed when computing thermal emission (the SSA theory is known to conserve power at a given order), so only the scattering coefficients are of interest in what follows. We introduce a revised notation to simplify consideration of polarimetric emission by defining

$f^{(N)}_{qp,\overline{n}'}$ as the complex amplitude of the Floquet mode indexed by $\overline{n}'$ at Nth order in scattered polarization q for incident polarization p, with p and q chosen from h or v for horizontal and vertical, respectively. For example, $f^{(N)}_{hh,\overline{n}'}$ would be defined as $\alpha^{(N)}_{\overline{n}'}$ for a horizontally polarized incident plane wave, with $\alpha^{(N)}_{\overline{n}'}$ representing the first row of the $\bar{\zeta}^{(N)}_{\overline{n}'}$ vector in Equation (6.1). Similarly we adopt the notation $g^{(N)}_{qp,\overline{n}'}$ for the Nth order SPM kernel function corresponding to $f^{(N)}_{hh,\overline{n}'}$. This notational modification is necessary due to the fact that Equation (6.1) must be considered separately for horizontal and vertical incident polarizations.

6.3 Fourth order emission theory

Kirchhoff's Law requires computation of the total surface reflectivity in order to determine surface emissivity. The total surface reflectivity is determined by integrating the total power scattered into the upper hemisphere under plane wave illumination. Furthermore, appropriate combinations of polarization coefficients [**?**] must be considered in order to compute polarimetric brightnesses. For a periodic surface with periods large compared to the electromagnetic wavelength, plane wave illumination results in a large set of Floquet modes scattered bistatically above the surface. The complex amplitude of each of these modes is expressed as a series up to fourth order in the SPM solution. Computation of the power in a given mode then results in a corresponding series for the scattered power in that mode. The fourth order contribution to the total surface reflectivity is then determined by adding (or integrating in the continuous surface limit) all fourth order power contributions from each scattered mode.

Following this process, the fourth order contribution of the Floquet mode indexed by $\overline{n}'$ to the total surface reflectivity in a given polarimetric quantity can be written as

$$\begin{aligned}
P^{(4)}_{h,\overline{n}'} &= 2\mathrm{Re}\Bigg\{ f^{(0)}_{hh} f^{(4)*}_{hh} + f^{(0)}_{vh} f^{(4)*}_{vh} \\
&\qquad +\mathrm{Re}\left\{ \frac{k_{z,\overline{n}'}}{k_{zi}} \right\} \left(f^{(1)}_{hh} f^{(3)*}_{hh} + f^{(1)}_{vh} f^{(3)*}_{vh} \right) \Bigg\} \\
&\quad +\mathrm{Re}\left\{ \frac{k_{z,\overline{n}'}}{k_{zi}} \right\} \left(|f^{(2)}_{hh}|^2 + |f^{(2)}_{vh}|^2 \right) \qquad (6.4) \\
P^{(4)}_{v,\overline{n}'} &= 2\mathrm{Re}\Bigg\{ f^{(0)}_{vv} f^{(4)*}_{vv} + f^{(0)}_{hv} f^{(4)*}_{hv} \\
&\qquad +\mathrm{Re}\left\{ \frac{k_{z,\overline{n}'}}{k_{zi}} \right\} \left(f^{(1)}_{vv} f^{(3)*}_{vv} + f^{(1)}_{hv} f^{(3)*}_{hv} \right) \Bigg\} \\
&\quad +\mathrm{Re}\left\{ \frac{k_{z,\overline{n}'}}{k_{zi}} \right\} \left(|f^{(2)}_{vv}|^2 + |f^{(2)}_{hv}|^2 \right) \qquad (6.5) \\
P^{(4)}_{U,\overline{n}'} &= 2\mathrm{Re}\Bigg\{ f^{(0)}_{vv} f^{(4)*}_{vh} + f^{(4)}_{hv} f^{(0)*}_{hh} \\
&\quad +\mathrm{Re}\left\{ \frac{k_{z,\overline{n}'}}{k_{zi}} \right\} \Big(f^{(1)}_{vv} f^{(3)*}_{vh} + f^{(2)}_{vv} f^{(2)*}_{vh} + f^{(3)}_{vv} f^{(1)*}_{vh} \\
&\quad + f^{(1)}_{hv} f^{(3)*}_{hh} + f^{(2)}_{hv} f^{(2)*}_{hh} + f^{(3)}_{hv} f^{(1)*}_{hh} \Big) \Bigg\} \qquad (6.6) \\
P^{(4)}_{V,\overline{n}'} &= 2\mathrm{Im}\Bigg\{ f^{(0)}_{vv} f^{(4)*}_{vh} + f^{(4)}_{hv} f^{(0)*}_{hh} \\
&\quad +\mathrm{Re}\left\{ \frac{k_{z,\overline{n}'}}{k_{zi}} \right\} \Big(f^{(1)}_{vv} f^{(3)*}_{vh} + f^{(2)}_{vv} f^{(2)*}_{vh} + f^{(3)}_{vv} f^{(1)*}_{vh} \\
&\quad + f^{(1)}_{hv} f^{(3)*}_{hh} + f^{(2)}_{hv} f^{(2)*}_{hh} + f^{(3)}_{hv} f^{(1)*}_{hh} \Big) \Bigg\} \qquad (6.7)
\end{aligned}$$

Here $*$, Re, and Im denote the complex conjugate, real, and imaginary part operators, respectively. The subscript $\overline{n}'$ is omitted above on the f quantities for simplicity, and the quantity $k_{zi} = k_0 \cos\theta_i$ is related to the radiometer polar observation angle θ_i, with k_0 the electromagnetic wavenumber. The quantity $k_{z,\overline{n}'}$ refers to the z component of the vector wavenumber of the Floquet mode indexed by $\overline{n}'$, as defined in [68]. Finally,

the subscripts h, v, U, and V of the P quantities refer to the horizontal, vertical, U, and V polarimetric radiometer channels, respectively. The above expressions are to be summed over all propagating modes (i.e. all values of $\overline{n}'$ corresponding to propagating Floquet modes.)

When the SPM solution for the $f^{(N)}_{qp,\overline{n}'}$ complex amplitudes from Equation (6.1) is substituted into the above and summed over $\overline{n}'$, a combination of sums over surface Fourier coefficients and SPM kernel functions results for determining $R^{(4)}_\zeta$, the total surface reflectivity. By shifting indices within these sums, it is possible to combine the multiple terms in this combination into a single "emission kernel" multiplying a single set of surface Fourier coefficients:

$$\begin{aligned} R^{(4)}_\zeta &= \sum_{\overline{n}_1}\sum_{\overline{n}_2}\sum_{\overline{n}_3} h_{\overline{n}_1} h_{\overline{n}_2} h_{\overline{n}_3} h_{-\overline{n}_1-\overline{n}_2-\overline{n}_3} \\ &\qquad \cdot g^{T,(4)}_\zeta\left(\overline{n}_1, \overline{n}_2, \overline{n}_3\right) \end{aligned} \tag{6.8}$$

Here ζ refers to h, v, U, or V, while $g^{T,(4)}_\zeta$ is the new reflectivity kernel obtained in this process. The resulting kernel for the horizontal reflectivity is

$$\begin{aligned} g^{T,(4)}_h &= \mathrm{Re}\left\{\frac{k_{z(\overline{n}_1+\overline{n}_3)}}{k_{zi}}\right\}\cdot \\ &\quad \Big(g^{(2)}_{hh}(\overline{n}_1+\overline{n}_3,\overline{n}_1)\; g^{(2)*}_{hh}(\overline{n}_1+\overline{n}_3,-\overline{n}_2) \\ &\quad + g^{(2)}_{vh}(\overline{n}_1+\overline{n}_3,\overline{n}_1)\; g^{(2)*}_{vh}(\overline{n}_1+\overline{n}_3,-\overline{n}_2)\Big) \\ &\quad +2\mathrm{Re}\Bigg\{\Gamma^*_h\; g^{(4)}_{hh}(\overline{0},\overline{n}_1,\overline{n}_2,\overline{n}_3) \\ &\qquad + \mathrm{Re}\left\{\frac{k_{z(-\overline{n}_3)}}{k_{zi}}\right\}\cdot \\ &\quad \Big(g^{(1)*}_{hh}(-\overline{n}_3)\; g^{(3)}_{hh}(-\overline{n}_3,\overline{n}_1,\overline{n}_2) \\ &\quad + g^{(1)*}_{vh}(-\overline{n}_3)\; g^{(3)}_{vh}(-\overline{n}_3,\overline{n}_1,\overline{n}_2)\Big)\Bigg\} \end{aligned} \tag{6.9}$$

where Γ_h is used to notate the horizontally polarized Fresnel reflection coefficient (as in [68]). The notation $k_{z,\overline{n}}$ again is utilized to indicate the z component of the vector wavenumber of the Floquet mode indexed by $\overline{n}$. The vertical reflectivity kernel $g_v^{T,(4)}$ can easily be obtained from the previous expression by interchanging the subscripts h and v.

The third Stokes' parameter reflectivity kernel is

$$
\begin{aligned}
g_U^{T,(4)} \;=\; & 2\mathrm{Re}\Bigg\{\Gamma_v \; g_{vh}^{(4)*}(\overline{0},-\overline{n}_1,-\overline{n}_2,-\overline{n}_3) \\
& \quad + \Gamma_h^* \; g_{hv}^{(4)}(\overline{0},\overline{n}_1,\overline{n}_2,\overline{n}_3) \\
& \quad + \mathrm{Re}\left\{\frac{k_{z(\overline{n}_3)}}{k_{zi}}\right\}\cdot \\
& \Big(g_{hv}^{(1)}(\overline{n}_3)\; g_{hh}^{(3)*}(\overline{n}_3,-\overline{n}_1,-\overline{n}_2) \\
& + g_{vv}^{(1)}(\overline{n}_3)\; g_{vh}^{(3)*}(\overline{n}_3,-\overline{n}_1,-\overline{n}_2)\Big) \\
& \quad + \mathrm{Re}\left\{\frac{k_{z(\overline{n}_1+\overline{n}_3)}}{k_{zi}}\right\}\cdot \\
& \Big(g_{hv}^{(2)}(\overline{n}_1+\overline{n}_3,\overline{n}_1)\; g_{hh}^{(2)*}(\overline{n}_1+\overline{n}_3,-\overline{n}_2) \\
& + g_{vv}^{(2)}(\overline{n}_1+\overline{n}_3,\overline{n}_1)\; g_{vh}^{(2)*}(\overline{n}_1+\overline{n}_3,-\overline{n}_2)\Big) \\
& \quad + \mathrm{Re}\left\{\frac{k_{z(-\overline{n}_3)}}{k_{zi}}\right\}\cdot \\
& \Big(g_{hv}^{(3)}(-\overline{n}_3,\overline{n}_1,\overline{n}_2)\; g_{hh}^{(1)*}(-\overline{n}_3) \\
& + \; g_{vv}^{(3)}(-\overline{n}_3,\overline{n}_1,\overline{n}_2)\; g_{vh}^{(1)*}(-\overline{n}_3)\Big)\Bigg\}
\end{aligned}
\tag{6.10}
$$

The fourth Stokes' parameter brightness kernel $g_V^{T,(4)}$ is obtained by replacing the Re operator at the beginning of Equation (6.10) with the Im operator.

If an ensemble average over a stochastic surface process is taken in Equation (6.8), the surface statistic of interest is

$$< h_{\overline{n}_1} h_{\overline{n}_2} h_{\overline{n}_3} h_{-\overline{n}_1-\overline{n}_2-\overline{n}_3} > \tag{6.11}$$

where the $< \cdot >$ notation refers to an ensemble average. In the continuous surface limit (i.e. as the surface periods approach infinity [22]), the fourth order reflectivity correction has the form of a six-fold integration:

$$\int\int d\mathbf{k}_1 \int\int d\mathbf{k}_2 \int\int d\mathbf{k}_3 \\ T(\mathbf{k}_1, \mathbf{k}_2, \mathbf{k}_3) g_\zeta^{T,(4)}(\mathbf{k}_1, \mathbf{k}_2, \mathbf{k}_3) \tag{6.12}$$

Here $\mathbf{k}$ represents the (k_x, k_y) couple and the integration limits are infinite. The previous ensemble averaged quantity is now expressed as T, which is the fourth moment of the random rough surface, given in terms of surface spectra W as follows:

$$\begin{aligned} T &= W(\mathbf{k}_1)W(\mathbf{k}_2)\delta(\mathbf{k}_3 + \mathbf{k}_2) \\ &\quad + W(\mathbf{k}_1)W(\mathbf{k}_2)\delta(\mathbf{k}_3 + \mathbf{k}_1) \\ &\quad + W(\mathbf{k}_3)W(\mathbf{k}_{22})\delta(\mathbf{k}_1 + \mathbf{k}_2) + T_{tri} \end{aligned} \tag{6.13}$$

The quantity T_{tri} is the surface tri-spectrum, which describes non-Gaussian sea surface properties at fourth order. However little empirical information is available on the sea surface tri-spectrum, making its further consideration difficult at this point in time.

For a Gaussian random process (GRP), the tri-spectrum (T_{tri}) vanishes, and the Dirac delta functions can be utilized in Equation (6.12) to obtain a four-fold integration for the fourth order brightness correction

$$\begin{aligned} \Delta T_\gamma^{(4)} &= -T_s \int dk_x \int dk_y \int dk'_x \int dk'_y W(k_x, k_y) \\ &\quad W(k'_x, k'_y) g_\zeta^{T,(4),shf}(k_x, k_y, k'_x, k'_y) \end{aligned} \tag{6.14}$$

where T_s is the surface physical temperature, and a modified kernel is used:

$$g_\zeta^{T,(4),shf}(\mathbf{k}_1,\mathbf{k}_2) = g_\zeta^{T,(4)}(\mathbf{k}_1,-\mathbf{k}_1,\mathbf{k}_2) + g_\zeta^{T,(4)}(\mathbf{k}_1,\mathbf{k}_2,-\mathbf{k}_1) + g_\zeta^{T,(4)}(\mathbf{k}_1,\mathbf{k}_2,-\mathbf{k}_2) \quad (6.15)$$

The integration limits above are again infinite.

Equation (6.14) presents the final form of the fourth order brightness correction to be utilized in the remainder of this paper. Note this form couples contributions from sea waves at distinct sea wavenumbers (i.e. (k_x, k_y) and (k'_x, k'_y)) so that emission "interaction" effects among two sea waves are included. The superscript shf will typically be omitted on the kernel functions in what follows for simplicity.

6.4 Reduction to the optical limit

The first examination of Equaton (6.14) to be performed involves its properties for computing interactions among pairs of "long" waves. The SSA4 theory is expected to reduce to a slope expansion of the physical optics theory in this limit, as has been shown previously [78]. Here the analysis is continued to fourth order to provide a complete verification, as well as a test of the SSA4 theory derivation.

6.4.1 "Long-long" wave expansion of SSA4 contributions

Coupling between pairs of "long" waves in Equation (6.14) implies that the region of interest in the integration domain lies near the origin of the four dimensional space. A Taylor expansion of the kernel functions about the origin to fourth order produces seventy terms, most of which vanish or are canceled by other terms in the Taylor expansion. The remaining non-zero fourth-order derivatives are multiplied by polynomial functions in k_x, k_y, k'_x, or k'_y, which allow the integrations over the spectra to be performed and result in double combinations of second order surface

slope moments. The final form for the obtained brightnesses is

$$\begin{aligned}\Delta T_{\zeta}^{(4)} \approx -T_s \Bigg(& \begin{bmatrix} \frac{1}{4}\left(g^{T,(4)}_{\zeta,(k_x)^2,(k'_x)^2} < S_x^2 >^2 + g^{T,(4)}_{\zeta,(k_y)^2,(k'_y)^2} < S_y^2 >^2\right) \\ \frac{1}{2}\left(g^{T,(4)}_{\zeta,(k_x)^2,k'_x,k'_y} + g^{T,(4)}_{\zeta,k_x,k_y,(k'_x)^2}\right) < S_x^2 >< S_x S_y > \end{bmatrix} \\ & + \begin{bmatrix} \frac{1}{4}\left(g^{T,(4)}_{\zeta,(k_x)^2,(k'_y)^2} + g^{T,(4)}_{\zeta,(k_y)^2,(k'_x)^2}\right) < S_x^2 >< S_y^2 > \\ \frac{1}{2}\left(g^{T,(4)}_{\zeta,(k_y)^2,k'_x,k'_y} + g^{T,(4)}_{\zeta,k_x,k_y,(k'_y)^2}\right) < S_x S_y >< S_y^2 > \end{bmatrix} \\ & + \begin{bmatrix} g^{T,(4)}_{\zeta,k_x,k_y,k'_x,k'_y} < S_x S_y >^2 \\ 0 \end{bmatrix} \Bigg) \end{aligned} \tag{6.16}$$

In the vector notation here (identical to [78]), the first row represents the horizontal and vertical polarizations, while the second row is for the third and fourth Stokes' parameters. The additional subscripts on the $g_{\zeta}^{T,(4)}$ quantities refer to the particular fourth order derivative in the Taylor series expansion of the original $g_{\zeta}^{T,(4)}$ function about the origin. Following [78], $< S_x^2 >$ and $< S_y^2 >$ are the large-scale surface slope variances along and perpendicular the radiometer look direction, respectively. This choice implies that the brightness kernels are evaluated with the radiometer azimuthal observation angle set to 0 degrees.

The slope moments in Equation (6.16) can be expressed in terms of up and cross wind slope variances $< S_u^2 >$ and $< S_c^2 >$ as follows:

$$\begin{aligned} < S_x^2 >^2 &= \frac{1}{8}\left[S_1^4 + 4\ S_2^4\ \cos(2\phi_w) + S_3^4\ \cos(4\phi_w)\right] \\ < S_y^2 >^2 &= \frac{1}{8}\left[S_1^4 - 4\ S_2^4\ \cos(2\phi_w) + S_3^4\ \cos(4\phi_w)\right] \\ < S_x S_y >^2 &= \frac{1}{8}\left[S_3^4 - S_3^4\ \cos(4\phi_w)\right] \\ < S_x^2 >< S_y^2 > &= \frac{1}{8}\left[S_4^4 - S_3^4\ \cos(4\phi_w)\right] \\ < S_x^2 >< S_x S_y > &= -\frac{1}{8}\left[2\ S_2^4\ \sin(2\phi_w) + S_3^4\ \sin(4\phi_w)\right] \\ < S_x S_y >< S_y^2 > &= -\frac{1}{8}\left[2\ S_2^4\ \sin(2\phi_w) - S_3^4\ \sin(4\phi_w)\right] \end{aligned} \tag{6.17}$$

where S_1^4, S_2^4, S_3^4, and S_4^4 are defined as:

$$\begin{aligned}
S_1^4 &= 3 < S_u^2 >^2 + 2 < S_u^2 >< S_c^2 > + 3 < S_c^2 >^2 \\
S_2^4 &= < S_u^2 >^2 - < S_c^2 >^2 \\
S_3^4 &= < S_u^2 >^2 - 2 < S_u^2 >< S_c^2 > + < S_c^2 >^2 \\
S_4^4 &= < S_u^2 >^2 + 6 < S_u^2 >< S_c^2 > + < S_c^2 >^2
\end{aligned} \tag{6.18}$$

and it is assumed that the radiometer look direction (i.e. the x axis) makes an angle ϕ_w with respect to the wind direction.

The azimuthal dependence of the fourth order long wave contributions in the optical limit then can be written explicitly as:

$$\begin{aligned}
\Delta T_\zeta^{(4)} &\approx -T_s \left(\begin{bmatrix} \frac{1}{32} S_1^4 \left[g^{T,(4)}_{\zeta,(k_x)^2,(k'_x)^2} + g^{(T,4)}_{\zeta,(k_y)^2,(k'_y)^2} + g^{T,(4)}_{\zeta,(k_x)^2,(k'_y)^2} + g^{T,(4)}_{\zeta,(k_y)^2,(k'_x)^2} \right] \\ 0 \end{bmatrix} \right. \\
&+ \begin{bmatrix} \frac{1}{8} S_2^4 \left[g^{T,(4)}_{\zeta,(k_x)^2,(k'_x)^2} - g^{T,(4)}_{\zeta,(k_y)^2,(k'_y)^2} \right] \cos(2\phi_w) \\ -\frac{1}{8} S_2^4 \left[\left(g^{T,(4)}_{\zeta,(k_x)^2,k'_x,k'_y} + g^{T,(4)}_{\zeta,k_x,k_y,(k'_x)^2} \right) + \left(g^{T,(4)}_{\zeta,(k_y)^2,k'_x,k'_y} + g^{T,(4)}_{\zeta,k_x,k_y,(k'_y)^2} \right) \right] \sin(2\phi_w) \end{bmatrix} \\
&\left. + \begin{bmatrix} \frac{1}{32} S_3^4 \left[g^{T,(4)}_{\zeta,(k_x)^2,(k'_x)^2} + g^{T,(4)}_{\zeta,(k_y)^2,(k'_y)^2} - 3 \left(g^{T,(4)}_{\zeta,(k_x)^2,(k'_y)^2} + g^{T,(4)}_{\zeta,(k_y)^2,(k'_x)^2} \right) \right] \cos(4\phi_w) \\ -\frac{1}{16} S_3^4 \left[\left(g^{T,(4)}_{\zeta,(k_x)^2,k'_x,k'_y} + g^{T,(4)}_{\zeta,k_x,k_y,(k'_x)^2} \right) - \left(g^{T,(4)}_{\zeta,(k_y)^2,k'_x,k'_y} + g^{T,(4)}_{\zeta,k_x,k_y,(k'_y)^2} \right) \right] \sin(4\phi_w) \end{bmatrix} \right) \\
&\approx -T_s \left(S_1^4 \; L^4_{\zeta,0}(\theta_i,\epsilon) + S_2^4 \; L^4_{\zeta,2}(\theta_i,\epsilon) \begin{bmatrix} \cos(2\phi_w) \\ \sin(2\phi_w) \end{bmatrix} \right. \\
&\left. + S_3^4 \; L^4_{\zeta,4}(\theta_i,\epsilon) \begin{bmatrix} \cos(4\phi_w) \\ \sin(4\phi_w) \end{bmatrix} \right)
\end{aligned} \tag{6.19}$$

The fact that $g^{T,(4)}_{\zeta,(k_x)^2,(k'_y)^2} + g^{T,(4)}_{\zeta,(k_y),(k'_x)^2} = 2 g^{T,(4)}_{\zeta,k_x,k_y,k'_x,k'_y}$ is used in obtaining this expression.

The final form for long wave contributions at fourth order (Equation (6.19)) is similar to the forms at second and third order [78], and shows the presence of zeroth, second, and fourth azimuthal harmonics in the emission signatures for a Gaussian

process sea. Surface effects are described only in terms of the long wave slope moments, as is typical in the optical limit, while emission effects are captured entirely by a set of "long wave functions" $L^4_{\zeta,k}$. The latter depend only on the observation angle and the surface permittivity.

Note that the slope factors that scale the long wave functions for distinct emission azmiuthal variations (i.e. $k = 0, 2,$ or 4) are likely to be significantly different for the sea surface: the zeroth harmonic term S^4_1 is a function only of the sum of the along and cross-wind slope variances, while S^4_2 which scales the second azimuthal harmonic involves a product of the sum and difference of the along and cross wind slope variances. The fourth harmonic slope factor S^4_3 finally is the square of the difference between the up and cross wind slope variances. Because differences between the up and cross wind slope variances for the sea surface are typically small, these facts indicate that fourth azimuthal harmonics should generally be much smaller than the corresponding zeroth and second azimuthal harmonics.

6.4.2 Fourth order expansion of physical optics theory

In the physical optics theory, brightness temperatures can be written as a double integration over the slope pdf [78]:

$$T_\zeta \;=\; T_s \int_{-\infty}^{\infty} d\alpha \int_{-\infty}^{\infty} d\beta \; g^{PO}_\zeta(\alpha,\beta)\; f(\alpha,\beta) \tag{6.20}$$

where the PO kernel function g^{PO}_ζ is described in [78]. Using a Taylor expansion of the PO kernel $g^{PO}_\zeta(\alpha,\beta)$ about the origin and considering only the fourth order terms produces:

$$\Delta T^{PO,(4)}_\zeta \;\approx\; -T_s \left[\begin{array}{c} \frac{1}{24}\left(g^{PO}_{\zeta,(\alpha)^4} < S^4_x > + g^{PO}_{\zeta,(\beta)^4} < S^4_y > \right) + \frac{1}{4}\left(g^{PO}_{\zeta,(\alpha)^2,(\beta)^2} < S^2_x \; S^2_y > \right) \\ \frac{1}{6}\left(g^{PO}_{\zeta,(\alpha)^3,\beta} < S^3_x \; S_y > + g^{PO}_{\zeta,\alpha,(\beta)^3} < S_x \; S^3_y > \right) \end{array} \right] \tag{6.21}$$

Sea surface fourth order slope moments can be expressed in terms of up and cross wind moments $< S_u^4 >$, $< S_u^2\ S_c^2 >$ and $< S_c^4 >$ as follows:

$$\begin{aligned}
< S_x^4 > &= \frac{3}{8}\left[< S_u^4 > +2\ < S_u^2\ S_c^2 > + < S_c^4 >\right] \\
&\quad +\frac{1}{2}\left[< S_u^4 > - < S_c^4 >\right]\cos 2\phi_w \\
&\quad +\frac{1}{8}\left[< S_u^4 > -6\ < S_u^2\ S_c^2 > + < S_c^4 >\right]\cos 4\phi_w \qquad (6.22) \\
< S_x^3\ S_y > &= -\frac{1}{4}\left[< S_u^4 > - < S_c^4 >\right]\sin 2\phi_w \\
&\quad -\frac{1}{8}\left[< S_u^4 > -6 < S_u^2 S_c^2 > + < S_c^4 >\right]\sin 4\phi_w \qquad (6.23) \\
< S_x^2\ S_y^2 > &= \frac{1}{8}\left[< S_u^4 > +2 < S_u^2\ S_c^2 > + < S_c^4 >\right] \\
&\quad -\frac{1}{8}\left[< S_u^4 > -6 < S_u^2\ S_c^2 > + < S_c^4 >\right]\cos 4\phi_w \qquad (6.24) \\
< S_x\ S_y^3 > &= -\frac{1}{4}\left[< S_u^4 > - < S_c^4 >\right]\sin 2\phi_w \\
&\quad +\frac{1}{8}\left[< S_u^4 > -6 < S_u^2\ S_c^2 > + < S_c^4 >\right]\sin 4\phi_w \qquad (6.25) \\
< S_x^4 > &= \frac{3}{8}\left[< S_u^4 > +2\ < S_u^2\ S_c^2 > + < S_c^4 >\right] \\
&\quad -\frac{1}{2}\left[< S_u^4 > - < S_c^4 >\right]\cos 2\phi_w \\
&\quad +\frac{1}{8}\left[< S_u^4 > -6\ < S_u^2\ S_c^2 > + < S_c^4 >\right]\cos 4\phi_w \qquad (6.26)
\end{aligned}$$

Noting that for a Gaussian process, $< S_u^4 >= 3\ < S_u^2 >$, $< S_c^4 >= 3\ < S_c^2 >$ and $< S_u^2\ S_c^2 >=< S_u^2 >< S_c^2 >$, the following form for the PO theory is obtained:

$$\begin{aligned}
\Delta T_\zeta^{PO,(4)} \approx -T_s \Bigg(& \begin{bmatrix} \frac{1}{64}S_1^4\left[g^{PO}_{\zeta,(\alpha)^4} + g^{PO}_{\zeta,(\beta)^4} + 2\ g^{PO}_{\zeta,(\alpha)^2,(\beta)^2}\right] \\ 0 \end{bmatrix} \\
& + \begin{bmatrix} \frac{1}{16}S_2^4\left[g^{PO}_{\zeta,(\alpha)^4} - g^{PO}_{\zeta,(\beta)^4}\right]\cos(2\phi_w) \\ -\frac{1}{8}S_2^4\left[g^{PO}_{\zeta,(\alpha)^3,\beta} + g^{PO}_{\zeta,\alpha,(\beta)^3}\right]\sin(2\phi_w) \end{bmatrix} \\
& + \begin{bmatrix} \frac{1}{64}S_3^4\left[g^{PO}_{\zeta,(\alpha)^4} + g^{PO}_{\zeta,(\beta)^4} - 6\ g^{PO}_{\zeta,(\alpha)^2,(\beta)^2}\right]\cos(4\phi_w) \\ -\frac{1}{16}S_3^4\left[g^{PO}_{\zeta,(\alpha)^3,\beta} - g^{PO}_{\zeta,\alpha,(\beta)^3}\right]\sin(4\phi_w) \end{bmatrix} \Bigg)
\end{aligned}$$

$$\approx \quad -T_s \left(S_1^4 \; L_{\zeta,0}^{PO,4}(\theta_i, \epsilon) + S_2^4 \; L_{\zeta,2}^{PO,4}(\theta_i, \epsilon) \begin{bmatrix} \cos(2\phi_w) \\ \sin(2\phi_w) \end{bmatrix} \right.$$
$$\left. + S_3^4 \; L_{\zeta,4}^{PO,4}(\theta_i, \epsilon) \begin{bmatrix} \cos(4\phi_w) \\ \sin(4\phi_w) \end{bmatrix} \right) \tag{6.27}$$

The final form obtained is identical to Equation (6.19), except for the use of $L_{\zeta,k}^{PO,4}$ as opposed to $L_{\zeta,k}^4$. Comparisons between the theories can therefore be performed solely in terms of the long wave functions themselves.

6.4.3 Comparison of SSA4 and PO theories

A comparison of the long wave functions $L_{\zeta,k}^4$ and $L_{\zeta,k}^{PO,4}$, $\{k = 0, 2, 4\}$, for sea water permitivity $(29.04 + i35.55)$ and in h, v, and U polarizations is provided in Figure 6.1. Both theories predict the long wave function for the fourth Stokes' parameter to vanish. Long wave functions from the two theories are in agreement, indicating that the SSA model continues to match PO to fourth order.

The long wave functions illustrated show similar amplitudes across azimuthal harmonics as well as polarizations, with all tending to show increasing amplitudes as the polar observation angle is increased. Second azimuthal long wave functions tend to have slightly larger amplitudes. Again these functions are scaled by the appropriate slope moments when computing brightness contributions; as discussed previously, the expected size of these slope moments results in small fourth azimuthal harmonic contributions as compared to the zeroth and second azimuthal harmonics.

6.5 "Interaction" effects among long and short sea waves

While a direct numerical computation of the four-fold integration of Equation (6.14) is possible, such computations yield little insight into the emission physics captured by the SSA4 model. Because all limits on the integrations of Equation

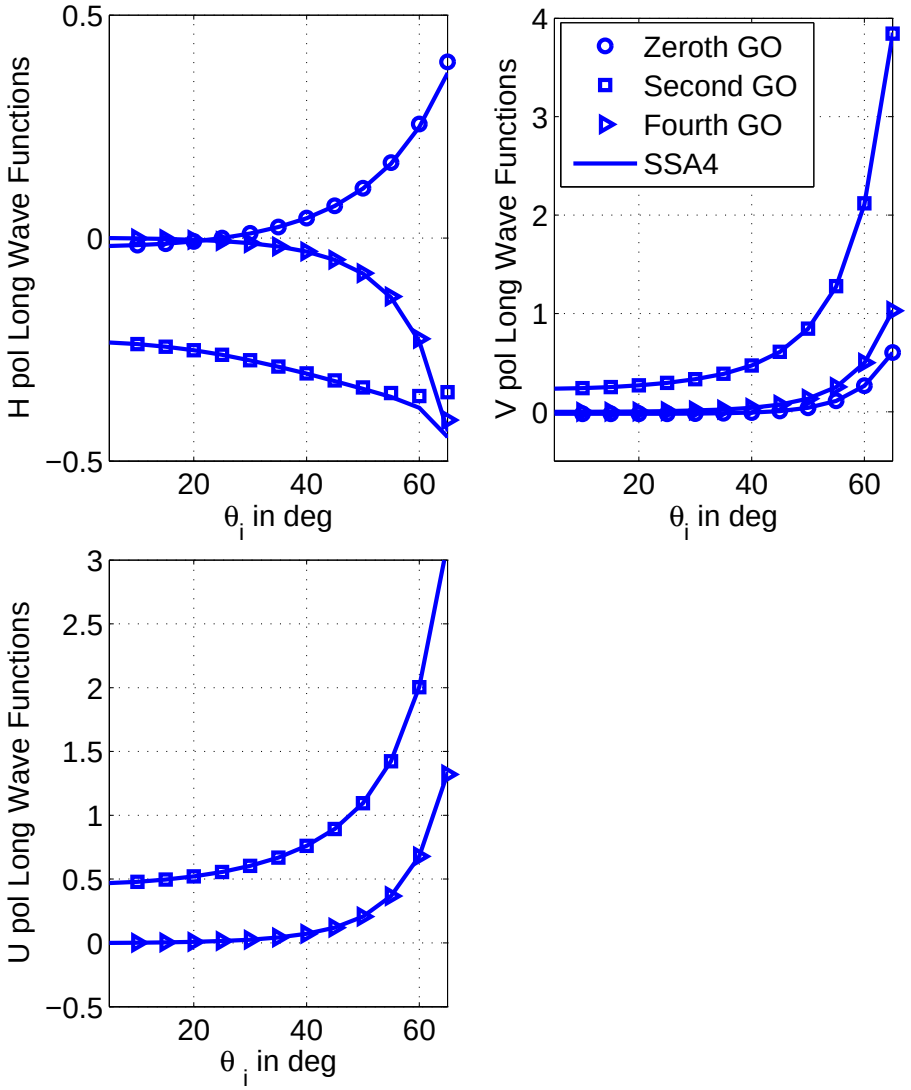

Figure 6.1: Comparison of the long wave functions $L^4_{\zeta,k}$ and $L^{PO,4}_{\zeta,k}$, $\{k = 0, 2, 4\}$, for sea water permitivity $(29.04 + i35.55)$ in h, v and U polarizations

(6.14) are infinite, such a computation includes interactions among all possible sea waves, including "long-long" (PO limit), "long-short", and "short-short". However the focus of the current paper is an examination of "long-short" interactions in order to assess a description of these interactions as "tilt" effects (as in the two-scale theory.) The process begins in Section 6.5.1 by identifying the portion of the integration region relevant for this purpose, and "critical phenomenon" behaviors of the SSA4 kernels are discussed in Section 6.5.2. A numerical integration scheme that is applicable to computation of the four-fold integral in this portion of the integration domain in then developed in Section 6.5.3. Description of an approximation to simplify the computations then follows in Section 6.6, along with interpretation of the results of this expansion.

6.5.1 Symmetrization of the SSA4 integration

To allow clear identification of "long-short" wave interactions in the four-dimensional integration domain, symmetry properties of the integrands are first applied to reduce this domain. Because the surface spectra involved in the integration by definition must be symmetric under the negation of both arguments, and also due to the "interchange" symmetric form (i.e. $(k_x, k_y) \leftrightarrow (k'_x, k'_y)$) of the product of two spectra involved, it is possible to consider 8 symmetric regions in the integrand of Equation (6.14). Using a symmetrization process based on these properties, a symmetrized kernel can be defined as

$$g_\zeta^{T,(4),sym}(k_x, k_y, k'_x, k'_y) = \Big\{ g_\zeta^{T,(4),shf}(k_x, k_y, k'_x, k'_y)$$
$$+ g_\zeta^{T,(4),shf}(-k_x, -k_y, k'_x, k'_y) + g_\zeta^{T,(4),shf}(k_x, k_y, -k'_x, -k'_y)$$
$$+ g_\zeta^{T,(4),shf}(-k_x, -k_y, -k'_x, -k'_y) + g_\zeta^{T,(4),shf}(k'_x, k'_y, k_x, k_y)$$

$$+ g_\zeta^{T,(4),shf}(-k'_x,-k'_y,k_x,k_y) + g_\zeta^{T,(4),shf}(k'_x,k'_y,-k_x,-k_y) \\ + g_\zeta^{T,(4),shf}(-k'_x,-k'_y,-k_x,-k_y)\Big\} \tag{6.28}$$

Under this symmetrization, the integration domain can be reduced to the region

$$k'_x > k_x > 0 \tag{6.29}$$

as illustrated in Figure 6.2(a) for $k_x = k_c$. If the coordinates (k'_x, k'_y) are now chosen to represent a "short wave" and (k_x, k_y) to represent a "long" wave, the portions of the domain corresponding to long-short wave interactions are as illustrated in Figure 6.2(b), where k_c refers to the maximum wavenumber of the long wave region. The integration regions in the long and short wave planes are approximated as annular regions in these two planes for convenience. The quantity k_c is chosen to be much less than the electromagnetic wavenumber to ensure only "long" waves are considered in the (k_x, k_y) plane, while the inner radius of the annulus in the (k'_x, k'_y) plane is chosen to be $>> k_c$ to ensure that "short" waves are modeled here. For the purposes of the expansion to be introduced later, "short" actually refers simply to short relative to the shortest "long" sea wave, rather than short relative to the electromagnetic wavelength.

In polar coordinates, Equation (6.14) can now be expressed on the defined integration domain as two coupled double integrals:

$$\begin{aligned} \Delta T_\zeta^{(4)} &= -T_s \int k_\rho \, dk_\rho \int d\phi \; W(k_\rho,\phi) \; \hat{g}(k_\rho,\phi) \\ \hat{g}(k_\rho,\phi) &= \int k_{\rho'} \, dk_{\rho'} \int d\phi' \; W(k_{\rho'},\phi') \; g(k_\rho,\phi,k_{\rho'},\phi') \end{aligned} \tag{6.30}$$

where the superscripts on the symmetrized kernel function are dropped; this kernel is to be used in all following discussions. The outer integration of Equation (6.30)

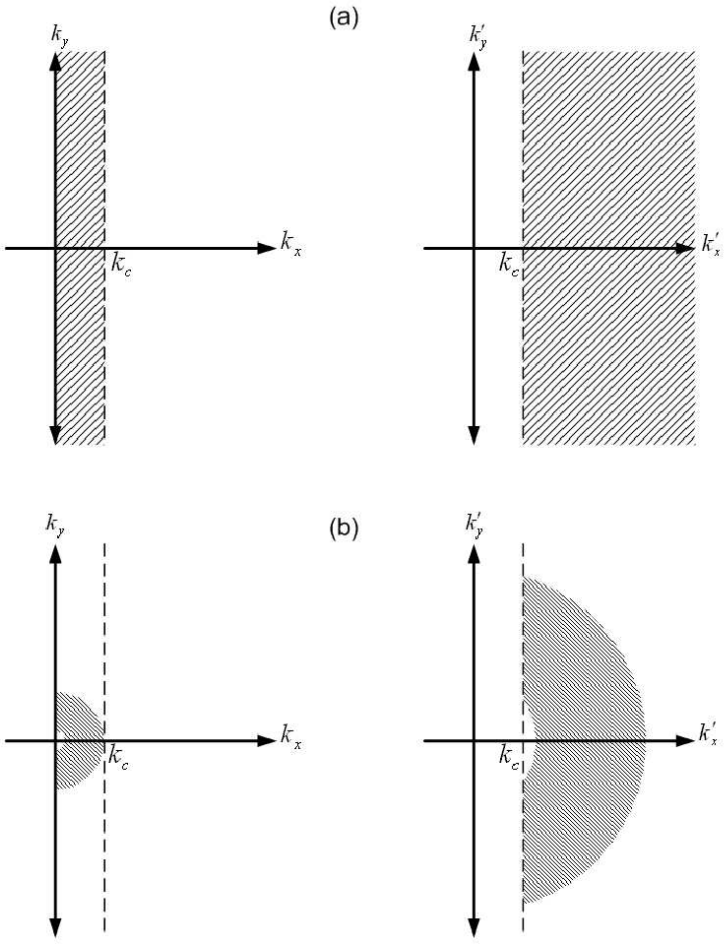

Figure 6.2: Integration regions (a) Following symmetrization of Equation (6.14) (b) Reduced integration region for modeling "long-short" sea wave interactions

is evaluated on the long wave plane, while the inner integration is evaluated on the short wave plane.

6.5.2 Critical phenomena in SSA4 kernels

It is well known that both the second and third order SSA emission kernels exhibit rapid variations (singular-like) behaviors on circular regions in their integration domains. These behaviors are called "critical phenomena" in the literature, and their presence requires numerical integrations involving the SSA kernels to be performed carefully. Because such variations are also likely in the fourth order SSA kernel, a study of the SSA4 kernel functions was performed to identify critical phenomenon behaviors and their locations in the domain of interest. This analysis showed that for a fixed point in the long wave plane, rapid variations in the kernels occurred in the vicinity of six distinct circles in the short wave plane. Tests varying the long wave point considered showed that these circles can be expressed in terms of (k_x, k_y) and (k'_x, k'_y) as:

$$\begin{aligned} (k'_x \pm k_{xi})^2 + (k'_y)^2 &= (k_o)^2 \\ (k'_x + k_x \pm k_{xi})^2 + (k'_y + k_y)^2 &= (k_o)^2 \\ (k'_x - k_x \pm k_{xi})^2 + (k'_y - k_y)^2 &= (k_o)^2 \end{aligned} \tag{6.31}$$

Here k_o is the electromagnetic wavenumber and $k_{xi} = k_o \sin(\theta_i)$. The first pair of circles do not depend on the long wave coordinates, and can be considered "fixed singular circles" as the long wave coordinates are varied. These are the same singular locations obtained in the second order SSA emission kernels. The other four circles involve the long wave coordinates (i.e. they move inside the short wave plane as the point in the long wave plane moves) and are called "moving singular circles".

Typically in the following presentations, the short wave plane will be discussed after fixing a reference point in the long wave plane.

An illustration of typical critical phenomenon behaviors of the SSA4 kernel functions is provided in Figures 6.3, 6.4, and 6.5, using a radiometer polar observation angle of 55 degrees and a medium relative permittivity of $\epsilon = 29.04 + i35.55$.

Plot (a) of Figure 6.3 illustrates a particular long wave point given as $(k_\rho, \phi) = (\frac{k_o}{4}, \frac{\pi}{6})$, and includes an illustration of the typical integration region boundaries (dashed lines) considered in long-short wave computations; the cutoff wavenumber (largest value of the k_ρ) is specified as $k_c = \frac{k_o}{2}$ here. These wavenumber choices are larger than would usually be used in order to emphasize distances between the multiple circles in the short-wave plane.

Plot (b) of Figure 6.3 illustrates the short wave plane, again with typical boundaries of the integration region marked as dashed lines. Critical phenomenon circles are also included in the plot. A line segment (thicker line) is also included in Figure 6.3; values of the kernel functions are examined along this line in Figures 6.4 and 6.5. Intersections of the line considered with the critical phenomenon circles are numbered from (1) to (3).

Figure 6.4 plots SSA4 kernel functions for all four polarimetric quantities (here VV refers to the fourth Stokes' parameter) on the line segment of Figure 6.3(b). Figure 6.5 zooms in on these functions near the intersection points, and normalizes the curves to their maximum in Figure 6.4. The results show the rapid variations of the kernels to be confined to small regions near the circular intersections; outside these regions the SSA4 kernels are relatively smooth. Note unlike the second order SSA kernels, the fourth order critical phenomenon behaviors typically show both large positive

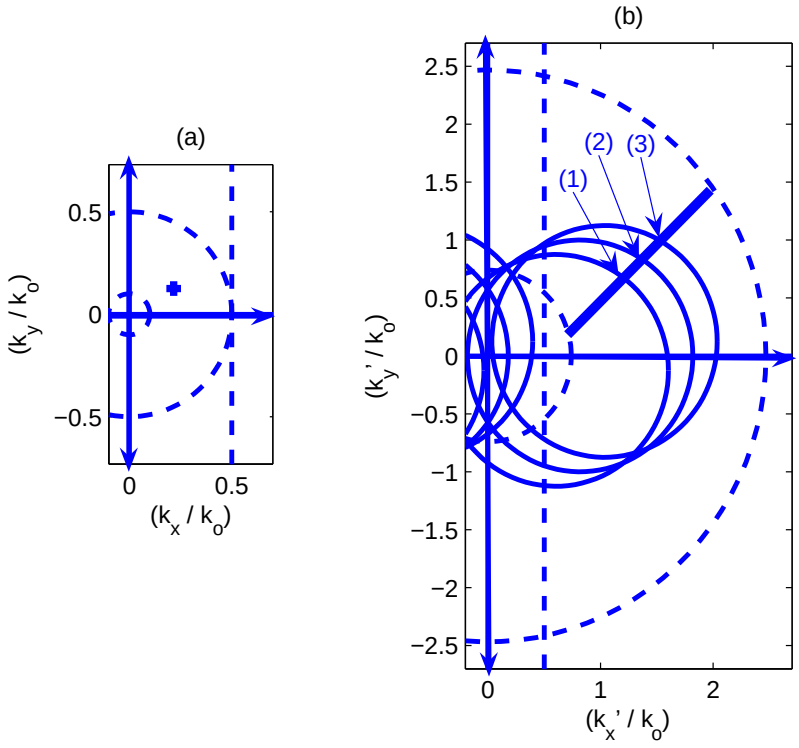

Figure 6.3: Illustration of critical phenomenon effects: (a) Long wave domain and a reference point $(k_\rho, \phi) = (\frac{k_o}{4}, \frac{\pi}{6})$, (b) Short wave domain, including domain boundaries (dashed), critical phenomenon circles (solid), and a line segment intersecting the critical phenomenon circles

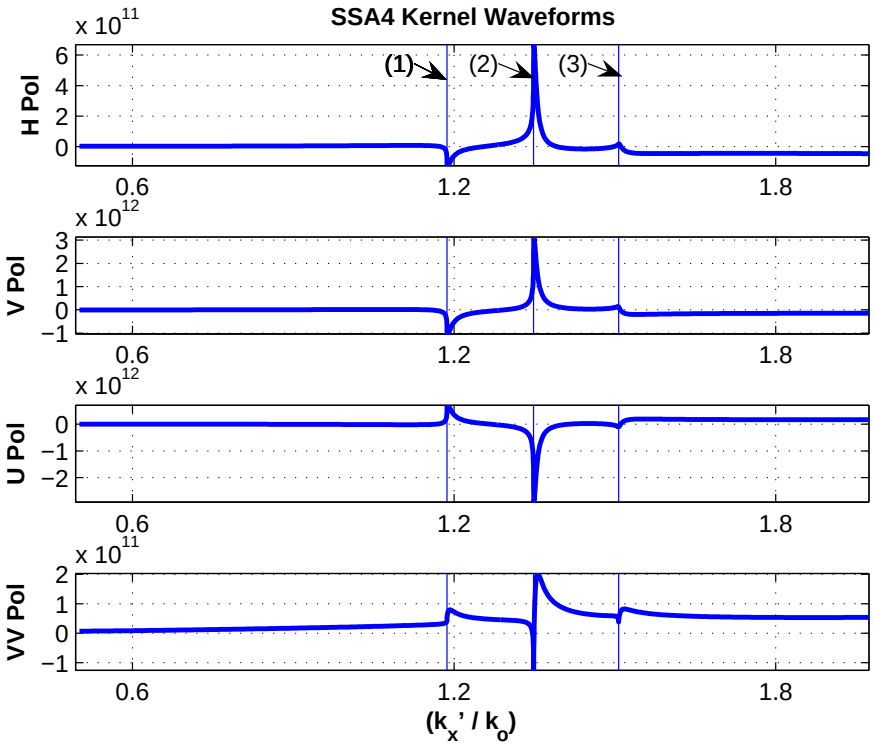

Figure 6.4: SSA4 kernel waveforms plotted on the line segment of Figure 6.3.

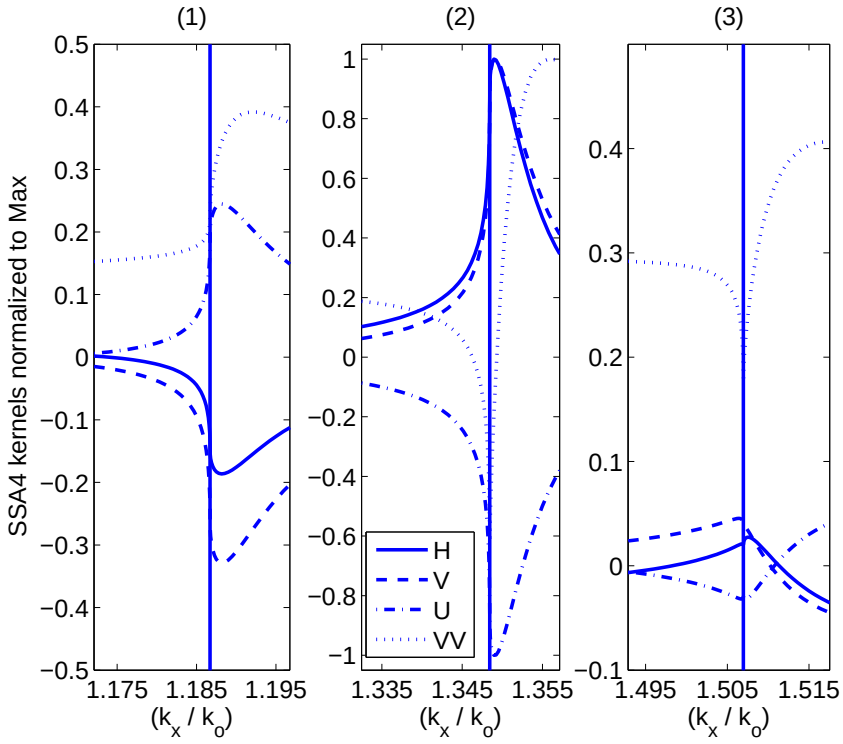

Figure 6.5: SSA4 kernel waveforms normalized to their maximum values in Figure 6.3, at the intersection points

and negative values (as in the vertical polarization kernel near point (1) compared to point (2) in Figure 6.5.) Therefore the critical phenomenon contributions tend to cancel out when the integration over the line segment is performed. Notice also that as the long-wave point considered is varied from the $(k_\rho, \phi) = (\frac{k_o}{4}, \frac{\pi}{6})$ value used to Figures 6.3-6.5, the locations of the intersections (1) to (3) vary. In particular, as the long wave is made longer (i.e. closer to the origin of the long wave plane), the intersections (1) and (3) move closer to the point (2), resulting in large positive and negative values of the kernel functions both being obtained near the point (2). These rapid variations make numerical computation of long-short wave interactions difficult. The next section presents a numerical integration method suited for these computations.

6.5.3 Numerical integration of long-short wave interaction contributions

Numerical integration of the SSA4 kernels can be simplified by dividing the full domain integration into piece-wise integrations between intersections with the critical phenomenon circles. For this purpose, a notation for the boundaries of these piece-wise integrations in the $k_{\rho'}$ and ϕ' variables of the short wave plane is introduced.

The set of $k_{\rho'}$ boundaries are defined as $k_{\rho,l}$ with $l = 0, 1, 2, \cdots, l_{max}$, with $k_{\rho,0}$ marking the lower boundary of the entire $k_{\rho'}$ integration and $k_{\rho,l_{max}}$ marking the outer boundary. Similarly, for a given value of l, integration boundaries in the ϕ' variable are written as the set $\phi_{l,m}$ for $m = 0, 1, 2, \cdots, m_{max(l)}$. Here $\phi_{l,0}$ and $\phi_{l,m_{max(l)}}$ mark the lower and upper boundaries of the ϕ' integration. Intermediate values of $\phi_{l,m}$ mark intersections with the critical phenomenon circles, as well as "buffer" points surrounding these intersections by a specified separation in ϕ'. Because the

ϕ' integration is performed first, intermediate values of $k_{\rho,l}$ were chosen based on intersections with the critical phenomenon circles for $\phi' = 0$, again with "buffer" points surrounding these boundaries included in the set of points.

Using these definitions, the short wave integral of Equation (6.30) can be rewritten as:

$$\hat{g}(k_\rho, \phi) = \sum_{l=1}^{l_{max}} \int_{k_{\rho,l-1}}^{k_{\rho,l}} k_{\rho'}\, dk_{\rho'} \sum_{m=1}^{m_{max(l)}} \int_{\phi_{m-1}}^{\phi_m} d\phi'\, W(k_{\rho'}, \phi')\, g(k_\rho, \phi, k_{\rho'}, \phi') \qquad (6.32)$$

Note it is also possible to reverse the order of these integrations by redefining the piece-wise limits first in terms of $k_{\rho'}$ then in terms of ϕ'; both approaches were evaluated and found to perform similarly.

The piece-wise integrations of Equation (6.32) now involve relatively smooth functions because the regions of rapid kernel variations are automatically resolved. Accordingly, a standard Gauss-Legendre quadrature is applied both in ϕ' and in $k_{\rho'}$ for computation of each of the piece-wise two-fold integrals.

Given this process for evaluating the short-wave plane integration, it remains to evaluate the integration over the long-wave plane. This integration is less numerically challenging because the short-wave integration smooths out kernel function variations. Therefore a standard Gauss-Legendre quadrature is applied for the k_ρ and ϕ integrations without further treatment.

Numerous tests of this approach were performed to ensure that a sufficient number of quadrature points, etc. was utilized to obtain convergence of model predictions. Results using the method described showed that convergence was obtained with use of only a moderate number (order to 100) quadrature points within each piece-wise integration. Because even a single evaluation of the symmetrized SSA4 kernel function is a relatively expensive operation, codes were developed to compute and output

a table of these kernels over the integration domain. These tables then allow more efficient computations of fourth order emission predictions as properties of the sea spectrum (for example, wind speed) are varied. Results from the numerical integration of long-short wave contributions will be discussed in Section 6.7, and compared with the approximation of long-short wave contributions defined in the next Section.

6.6 Approximations for long-short wave contributions

6.6.1 Long-wave expansion of SSA4 short-wave integrations

Due to the rapidly varying nature of the SSA4 kernel functions and the presence of the "moving singular circles" in the short wave plane, extreme care must be exercised when attempting to expand the SSA4 kernel functions in terms of long wave parameters. To address this issue, expansion of the result of the short wave integration is first considered before proceeding to expansion of the SSA4 kernel functions themselves.

Based on the slope expansion implicit in the SSA4 theory, it is to be expected that an expansion of the $\hat{g}(k_x, k_y)$ quantity in terms of k_x and k_y should be applicable near the origin (i.e. very long long waves); the return to rectangular wavenumber coordinates is made for convenience in what follows. It is also to be expected that the zeroth and first order terms in such an expansion will vanish, leaving

$$\hat{g}(k_x, k_y) \approx \frac{k_x^2}{2}\, \hat{g}_{k_x^2}(0,0) + \frac{k_y^2}{2}\, \hat{g}_{k_y^2}(0,0) \tag{6.33}$$

The subscripts k_x^2 and k_y^2 again represent second partial derivatives with respect to k_x and k_y, and the cross $k_x k_y$ term is found to vanish when it is assumed that the radiometer observes along the x axis of the coordinate system. With this expansion,

the fourth order brightness contribution reduces to

$$\Delta T^{(4)} \approx \frac{-T_s}{2}\left[< S_x^2 > \hat{g}_{k_x^2}(0,0) + < S_y^2 > \hat{g}_{k_y^2}(0,0)\right] \tag{6.34}$$

where $< S_x^2 >$ and $< S_y^2 >$ are the along- and cross-look slope variances of the long waves considered. This form is attractive for evaluating long-short wave contributions due to its efficiency when compared to the four-fold integration. Note this expansion is performed following the integration over the short-wave plane, so that the derivatives considered depend on the short wave spectrum.

Numerical tests using a centered difference algorithm for the Taylor expansion of $\hat{g}(k_x, k_y)$ near the origin confirmed that the zeroth and first order terms vanish. The remaining second order derivatives were computed as

$$\hat{g}_{k_x^2}(0,0) = \lim_{h\to 0} \frac{2\ \hat{g}(h,0)}{h^2}, \qquad \hat{g}_{k_y^2}(0,0) = \lim_{h\to 0} \frac{2\ \hat{g}(0,h)}{h^2} \tag{6.35}$$

due to the symmetry properties of $\hat{g}(k_x, k_y)$. The k_x^2 derivative can be more explicitly written as

$$\hat{g}_{k_x^2}(0,0) = \lim_{h\to 0} \int k_{\rho'}\ dk_{\rho'} \int d\phi'\ W(k_{\rho'}, \phi')\ \frac{2\ g(h,0,k_{\rho'},\phi')}{h^2} \tag{6.36}$$

Expressions for k_y^2 derivative are almost identical, and therefore not discussed specifically in what follows. Results from this approach will not be considered further, but were used in verifying the accuracy of the expansion discussed in the next paragraph.

6.6.2 Long wave expansion of SSA4 kernel functions

A more useful and efficient form of the long-short wave expansion can be obtained by moving the limit operator inside the integrals, so that derivatives of the SSA4 kernels, rather than the result of the short wave plane integration, are involved. The

result of such an interchange for the k_x^2 term is

$$\hat{g}_{k_x^2}(0,0) \approx \int k_{\rho'}\, dk_{\rho'} \int d\phi'\, W(k_{\rho'}, \phi')\, g_{k_x^2}(0,0,k_{\rho'},\phi') \tag{6.37}$$

where $g_{k_x^2}(0,0,k_{\rho'},\phi')$ represents the SSA4 kernel derivative $\lim_{h\to 0} \frac{2g(h,0,k_{\rho'},\phi')}{h^2}$.

Equation (6.37) along with Equation (6.34) shows $g_{k_x^2}(0,0,k_{\rho'},\phi')$ (and a similar $g_{k_y^2}(0,0,k_{\rho'},\phi')$ term) to be spectrum independent "weighting functions" that describe contributions of a particular short wave $(k_{\rho'},\phi')$ to the total long-short wave brightness when multiplied by the long wave slope variance. This form approximates the tilting process, and is therefore relevant for use in comparisons with the two-scale theory. In such a comparison, the original two-scale model equations can be expanded into a similar series in long-wave slopes; results show the zeroth order term to be that of a flat surface, the second order term to be identical to the second order small slope theory, and the fourth order term to be identical to Equation (6.34) except that two-scale model derivatives $g_{k_x^2}^{two}(0,0,k_{\rho'},\phi')$ are involved as opposed to those from the SSA4. Therefore sea spectrum independent comparisons of the two theories and their predictions of long-short wave tilt effects can be performed in terms of the kernel function derivatives alone.

Because the SSA4 kernels are not truly singular, the required expansion of the SSA4 kernels is possible, but remains numerically difficult due to critical phenomenon effects. The h dependence of the $k_{\rho'}$ and ϕ' grids in the short wave plane further complicates this process. Although this dependence should vanish identically as $h \to 0$, the effects of finite h values in finite precision computations remain observable particularly near the critical phenomenon regions. For this reason, the weighting functions to be illustrated should be considered only "semi-stable" representations, with some degree of h dependence remaining. However it is again emphasized that the

extreme SSA4 kernel function values obtained near the critical phenomenon regions largely cancel out when integrated, so that the effect of this "semi-stable" nature is not significant when computing final fourth order brightnesses. Evidence supporting this statement will be provided in Section 6.7 through comparisons with numerically integrated long-short wave contributions.

Further simplification of the final fourth order brightness in this approximation can be obtained by substituting an assumed form for the sea spectrum:

$$W(k_\rho, \phi) = \frac{1}{k_\rho^4} \left[C_0(k_\rho) + C_2(k_\rho) \cos\left(2\left(\phi - \phi_w\right)\right) \right] \tag{6.38}$$

with ϕ_w representing the wind direction; it is assumed that the radiometer look direction is along x in what follows (i.e. the azimuthal angle of the radiometer observation direction is zero). The fourth order brightness is then

$$\begin{aligned} \Delta T_\zeta^{(4)} \approx \frac{-T_s}{2} \Bigg(& < S_x^2 > \int dk_{\rho'} \begin{bmatrix} C_0(k_{\rho'}) \\ C_2(k_{\rho'}) \end{bmatrix}^T \int d\phi' \begin{bmatrix} 1 \\ \cos(2\left(\phi' - \phi_w\right)) \end{bmatrix} \frac{g_{k_x^2}(0, 0, k_{\rho'}, \phi')}{k_{\rho'}^3} \\ & + < S_y^2 > \int dk_{\rho'} \begin{bmatrix} C_0(k_{\rho'}) \\ C_2(k_{\rho'}) \end{bmatrix}^T \int d\phi' \begin{bmatrix} 1 \\ \cos(2\left(\phi' - \phi_w\right)) \end{bmatrix} \frac{g_{k_y^2}(0, 0, k_{\rho'}, \phi')}{k_{\rho'}^3} \Bigg) \end{aligned} \tag{6.39}$$

This expression is valid in general, but, in order to extract the azimuthal harmonics in wind direction, it is more convenient to expand the original multiplication of long and short wave spectra into terms involving $[1, \cos(2\phi_w), \sin(2\phi_w), \cos(4\phi_w), \sin(4\phi_w)]$ as follows:

$$\begin{aligned} k_\rho^4 k_{\rho'}^4 W(k_\rho, \phi) W(k_{\rho'}, \phi') = & \Bigg[\Big(C_0(k_\rho) C_0(k_{\rho'}) + \frac{1}{2} C_2(k_\rho) C_2(k_{\rho'}) \cos\left(2\left(\phi - \phi'\right)\right) \Big) \\ & + \Big(C_0(k_\rho) C_2(k_{\rho'}) \cos(2\phi') + C_2(k_\rho) C_0(k_{\rho'}) \cos(2\phi) \Big) \cos(2\phi_w) \\ & + \Big(C_0(k_\rho) C_2(k_{\rho'}) \sin(2\phi') + C_2(k_\rho) C_0(k_{\rho'}) \sin(2\phi) \Big) \sin(2\phi_w) \end{aligned}$$

$$+\left(\frac{1}{2}C_2(k_\rho)C_2(k_{\rho'})\cos(2\left(\phi+\phi'\right))\right)\cos(4\phi_w)$$
$$+\left(\frac{1}{2}C_2(k_\rho)C_2(k_{\rho'})\sin(2\left(\phi+\phi'\right))\right)\sin(4\phi_w)\Big] \tag{6.40}$$

Use of this representation along with expansion of the sinusoidal terms in $\phi+\phi'$ and $\phi-\phi'$ allows a combination of terms to be defined for determining a specific azimuthal harmonic of the observed brightnesses.

The result of the ϕ' integration of individual terms in this combination is defined through

$$w^{(1,c,s)}_{\zeta,(x,y)}(k_{\rho'}) = \int d\phi' \begin{bmatrix} 1 \\ \cos(2\phi') \\ \sin(2\phi') \end{bmatrix} \frac{g_{\zeta,k^2_{(x,y)}}(0,0,k_{\rho'},\phi')}{k^3_{\rho'}} \tag{6.41}$$

and denoted as a "weighting function" in what follows. It is these weighting functions that can be compared with similar weighting functions from the expanded two-scale theory. Here the subscript ζ represents the polarization, the subscripts (x,y) represent either the second order x or y derivative, and the superscripts $(1,c,s)$ represent use of either constant, $\cos(2\phi')$, or $\sin(2\phi')$ factors in the ϕ' integration.

Finally, harmonics of the fourth order brightness contribution are written using the weighting functions defined above as

$$\begin{aligned} H^{(0)}_\zeta &= -\frac{\pi}{4}T_s\Big[I_0\int dk_{\rho'}C_0(k_{\rho'})\left(w^{(1)}_{\zeta,(x)}(k_{\rho'})+w^{(1)}_{\zeta,(y)}(k_{\rho'})\right) \\ &\qquad +\frac{I_2}{4}\int dk_{\rho'}C_2(k_{\rho'})\left(w^{(c)}_{\zeta,(x)}(k_{\rho'})-w^{(c)}_{\zeta,(y)}(k_{\rho'})\right)\Big] \\ H^{(2)}_\zeta &= -\frac{\pi}{4}T_s\Big[I_0\int dk_{\rho'}C_2(k_{\rho'})\left(w^{(c)}_{\zeta,(x)}(k_{\rho'})+w^{(c)}_{\zeta,(y)}(k_{\rho'})\right) \\ &\qquad +\frac{I_2}{2}\int dk_{\rho'}C_0(k_{\rho'})\left(w^{(1)}_{\zeta,(x)}(k_{\rho'})-w^{(1)}_{\zeta,(y)}(k_{\rho'})\right)\Big] \end{aligned} \tag{6.42}$$

which applies to the linearly polarized channels. Here $H^{(0)}$ represents the zeroth harmonic, and $H^{(2)}$ represents the second azimuthal harmonic; fourth harmonics are

small and not considered further in what follows. For the third and fourth Stokes' parameters, the zeroth harmonic vanishes and the second harmonic is obtained through

$$H_{\zeta}^{(2)} = -\frac{\pi}{4} T_s I_0 \int dk_{\rho'} C_2(k_{\rho'}) \left(w_{\zeta,(x)}^{(s)}(k_{\rho'}) + w_{\zeta,(y)}^{(s)}(k_{\rho'}) \right) \tag{6.43}$$

In the above equations, the terms $I_{(0,2)}$ are defined through

$$I_{(0,2)} = \int dk_{\rho} \frac{C_{(0,2)}(k_{\rho})}{k_{\rho}} \tag{6.44}$$

with the integration evaluated on long wave domain.

The preceeding equations show that the expanded SSA4 model expresses "long-short" interaction effects in terms of an integration of a combination of the weighting functions defined in equation (6.41) multiplied by the short wave curvature spectrum. The result of this integration is multiplied by a function resembling the long wave slope variance. Therefore the weighting functions provide sea-surface-independent insight into the relative contributions of particular short scale sea waves to the total observed "long-short" interaction brightnesses.

6.6.3 Comparison of SSA4 and Two-scale weighting functions

Figures 6.6 and 6.7 present comparison of the SSA4 and two-scale "semi-stable" weighting functions for radiometer polar observation angle 55 degrees and $\epsilon = 29.04 + i35.55$. Plots of the zeroth azimuthal harmonic weighting function $w_{h,(x)}^{(1)}(k_{\rho'})$ (horizontal polarization) in Figure 6.6 include additional plots that provide higher resolution near the critical phenomenon regions marked as (1) through (3), while Figure 6.7 illustrates the zeroth azimuthal harmonic weighting function for vertical polarization and the second azimuthal harmonic weighting functions for third and fourth Stokes'

parameters without further detail. The figures illustrate weighting function magnitudes, and also include plots of the signs (shifted by 5 units for the multiple curves for convenience).

The weighting functions in Figure 6.6 are very different near the critical phenomena regions, with the SSA4 kernels showing much larger variations than two scale; note the rapid nulling behavior observed in both SSA4 and two-scale weighting functions results on sign changes of the weighting functions due to the use of a logarithmic vertical axis. However such rapid variations are not expected to make significant brightness contributions due to cancellation effects discussed previously.

Overall the comparison of the SSA4 and two-scale weighting functions shows the two to have similar properties, both in magnitude and signs, particularly in regions far from the critical phenomenon boundaries. However even in such regions, differences between the two models are observed, so that a complete agreement between the two theories is not achieved. Because development of a simple description of the differences between the two weighting functions is not easily obtained, more concrete examples of comparisons with two-scale theory predictions are provided in the next Section.

6.7 Comparisons of numerically integrated, expanded, and two-scale long-short wave brightness contributions

Numerically integrated (Section 6.5.3), expanded (Section 6.6.2), and two-scale model predictions of the azimuthal harmonics of the fourth order long-short wave brightness contributions are compared in this Section. The radiometer frequency is assumed to be 19.35GHz (wavelength $\lambda_o = 1.55$cm, wavenumber $k_o = 405$ rads/m) and a surface relative permitivity $\epsilon = 29.04 + i35.55$ is used. The sea spectrum

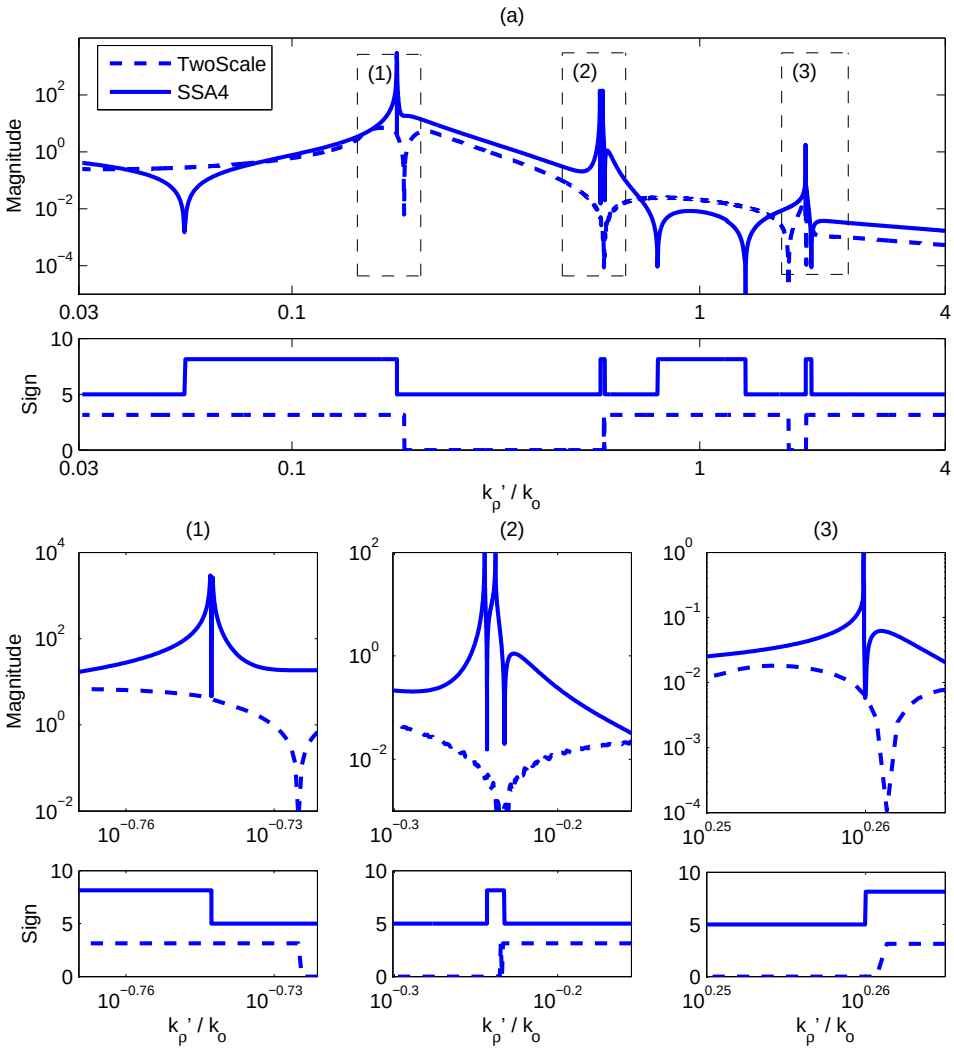

Figure 6.6: "Semi-stable" horizontally polarized weighting functions $w^{(1)}_{h,(x)}(k_{\rho'})$, including higher resolution plots near critical phenomenon regions (1) to (3)

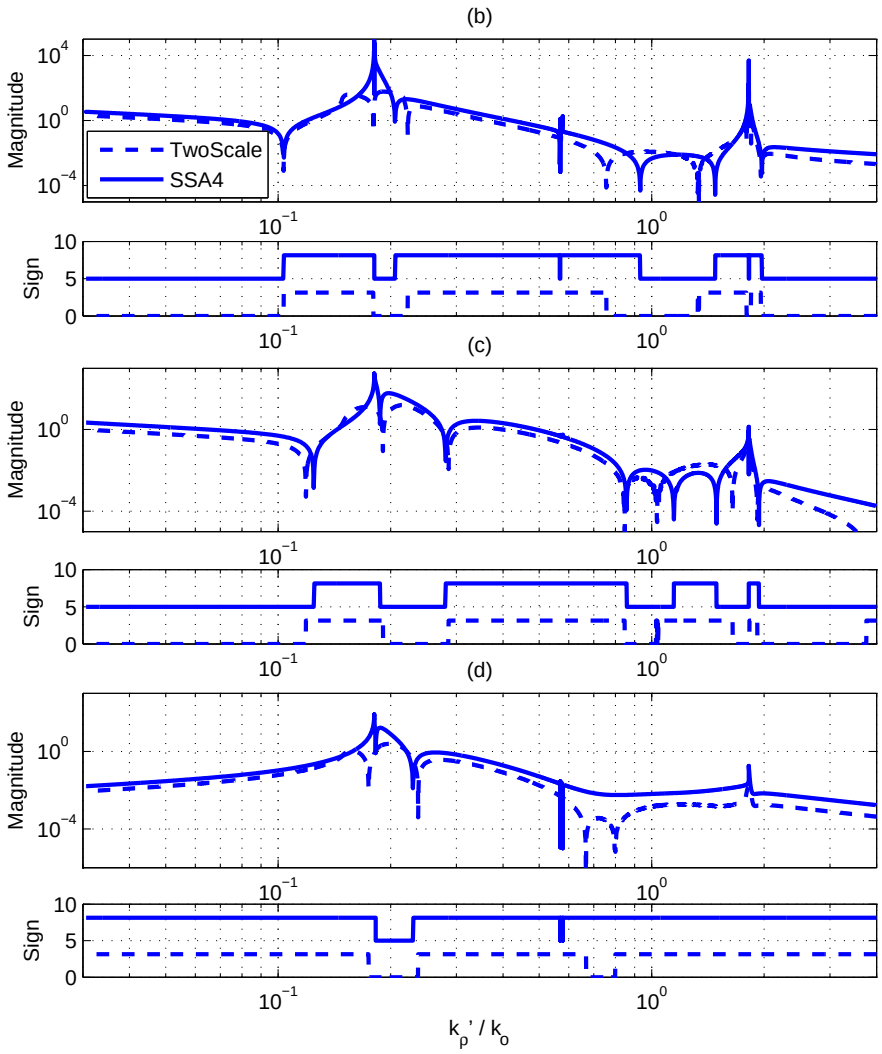

Figure 6.7: "Semi-stable" weighting functions b)-Vertical Pol.($w^{(1)}_{v,(x)}(k_{\rho'})$) , c)-U pol.($w^{(s)}_{u,(x)}(k_{\rho'})$), d)-VV Pol.($w^{(s)}_{VV,(x)}(k_{\rho'})$)

is modeled using the modified "Durden-Vesecky" spectrum described in [79], and the sea surface physical temperature is set to 283 K. While all theories predict the possibility of zeroth, second, and fourth azimuthal harmonics in this process, fourth azimuthal harmonics are found to be extremely small and therefore not described further. Azimuthal harmonic brightnesses are plotted either with respect to wind speed (from 0 to 20m/s) for a fixed radiometer observation angle $\theta_i = 55$ degrees, or with respect to observation angle ranging from 40^o to 75^o for a fixed wind speed of 10m/s. In all cases, the boundaries of the short-wave integration correspond to short sea waves of wavelengths ranging from 0.5m down to 4mm.

Two distinct descriptions of the long-wave integration domain are utilized. In the first case (labeled Case A), the long wave domain includes all long waves longer than 62.5 m; the long wave spectrum considered of course varies as the wind speed is varied. In this case, the long waves included are certainly much longer than the short waves of interest, so that the SSA4 expansion should be more applicable. In the second case (Case B), a shorter set of long waves ranging from 62.5 m maximum wavelength down to 0.625 m is used to assess the applicability of the SSA4 expansion as the separation between "long" and "short" waves is decreased.

Figures 6.8 (versus wind speed) and 6.9 (versus angle) plot the comparisons for Case A. First note that the brightness harmonics obtained in Case A are all less than 0.1 K, with the exception of the 0th harmonics at large wind speeds and/or observation angles. This is due to the small rms slopes obtained when only extremely long long waves are included. The wind speed dependence observed arises both from increases in the long wave slope variance considered, but also from changes in the short wave spectrum [79] with windspeed. The comparison among theories shows the SSA4

expansion to be highly accurate in this case when compared to the numerical SSA4 integration, even given the difficulties in evaluation of the kernel function derivatives required in the expansion. Two-scale predictions again are similar to the SSA4 results in terms of general trends and relative amplitudes, but do show observable differences.

Results for Case B in Figures 6.10 and 6.11 show larger but still relatively small fourth order effects with maximum amplitudes on the order of 1 K in the zeroth harmonics while remaining less than 0.1 K in second azimuthal harmonics. The expanded SSA4 theory is found to provide reduced accuracy compared to case A, but to still achieve good agreement with the full SSA4 numerical integration. Differences with the two-scale model are more significant, particularly for the zeroth azimuthal harmonic of horizontal polarization, but overall the two-scale model shows similar trends and amplitudes.

6.8 Conclusion

In this Chapter, expressions for the fourth-order SSA theory of emission from one layer rough surfaces were derived and presented. For the case of a Gaussian random process surface model, evaluation of the theory required computation of a four-fold integration over a product of two surface spectra. This form was described as providing information on contributions from interactions of multiple sea waves in the surface spectrum. Predictions of the model were evaluated in two situations: coupling between "long-long" waves and between "long-short" waves. The former contributions were shown to remain consistent with the physical optics theory, as has been previously demonstrated for the second and third order SSA models. "Long-short" wave

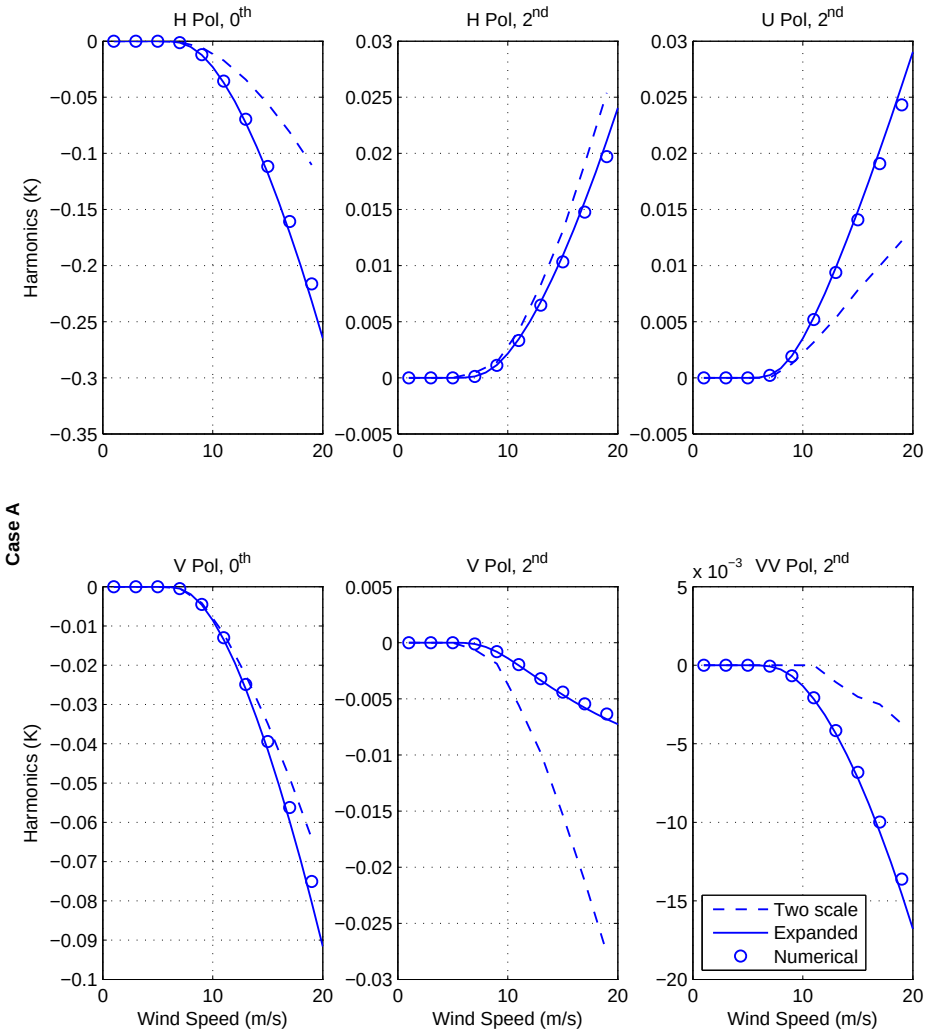

Figure 6.8: Case A, brightness tempreature azimuthal harmonics versus wind speed

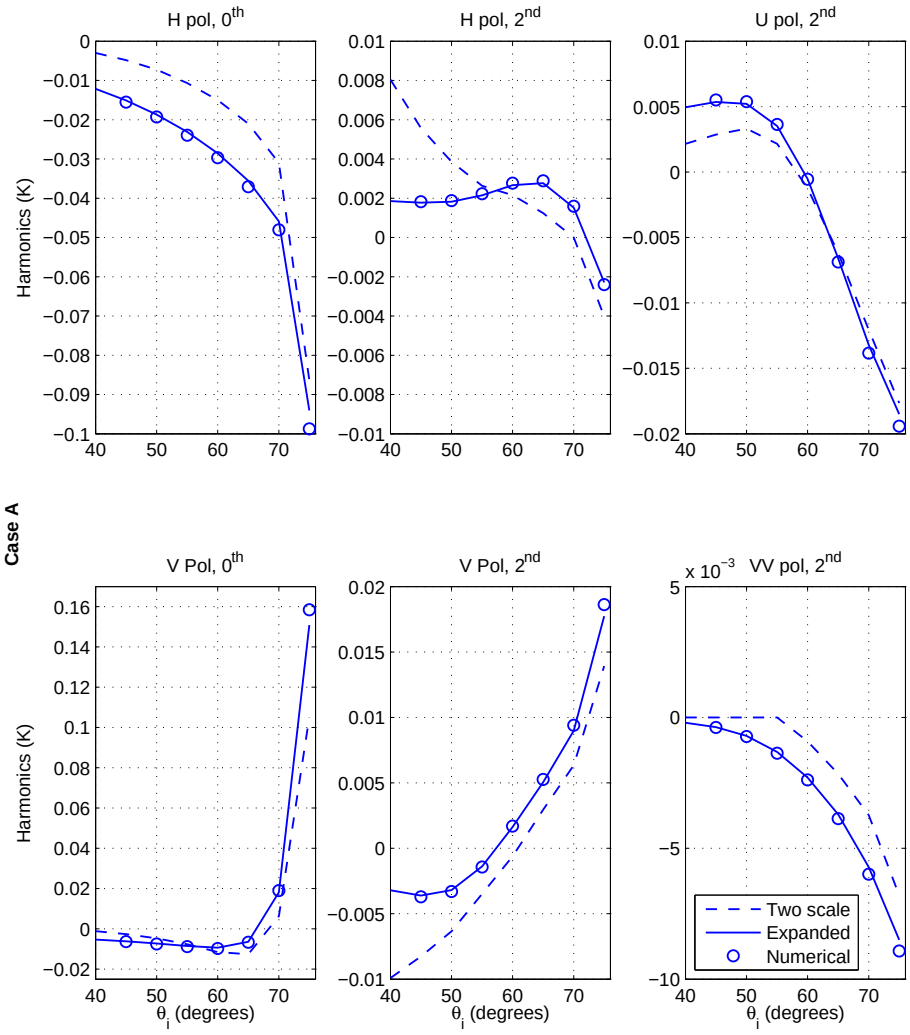

Figure 6.9: Case A, brightness temperature azimuthal harmonics versus θ_i

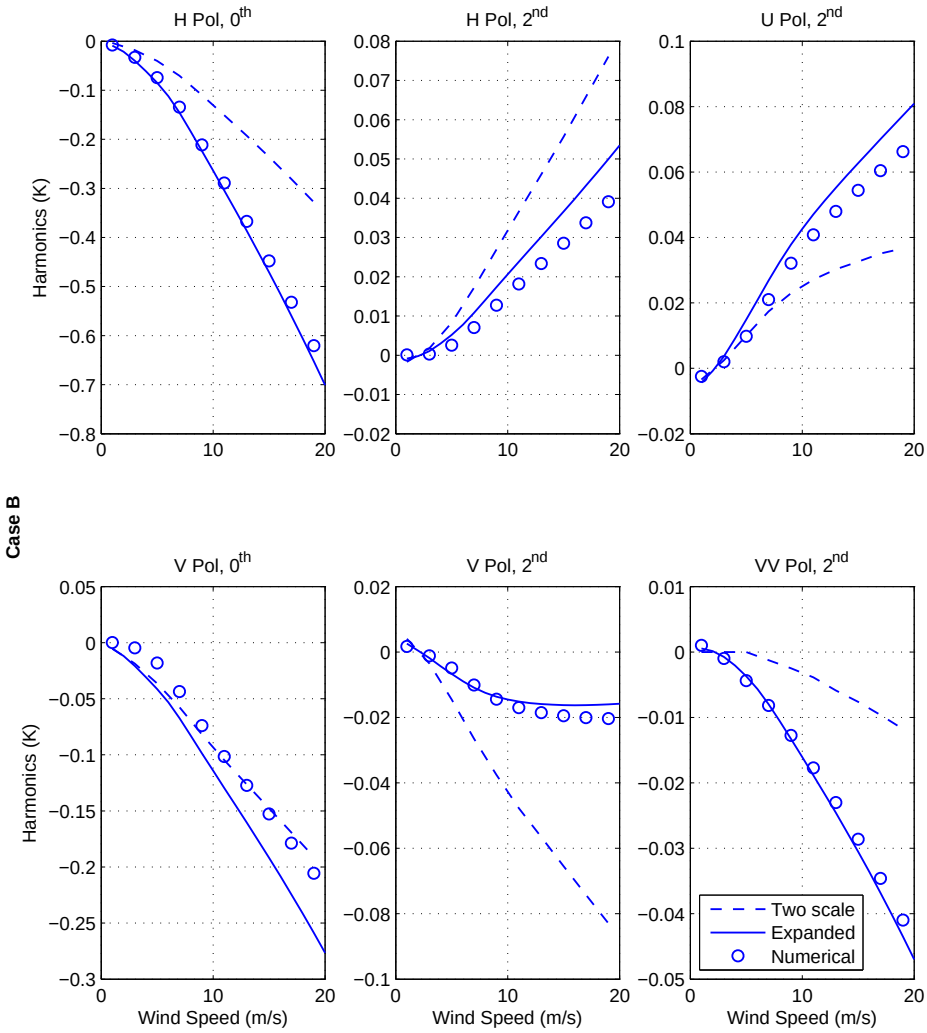

Figure 6.10: Case B, brightness temperature azimuthal harmonics versus wind speed

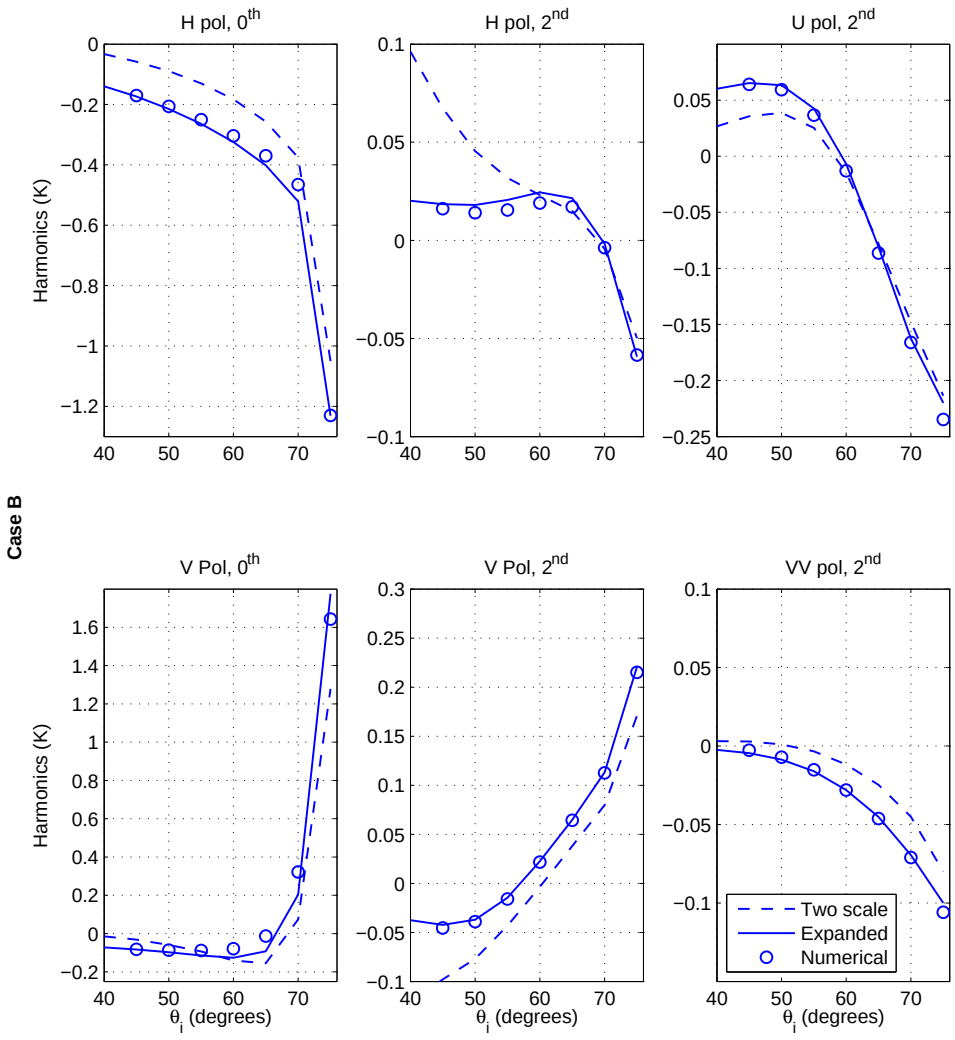

Figure 6.11: Case B, brightness temperature azimuthal harmonics versus θ_i

interactions were studied through the use of a symmetrized kernel function, and by consideration of critical phenomenon effects in the SSA4 kernel functions. A numerical integration procedure for evaluation of "long-short" wave effects was described, as well as an expansion in long wave slopes that yielded a simplified approximation in terms of spectrum independent "weighting functions." A study of these interactions was performed, and it was found that the expansion provided reasonable predictions, even though finite computational precision limited the accuracy of the kernel function derivative evaluation in some cases. One of the primary goals of this part was an assessment of the commonly applied "two-scale" theory through comparison with the SSA4. This was performed by comparing the "weighting functions" of the SSA4 expansion with those obtained from a similar expansion of the two-scale theory, as well as through direct comparison of fourth order brightnesses between the theories. Results showed the two methods not to be identical, indicating that the SSA4 model captures long-short wave interactions beyond the simple "tilting" process implicit in the two-scale theory.

CHAPTER 7

CONCLUSION

In this dissertation, complete SPM solution of the two layer problem has been investigated, along with its applications and applications of previously developed one layer complete SPM theory. The purpose of this study was to improve our understanding of given rough surface scattering problems by utilizing higher order SPM solutions. SPM is one of the fundamental and most useful approaches in classical rough surface scattering theory, mostly because of its ability to decouple the surface and the scattering effects. The lower order SPM solutions are well studied in the literature and provide sufficient insight to several rough surface scattering problems. But, if problems such as multi layer roughness or multi scale roughnesses are considered, then higher order SPM solutions are necessary to provide more descriptive information on scattering properties. This dissertation was focused on such applications. In the first part, where the two layer SPM solution was derived rigorously, the interaction of rough surfaces was investigated, assuming the surfaces are uncorrelated GRPs. Moreover, one final chapter was devoted to applications of one layer SPM theory, where the fourth order emission theory of rough surface was considered. In this part, the fourth order SPM theory was utilized, and an alternative to the so called two-scale theory was derived.

The main contributions of this dissertation can be summarized as follows:

- A numerical SPM solution procedure is described for the two layer problem at arbitrary order, which is more suitable for deterministic problems.
- The numerical SPM solution for two layer problem was extended to an arbitrary number of layers case.
- Explicit expressions for the SPM kernels were presented analytically up to the second order.
- The complete SPM solution was provided as an arbitrary order analytical solution, the solution was expressed iteratively.
- A power analysis of the two layer problem was given at third order for both coherent and incoherent fields, and the total scattering of the two layer problem was decomposed into upper, lower and interaction effects and the importance of interactions of rough surfaces are investigated.
- One layer arbitrary order solution is utilized to compute fourth order emission theory of rough surfaces.
- In the case, when multi scale roughness description of the surface is relevant, a theoretically sound alternative is developed to the commonly used heuristic two-scale theory.

Specifically in Chapter 2, detailed formulations for fundamental rough surface scattering models, 1-D, rough, PEC interfaces. Both approximate and exact models were described. The approximate models discussed include, small perturbation

method (SPM), second order small slope approximation (SSA2), the physical optics (PO), and the lowest order modified non-local SSA (MNLSSA). As an exact numerical solution, the extended boundary condition (EBC) method was considered. The 1-D Dirichlet treatment of the SPM, was highlighted in great detail for the deterministic case. And later, as a non-classical rough surface scattering model example, the SSA2 model was described for the same problem, since the SSA2 model can be considered as an advanced application of SPM model. The rest of the chapter, was mostly specialized for a deterministic problem: scattering from sinusoidal gratings. Formulations of each model mentioned above was presented and one final section was also included, for comparison of these models, in order to give insight on the limitations of each model.

Then, in Chapter 3, basic problem setup for the two-layer problem was introduced. In this chapter, first, the notational conventions were provided. Next, the boundary conditions were studied. Each boundary condition brought a so called forcing function, which were utilized to express the solution of the problem as a set of two linear system of equations, for horizontal and vertical polarizations, respectively. The solution for these systems of equations was provided analytically. Later, a Fast Fourier Transform(FFT) based numerical solution was described, in the Fourier-Rayleigh sense. For validation purposes, the numerical perturbation solution was compared against an existing two and a half dimensional extended boundary condition(EBC) solution for two sine surfaces on top of each other, in the propagating modes. Arbitrary number of layers case was also considered as a final section in this chapter in a numerical sense. This section can also be considered as a generalization

of the two-layer numerical solution, which might be very useful in a possible future work involving analytical arbitrary layer SPM solutions.

Next, in Chapter 4, analytical solution procedure for the two-layer problem was presented. In this chapter, first, the zeroth order solution was provided, in terms of the $K_{E,H}$ terms, defined in Chapter 3. The zeroth and arbitrary order contributions to the general N^{th} order solution was studied from the forcing functions, provided in Chapter 3. The zeroth order contribution terms were studied separately for horizontal and vertical incidence cases, but the arbitrary order contributions were identical for both incidence cases. Next, partial SPM solutions for zeroth and lower order contribution terms were obtained. Later, these partial solutions were utilized to obtain the complete first and second order solutions. Then, general form of higher order solutions were studied, and based on those generalizations, a new tensor based notation was introduced. The tensor notation was applied to the partial SPM solutions, and the arbitrary order SPM solution procedure was constructed with them. Finally, a convergence analysis of SPM solutions were presented using the ratio test of convergence. The main conclusion, based on this study was the fact that The two layer SPM theory have better predictions if the surfaces posses similar heights. This is mostly due to numerical accuracy of the computations: the kernels produce huge values especially at the higher orders, several addition operations occur above machine limit.

Later, in Chapter 5, power analysis of the two-layer problem was provided. Given the field solution to the third order in surface height, reflected, intermediate and transmitted powers were derived to third order. In this chapter, first, a general discussion on the power calculations was provided. Assumptions on the statistical

surface properties were highlighted. Then, under the assumption of Gaussian Random Process (GRP), the zeroth and the second order coherent reflectivity and the second and the fourth order incoherent bi-static Radar Cross Sections (RCS) were derived. For the case, when the two surfaces are uncorrelated, the bi-static RCS term was studied thoroughly and the effects of upper and lower roughness and the interaction of roughness effects were identified. A special term was defined as the ratio of the interaction effect to the overall RCS, and it was studied for several setups. The results had confirmed that the surface interactions are important for two layer problem, and consequently, higher order solutions are necessary for analyzing layered roughness.

Last, in Chapter 6, expressions for the fourth-order SSA theory of emission from one layer rough surfaces were derived and presented. For the case of a Gaussian random process surface model, evaluation of the theory required computation of a four-fold integration over a product of two surface spectra. This form was described as providing information on contributions from interactions of multiple sea waves in the surface spectrum. Predictions of the model were evaluated in two situations: coupling between "long-long" waves and between "long-short" waves. The former contributions were shown to remain consistent with the physical optics theory, as has been previously demonstrated for the second and third order SSA models. "Long-short" wave interactions were studied through the use of a symmetrized kernel function, and by consideration of critical phenomenon effects in the SSA4 kernel functions. A numerical integration procedure for evaluation of "long-short" wave effects was described, as well as an expansion in long wave slopes that yielded a simplified approximation in terms of spectrum independent "weighting functions." A study of

these interactions was performed, and it was found that the expansion provided reasonable predictions, even though finite computational precision limited the accuracy of the kernel function derivative evaluation in some cases.

One of the primary goals of this part was an assessment of the commonly applied "two-scale" theory through comparison with the SSA4. This was performed by comparing the "weighting functions" of the SSA4 expansion with those obtained from a similar expansion of the two-scale theory, as well as through direct comparison of fourth order brightnesses between the theories. Results showed the two methods not to be identical, indicating that the SSA4 model captures long-short wave interactions beyond the simple "tilting" process implicit in the two-scale theory. However studies showed that brightness differences between the two theories were generally small, and can be considered negligible for second azimuthal harmonic variations in particular. Further studies using the SSA4 theory to compute "short-short" wave interaction effects may also yield additional motivation for further application of the method.

BIBLIOGRAPHY

[1] Elfouhaily, T. M., Guerin, C. A. "A critical survey of approximate scattering wave theories from random rough surfaces", *Waves in Random Media*, vol. 14, pp. 1-40, 2004.

[2] Tabatabaeenejad A., Moghaddam, M., "Backscattering of Electromagnetic waves from layered rough surfaces and its applications in estimating deep soil moisture", *Proc. IEEE IGARSS*, vol. 5, pp. 3526-3528, 2004

[3] Kuo, C., Moghaddam, M., "Electromagnetic scattering from multilayer Rough surfaces based on Extended boundary condition formulation and transition matrix approach", *Proc. IEEE IGARSS*,vol. 1, pp. 4 , 2005

[4] Hussein, Z. A., Holt, B.,McDonald, K. C., Jordan, R., Huang, J., Chu, A., Pak, K., Gradziel, M., Kuga, Y., Ishimaru, A., Jaruwatanadilok, S., Gogineni, P., Akins, T., Heavey, B., Perovich, D., Sturm, M., "A combined spatial and frequency domain interferometer for sea ice thickness measurement", NASA ESTC, 2005.

[5] Sourbet, A., Berginc, G.,Bourrely, C., "Application of reduced Rayleigh equations to electromagnetic wave scattering by two-dimensional randomly rough surfaces", *Physical Rev. B*, Vol. 63, 245411, 2001.

[6] Sourbet, A., Berginc, G.,Bourrely, C., "Backscattering enhancement of an electromagnetic wave scattered by two-dimensional rough layers" *J. Opt. Soc. Am. A*, vol.18 pp. 2778-2788, 2001.

[7] Moss, D. M.,Grzegorczyk, T. M., Han, H. C., Kong, J. A., "Forward-backward method with spectral acceleration for scattering from layered rough surfaces", *IEEE Trans. Antennas Prop.*, vol. 54, pp 1006-1016, March 2006.

[8] Harrington R. F., "Time Harmonic Electromagnetic Fields" McGraw-HILL, 1961

[9] Kong Jin A., "Electromagnetic Wave Theory" John Willey & Sons, Inc., 1990

[10] Leung Tsang, Jin Au Kong, Kung-Hau Ding, "Scattering of Electromagnetic Waves: Theories and Applications", John Willey & Sons, Inc., 2000.

[11] Leung Tsang, Jin Au Kong, Kung-Hau Ding, Chi On Ao, "Scattering of Electromagnetic Waves: Numerical Simulations", John Willey & Sons, Inc., 2001.

[12] Leung Tsang, Jin Au Kong, "Scattering of Electromagnetic Waves: Advanced Topics." , John Willey & Sons, Inc., 2001.

[13] Elfouhaily, T., Bourlier, C., Johnson, J. T., "Two families of non-local scattering models and the weighted curvature approximation", *Waves Random Media*, vol. 14, pp. 563-580, 2004.

[14] Fung, A. K., "Microwave Scattering and Emission Model and Their Applications.", Norwood, MA: Artech House, 1994.

[15] Voronovich, A. G., "Non-local small-slope approximation for wave scattering from rough surfaces", *Waves Random Media*, vol. 6, pp. 151-167, 1996.

[16] Stogryn, A., "Electromagnetic scattering from rough finitely conducting surfaces", *Radio Sci.*, vol. 2, no. 4, pp. 415-428, 1967.

[17] Ulaby, F., Moore, R. ,Fung A., "Microwave Remote Sensing: Active and Passive. Radar Remote Sensing and Surface Scattering and Emission Theory.", *Reading, MA: Addison-Wesley*, vol. 3, 1982

[18] Fuks, M. I., Voronovich, A. G. "Wave diffraction by rough interfaces in an arbitrary plane-layered medium", *Waves in Random Media*, vol. 10, pp. 253-272, 2000

[19] Voronovich, A. G., "Wave scattering from rough surfaces", *Springer-Verlag*, 1994

[20] Ishimaru, A., "Wave propagation and scattering in random media", New York: Academic, 1978

[21] Ishimaru, A., "Electromagnetic wave propagation, radiation and scattering", *Prentice-Hall*, 1991.

[22] Rice, S. O., "Reflection of electromagnetic waves from slightly rough surfaces," *Commun. Pure Appl. Math,* vol. 4, pp. 361-378, 1951.

[23] Valenzuela, G. R., "Depolarization of EM waves by slightly rough surfaces," *IEEE Trans. Ant. Prop.,* vol. AP-15, pp. 552-557, 1967.

[24] Valenzuela, G. R., "Scattering of electromagnetic waves from a tilted slightly rough surface," *Radio Science,* vol. 3, pp. 1057-1066, 1968.

[25] Ogilvy, J. A. ,"Theory of Wave Scattering from Random Rough Surfaces", Adam Hilger, 1991

[26] Beckmann, P., Spizzichino, A., "The scattering of electromagnetic waves from rough surfaces," Pergamon Press, Oxford, England, 1963

[27] Ohlidal, K. Navratil, and M. Ohlidal, "Scattering of light from multilayer systems with rough boundaries," *Prog. Opt.*, vol. 34, pp. 251-334, 1995.

[28] R. Garcia-Llamas, L. E. Regalado, and C. Amra, "Scattering of light from a two-layer system with a rough surface," *J. Opt. Soc. Am. A*, vol. 16, pp. 2713-2719, 1999.

[29] P. Bousquet, F. Flory, and P. Roche, "Scattering from multilayer thin films: theory and experiment," *J. Opt. Soc. Am.*, vol. 71, pp. 1115-1123, 1981.

[30] J. M. Elson, "Multilayer-coated optics: guided-wave coupling and scattering of interface random roughness," *J. Opt. Soc. Am. A*, vol. 12, pp. 729-742, 1995.

[31] G. C. Brown, V. Celli, M. Haller, and A. Marvin, "Vector theory of light scattering from a rough surface: unitary and reciprocal expansions," *Surf. Sci.*, vol. 136, pp. 381-397, 1984.

[32] A. R. McGurn, A. A. Maradudin, and V. Celli, "Localization effects in the scattering of light from a randomly rough grating," *Phys. Rev. B*, vol. 31, pp. 4866-4871, 1985.

[33] V. Celli, A. A. Maradudin, A. M. Marvin, and A. R. McGurn, "Some aspects of light scattering from a randomly rough metal surface," *J. Opt. Soc. Am. A.*, vol. 2, pp. 2225-2239, 1985.

[34] A. R. McGurn and A. A. Maradudin, "Localization effects in the elastic scattering of light from a randomly rough surface," *J. Opt. Soc. Am. B.*, vol. 4, pp. 910-926, 1987.

[35] A. A. Maradudin and E. R. Mendez, "Enhanced backscattering of light from weakly rough, random metal surfaces," *Appl. Opt.*, vol. 32, pp. 3335-3343, 1993.

[36] C. S. West and K. A. O'Donnell, "Observations of backscattering enhancement from polaritons on a rough metal surface," *J. Opt. Soc. Am. A.*, vol. 12, pp. 390-397, 1995.

[37] V. Freilikher, E. Kanzieper, and A. A. Maradudin, "Coherent scattering enhancement in systems bounded by rough surfaces," *Phys. Rep.*, vol. 288, pp. 127-204, 1997.

[38] A. Ishimaru, C. Le, Y. Kuga, L. A. Sengers, and T. K. Chan, "Polarimetric scattering theory for high slope rough surfaces," Progress in Electromagnetic Research, M. Tateiba and L. Tsang, eds. *Elsevier, New York*, vol. 14, pp. 1-36, 1996.

[39] A. R. McGurn and A. A. Maradudin, "Perturbation theory results for the diffuse scattering of light from twodimensional randomly rough metal surfaces," *Waves Random Media*, vol. 6, pp. 251-267, 1996.

[40] M. I. Charnotskii, V. I. Tatarskii, "Tilt-invariant theory of rough surface scattering," *Waves Random Media*, vol. 5, pp. 361-80, 1995.

[41] A. B. Isers, A. A. Puzenko and I. M. Fuks, "The local perturbation method for solving the problem of diffraction from a surface with small slope irregularities," *J. Electromagn. Wave Appl.*, vol. 5, pp. 1419-35, 1991.

[42] E. Bahar "Scattering cross sections for composite random surfaces: fullwave analysis," *Radio Sci.*, vol. 16, pp. 1327-35, 1981.

[43] D. P. Winebrenner and A. Ishimaru, "Investigation of a surface-field phase-perturbation technique for scattering from rough surfaces," *Radio Sci.*, vol. 20, pp. 161-70, 1985.

[44] B. F. Kuryanov, "The scattering of sound at a rough surface with two types of irregularity," *Sov. Phys.-Acoust.*, vol. 8, pp. 252-7, 1962.

[45] G. R. Valenzuela, "Theories for the interaction of electromagnetic and oceanic waves,"-*a review Boundary Layer Meteorol.*, vol. 31, pp 61-5, 1978.

[46] J. W. Wright, "A new model for sea clutter," *IEEE Trans. Antennas Propag.*, vol. 16, pp 217-23, 1968.

[47] G. S. Brown, "A new approach to the analysis of rough surface scattering," *IEEE Trans. Antennas Propag.*, vol. 39, pp. 943-8, 1991.

[48] A. A. Maradudin and D. L. Mills, "Scattering and absorption of electromagnetic radiation by semi-infinite medium in the presence of surface roughness,"*Phys. Rev. B*, vol. 11, pp. 1392-415, 1975.

[49] A. A. Maradudin, T. Michel, A. R. McGurn and E. R. Mendez, "Enhanced backscattering of light from random grating," *Ann. Phys.*, NY 203, pp. 255-307, 1990.

[50] Ch, Elachi, L. E. Roth, and G. G. Schaber, "Spaceborne radar subsurface imaging in hyperarid regions," *IEEE Trans. Geosci. Rem. Sens.*, vol. 22, pp. 383-7, 1984.

[51] A. K. Fung and M. E. Chen, "Emission from an inhomogeneous layer with irregular interfaces," *Radio Sci.*, vol. 16, pp. 289-97, 1981.

[52] N. P. Zhuk, A. V. Frankov and A. G. Yarovoy, "Backward scattering of electromagnetic waves by the rough surface of a medium whose dielectric permittivity has an exponential profile," *J. Commun. Tech. Electron.*, vol. 38, pp. 108-11, 1993.

[53] N. P. Zhuk, S. N. Shulga and A. G. Yarovoy, "Backscattering of waves by a rough conducting substrate covered by a homogeneous dielectric layer," *J. Commun. Tech. Electron.*, vol. 36, pp. 131-3, 1991.

[54] A. G. Yarovoy , R. V. de Jongh and L. P. Ligthart, "Scattering properties of a statistically rough interface inside a piecewise homogeneous stratified medium," *Int. Symp. Electromagnetic Theory (Thessaloniki)*, pp. 680-2, 1998.

[55] A. Kalmykov, I. Fuks, I. Scherbinin, V. Tsymbal, A. Matveev, A. Gavrilenko, M. Fix and V. Freilikher, "Radar observations of strong subsurface scatterers. A model of backscattering," *IEEE Proc. IGARSS95 Quantitative Remote Sensing*, vol. 3, pp. 1702-4, 1995.

[56] I. M. Fuks, "Radar contrast polarization dependence on subsurface sensing," *IEEE Proc. IGARSS98* (Seattle, WA), vol. 3, pp. 1455-9, 1998.

[57] D. L. Mills and A. A. Maradudin, "Surface roughness and the optical properties of a semi-infinite material: the effect of a dielectric overlayer," *Phys. Rev. B*, vol. 12, pp. 2943-58, 1975.

[58] J. M. Elson, "Infrared light scattering from surfaces covered with multiple dielectric overlayers," *Appl. Opt.*, vol. 16, pp. 2872-81, 1977.

[59] C. Amra, G. Albrand and P. Roche, "Theory and application of antiscattering single layers: antiscattering and antireflection coatings," *Appl. Opt.*, vol. 25, pp. 2695-702, 1986.

[60] C. Amra, "First-order vector theory of bulk scattering in optical multilayers," *J. Opt. Soc. Am. A*, vol. 10, pp. 365-74, 1993.

[61] C. Amra, "From light scattering to microstructure of thin-film multilayers," *Appl. Opt.*, vol. 32, pp. 5481-91, 1993.

[62] V. Freilikher, M. Pustilnik, I. Yurkevich and V. I. Tatarskii, "Polarization of light scattering from slightly rough dielectric film," *Opt. Lett.*, vol. 19, pp. 1382-4, 1994.

[63] A. Sentenac and J. J. Greffet, "Mean-field theory of light scattering by one-dimensional rough surface," *J. Opt. Soc. Am. A*, vol. 15, pp. 528-32, 1998.

[64] O. Calvo-Perez, J. J. Greffet, and A. Sentenac, "Scattering by randomly rough dielectric surfaces and rough dielectric films: influence of the height distribution," *J. Opt. A: Pure Appl. Opt.*, vol. 1, pp. 560-5, 1999.

[65] O. Calvo-Perez, A. Sentenac and J. J. Greffet, "Light scattering by a two-dimensional, rough penetrable medium: a mean-field theory," *Radio Sci.*, vol. 34, pp. 311-55, 1999.

[66] N. P. Zhuck, "Scattering of EM waves from a slightly rough surface of a generally anisotropic plane-layered half-space," *IEEE Trans. Antennas Propag.*, vol. 45, pp. 1774-82, 1997.

[67] V. I. Tatarskii, "Relation between the Rayleigh equation in diffraction theory and the equation based on Greens formula," *J. Opt. Soc. Am. A*, vol. 12, pp. 1254-60, 1995.

[68] Johnson, J. T., "Third order small perturbation method for scattering from dielectric rough surfaces," *J. Opt. Soc. Am. A.,* vol. 16, pp. 2720-2726, 1999.

[69] M. A. Demir, J. T. Johnson "Fourth and higher-order small perturbation solution for scattering from dielectric rough surfaces," *J. Opt. Soc. Am. A*, vol. 20, pp. 2330-2337, 2003.

[70] M. A. Demir, "Fourth order theories of emission and scattering from rough surfaces," M. S. Thesis, Dept. of Electrical and Computer Engineering, The Ohio State University, 2003.

[71] M. A. Demir, J. T. Johnson "Fourth Order Small Slope Theory of Sea Surface Brightness Temperatures" *IEEE Trans. Geosc. Remote Sens.*, vol. 45, pp. 175-186, 2007.

[72] Kim, H.,"Radar Image studies of scattering from random rough surfaces", *Dissertation*, The Ohio State University, 2002.

[73] Irisov, V. G., "Small-slope expansion for thermal and reflected radiation from a rough surface," *Waves in Random Media,* vol. 7., pp. 1-10, 1997.

[74] Johnson, J. T., Kong J. A., Shin R. T., Staelin D. H., O'Neill K., Lohanick A. W., "Third stokes parameter emission from a periodic water surface," *IEEE Trans. Geosc. Remote Sens.,* vol. 31, no5, pp. 1066-1080, 1993.

[75] Johnson, J. T., and M. Zhang, "Theoretical study of the small slope approximation for ocean polarimetric thermal emission," *IEEE Trans. Geosc. Remote Sens.,* vol. 37, pp. 2305-2316, 1999.

[76] Irisov, V. G., "Azimuthal variations of the microwave radiation from a slightly non-Gaussian sea surface," *Radio Science,* vol. 53, pp. 65-82, 2000.

[77] Johnson, J. T. and Y. Cai, "A theoretical study of sea surface up/down wind brightness temperature differences," *IEEE Trans. Geosc. Remote Sens.,* vol. 40, pp. 66-78, 2002.

[78] J. T. Johnson, "Comparison of the physical optics and small slope theories for polarimetric thermal emission from the sea surface," *IEEE Trans. Geosc. Rem. Sens.,* vol. 40, pp. 500-504, 2002.

[79] Yueh, S. H., "Modeling of wind direction signals in polarimetric sea surface brightness temperatures," *IEEE Trans. Geosc. Remote Sens.*, vol. 35, pp. 1400-1418, 1997.

[80] Johnson, J. T., "An efficient two-scale model for the computation of thermal emission and atmospheric reflection from the sea surface," *IEEE Trans. Geosc. Remote Sens.,* vol. 44, pp. 560-568, 2006.